IRE Transactions

on Microwave Theory and Techniques

Volume MTT-7 JULY, 1959 Number 3

In This Issue

PUBLISHED BY THE

Professional Group on Microwave Theory and Techniques

IRE PROFESSIONAL GROUP ON MICROWAVE THEORY AND TECHNIQUES

The Professional Group on Microwave Theory and Techniques is an association of IRE members with professional interest in the field of Microwave Theory and Techniques. All IRE members are eligible for membership and will receive all Group publications upon payment of the prescribed annual fee of \$3.00. Members of the American Physical Society and the Institution of Electrical Engineers of Great Britain may become affiliated with PGMTT and receive all Group publications upon payment of the Affiliate fee of \$7.50 per year.

IRE TRANSACTIONS®

on Microwave Theory and Techniques

Published by the Institute of Radio Engineers, Inc., for the Professional Group on Microwave Theory and Techniques, at 1 East 79th Street, New York 21, New York. Responsibility for the contents rests upon the authors, and not upon the IRE, the Group, or its members. Price per copy: IRE PGMTT members, \$1.65; IRE members, \$2.45, nonmembers, \$4.95. Annual subscription price: IRE members, \$8.50; colleges and public libraries, \$12.75; nonmembers, \$17.00.

Address all manuscripts to Donald D. King, PGMTT Editor, Electronic Communications, Inc., 1830 York Road, Timonium, Md. Submission of three copies of manuscripts, including figures, will expedite the review.

IRE Transactions on Microwave Theory and Techniques

Volume MTT-7 JULY, 1959 Number 3

TABLE OF CONTENTS

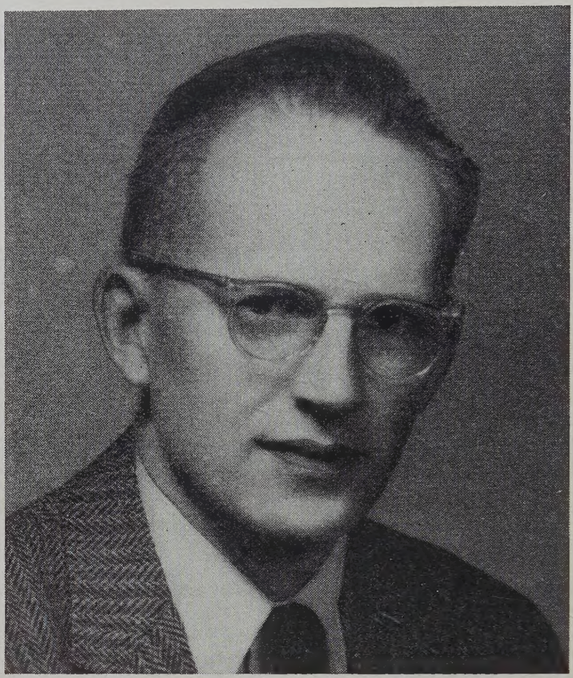

Henry J. Riblet

Henry J. Riblet (A'45–M'55–F'58) was born on July 21, 1913, in Calgary, Can. He graduated from Yale University, New Haven, Conn., with the B.S. degree in mathematics in 1935. He received the M.A. and the Ph.D. degrees in mathematics from Yale in 1937 and 1939, respectively.

For the next three years he taught mathematics at Adelphi College and then at Hofstra College, Long Island, N. Y. He first encountered radio engineering when, with the encouragement of W. W. Hansen, he modified Hansen's method and obtained accurate klystron resonant frequencies using a procedure numerically equivalent to the "variational principle."

He joined the M.I.T. Radiation Laboratory, Cambridge, Mass., in 1942, and at the close of the war was in charge of the developmental section of the antenna group devoted to the design of linear arrays, beacon and special broad-band antennas. From 1946 to 1948 he headed the microwave group at the Submarine Signal Company. He is presently President of the Microwave Development Laboratories, the Fab-Braze Corporation, Strand Laboratories, and the Elevator Scaffold Corporation, as well as being Treasurer of Ferrotec, Inc.

Dr. Riblet is the author of approximately twenty technical articles dealing with theory and practice in mathematics, physics, and engineering, and has been awarded over fifty patents on mechanical and electrical devices.

He is a member of the American Mathematical Society and the American Physical Society.

Pure or Applied?

IT seems that in the general desire to acknowledge and recognize the contributions of science to our present society, there is a tendency to glamorize the basic sciences at the expense of their engineering counterparts. It is almost as if a descending hierarchy has been established between theory at one end and practice at the other. Perhaps this is not the case, but articles on the danger of neglecting pure research in the interest of its applications and lamenting the distribution of research and development funds are a familiar sight, while it is seldom noted that only rarely can pure research proceed faster than the engineering technology on which it rests. Such articles foster the idea that research is reserved to pure science while the design engineer is relegated to the role of skillful computer.

This editorial permits me the opportunity to state the case for engineering; for utility must be the gauge. Even those who decry our lack of interest in basic science ultimately justify it by pointing to the many contributions which have been made to our technology by seemingly irrelevant investigation. Of course, usefulness is a broad term and includes much of human activity. In the mathematical fraternity in which I traveled for a time, it was not unusual to encounter a certain pride in research having no foreseeable application. But isn't curiosity itself a fundamental hunger? And who can say that knowledge for its own sake may not become man's principal justification for his scientific efforts, or even, for that matter, tell what mathematical theorem is useless?

Clearly then, the curve of worth cannot continually slope upward as the research effort recedes from its applications without our concluding that the useless work is the most valuable.

Applied or Pure, all research is a quest for knowledge. Both are equally interesting, equally difficult and, when progress is made, give equal pleasure. Pure research is so vital to us, not because it is "pure," but because it is basic to the engineering sciences. The engineering sciences are equally important because without them, our basic knowledge would effect our lives in only a minor way.

Society is enormously indebted to those who work without the satisfaction of seeing their efforts immediately put to use but, as one draws farther and farther from the application, the special requirements of a problem become less onerous. The path in some ways is easier. Projects can be selected at the frontier of knowledge, often in a virgin field, on the basis of interest and solvability rather than immediate need. The design engineer, on the other hand, who works at a "nerve-fraying" problem with constraints that are given in terms of rigid specifications, bounded by definite limits on time and money, has, in general, a more frustrating task and is entitled to every credit and consideration.

After all, it is not a question of pure research vs developmental engineering, because neither can proceed far without the other; but rather, where they should devote their time working together as a team.

—HENRY J. RIBLET

Report of Advances in Microwave Theory and Techniques in U.S.A.—1958*

R. E. BEAM† AND M. E. BRODWIN†

Introduction

THIS report on advances in microwave theory and techniques is based on papers appearing in American journals. Advances in the realm of sources and detectors, transmission lines, circuits and circuit elements, components, and measurements are reported. No attempt is made to cover advances in the realm of antennas and wave propagation.

Advances in 1958 were dominated by extensions in knowledge and understanding of solid-state phenomena and by the application of solid-state materials for sources, detectors, and microwave components. Methods of inducing emission of internal molecular energy to achieve microwave amplification have been studied intensively and extensively.

Molecular beam types of masers have characteristics which are serious limitations to extensive practical utilization except for very specialized application requiring very small noise figures. One of the greatest disadvantages is the requirement for operation at liquid helium temperatures; a second serious disadvantage is the very narrow bandwidth; and a third is the requirement of pumping power, usually at frequencies higher than the signal frequency.

These disadvantages are not as great for the new solid-state masers which have received a greater measure of attention during the past year. New materials such as ruby and garnet have been studied. The promise of large scale improvements is not great.

Parametric amplifiers which utilize nonlinear reactances appear to offer significant advantages over masers. Following Suhl's proposal for a ferromagnetic amplifier in the microwave range utilizing a ferrite to obtain, in effect, a time-varying inductance, interest in parametric amplifiers, in general, increased. The well-known nonlinear capacitance characteristic of semiconductor diodes led to considerable efforts to utilize them and to improve their characteristics for such microwave applications. The future of parametric amplifiers utilzing semiconductor diodes at microwave frequencies as low-noise devices appears to be very bright. Traveling-wave forms of parametric amplifiers are considered by some to be very promising. Since low noise figures (as low as can be justified for most applications) are realizable in a simple manner by parametric means without cooling, the great interest in them seems justified.

* Manuscript received by the PGMTT, April, 1959.
† Elec. Engrg. Dept., Northwestern Univ., Evanston, Ill.

The interest in, and development of, traveling-wave tubes as versatile sources of microwave energy having unequaled gain-bandwidth products continued unabated. These efforts have resulted in much smaller, lighter, and more easily adjustable tubes of low, medium, and high power capabilities. Commercial use of these tubes will undoubtedly increase significantly as the result of recent advances.

Klystrons remain the work horses of the microwave tubes and as such are of great importance and have received considerable study. Of especial significance among the developments of the year is the clarification of the low noise-figure potentialities of kylstrons as amplifiers with wide dynamic range for application in RF amplifiers of microwave receivers. Microwave receivers having high sensitivity, high gain, and great dynamic range now appear to be feasible.

It is interesting to note that both traveling-wave tubes and reflex klystrons, respectively, have been operated in a parametric fashion with pumping signals to achieve operation over an extended frequency band and to achieve regenerative amplifier action with the aid of isolators or circulators.

Magnetrons, *per se*, and ordinary vacuum tubes for microwave use received comparatively little study.

Transmission lines and components for transmission systems were investigated extensively. Investigations of TEM lines continue to be dominated by such needs as wider operating bandwidths and smaller size. The large circular waveguide operating in the low-attenuation TE_{01} mode continued to attract study. Mode-purity problems hinder commercial application of these large waveguides. Interest in open or surface waveguides was dominated by their potential usefulness at millimeter wavelengths. Launching methods for surface waves were studied.

Transmission lines containing anisotropic media and microwave components utilizing such media accounted for much activity. The theory of wave propagation in anisotropic waveguides of various geometries, the development of such components as isolators, circulators, and phase shifters, and the search for new anisotropic materials were areas of major interest. Study of the utility of yttrium garnet in components for operation at lower frequencies than are possible with ferrites is noteworthy.

Advances in microwave measurements were principally of the nature of refinements of well-established techniques.

The individual work on the subjects mentioned above

is listed in the following three sections; Sources and Detectors, Transmission Lines, and Measurements. Studies of microwave components and devices which utilize anisotropic materials are also listed in these sections.

Sources and Detectors

Activity in the field of sources of microwave energy has been extensive. Well-established types continue to receive attention. Traveling-wave-tube studies were especially numerous and have resulted in tubes with characteristics which should make them acceptable for field use.

Interest in masers has continued but has been greatest in solid-state rather than in gaseous-state types. The principal advance in sources appears to be in the field of cavity and traveling-wave types of parametric amplifiers, especially those using semiconductor diodes as nonlinear reactive elements.

The results of recent studies of semiconductor diodes indicate that greatly improved diodes for microwave applications will be forthcoming.

Parametric Amplifiers

Most devices which amplify at microwave frequencies use dc sources of power, however, the required power can be supplied from a CW source. The CW source, or "pump," functions to vary the reactance of a circuit. Amplifiers which depend upon the variation of a circuit parameter for their operation are called parametric amplifiers. A parametric amplifier, utilizing a ferromagnetic sample in a microwave cavity for amplification of microwaves, was proposed about two years ago by Suhl. He showed that if the ferromagnetic sample is placed in a cavity which is resonant at three frequencies such that one of the frequencies is equal to the sum of the other two, amplification may occur at either of the two lower frequencies. The simplest case is that for which the RF power source is operated at twice the frequency of the signal to be amplified.

Suhl's proposal and the availability of suitable nonlinear reactances for microwave operation supplied a great stimulus to the development of parametric amplifiers utilizing nonlinear reactances in cavity and traveling-wave structures. Another important stimulus is the promise of low noise figures without cooling since variable-reactnace amplifiers do not depend upon resistive elements for their operation.

A critical evaluation of the relative merits of masers and parametric amplifiers was favorable to the parametric amplifier. Traveling-wave types were considered the most promising of all. Ferrite parametric amplifiers require high pumping powers for reasonably large gain-bandwidth products and strong static magnetic fields. These characteristics place ferrite amplifiers in a poor competitive position relative to semiconductor-diode and electron-beam types of parametric amplifiers.

[1] H. Heffner, "Masers and parametric amplifiers—introduction," 1958 IRE WESCON Convention Record, pt. 3, pp. 3–8.

A basic study of the general energy relations for nonlinear lumped circuit elements was published by Manley and Rowe two years ago. In a continuation of this study the simplest types of nonlinear capacitor modulators, demodulators, and negative conductance amplifiers in which components at two signal frequencies are present were studied by the methods of small-signal theory.

[2] H. E. Rowe, "Some general properties of nonlinear elements· II. Small signal theory," Proc. IRE, vol. 46, pp. 850–860; May, 1958.

A generalization of the Manley-Rowe relations to include power flow in systems involving nonlinear anisotropic electric and magnetic media and nonreciprocal circuits was reported.

[3] H. A. Haus, "Power-flow relations in lossless nonlinear media," IRE Trans. on Microwave Theory and Techniques, vol. MTT-6, pp. 317–324; July, 1958.

An analysis of the variable reactance amplifier in terms of a low-frequency analog in which a variable energy storage is coupled to two resonant circuits looks promising as a simple guide for a parametric amplifier design.

[4] H. Heffner and G. Wade, "Gain, bandwidth, and noise characteristics of the variable-parameter amplifier," *J. Appl. Phys.*, vol. 29, pp. 1321–1331; September, 1958.

The principles of a ferromagnetic resonance frequency converter which are those of the Suhl amplifier were described and checked experimentally. The results obtained are pertinent to the original amplifier as well as to the frequency converter.

[5] K. M. Poole and P. K. Tien, "A ferromagnetic resonance frequency converter," Proc. IRE, vol. 46, pp. 1387–1396; July, 1958.

A mode of operation which is characterized by the use of the uniform precession in a ferrite as the idling magnetostatic mode was described. Although this mode is similar to Suhl's semistatic mode, it differs in that the biasing field is tuned to the difference between the pump and signal frequencies rather than to the pump frequency.

[6] A. D. Berk, L. Kleinman, and C. E. Nelson, "Modified semistatic ferrite amplifier," 1958 IRE WESCON Convention Record, pt. 3, pp. 9–12.

As an indication of the advances in the use of semiconductors, a back-biased germanium junction diode was used in a rectangular cavity which was resonant at 3500, 2300, and 1200 mc. Values of gain as high as 40 db were obtained at 1200 and 2300 mc with a pump frequency of 3500 mc. At 16-db gain, a noise figure of less than 4.8 db was observed.

[7] H. Heffner and K. Kotzebue, "Experimental characteristics of a microwave parametric amplifier using a semiconductor diode," Proc. IRE, vol. 46, p. 1301; June, 1958.

The following studies indicate that operation with lower-frequency pumping instead of with higher-frequency pumping is possible and that lower noise figures are to be achieved by this type of operation.

[8] S. Bloom and K. K. N. Chang, "Parametric amplification using low-frequency pumping," *J. Appl. Phys.*, vol. 29, p. 594; March, 1958.
[9] K. K. N. Chang and S. Bloom, "A parametric amplifier using lower-frequency pumping," Proc. IRE, vol. 46, pp. 1383–1386; July, 1958.
[10] K. K. N. Chang and S. Bloom, "A parametric amplifier using lower-frequency pumping," 1958 IRE WESCON Convention Record, pt. 3, pp. 23–27.
[11] C. L. Hogan, R. L. Jepsen, and P. H. Vartanian, "A new type of ferromagnetic amplifier," *J. Appl. Phys.*, vol. 29, pp. 422–423; March, 1958.
[12] G. F. Herrmann, M. Uenohara, and A. Uhlir, Jr., "Noise figure measurements on two types of variable reactance amplifiers using semiconductor diodes," Proc. IRE, vol. 46, pp. 1301–1303; June, 1958.

An analysis of the traveling-wave type of parametric amplifier which is based on a low-frequency model was made. The existence of a growing wave was demonstrated. The amplifying system consisted of two coupled transmission lines with time-dependent coupling. A theory was then developed for a structure which consisted of four parallel wires imbedded in a ferrite rod.

[13] P. K. Tien and H. Suhl, "A traveling-wave ferromagnetic amplifier," Proc. IRE, vol. 46, pp. 700–706; April, 1958.

A closely related study, which expands the general theory and cites applications to broad-band frequency converters, frequency channel selectors, wide-band amplifiers, tunable narrow-band amplifiers and oscillators, was described.

[14] P. K. Tien, "Parametric amplification and frequency mixing in propagating circuits," *J. Appl. Phys.*, vol. 29, pp. 1347–1357; September, 1958.

Somewhat pertinent to the study of traveling-wave parametric amplifiers is a discussion of the solution of Maxwell's equations for media in which the permittivity and permeability vary independently with time.

[15] F. R. Morgenthaler, "Velocity modulation of electromagnetic waves," IRE Trans. on Microwave Theory and Techniques, vol. MTT-6, pp. 167–172; April, 1958.

The results obtained with an experimental UHF traveling-wave parametric amplifier utilizing diffused-junction silicon diodes as nonlinear capacitors were summarized in the following paper. A noise figure of 3.5 db, a bandwidth of 10 to 20 mc, a forward gain of about 12 db for a signal frequency of 380 mc were reported.

[16] R. S. Engelbrecht, "A low-noise nonlinear reactance traveling-wave amplifier," Proc. IRE, vol. 46, p. 1655; September, 1958.

It was suggested early in 1958 that an electron beam be used instead of the ferrite to vary the reactance of a microwave cavity for parametric amplification. A tube for a signal frequency of 4130 mc, and a pump frequency of 8300 mc was constructed and tested. This amplifier was of the regenerative type utilizing the electronic reactance of a double-gap cavity to give parametric excitation. Results obtained were substantially as predicted.

[17] T. J. Bridges, "A parametric electron beam amplifier," Proc. IRE, vol. 46, pp. 494–495; February, 1958.

A distributed parametric amplifier, using an electron beam and deriving its power from a CW source equal to twice the operating frequency, was described. It was found that the normal space-charge waves in a drifting electron beam will convert to exponentially growing waves if one modulates the beam with a pumping frequency equal to twice the signal frequency. Either the fast or slow space-charge wave can be made to grow. Previous microwave amplifiers have amplified only the slow wave and theorems on minimum noise figure for slow-wave tubes are not valid for fast-wave amplifiers. Emphasis is placed on the fast wave.

[18] W. H. Louisell and C. F. Quate, "Parametric amplification of space charge waves," Proc. IRE, vol. 46, pp. 707–716; April, 1958.

An experimental fast-wave amplifier utilizing double-gap cavities as fast-wave couplers was proposed and built. A gain of 30 db was measured. A gain of 13 db per plasma wavelength for a pump frequency of 8400 mc and a signal frequency of 4200 mc was obtained by utilizing a demountable tube with a fixed input and pump cavities but movable signal pick-up cavity. It was also demonstrated that parametric amplification of space-charge waves is possible with the pump frequency lower than the signal frequency or with the pump frequency slightly different from twice the signal frequency.

[19] A. Ashkin, T. J. Bridges, W. H. Louisell, and C. F. Quate, "Parametric electron beam amplifiers," 1958 IRE WESCON Convention Record, pt. 3, pp. 13–22.
[20] A. Ashkin, "Parametric amplification of space charge waves," *J. Appl. Phys.*, vol. 29, pp. 1646–1651; December, 1958.

In principle fast-wave amplifiers should be less noisy than slow-wave amplifiers because noise cancellation is possible for the fast electron wave. A device was described which employs fast-wave interaction in its input and output sections and in which the amplitude of the transverse motion of the electrons is increased by parametric amplification between its input and output sections. It was reported that a gain of 20 db was easy to obtain with a few milliwatts of pump power and that a noise figure of 1.3 db was measured.

[21] R. Adler, "Parametric amplification of the fast electron wave," Proc. IRE, vol. 46, pp. 1300–1301; June, 1958.
[22] R. Adler, G. Hrbek, and G. Wade, "A low-noise electron-beam parametric amplifier," Proc. IRE, vol. 46, pp. 1756–1757; October, 1958.

Chu's kinetic power theorem which provided the key to the solution of noise problems in conventional longitudinal beam amplifiers was not general enough to apply to the parametric beam amplifier. This power theorem was generalized to apply to parametric beam amplifiers.

[23] H. A. Haus, "The kinetic power theorem for parametric, longitudinal, electron-beam amplifiers," IRE Trans. on Electron Devices, vol. ED-5, pp. 225–232; October, 1958.

An interesting development which may well include the parametric effects in electron beams was that of the utilization of a high-level pumping signal to extend the frequency range of amplification in a traveling-wave tube. The small signal gain of an S-band tube operating at L band was increased by 33 db by adding a saturating S-band signal to the input of the tube.

[24] L. D. Buchmiller and G. Wade, "Pumping to extend traveling-wave-tube frequency range," Proc. IRE, vol. 46, pp. 1420–1421; July, 1958.

Nonlinear Devices

The need for extending the frequency range, in which the detection sensitivity is good, and for improving nonlinear capacitors for parametric amplifiers has had considerable influence in the study of methods of improving solid-state diodes. The upper frequency limit of operation of semiconductor diodes is being increased; the Q, decreased; new materials are being used; new design techniques are being developed; and an appreciation of their potential fields of usefulness is developing. The following papers are representative of those which treated some aspect of solid-state diodes.

[25] A. Uhlir, "The potential of semiconductor diodes in high-frequency communications," Proc. IRE, vol. 46, pp. 1099–1155; June, 1958.
[26] G. C. Messenger, "New concepts in microwave mixer diodes," Proc. IRE, vol. 46, pp. 1116–1121; June, 1958.
[27] C. T. McCoy, "Present and future capabilities of microwave crystal receivers," Proc. IRE, vol. 46, pp. 61–66; January, 1958.
[28] D. A. Jenny, "A gallium arsenide microwave diode," Proc. IRE, vol. 46, pp. 717–722; April, 1958.
[29] L. K. Anderson and A. Hendry, "An investigation of the properties of germanium mixer crystals at low temperatures," IRE Trans. on Microwave Theory and Techniques, vol. MTT-6, pp. 393–398; October, 1958.
[30] S. M. Bergmann, "One aspect of minimum noise figure microwave mixer design," IRE Trans. on Microwave Theory and Techniques, vol. MTT-6, pp. 324–326; July, 1958.
[31] S. Kita, "A harmonic generator by use of nonlinear capacitance of germanium diode," Proc. IRE, vol. 46, p. 1307; June, 1958.
[32] K. K. N. Chang, "Harmonic generation with non-linear reactances," *RCA Rev.*, vol. 19, pp. 455–464; September, 1958.
[33] J. L. Moll, A. Uhlir, Jr. and B. Senitzky, "Microwave transients from avalanching silicon diodes," Proc. IRE, vol. 46, pp. 1306–1307; June, 1958.
[34] W. T. Read, Jr., "A proposed high-frequency, negative-resistance diode," *Bell. Sys. Tech. J.*, vol. 37, pp. 401–446; March, 1958.

The use of the nonlinear characteristics of ferrites and similar materials for detection, harmonic generation, frequency conversion and related functions, has continued. The following papers are indicative of experimental investigations in this area.

[35] D. Jaffe, J. C. Cacheris and N. Karayianis, "Ferrite microwave detector," Proc. IRE, vol. 46, pp. 594–601; March, 1958.
[36] E. N. Skomal and M. A. Medina, "Microwave frequency conversion studies in magnetized ferrites," *J. Appl. Phys.*, vol. 29, pp. 423–424; March, 1958.

Masers

The utilization of direct interaction of microwave fields with the molecules in uncharged matter has received much study during this year. Emphasis has been placed on the three-level solid-state maser rather than the ammonia-beam type. New paramagnetic materials such as cobalticyanide, ruby, and yttrium-iron garnet have been introduced, and traveling-wave propagating structures have been used instead of cavities. Methods of increasing gain and bandwidth and of decreasing the lower limit on operating frequency have been sought. A unidirectional quantum-mechanical amplifier which affords a natural isolation of output and input without the use of isolators or circulators was described, and the results of gain and noise measurement were recorded. The amplifying medium consisted of a prestimulated beam of ammonia molecules which was first passed through a state selector where only the excited or upper state molecules were retained. The beam was then passed, in turn, through two cavities which were resonant at the same frequency (23.87 kmc). Beyond-cut-off-waveguide sections were used to prevent RF leakage at the beam entrance and exit points and between the cavities.

[37] N. Sher, "A two-cavity unilateral maser amplifier," 1958 IRE National Convention Record, pt. 1, pp. 27–35.

In another study of two cavity masers a method which involves a geometrical representation of the Schroedinger equation was found especially useful in finding the approximate behavior of a complicated maser system. The theory of an experimental observation by Higa was developed. In this experiment the two cavities were tuned to the molecular frequency under such conditions that each maintained oscillations without the other. The first cavity, A, through which the beam passed, was then detuned. Oscillations in the second cavity, B, were observed to follow the frequency of A up to the critical point, a few kilocycles from the molecular frequency. Without further detuning of A, cavity B began to oscillate simultaneously at the molecular frequency to which it was tuned and at the frequency of A.

[38] W. H. Wells, "Maser oscillator with one beam through two cavities," *J. Appl. Phys.*, vol. 29, pp. 714–717; April, 1958.

The results of a theoretical analysis of the respective merits of reflection-type and transmission-type cavities for use in maser amplifiers were reported. Consideration was given to noise temperature, bandwidth, and gain modulation characteristics. The reflection type of maser was shown to be superior in most respects to the transmission type. However, they are limited by the isolation obtainable from available circulators. A figure of merit for both types was included.

[39] M. L. Stich, "Maser amplifier characteristics for transmission and reflection cavities," *J. Appl. Phys.*, vol. 29, pp. 782–789; May, 1958.

The three-level, solid-state maser has received considerable study during the past year. The theoretical principles of operation were discussed; the relevant physical properties of paramagnetic salts were elucidated, and a 6-kmc maser using lanthanum ethylsulphate crystals containing one-half per cent cerium was described in the following paper.

[40] H. E. D. Scovil, "The three-level solid-state maser," IRE Trans. on Microwave Theory and Techniques, vol. MTT-6, pp. 29–38; January, 1958.

In this investigation a gain of 20 db with a bandwidth of approximately 100 kc and an effective noise temperature of about 150°K were obtained experimentally. The stability margin was small. Both bandwidth and stability, it was claimed, could be improved if an appropriate unidirectional slow-wave structure were employed.

Solid-state masers using potassium cobalticyanide with one-half per cent chromicyanide as the paramag-

netic salt received appreciable attention. This material is considered to be well-suited for maser application because it has a long spin-lattice relaxation time; a value of 0.2 seconds at 1.25°K was reported. This salt was used in cavities with dual resonant frequencies to obtain S-band and L-band amplification and oscillation.

[41] A. L. McWhorter and J. W. Meyer, "Solid-state maser amplifier," *Phys. Rev.*, vol. 109, pp. 312–318; January 15, 1958.
[42] A. L. McWhorter and F. R. Arams, "System-noise measurement of a solid-state maser," PROC. IRE, vol. 46, pp. 913–914; May, 1958.
[43] J. O. Artman, N. Bloembergen, and S. Shapiro, "Operation of a three-level solid-state maser at 21 cm," *Phys. Rev.*, vol. 109, pp. 1392–1393; February 15, 1958.
[44] S. H. Autler and N. McAvoy, "21-centimeter solid-state maser," *Phys. Rev.*, vol. 110, pp. 280–281; April 1, 1958.

A UHF maser which had two separate resonant structures instead of the usual one was described. A cavity, which was resonant at the pumping frequency, and a lumped circuit, which was resonant at the amplifying frequency, were used. The paramagnetic material was potassium cobalticyanide.

[45] R. H. Kingston, "A UHF solid-state maser," PROC. IRE, vol. 46, p. 916; May, 1958.

To prevent noise from being fed back into the resonant cavities, ferrite circulators have been widely used. For lower microwave frequencies, such as 300 mc and 1380 mc, satisfactory circulators were not available. To eliminate the circulator, a system involving two matched masers coupled to the side arms of a magic T was proposed.

[46] S. H. Autler, "Proposal for a maser-amplifier system without nonreciprocal elements," PROC. IRE, vol. 46, pp. 1880–1881; November, 1958.

The application of three-level solid-state masers is hindered by the limited number of suitable paramagnetic materials, and by the requirement for pumping signal powers at frequencies above the signal frequency. Therefore the two-level solid-state maser, even though basically intermittent in operation instead of continuous as is the three-level one, was carefully examined for possible modes of continuous operation. In principle, it was concluded that a continuous two-level maser which would have some advantage over the three-level maser was possible using paramagnetic materials and the principle of nonadiabatic field reversal.

[47] D. I. Bolef and P. F. Chester, "Some techniques of microwave generation and amplification using electron spin states in solids," IRE TRANS. ON MICROWAVE THEORY AND TECHNIQUES, vol. MTT-6, pp. 47–52; January, 1958.

In another paper on two-level solid-state masers, an analysis of the emission from a matched cavity at paramagnetic resonance was given.

[48] H. H. Theissing, F. A. Dieter, and P. J. Caplan, "Analysis of the emissive phase of a pulsed maser," *J. Appl. Phys.*, vol. 29, 1673–1678; December, 1958.

Cavity-type masers are quite limited in bandwidth and gain. Greatly improved performance was obtained by using a slow-wave propagation structure instead of a cavity; wider amplifying bandwidth, high gain, and unidirectional amplification resulted. As representative of the results obtained, a ruby traveling-wave maser gave a net gain of 23 db, a bandwidth of 25 mc, and a tuning range of 350 mc centered about 5900 mc.

[49] R. W. DeGrasse, "Slow-wave structures for unilateral solid-state maser amplifiers," 1958 IRE WESCON CONVENTION RECORD, pt. 3, pp. 29–35.

Noise in maser amplifiers was the object of considerable study. One study resulted in a theoretical treatment and experimental data on the noise of an ammonia-beam maser. An equivalent circuit was developed, and expressions for the gain and effective noise input temperature were derived for both transmission and reflection types of masers.

[50] J. P. Gordon and L. D. White, "Noise in maser amplifiers—theory and experiment," PROC. IRE, vol. 46, pp. 1588–1594; September, 1958.
[51] J. C. Helmer and M. W. Muller, "Calculation and measurement of the noise figure of a maser amplifier," IRE TRANS. ON MICROWAVE THEORY AND TECHNIQUES, vol. MTT-6, pp. 210–214; April, 1958.
[52] F. R. Arams and G. Krayer, "Design considerations for circulator maser systems," PROC. IRE, vol. 46, pp. 912–913; May, 1958.

In another endeavor to find paramagnetic materials suitable for masers, the spin properties of ruby (Al_2O_3:Cr) were investigated. Using the regenerative cavity system, K- and X-band absorption lines characteristic of the ruby were observed; no interaction between the two bands was detected. Net gain as high as 20 db was observed at 9300 mc for a pumping frequency of 24,000 mc.

[53] G. Makhov, C. Kikuchi, J. Lambe, R. W. Terhune, "Maser action in ruby," *Phys. Rev.*, vol. 109, pp. 1399–1400; February 15, 1958.

The spin-lattice relaxation time of yttrium-ion garnet was measured and found to be 7×10^{-8} second. The ferromagnetic resonance line width was 2.3 oersteds at 9300 mc, reportedly the narrowest line width of any known ferromagnetic material. Low-frequency resonances at frequencies as low as 44 mc, for an applied field of 1000 oersteds, was observed in another investigation.

[54] R. C. LeCraw, E. G. Spencer, and C. S. Porter, "Ferromagnetic resonance and nonlinear effects in yttrium iron garnet," *J. Appl. Phys.*, vol. 29, pp. 326–327; March, 1958.
[55] E. G. Spencer, and R. C. LeCraw, C. S. Porter, "Ferromagnetic resonance in yttrium garnet at low frequencies," *J. Appl. Phys.*, vol. 29, pp. 429–430; March, 1958.

Traveling-wave Tubes

Taveling-wave tubes operate over a wide band of frequencies and provide appreciable gain. These characteristics are desirable ones for application in systems requiring frequency diversification. The use of heavy, power-thirsty electromagnets for focusing the electron beam has been the greatest factor limiting their application. Other factors include the need for precise alignment of the focusing structure, the large size, the fragility, and the cost. The size and weight were considerably reduced by the use of convergent flow shielded electron guns and by the imposition of proper relationships upon beam diameter, beam current, and magnetic

field to produce a balance between the magnetic force on the electrons and the forces due to space-charge and centrifugal acceleration. Periodic-permanent-magnet focusing was then developed to obtain further reductions. The need for accurate alignment of the focusing structure with the axis of the tube remained. To achieve further reductions in size and weight and the elimination of the alignment problem, studies of periodic electrostatic focusing were initiated. These means of focusing are still being studied.

A new traveling-wave tube, called the Estiatron, was announced. Instead of one helix, this tube utilizes two helices which are interwound in a bifilar manner, imbedded in the glass envelope, and operated at different potentials to produce periodic electrostatic focusing of the electron beam. A continuous-wave output in excess of 9 watts over the frequency range from 2000 to 3000 mc and a maximum gain of 25 db were reported. The weight of the tube was less than 1 pound.

[56] D. Blattner and F. Vaccaro, "The Estiatron—an electrostatically focused medium-power traveling-wave tube," 1958 IRE National Convention Record, pt. 3, pp. 101–105.

A new traveling-wave tube which utilizes an annular gun and a pair of concentric bifilar helices in a biperiodic electrostatic focusing system was also described. An experimental tube had a gain of 10 db at a power level of 100 milliwatts at a frequency of 2970 mc.

[57] K. K. N. Chang, "An electrostatically focused traveling-wave-tube amplifier," *RCA Rev.*, vol. 19, pp. 86–97; March, 1958.

A new type of voltage-tuned microwave oscillator, called the Helitron, was described. It employs an electron beam which travels in a helical path around a four-conductor transmission line. The beam interacts on a radial and angular basis with a TEM wave on the line in such a way as to lose potential energy to the wave. The interaction is similar to that in an M-type traveling-wave tube. Electron focusing is accomplished by balancing centrifugal force against a radial electric-field force; no focusing magnets are required. Continuous voltage tuning over the frequency range from 1200 to 2400 mc with a change in tuning voltage from 650 to 1700 volts and power output between 1 and 10 milliwatts were reported.

[58] D. A. Watkins and G. Wada, "The helitron oscillator," Proc. IRE, vol. 46, pp. 1700–1705; October, 1958.

Design considerations for traveling-wave tubes for use in airborne equipment were surveyed and examples of current tubes with desirable characteristics were given.

[59] M. Nowogrodzki, "Design of traveling-wave tubes for airborne applications," 1958 IRE WESCON Convention Record, pt. 3, pp. 66–71.

Factors affecting the design of a high-power traveling-wave tube using periodic magnetic focusing were described in another paper. The design considerations, construction, and performance were given for an S-band tube which yielded a saturated power gain of 30 db, a 3-db bandwidth of 2200–4000 mc, a mid-band peak power of about 2 kw, good reproducibility characteristics, and a weight of about 17 pounds.

[60] O. T. Purl, J. R. Anderson, and G. R. Brewer, "A high-power periodically focused traveling-wave tube," Proc. IRE, vol. 46, pp. 441–448; February, 1958.

Another study of periodic magnetic focusing structures yielded charts to facilitate the design of periodic permanent magnets for focusing electron beams in tubes with parallel-flow guns.

[61] J. E. Sterrett and H. Heffner. "The design of periodic magnetic focusing structures," IRE Trans. on Electron Devices, vol. ED-5, pp. 35–42; January, 1958.

Formulas and graphs which describe the distribution of leakage flux around a tubular permanent magnet were also discussed.

[62] M. S. Glass, "Distribution of leakage flux around a TWT-tron focusing magnet—a graphic analysis," Proc. IRE, vol. 46, pp. 1751–1756; October, 1958.

There is a growing need for permanent magnets of higher coercive force for focusing of electron beams. An appraisal of such materials and some design techniques which enable the use of materials with relatively low remanence for compact tubular magnets for strong focusing fields were given.

[63] M. S. Glass, "Appraisal of permanent magnet materials for magnetic focusing of electron beams," *J. Appl. Phys.*, vol. 29, pp. 403–404; March, 1958.

Periodic electrostatic focusing of a hollow electron beam was studied in an attempt to obtain useful design information. The system studied was one in which combined uniform radial electric and periodic radial and longitudinal electric fields were used to focus the hollow beam. The beam was confined between an inner cylinder and a concentric outer series of focusing rings whose potentials were alternated.

[64] C. C. Johnson, "Periodic electrostatic focusing of hollow electron beam," IRE Trans. on Electron Devices, vol. ED-5, pp. 233–243; October, 1958.

The practical realization of improved signal-to-noise ratios in traveling-wave tubes stimulate considerable activity. Improvements in design and techniques which have lowered the noise figure of a developmental traveling-wave tube from 9 db to 6 db and which have resulted in noise figures as low as 4.8 db in selected tubes were discussed. The most important factor contributing to the smaller noise figure was claimed to be a smooth and highly-emissive dense-oxide cathode operating at about 600°C.

[65] E. W. Kinaman and M. Magid, "Very low-noise traveling-wave amplifier," Proc. IRE, vol. 55, pp. 861–867; May, 1958.

A study has shown that backward-wave tubes are capable of very low noise figures and experimental S-band tubes with special low-noise guns have yielded noise figures of less than 4.5 db for a 25 per cent tuning range.

[66] M. R. Currie and D. C. Forster, "Low noise tunable preamplifiers for microwave receivers," Proc. IRE, vol. 46, pp. 570–579; March, 1958.

Measured noise figures in the vicinity of 3.5 db were reported for backward-wave tubes. Features of the low-noise gun are that emission originated predominately from the edge and side of the cathode and that the potential profile in the cathode region departed drastically from the usual approximate Fry-Langmuir distribution.

[67] M. R. Currie, "A new type of low-noise electron gun for microwave tubes," PROC. IRE, vol. 46, p. 911; May, 1958.

In another experiment it was demonstrated that the nature of the potential profile in the vicinity of the cathode is the important factor in achieving a low-noise electron gun. Tests on a conventional low-noise traveling-wave tube which had the usual circular-disk type of emitting surface, but the new potential profile also yielded noise figures as low as 3.5 db.

[68] M. Caulton and G. E. St. John, "S-band traveling-wave tube with noise figure below 4 db," PROC. IRE, vol. 46, pp. 911–912; May, 1958.

The minimum noise-power output of traveling-wave tubes is a unique function of the noise pattern in the electron beam. Achievement of minimum noise-power output involves optimizing the standing-wave ratio and position in the vicinity of the potential minimum. Calculations of optimum noise parameters for common types of backward wave tubes were presented along with a discussion of noise reduction as the pass bands of these tubes are tuned in frequency.

[69] M. R. Currie and D. C. Forster, "Conditions for minimum noise generation in backward-wave amplifiers," IRE TRANS. ON ELECTRON DEVICES, vol. ED-5, pp. 88–98; April, 1958.

In a study of the noise characteristics of a backward-wave oscillator, it was shown that a backward-wave oscillator is representable as a CW generator in which both amplitude and frequency are simultaneously modulated by noise in a partially correlated manner. It was also demonstrated that there is a rough correspondence between the regions of high slope of the power and frequency vs beam current curves and the regions of high AM and FM noise. The noise modulation was found to be influenced principally by variations in the beam and magnet currents.

[70] J. B. Cicchetti and J. Munushian, "Noise characteristics of a backward-wave oscillator," 1958 IRE NATIONAL CONVENTION RECORD, pt. 3, pp. 84–100.

Other papers of interest on noise in traveling-wave tubes include the following:

[71] R. C. Knechtli, "Effect of electron lenses on beam noise," IRE TRANS. ON ELECTRON DEVICES, vol. ED-5, pp. 84–88; April, 1958.
[72] R. P. Little, H. M. Ruppel, and S. T. Smith, "Beam noise in crossed electric and magnetic fields," *J. Appl. Phys.*, vol. 29, pp. 1376–1377; September, 1958.
[73] S. Saito, "New method of measuring the noise parameters of an electron beam," IRE TRANS. ON ELECTRON DEVICES, vol. ED-5, pp. 264–275; October, 1958.

There was considerable study directed towards improving the power output and efficiency of traveling-wave tubes. A general design procedure for high-efficiency, large-signal amplifiers involving design curves was described. The procedure facilitates the design of tubes with near-maximum power output and efficiency at any frequency range. The chief limiting assumption is that the electric field is constant across the stream radius.

[74] J. E. Rowe and H. Sobol, "General design procedure for high-efficiency traveling-wave amplifiers," IRE TRANS. ON ELECTRON DEVICES, vol. ED-5, pp. 288–300; October, 1958.

The improvement of traveling-wave-tube efficiency by adjustment of collector potential was studied. By using single-stage and double-stage collectors which can be operated at depressed potentials, over-all efficiencies of 46 and 57 per cent respectively, were obtained.

[75] F. Sterzer, "Improvement of traveling-wave tube efficiency through collector potential depression," IRE TRANS. ON ELECTRON DEVICES. vol. ED-5, pp. 300–305; October, 1958.

In a related paper it was shown that it is necessary to inhibit secondary electron emission to achieve higher efficiency by reduction of collector potential. The application of this and other results increased collector efficiency to about 35 per cent.

[76] H. J. Wolkenstein, "Effect of collector potential on the efficiency of traveling-wave tubes," *RCA Rev.*, vol. 19, pp. 259–282; June, 1958.

In achieving high-power traveling-wave tubes, loaded waveguide circuits are of particular interest. The interaction of an electron beam with a chain of coupled resonators was studied. Other topics considered were impedance matching, frequency dependence of the gain, and the transition from backward-wave oscillation to forward-wave oscillation as the operating voltage is varied.

[77] R. W. Gould, "Characteristics of traveling-wave tubes with periodic circuits," IRE TRANS. ON ELECTRON DEVICES, vol. ED-5, pp. 186–195; July, 1958.
[78] E. Belohoubek, "Propagation characteristics of slow-wave structures derived from coupled resonators," *RCA Rev.*, vol. 19, pp. 283–310; June, 1958.

Attempts to extend the tuning range and the upper limit of operating frequency of traveling-wave tubes have continued. The feasibility of obtaining voltage-tunable backward-wave oscillators having useful power output over very wide frequency ranges at millimeter wavelengths was demonstrated. The possibility of obtaining useful powers at frequencies as high as 150,000 mc was indicated.

[79] D. J. Blattner and F. Sterzer, "Two backward-wave oscillator tubes for the 29,000 to 74,000 megacycle frequency range," *RCA Rev.*, vol. 19, pp. 584–597; December, 1958.
[80] R. W. Grow, D. A. Dunn, J. W. McLaughlin, and R. P. Lagerstrom, "A 20 to 40-KMC backward-wave oscillator," IRE TRANS. ON ELECTRON DEVICES, vol. ED-5, pp. 152–156; July, 1958.

As the frequency of operation of conventional low-voltage helix-type backward-wave oscillators is decreased, a rapid rise in starting current has been observed. Theory indicates that the low-frequency end of the tuning range can be extended by creating the proper velocity distribution across the electron beam. The high-frequency end of the tuning range of such an oscillator is usually limited by the crossover of the forward- and backward-wave interactions. The upper end is controlled

by such factors as tube dimensions and dielectric loading of the helix. The design, construction, and experimental results on modified conventional L- and S-band oscillators were given. Significant extensions of tuning range resulted.

[81] L. Maninger, "A low voltage helix type backward wave oscillator with extended tuning range," 1958 IRE WESCON Convention Record, pt. 3, pp. 42–54.

Electron beam and circuit interaction phenomena, including such topics as thermal velocity effects, beam dynamics, current and charge distributions, spurious oscillations, efficiency of conversion, and power output were studied extensively. These studies are applicable to most types of microwave tubes and are not limited to traveling wave tube designs.

[82] G. Herrmann, "Optical theory of thermal velocity effects in cylindrical electron beams," *J. Appl. Phys.*, vol. 29, pp. 127–136; February, 1958.
[83] A. Szabo, "Thermal velocity effects in magnetically confined beams," IRE Trans. on Electron Devices. vol. ED-5, pp. 183–185; July, 1958.
[84] A. Ashkin, "Dynamics of electron beams from magnetically shielded guns," *J. Appl. Phys.*, vol. 29, pp. 1594–1604; November, 1958.
[85] M. Chodorow, H. J. Shaw, and D. A. Winslow, "Current distribution in modulated magnetically focussed electron beams," *J. Appl. Phys.*, vol. 29, pp. 1525–1533; November, 1958.
[86] J. W. Gewartowski, "Velocity and current distributions in the spent beam of the backward-wave oscillator," IRE Trans. on Electron Devices, vol. ED-5, pp. 215–222; October, 1958.
[87] T. T. Kirstein and G. S. Kino, "Solutions to the equations of space-charge flow by the method of the separation of variables," *J. Appl. Phys.*, vol. 29, pp. 1758–1767; December, 1958.
[88] I. P. Shkarofsky, "A symmetry property of space-charge waves in accelerated electron beams," IRE Trans. on Electron Devices, vol. ED-5, pp. 283–288; October, 1958.
[89] M. Chodorow and C. Susskind, "Space-charge-balanced hollow beam with uniform charge distribution," Proc. IRE, vol. 46, pp. 497–498; February, 1958.
[90] H. G. Kosmahl, "Influence of magnetic focusing fields and transverse electron motion on starting conditions for spurious oscillations in O-type backward-wave oscillators," IRE Trans. on Electron Devices, vol. ED-5, pp. 252–257; October, 1958.
[91] W. E. Waters, "Rippling of thin electron ribbons," *J. Appl. Phys.*, vol. 29, pp. 100–104; January, 1958.
[92] W. W. Rigrod, "Space-charge waves along magnetically-focused electron beams," Proc. IRE, vol. 46, pp. 358–359; January, 1958.
[93] D. V. Geppert, "Analysis of traveling-wave tubes with tapered velocity parameter," Proc. IRE, vol. 46, p. 1658; September, 1958.
[94] W. H. Louisell, "Approximate analytic expressions for TWT propagation constants," IRE Trans. on Electron Devices, vol. ED-5, pp. 257–259; October, 1958.
[95] A. Kiel, M. Scotto, and P. Parzen, "Propagation in a crossed field periodic structure," IRE Trans. on Electron Devices, vol. ED-5, pp. 76–84; April, 1958.
[96] A. Yariv, "On the coupling coefficients in the coupled-mode theory," Proc. IRE, vol. 46, pp. 1956–1957; December, 1958.

Klystrons

The great practical importance of klystrons continues to provide considerable motivation for improving their performance and for gaining a better understanding of their potential. Higher operating frequencies, wider operating bandwidths, higher efficiencies, greater power outputs, and lower noise levels are representative of the areas in which studies have been made.

Much of the work listed under other headings in this review might well have been listed under this heading; examples include studies of electron guns, beam and circuit interaction, and noise. Of course the resemblance between a traveling-wave tube with periodic circuits and a klystron is very great. If the resonator coupling coefficient is small, and the ratio of the power flowing along the slow-wave circuit to the power dissipated in a resonator is much less than unity, the traveling-wave device becomes a klystron. The results of an analysis of traveling-wave amplifiers were extended to klystron amplifiers in the following paper.

[97] R. W. Gould, "Characteristics of traveling-wave tubes with periodic circuits," IRE Trans. on Electron Devices, vol. ED-5, pp. 186–195; July, 1958.

Klystrons are usually considered to be inherently noisy with noise figures of the order to 25 to 40 db. Actually low-noise amplifiers can be built. A klystron amplifier with a noise figure of 6.7 db was reported. It was found that to achieve low-noise operation much higher beam currents were required than for low-noise traveling-wave tubes. The greater dynamic range of klystrons as compared with traveling-wave tubes and parametric amplifiers was also emphasized.

[98] R. G. Rockwell, "Are klystron amplifiers inherently noisy?" 1958 IRE WESCON Convention Record, pt. 3, pp. 55–59.

An investigation of millimeter-wave klystron power amplifiers demonstated that it is possible to obtain CW powers of at least 75 watts in the 8-mm wave band. Cathode emission densities of 1.5 amperes per square centimeter in an electron gun with a density multiplication of 100 was required.

[99] T. J. Bridges and H. J. Curnow, "Experimental 8-mm klystron power amplifiers," Proc. IRE, vol. 46, pp. 430–432; February, 1958.

Another investigation of millimeter-wave klystrons was concerned with double-cavity designs for the ranges, 4.3 to 5.2 mm, 5.0 to 6.4 mm, and 5.8 to 6.8 mm. All three were operated at 800 volts or less. An output of 175 mw at a wavelength of 6.0 mm was reported. An X-band design which gave 20 mw output for an operating voltage of 200 volts was described in the same paper.

[100] C. J. Carter and W. H. Cornetet, Jr., "Low voltage operation of the retarding-field oscillator at X band and in the millimeter wavelength region," IRE Trans. on Electron Devices, vol. ED-5, pp. 139–143; July, 1958.

Bunching in two-cavity and multicavity klystrons in the presence of space charge was studied. Computed results were synthesized to provide a qualitative picture of the manner in which bunching velocity spread and circuit efficiency contribute to the efficiency of energy conversion at the output gap.

[101] S. E. Webber, "Ballistic analysis of a two-cavity finite beam klystron," IRE Trans. on Electron Devices, vol. ED-5, pp. 98–108; April, 1958.
[102] S. E. Webber, "Large signal analysis of the multicavity klystron," IRE Trans. on Electron Devices, vol. ED-5, pp. 306–315; October, 1958.

The successful operation of a reflex klystron as a narrow-band regenerative parametric amplifier at 11,000 mc was reported. The performance was pre-

dicted quite accurately from simple theory. A circulator was used to separate input from output.

[103] C. F. Quate, R. Kompfner, and D. A. Chisholm, "The reflex klystron as a negative resistance type amplifier," IRE Trans. on Electron Devices, vol. ED-5, pp. 173–179; July, 1958.

General formulas for calculating the equivalent circuit constants of reentrant cavities were derived using the theory of Green's function. A very impressive number of resonant cavity dimensions were given for a number of resonant frequencies.

[104] K. Fujisawa, "General treatment of klystron resonant cavities," IRE Trans. on Microwave Theory and Techniques, vol. MTT-6, pp. 344–358; October, 1958.

A 10-kw six-cavity klystron was described. By the use of double-tuned coupled circuits at the gaps of the cavities it was possible to obtain a 3-db band-width of 20 mc at the frequency of 840 mc.

[105] H. Goldman, L. F. Gray, and L. Pollack, "Wideband uh-klystron amplifier," 1958 IRE National Convention Record, pt. 3, pp. 114–123.

A brief, but helpful, discussion was presented of the conditions under which broad-band operation of multi-cavity klystrons is profitable.

[106] S. V. Yadavalli, "Effect of beam coupling coefficient on broad band operation of multi-cavity klystrons," Proc. IRE, vol. 46, pp. 1957–1958; December, 1958.

At present little data are available on the velocity spread and the current distribution for practical klystron beams. If such data were known, it is possible to determine their effect on the fundamental component of the beam current by a method reported in the following paper:

[107] L. A. Harris, "The effect of an initial velocity spread on klystron performance," IRE Trans. on Electron Devices, vol. ED-5, pp. 157–160; July, 1958.

Instead of the usual bunching theory of an electron beam in transit through an accelerating aperture of such velocity modulation devices as klystrons, another theory which is based upon a potential-well model was presented. An expression for the radiated power resulting from the acceleration of the electrons was developed from this model.

[108] L. Gold, "Potential well theory of velocity modulation," Proc. IRE, vol. 46, p. 1952; December, 1958.

The generation of second harmonic in a velocity-modulated beam of a klystron was analyzed. The analysis gave results which were consistent with the experimental observations that the second harmonic current is not a periodic function of distance; that the maxima of the second harmonic current are closer to the input cavity than are the corresponding maxima of the fundamental; and that the second harmonic current grows with distance for thin beams.

[109] F. Pasche, "Generation of second harmonic in a velocity-modulated electron beam of finite diameter," *RCA Rev.*, vol. 19, pp. 617–627; December, 1958.

Barkhausen-Kurz oscillators *per se* have received very little attention during recent years. The necessity for an accelerating grid mesh has hindered commercial development. The Osaka tube in which the grid mesh is replaced by the interaction gap of a resonant cavity has resulted in an efficient oscillator. A magnetically-focused Barkhausen-Kurz oscillator which is an improved version of the Osaka tube for operation at centimeter or millimeter wavelengths received attention. At K-band, 430 mw of power, and an efficiency of 12.2 per cent were reported. The results give promise that a high-power tube with high efficiency may be possible.

[110] E. M. Boone, M. Uenohara, and D. T. Davis, "A Barkhausen-Kurz oscillator at centimeter wavelengths," IRE Trans. on Electron Devices, vol. ED-5, pp. 196–205; July, 1958.

The need for pulsed signals with minimum possible sideband energy in air navigation systems resulted in a method of generation in which the anode of a klystron final amplifier is modulated by a special modulating circuit.

[111] D. H. Preist, "The generation of shaped pulses using microwave klystrons," 1958 IRE National Convention Record, pt. 3, pp. 106–113.

The problem of generation of appreciable amounts of power at millimeter and submillimeter wavelengths is one of the most difficult and challenging problems facing designers of energy sources. Several new types of coupling structures for extracting energy from a megavolt electron beam at a harmonic of the frequency used to modulate the beam were described. Emphasis was placed on the use of dielectric-tubes as coupling structures and Cerenkov radiations.

[112] R. H. Pantell, P. D. Coleman, and R. C. Becker, "Dielectric slow-wave structures for the generation of power at millimeter and submillimeter wavelengths," IRE Trans. on Electron Devices, vol. ED-5, pp. 167–173; July, 1958.

Transmission Lines

The accepted definition of transmission lines encompasses ordinary transmission lines, closed waveguides, and surface-wave structures. The large amount of literature on transmission lines containing anisotropic media has led to the division of the references in this section into those in which isotropy prevails and those in which anisotropy plays a dominant role. Isotropic lines are reviewed first.

TEM Lines

The broad bandwidth characteristics and mechanical simplicity of various types of strip and planar lines continue to stimulate the development of components for such lines, and the study of methods of improving their characteristics. Specialized aspects of coaxial lines were also studied.

The field configuration in a duo-dielectric parallel-plane waveguide was discussed qualitatively in an effort to clarify a point of confusion associated with the field configuration for a particular mode in a coaxial line which was filled throughout 180° of arc with a low-loss material of high dielectric constant. A more exact analysis of the parallel-plane guide yielded results

which partially contradict the field structure previously described.

[113] B. J. Duncan, L. Swern, K. Tomiyasu, "Microwave magnetic field in dielectric loaded coaxial line," PROC. IRE, vol. 46, pp. 500–502; February, 1958.
[114] M. Cohn, "Parallel plane waveguide partially filled with a dielectric," PROC. IRE, vol. 46, pp. 1952–1953; December, 1958.

The same structure and a double-slab version were studied for application at millimeter wavelengths. For this application, the important mode is one in which the E field is parallel to the walls. Low attenuation was observed. The use of laminated dielectrics was suggested.

[115] F. J. Tischer, "Properties of the H-guide at microwaves and millimeter waves," 1958 IRE WESCON CONVENTION RECORD, pt. 1, pp. 4–12.

Other structures which were investigated are the shielded balanced pair, the double-slotted coaxial line, and the slab line. The shielded balanced pair was studied experimentally over a range of variables to evaluate the relative merit of each of three different formulas for the capacitance. The use of the simplest of these formulas was recommended.

[116] B. G. King, J. McKenna, and G. Raisbeck, "Experimental check of formulas for capacitance of shielded balanced-pair transmission line," PROC. IRE, vol. 46, pp. 922–923; May, 1958.

The double-slotted coaxial lines can support two types of TEM waves; approximate formulas for the characteristic impedance for each type of wave were derived by a conformal mapping method.

[117] J. Smolarska, "Characteristic impedances of the less slotted coaxial line," IRE TRANS. ON MICROWAVE THEORY AND TECHNIQUES, vol. MTT-6, pp. 161–166; April, 1958.

Slab lines, consisting of a circular inner conductor between two parallel planes, were studied to determine the breakdown conditions. The power handling capacity was found to be on the order of 60 to 96 per cent of an equivalent coaxial line.

[118] G. M. Badoyannis, "The power handling capacity of slab lines," 1958 IRE WESCON CONVENTION RECORD, pt. 1, pp. 35–38.

Further advances were reported in the use of nonuniform transmission lines as broad-band terminations. It was shown that if the fractional change in shunt admittance was maintained constant, a fixed length of line can lead to an arbitrarily large effective length without destroying the match at the input. The analysis was applied to the problem of broad-band terminations.

[119] I. Jacobs, "The nonuniform transmission line as a broadband termination," *Bell Sys. Tech. J.*, vol. 37, pp. 913–924; July, 1958.

The design of monotonic stepped transmission-line transformers for prescribed reflection coefficients and bandwidth ratio was studied. A design method was evolved which for a specified number of steps provides the maximum possible bandwidth for a specified reflection coefficient, or the minimum possible reflection coefficient for a given bandwidth.

[120] L. Solymar, "Some notes on the optimum design of stepped transmission-line transformers," IRE TRANS. ON MICROWAVE THEORY AND TECHNIQUES, vol. MTT-6, pp. 373–378; October, 1958.

The inherent wide bandwidth of TEM lines was utilized for the design of broad-band baluns. A balun with ferrite loading to obtain high permeability was analyzed and constructed. The insertion loss fluctuated between 1 and 2 db over the frequency range of 5 to 1000 mc. Another design, using coaxial cavities was operated over a 13-to-1 frequency range. The nondispersive nature of TEM lines was also used for circuits with constant phase shift over a five-to-one frequency range.

[121] T. M. O'Meara and R. L. Sydnor, "A very-wide band balun transformer for VHF and UHF," PROC. IRE, vol. 46, pp. 1848–1860; November, 1958.
[122] J. W. McLaughlin, D. A. Dunn, and R. W. Grow, "A wide-band balun," IRE TRANS. ON MICROWAVE THEORY AND TECHNIQUES, vol. MTT-6, pp. 314–316; July, 1958.
[123] B. M. Schiffman, "A new class of broad-band microwave 90-degree phase shifters," IRE TRANS. ON MICROWAVE THEORY AND TECHNIQUES, vol. MTT-6, pp. 232–237; April, 1958.

Isotropic Hollow Waveguides

The low-attenuation and wide-bandwidth characteristics of large circular waveguides have stimulated further study of the problems which have delayed their practical application. These difficulties are principally due to the excitation of spurious modes.

A study of the effect of random geometric imperfections upon mode conversion in circular cylindrical waveguides was reported. It was shown that coupling to spurious modes caused by random deviations of the guide axis from a straight line is more serious than that caused by joints and by small deviations of the cylinders from circularity.

[124] W. D. Warters and H. E. Rowe, "The effects of mode conversion in long circular waveguide," 1958 IRE WESCON CONVENTION RECORD, pt. 1, pp. 13–20.

In the study of conically tapered transition sections, both constant and variable cone angle designs were investigated. In constant angle types, it was found that the magnitude of the next higher mode caused significant reflections. An improved design, in which the cone angle was gradually varied, exhibited reduced reflection. A 3-foot transition, using a variable cone angle, was found to be as effective as a 58-foot transition with constant cone angle.

[125] L. Solymar, "Design of a conical taper in circular waveguide system supporting H_{01} mode," PROC. IRE, vol. 46, pp. 618–619; March, 1958.
[126] H. G. Unger, "Circular waveguide taper of improved design," *Bell Sys. Tech. J.*, vol. 37, pp. 899–921; July, 1958.

It was noted that the mode conversion effects are much less significant in helical waveguides, operating in a TE_{01} mode, than in solid waveguides. This aspect of helical waveguides prompted an extensive examination of other effects in this structure. The power loss is one effect which was studied. When the wires of the helix are in contact, the loss is 8.5 per cent higher than the loss in the equivalent circular waveguide. When the wires are separated by a distance equal to their diameter, the loss is increased to 22.5 per cent more than that for a smooth surface.

[127] J. A. Morrison, "Heat loss of circular electric waves in helix waveguides," IRE TRANS. ON MICROWAVE THEORY AND TECHNIQUES, vol. MTT-6, pp. 173–177; April, 1958.

Another helical waveguide structure that appears promising as a solution to the difficulties of solid-wall waveguides, is the helix with a jacket of lossy material. The principal effect of the lossy jacket is to attenuate spurious modes. The structure was evaluated for use as mode filters between sections of solid waveguide, as mode suppressors in bends, and as a substitute for the solid waveguide in transmission systems. Sections of helix waveguides with lossy jackets and diametral resistance sheets were found to be effective mode filters for all spurious modes including the TE_{12} mode. At sharp bends, the most effective construction was found to be a low-loss dielectric jacket within a coaxial shield. As a replacement for solid circular waveguide, the preferred design is a helix within a jacket of medium loss surrounded by a metal shield. Examples of different constructions and their characteristics were presented.

[128] W. D. Warters, "The effects of mode filters on the transmission characteristics of circular electric waves in a circular waveguide," *Bell Sys. Tech. J.*, vol. 37, pp. 657–677; May, 1958.
[129] H. G. Unger, "Helix waveguide theory and application," *Bell Sys. Tech. J.*, vol. 37, pp. 1599–1647; November, 1958.
[130] D. Marcuse, "Continuation of the TE_{01} wave within the curved helix waveguide," *Bell Sys. Tech. J.*, vol. 37, pp. 1649–1662; November, 1958.
[131] C. F. E. Rose, "Research models of helix waveguide," *Bell Sys. Tech. J.*, vol. 37, pp. 679–688; May, 1958.

An interesting component, a phase shifter using coupling between coaxial helical waveguides operating in a lower mode, was reported. The phase shifter had a trombone-like shape.

[132] P. A. Crandall and F. J. Dominick "A helical phase shifter for VHF," *Microwave J.*, pp. 29–32; January, 1958.

The attenuation of waveguides for frequencies far above cut off and approaching the frequencies of visible light were studied. It was found that the attenuation of transverse magnetic waves (including TEM waves) increased for a limited range of frequencies above cut off and then decreased. The attenuation of the TE_{on} modes always decreased with higher frequency. In the visible region, the attenuation of TE waves was lower than that of TM waves.

[133] A. E. Karbowiak, "Guided wave propagation in submillimetric region," PROC. IRE, vol. 46, pp. 1706–1711; October, 1958.

The effect of geometrical and electrical imperfections on the propagation of energy through a waveguide was studied. In the immediate vicinity of localized imperfections, such as irregularities in the wall of a waveguide, higher mode fields which do not propagate are excited. These "ghost" modes behave like resonant structures. The finite conductivity of the walls affects the propagation of a pulse-modulated wave in a waveguide. Assuming small losses, it was shown that the damping factor for a pulse is the same as for the carrier.

[134] E. T. Jaynes, "Ghost modes in imperfect waveguides," PROC. IRE, vol. 46, pp. 416–418; February, 1958.
[135] G. Ryszard, "Influence of wall losses on pulse propagation in waveguides," *J. Appl. Phys.*, pp. 22–24; January, 1958.

The design of transitions between waveguides of different characteristics was the subject of continuing study. Cohn's design procedure for Tchebycheff-stepped transformers was used to design a transformer for coupling a rectangular to a double-ridged waveguide and for coupling an air-filled to a dielectric-filled rectangular waveguide. Linear and sinusoidal E-plane tapers for coupling rectangular waveguides were also studied and convenient design curves were presented. Formulas for the complex reflection coefficient were derived.

[136] E. S. Hensperger, "Broad-band stepped transformers from rectangular to double-ridged waveguide," IRE TRANS. ON MICROWAVE THEORY AND TECHNIQUES, vol. MTT-6, pp. 311–314; July, 1958.
[137] R. W. Whiteman, H. Zucker, C. M. Knop, "A low reflection dielectric waveguide stepped taper," *Proc. Natl. Electronics Conf.*, vol. 14; 1958.
[138] K. Matsumaru, "Reflection coefficient of E-plane tapered waveguides," IRE TRANS. ON MICROWAVE THEORY AND TECHNIQUES, vol. MTT-6, pp. 143–149; April, 1958.

The harmonic power present in high-power waveguides of rectangular cross section was studied experimentally. The relative amplitudes of the higher modes was determined. A 31-kw x-band signal was observed in the radiation from a 5-mgw S-band magnetron.

[139] M. P. Forrer and K. Tomiyasu, "Determination of higher order propagating modes in wave-guide systems," *J. Appl. Phys.*, vol. 29, pp. 1040–1045; July, 1958.

The power handling capacity of a rectangular waveguide, with a centered dielectric slab and sides parallel to the E-plane, was related to the dielectric constant and the thickness of the slab. For realizable values of dielectric constant and thickness, the power handling capacity could be made twice that of the empty guide.

[140] P. H. Vartanian, W. P. Ayres, and A. L. Holgesson, "Propagation in dielectric slab loaded rectangular waveguide," IRE TRANS. ON MICROWAVE THEORY AND TECHNIQUES, vol. MTT-6, pp. 215–222; April, 1958.

It was shown that breakdown of high power waveguides may be initiated by cosmic rays.

[141] S. W. Lichtman, "Influence of sea level cosmic radiation on power breakdown of air filled waveguide," *Proc. Natl. Electronics Conf.*, vol. 14; 1958.

Surface Waves

Surface waves may be defined as waves which propagate without radiation along the interface between two media and which have an evanescent field structure over an equiphase surface. A brief survey of the characteristics of surface waves was published. Attention was focused on the inhomogeneous plane wave (Zenneck wave), the radial surface wave, and the axially propagating cylindrical wave (Goubau wave).

[142] H. M. Barlow, "Surface waves," PROC. IRE, vol. 46, pp. 1413–1417; July, 1958.

The need for supporting dielectric-rod waveguides in space at some distance from objects has led to the investigation of waveguides consisting of half-round dielectric rods mounted on conducting image planes. The use of the image plane permits transmission of the low-loss hybrid mode but excludes certain other modes.

Field purity predictions were verified experimentally, and the effects of dielectric geometry and dielectric constant on field extension, loss, and dispersion were discussed. The case in which the dielectric was partially submerged in the ground plane was also considered.

[143] S. P. Schlesinger and D. D. King, "Dielectric image lines," IRE Trans. on Microwave Theory and Techniques, vol. MTT-6, pp. 291–299; July, 1958.

In order to excite the surface waves, it is necessary that the fields of the launching structure conform with the field distribution of the surface waves. Horns have been widely used for launching waves on dielectric rods. Other launching devices, such as wires, rings, and slots were investigated for exciting image lines.

[144] C. M. Angulo and W. S. C. Chang, "The excitation of a dielectric rod by a cylindrical waveguide," IRE Trans. on Microwave Theory and Techniques, vol. MTT-6, pp. 389–393; October, 1958.
[145] R. H. DuHamel and J. W. Duncan, "Launching efficiency of wires and slots for a dielectric rod waveguide," IRE Trans. on Microwave Theory and Techniques, vol. MTT-6, pp. 277–284; July, 1958.

A theoretical study of surface wave phenomena was concerned with the problem of propagation of electromagnetic waves produced by a line source of magnetic dipoles located at the corner of a right-angle wedge. An impedance-type boundary condition was prescribed on the surface of the wedge.

[146] S. N. Karp and F. C. Karal, Jr., "Surface waves on a right angled wedge," 1958 IRE WESCON Convention Record, pt. 1, pp. 101–103.

Artificial Dielectrics

If the elements of an artificial dielectric forms a cubic lattice and the lattice is small compared with the wavelength, the structure behaves isotropically. A change in structure or an enhanced behavior of the elements in a specific direction leads to a dielectric with anisotropic properties. Several studies of artificial dielectrics were reported. The anisotropy, which arises in a cubic lattice when the inter-element spacing is large, was investigated, and an anisotropy tensor was derived. An experimental investigation of planar arrays of thin metallic rectangles was made. The anomalous dispersion was strongly affected by lateral interaction between the elements of the array. Another structure, which consisted of thin dielectric sheets separated by thin sheets of different dielectric constant, was investigated theoretically. To obtain an isotropic dielectric of light weight, a random array of concentric metal and dielectric shells was suggested.

[147] Z. A. Kaprielian, "Anisotropic effects in geometrically isotropic lattices," *J. Appl. Phys.*, vol. 29, pp. 1052–1063; July, 1958.
[148] A. F. Wickersham, Jr., "Anomalous dispersion in artificial dielectrics," *J. Appl. Phys.*, vol. 29, pp. 1537–1542; November, 1958.
[149] R. E. Collin, "A simple artificial anisotropic dielectric medium," IRE Trans. on Microwave Theory and Techniques, vol. MTT-6, pp. 206–209; April, 1958.
[150] M. K. Hu and D. K. Cheng, "A new class of artificial dielectrics," 1958 IRE WESCON Convention Record, pt. 1, pp. 21–25.

In a related area, the problem of propagation through a random distribution of dielectric spheres was considered. Time-averaged attenuation and phase shift were measured for foamed dielectric spheres suspended by a turbulent air column.

[151] C. I. Beard and V. Twersky, "Propagation through random distributions of spheres," 1958 IRE WESCON Convention Record, pt. 1, pp. 87–100.

Junctions

Several studies of junctions, directional couplers, and hybrid structures were reported.

An analysis of two-part networks utilized a stereographic mapping of the output and input parameters on the Reimann sphere.

[152] E. F. Bolinder, "General method of analyzing bilateral two port networks from three arbitrary impedance or reflection coefficient measurements," *Proc. Natl. Electronics Conf.*, vol. 14; 1958.

Multiple-branch couplers are most useful for applications requiring tight coupling. A design method which is based on the use of n series branches in rectangular waveguide was presented. In another paper, distributed coupling between strip lines was studied. Couplings over one-quarter and three-quarter wavelengths were treated in detail. The former gave almost constant coupling over a two-to-one frequency band while the latter gave a similar result over a five-to-one frequency band.

[153] J. Reed, "The multiple branch waveguide coupler," IRE Trans. on Microwave Theory and Techniques, vol. MTT-6, pp. 398–403; October, 1958.
[154] J. K. Shimizu and E. M. T. Jones, "Coupled-transmission-line directional couplers," IRE Trans. on Microwave Theory and Techniques, vol. MTT-6, pp. 403–410; October, 1958.

A broad-band coaxial hybrid ring which has excellent isolation and balance characteristics was described. An equivalent admittance circuit was developed and used as a basis for the determination of the admittance and VSWR at the input arms. An isolation of 13.5 db or better was observed over a 50 per cent bandwidth.

[155] V. J. Albanese and W. P. Peyser, "An analysis of a broad-band coaxial hybrid ring," IRE Trans. on Microwave Theory and Techniques, vol. MTT-6, pp. 369–373; October, 1958.

Resonators and Filters

Accurate methods of measuring the characteristics of resonators were subjects of considerable study in 1958. It was shown that a graph of susceptance vs frequency is a straight line with a slope related to the Q. In this way, all of the impedance-frequency data is averaged so that a more accurate value for the Q is obtained. In another report, the phase shift introduced by a small perturbing element was used to determine the shunt impedance.

[156] A. Singh, "An improved method for the determination of Q of cavity resonators," IRE Trans. on Microwave Theory and Techniques, vol. MTT-6, pp. 155–160; April, 1958.
[157] K. B. Mallory, "Measurement of shunt impedance of a cavity," *J. Appl. Phys.*, vol. 29, p.p. 790–793; May, 1958.

The problems associated with the measurements of the Q of the resonators in the presence of coupling losses were studied. The analysis demonstrated that series

losses were separable from cavity losses. Shunt losses, however, could not be distinguished from the cavity losses without separate measurements of the coupling network.

[158] E. L. Ginzton, "Microwave Q measurements in the presence of coupling losses," IRE TRANS. ON MICROWAVE THEORY AND TECHNIQUES, vol. MTT-6, pp. 383–389; October, 1958.

A discussion of the case in which the resonant frequencies of two or more modes are sufficiently close to affect the observed impedance loci was presented.

[159] M. G. Keeney, "On the measurement of resonant cavity Q," *Proc. Natl. Electronics Conf.*, vol. 13, pp. 442–451; 1957.

A contribution to the theoretical analysis of cavity resonators was made which clarified the assumptions underlying Slater's analysis. By expanding the fields in terms of complete orthonormal functions and determining the expansion coefficients, the input impedance of the cavity could be determined. A corrected set of functions for the expansion was presented.

[160] K. Kurokawa, "The expansions of electromagnetic fields in cavities," IRE TRANS. ON MICROWAVE THEORY AND TECHNIQUES, vol. MTT-6, pp. 178–187; April, 1958.

A traveling-wave resonator, a ring circuit directionally coupled to the main guide, has the property that fields within the ring are larger than the fields in the main guide. This property was employed to obtain higher powers for testing microwave components. An effective power of 8 mgw was obtained from an 800 kw source.

[161] L. J. Milosevic and R. Vautey, "Traveling-wave resonators," IRE TRANS. ON MICROWAVE THEORY AND TECHNIQUES, vol. MTT-6, pp. 136–143; April, 1958.

The general synthesis procedure for high-Q waveguide filters was further clarified. The approximations required for synthesis based upon a ladder-network prototype were placed upon a formal basis.

[162] H. J. Riblet, "A unified discussion of high-Q waveguide filter design theory," IRE TRANS. ON MICROWAVE THEORY AND TECHNIQUES, vol. MTT-6, pp. 359–368; October, 1958.

A number of papers giving examples of specific designs appeared.

[163] S. B. Cohn, "Parallel-coupled transmission-line-resonator filters," IRE TRANS. ON MICROWAVE THEORY AND TECHNIQUES, vol. MTT-6, pp. 223–231; April, 1958.
[164] G. L. Matthaei, "Direct-coupled, band-pass filters with $\lambda_0/4$ resonators," 1958 IRE NATIONAL CONVENTION RECORD, pt. 1, pp. 98–111.
[165] A. I. Grayzel, "A band separation filter for the 225–400 mc band," 1958 IRE NATIONAL CONVENTION RECORD, pt. 1, pp. 91–97.
[166] J. H. Vogelman, "High power microwave filters," 1958 IRE NATIONAL CONVENTION RECORD, pt. 1, pp. 84–90.
[167] R. E. Saxe "Analysis of a lossy transmission line filter," *Proc. Natl. Electronics Conf.*, vol. 13, pp. 470–481; 1957.
[168] D. Alstadter and E. O. Houseman, Jr., "Some notes on strip transmission line and waveguide multiplexers," 1958 IRE WESCON CONVENTION RECORD, pt. 1, pp. 54–69.

Microwave components

Advances in switching techniques, matched windows, and absorbing materials were prominent among the reports on microwave components.

At low-power levels, semiconductor diodes in novel circuits were used for rapid switching. The equivalent circuit of the diode as a function of bias was analyzed to to predict the switching behavior. Germanium diodes were found to be preferable to silicon diodes since they have lower spreading resistance and higher nonlinear resistance with reverse bias. A millimicrosecond switching time appears to be feasible. The RF power that can be switched depends upon the Zener voltage and the resistivity of the crystal. The control of powers up to 50 mw were reported. The diodes were mounted across the waveguide in single and cascade arrangements. A hybrid-T configuration produced an insertion loss of 0.7 db with an isolation of 50 db.

[169] M. R. Millet, "Microwave switching by crystal diodes," IRE TRANS. ON MICROWAVE THEORY AND TECHNIQUES, vol. MTT-6, pp. 284–290; July, 1958.
[170] R. V. Garver, E. G. Spencer, and M. A. Harper, "Microwave semiconductor switching techniques," IRE TRANS. ON MICROWAVE THEORY AND TECHNIQUES, vol. MTT-6, pp. 378–383; October, 1958.

For rapid switching of high-power levels, the duplexer is the accepted component. A new duplexer, consisting of a microwave bridge and a power sensitive phase shifter was reported to be capable of handling twice the power of conventional balanced duplexers.

[171] P. D. Lomer and R. M. O'Brien, "A new form of high-power microwave duplexer," IRE TRANS. ON MICROWAVE THEORY AND TECHNIQUE, vol. MTT-6, pp. 264–267; July, 1958.

Dielectric windows for low- and high-power operation were described. The matching of the low-power window was accomplished by recessing the dielectric slab into the walls of the waveguide and using a matching iris. For high-power applications, a ceramic slab was used as one element of a three-element filter. This structure was successfully operated at powers in excess of one mgw over a 15 per cent bandwidth at X band.

[172] H. Zucker and C. M. Knop "A low reflections dielectric waveguide window for X band," *Proc. Natl. Electronics Conf.*, vol. 13, pp. 254–268; 1957.
[173] H. J. Shaw and L. M. Winslow, "A broad-band high-power vacuum window for X band," IRE TRANS. ON MICROWAVE THEORY AND TECHNIQUES, vol. MTT-6, pp. 326–330; July, 1958.

Further work on the properties of single layer microwave absorbing materials was carried out. The effects of magnetic and electric losses were studied as well as the design of the material for greatest bandwidth and minimum thickness.

[174] D. L. Waidelich, "The design of a single-layer microwave absorbing material," *Proc. Natl. Electronics Conf.*, vol. 14; 1958.

A rotary joint for use with mast-mounted antennas was developed.

[175] W. E. From, E. G. Fubini, and H. S. Keen, "A new microwave rotary joint," 1958 IRE NATIONAL CONVENTION RECORD, pt. 1, pp. 78–72.

Anisotropic waveguides

With the development of ferrite materials, a new dimension was added to the field of microwave engineering. The ferrites are characterized by large spin resonances and low conductivity. The existence of a large

number of uncoupled electron spins results in a tensor permeability with a strong anisotropy. Although other ferromagnetic materials are anisotropic, the low conductivity of ferrites has resulted in their wide application to microwaves.

Developments in the theory and application of waveguides loaded with anisotropic media proceeded rapidly during the year. The general theory of wave propagation in waveguides of various geometries was discussed; isolators, circulators, and other microwave components were studied; and new materials were introduced. Ferrites were most widely used, but other anisotropic materials and gas plasmas increased in importance.

A comprehensive survey of recent developments in ferrites and semiconductors was published early in 1958. Emphasis was placed on the application of nonreciprocal devices at low frequencies and at high-power levels. The study of nonlinear behavior in ferrites for frequency doubling, mixing, and amplification was reviewed. In other semiconductors, experiments in cyclotron resonance and spin resonance were reported.

[176] B. Lax, "The status of microwave applications of ferrites and semiconductors," IRE Trans. on Microwave Theory and Techniques, vol. MTT-6, pp. 5–18; January, 1958.

The theory of propagation in anisotropic media was expanded by the derivation of orthogonality properties of uniform waveguides filled with this material. Specific orthogonality relationships were derived which permit the expansion of the field components in terms of a complete set of waveguide modes.

[177] A. D. Bresler, G. H. Joshi, and N. Marcuvitz, "Orthogonality properties for modes in passive and active uniform waveguides," *J. Appl. Phys.*, vol. 29, pp. 794–799; May, 1958.

Early ferrite devices employed Faraday rotation in circular waveguide. Later discoveries of nonreciprocal effects in rectangular waveguides loaded with transversely magnetized ferrite slabs stimulated investigations of this preferred structure. The propagation constants and field configurations in the region of resonance were presented, and confirming measurements of the distribution of the transverse electric field were reported. The conditions for cut off of slab-loaded and completely filled rectangular guide were established and verified experimentally.

[178] W. J. Crowe, "Behavior of the T.E. modes in ferrite loaded rectangular waveguide in the region of ferri-magnetic resonance," *J. Appl. Phys.*, vol. 29, pp. 397–398; March, 1958.

[179] T. M. Straus, "Field displacement effects in dielectric and ferrite loaded waveguides," 1958 IRE WESCON Convention Record, pt. 1, pp. 135–146.

[180] R. F. Soohoo, "Cutoff phenomena in transversely magnetized ferrites," Proc. IRE, vol. 46, pp. 788–789; April, 1958.

The theory of the field displacement isolator was studied, and it was found that a thick slab placed close to a side wall produced the maximum ratio of reverse to forward attenuation.

[181] K. J. Button, "Theoretical analysis of the operation of the field displacement ferrite isolator," IRE Trans. on Microwave Theory and Techniques, vol. MTT-6, pp. 303–308; July, 1958.

The theoretical determination of reflection from an air-to-ferrite interface was presented. The transversely magnetized ferrite completely filled the waveguide, and the components of the equivalent circuit representation for the interface were calculated.

[182] C. B. Sharpe and D. S. Heim, "A ferrite boundary-value problem in a rectangular waveguide," IRE Trans. on Microwave Theory and Techniques, vol. MTT-6, pp. 42–46; January, 1958.

In cylindrical waveguide, a thick axially-magnetized rod and a circumferentially magnetized cylinder were studied. The propagation constants for the rod structure are well-known for the case of thin rods, and have been computed by approximate methods. The propagation constants for the thick rod were found by machine computation. The boundary value problem for the circumferentially magnetized ring was solved. It was found that the E-field displacement for a TE_{01} mode was suitable for an isolator.

[183] J. E. Tompkins, "Energy distribution in partially ferrite-filled waveguides," *J. Appl. Phys.*, vol. 29, pp. 399–400; March, 1958.

[184] N. Kumagai and K. Takeuchi, "Circular electric waves propagating through the circular waveguide containing a circumferentially magnetized ferrite cylinder," 1958 IRE WESCON Convention Record, pt. 1, pp. 123–130.

Ferrite-loaded TEM lines (microstrip and coaxial lines) were also studied to determine their reciprocal and nonreciprocal properties. The theoretical analysis of infinite parallel plane waveguide filled with longitudinally magnetized ferrite was applied to the microstrip structure. The reciprocal behavior was verified and the predicted variation of propagation constant with applied magnetic field was observed. The problem of the coaxial line, with transversely magnetized ferrite, was approached by the analysis of the equivalent parallel-plane structure. The geometry consisted of a dielectric slab between ferrite slabs; the differential phase shift was calculated.

[185] M. E. Brodwin, "Propagation in ferrite-filled microstrip," IRE Trans. on Microwave Theory and Techniques, vol. MTT-6, pp. 150–155; April, 1958.

[186] K. J. Button, "Theory of non-reciprocal ferrite phase shifters in dielectric-loaded coaxial line," *J. Appl. Phys.*, vol. 29, pp. 998–1000.

Reciprocity was investigated to determine how the impedance, admittance and scattering matrices were affected by reversal of the dc magnetic field. It was found that the usual reciprocity relations hold when the source and load are interchanged if the field is reversed.

[187] R. F. Harrington and A. T. Villeneuve, "Reciprocity relationships for gyrotropic media," IRE Trans. on Microwave Theory and Techniques, vol. MTT-6, pp. 308–310; July, 1958.

Isolators and Circulators

Improvements in the design of isolators consisted of new techniques for increasing bandwidth and for reducing the low-frequency limit. The bandwidth of isolators in rectangular waveguide was increased by using ferrites with different saturation magnetizations located

at different positions in the wave-guide. The result is equivalent to cascaded narrow band isolators. Another approach to this problem was the use of inherently wideband structures with the ferrite as a coupling medium. Devices operating over 6–11 kmc were reported.

[188] B. J. Duncan and B. Vafiades, "Design of a full waveguide bandwidth high-power isolator," IRE TRANS. ON MICROWAVE THEORY AND TECHNIQUES, vol. MTT-6, pp. 411–414; October, 1958.
[189] E. M. T. Jones, S. B. Cohn and J. K. Shimizu, "A wideband nonreciprocal tem-transmission-line network," 1958 IRE WESCON CONVENTION RECORD, pt. 1, pp. 131–134.

Factors affecting the low-frequency limit of operation were shown to be functions of the ferrite material and the geometry. Materials with small saturation magnetization and narrow line width are desireable. The optimum arrangement is thin ferrite slabs placed along the broad walls of the waveguide.

[190] F. O. Schulz-DuBois, G. J. Wheeler, and M. H. Sirvetz, "Development of a highpower L-band resonance isolator," IRE TRANS. ON MICROWAVE THEORY AND TECHNIQUES, vol. MTT-6, pp. 423–428; October, 1958.
[191] G. S. Heller and G. W. Catuna, "Measurement of ferrite isolation at 1300 mc," IRE TRANS. ON MICROWAVE THEORY AND TECHNIQUE, vol. MTT-6, pp. 97–100; January, 1958.

A new circulator design was reported in which a ferrite rod was placed along an axis of symmetry of an H-plane waveguide junction.

[192] W. E. Swanson and G. J. Wheeler, "Tee circulator," 1958 IRE WESCON CONVENTION RECORD, pt. 1, pp. 151–156.

Switches, Filters, and other Components

The effects of anisotropy were the principal features of a number of components; switches, attenuators, phase shifters, and a power limiter. The principal problem in rapidly switching ferrite devices is the high power requirements of the external magnet. One reported solution is to use a thin-walled waveguide to reduce eddy-current loss but with sufficient thickness for low-loss wave propagation. Another solution is to place the entire magnetic circuit within the waveguide structure and use an internal conductor to control the magnetic properties. Switching times of 0.1 μsec and with a power of 50 watts were reported.

[193] E. H. Turner, "A fast ferrite switch for use at 70 kmc," IRE TRANS. ON MICROWAVE THEORY AND TECHNIQUES, vol. MTT-6, pp. 300–303; July, 1958.
[194] M. A. Treuhaft and L. M. Silber, "Use of microwave ferrite toroids to eliminate external magnets and reduce switching power," PROC. IRE, vol. 46, p. 1538; August, 1958.

Ferrites were used to control the characteristics of filters by using the ferrite as an integral part of a cavity, and by employing isolators to prevent interaction between networks.

[195] W. L. Whirry and C. E. Nelson, "Ferrite-loaded, circularly polarized microwave cavity filters," IRE TRANS. ON MICROWAVE THEORY AND TECHNIQUES, vol. MTT-6, pp. 59–65; January, 1958.
[196] H. Rapaport, "A microwave ferrite frequency separator," IRE TRANS. ON MICROWAVE THEORY AND TECHNIQUES, vol. MTT-6; pp. 53–58; January, 1958.

A reciprocal phase shifter which operated at a power of 15 kw and a ferrite attenuator for compensating the gain variation of traveling wave tubes were also reported.

[197] W. H. Hewitt Jr. and W. H. VonAulock, "A reciprocal ferrite phase shifter for X band," *Proc. Natl. Electronics Conf.*, vol. 13, pp. 459–469; 1957.
[198] F. Fleri and B. J. Duncan, "Reciprocal ferrite devices in TEM mode transmission lines," IRE TRANS. ON MICROWAVE THEORY AND TECHNIQUES, vol. MTT-6, pp. 91–96; January, 1958.

The saturation effects in ferrites were used to limit high microwave powers. At high levels, spin wave effects produce an anomalous absorption on the low field side of the main ferromagnetic resonance. This effect was used to construct a simple limiter with a threshold of 300 watts.

[199] R. F. Soohoo, "Power limiting using ferrites," 1958 IRE NATIONAL CONVENTION RECORD, pt. 1, pp. 36–47.

Radiation from Ferrite Filled Apertures

Ferrite properties were employed to control the phase and amplitude distribution of radiating apertures. Rectangular, square and circular apertures were investigated. The previously reported experimental investigations of ferrite-filled rectangular waveguide apertures were analyzed. The contributions of higher modes were considered and the far-field behavior was related to the aperture distribution.

[200] B. Tyras and G. Held, "Radiation from a rectangular waveguide filled with ferrite," IRE TRANS. ON MICROWAVE THEORY AND TECHNIQUES. vol. MTT-6, pp. 268–277; July, 1958.

Experimental investigations of the radiation from square and circular apertures were reported. Beam displacements of $\pm 30°$ were observed for the completely-filled square aperture and a system was devised for sequential lobing. The circular aperture containing a ferrite ball was studied for possible application to conical scanning.

[201] D. B. Medved, "An electronic scan using a ferrite aperture Luneberg lens system," IRE TRANS. ON MICROWAVE THEORY AND TECHNIQUES, vol. MTT-6, pp. 101–103; January, 1958.
[202] M. S. Wheller, "Nonmechanical beam steering by scattering from ferrites," IRE TRANS. ON MICROWAVE THEORY AND TECHNIQUES, vol. MTT-6, pp. 38–42; January, 1958.

Measurement of Ferrite Properties

When the sample is placed in an inhomogeneous RF magnetic field, anomalous resonances were observed. The origin of these anomalies was studied; it was shown that they are caused by the free modes of the magnetic dipoles in the material.

[203] L. R. Walker, "Ferro-magnetic resonance: line structure," *J. Appl. Phys.*, vol. 29, pp. 318–322; March, 1958.

Cavity techniques for the measurement of disc and rod samples were reported. In one paper, the frequency shift, produced by a ferrite disc in a cavity of generalized cross section, was related to the tensor components. For rod-shaped samples, the solution to the boundary value problem in cylindrical waveguide was used for the measurement. A different approach to this problem employed a bimodal cavity. A relationship was derived for the coupling between the modes and the properties of the material.

[204] H. Seidel and H. Boyet, "Frequency shifts in cavities with longitudinally magnetized small ferrite discs," *Bell Sys. Tech. J.*, vol. 37, pp. 637–655; May, 1958.
[205] H. E. Bussey and L. A. Steinert, "Exact solution for a gyromagnetic sample and measurements on a ferrite," IRE Trans. on Microwave Theory and Techniques, vol. MTT-6, pp. 72–76; January, 1958.
[206] A. M. Portis, and D. Teaney, "Microwave Faraday rotation: design and analysis of a bimodal cavity," *J. Appl. Phys.*, vol. 29, pp. 1692–1698; December, 1958.

A technique for the measurement of line width which is insensitive to the sample size was developed. It was found that the surface finish had a strong effect on the measured line width.

[207] D. C. Stinson, "Experimental techniques in measuring ferrite line widths with a cross-guide coupler," 1958 IRE WESCON Convention Record, pt. 1, pp. 147–150.

The use of ring circuits for the measurement of ferrite properties led to a theoretical analysis of the effects of ferrites on the resonant frequency and Q.

[208] F. J. Tischer, "Resonant properties of nonreciprocal ring circuits," IRE Trans. on Microwave Theory and Techniques, vol. MTT-6, pp. 66–71; January, 1958.

For the measurement of ferrite parameters at low frequencies, a new technique was developed and results of measurements on foreign materials were given.

[209] P. P. Lombardini, R. F. Schwartz, and R. J. Doviak, "Measurement of the properties of various ferrites used in magnetically tuned resonant circuits in the 2.5–45 mc. region," *J. Appl. Phys.*, vol. 29, pp. 395–296; March, 1958.

Ferrite Materials

The search for improved materials included an examination of polycrystalline rare earth garnets as possible solutions to the low-frequency ferrite problem. The desired characteristics are narrow line width and low saturation magnetization.

Different compositions were examined and their application to L-band and S-band isolators was reported.

[210] B. Ancker-Johnson and J. J. Rowley, "Mixed garnets for nonreciprocal devices at low microwave frequencies," Proc. IRE, vol. 46, pp. 1421–1422; July, 1958.

The effect of partial substitution of gadolinium for yttrium in rare earth garnets was determined and it was shown that the gadolinium reduces the saturation magnetization with a small effect on line width.

[211] H. R. Sirvetz and J. E. Zniemer, "Microwave properties of polycrystalline rare earth garnets," *J. Appl. Phys.*, vol. 29, pp. 431–434; March, 1958.

The behavior of materials of different compositions were reported in the following papers:

[212] J. E. Pippin and C. L. Hogan, "Resonance measurements on nickel-cobalt ferrites as a function of temperature and on nickel ferrite-aluminates," IRE Trans. on Microwave Theory and Techniques, vol. MTT-6, pp. 77–82; January, 1958.
[213] G. P. Rodrique, J. E. Pippin, W. P. Wolf, and C. L. Hogan, "Ferrimagnetic resonance in some polycrystalline rare earth garnets," IRE Trans. on Microwave Theory and Techniques, vol. MTT-6, pp. 83–91; January, 1958.

Ionized Gases and Hall Effect

Ionized gases were investigated and nonreciprocal effects were reported. Among other reports on gaseous media were improvements in discharge tubes and noise sources. A Hall effect circulator was described.

A valuable survey was presented which outlined the present knowledge of the application of gas plasmas to microwave propagation. The paper discussed the isotropic gas plasma and the anisotropy produced by a static magnetic field. The problem of guided-wave propagation was reviewed and data were presented on resonant phenomena in the gyromagnetic plasma.

[214] L. Goldstein, "Nonreciprocal electromagnetic wave propagation in ionized gaseous media," IRE Trans. on Microwave Theory and Techniques, vol. MTT-6, pp. 19–29; January, 1958.

The case of an ion-filled rectangular waveguide with an axial magnetic field was investigated and the propagation characteristics determined.

[215] L. D. Smullin and P. Chorney, "Properties of ion-filled waveguides," Proc. IRE, vol. 46, pp. 360–361; January, 1958.

Advances in gas discharge switching included the use of a magnetic field and cyclotron resonance phenomena to control the firing of a discharge tube, and the application of a shaped pulse to the keep-alive electrode to modify the electron density.

[216] S. J. Tetenbaum and R. M. Hill, "High power, broadband, microwave gas discharge switch tube," 1958 IRE National Convention Record, pt. 1, p. 83.
[217] R. E. Hovda and E. R. Roehl, "Characteristics and control of gas tube duplexers during their recovery time," 1958 IRE WESCON Convention Record, pt. 3, pp. 105–114.

Close agreement was found between the noise temperature and the electron temperature for argon tubes at 3000 mc; it was recommended that these tubes be adopted as standard noise sources.

[218] E. W. Collings, "Noise and electron temperatures of some cold cathode argon discharges," *J. Appl. Phys.*, vol. 29, pp. 1215–1219; August, 1958.

An unusual device was reported for the production of high-power noise. An impulse generator was described with significant power output in the 200-to-7000 mc frequency range. The output power varied from 120 to 145 db above KTB.

[219] R. H. George and H. J. Heim, "Recent developments with spark gap impulse noise generators" *Proc. Natl. Electronics Conf.* vol. 13, pp. 287–295; 1957.

The Hall effect was studied to determine possible applications to circulators. A three-port device was constructed consisting of a slab of germanium with six wire connections. Although this design is expected to operate between dc and 100 mc, the principle could be extended to the microwave region.

[220] W. J. Grubbs, "The Hall effect circulator—a passive transmission device," 1958, IRE WESCON Convention Record, pt. 3, pp. 83–93.

Measurements

Advances in measurements include the use of the Hall effect and the use of the torque developed on thin metal vanes to measure microwave power; improved design methods for broad-band calorimeters as standards for microwave power measurements; the development of semiautomatic techniques for broad-band measure-

ments; the design of new atomic frequency standards; and a more comprehensive treatment of considerations which limit the sensitivity of microwave radiometers.

Power Measurements

The Hall effect was applied to the measurement of power with the noteworthy result that the technique is independent of standing-wave ratio. A device is described which has a sensitivity of 50 mw.

[221] H. M. Barlow, "The Hall effect and its application to microwave power measurement," PROC. IRE, vol. 46, pp. 1411–1413; July, 1958.

Another novel technique employed a thin metallic vane suspended in the waveguide. The electric field produces a torque tending to rotate the vane in line with the unperturbed field. The device shows promise as a primary standard.

[222] A. L. Cullen, B. Rogal, and S. Okamura, "A wide-band double-vane torque-operated wattmeter for 3-cm microwaves," IRE TRANS. ON MICROWAVE THEORY AND TECHNIQUES, vol. MTT-6, pp. 133–136; April, 1958.

The present primary standard of power measurement is still the calorimeter. A commercial dry calorimeter was described.

[223] M. Sucher and H. J. Carlin, "Broad-band calorimeters for the measurement of low and medium level microwave power. I. Analysis and design," IRE TRANS. ON MICROWAVE THEORY AND TECHNIQUES, vol. MTT-6, pp. 188–194; April, 1958.
[224] A. V. James and L. O. Sweet, "Broad-band calorimeters for the measurement of low and medium level microwave power. II. Construction and performance," IRE TRANS. ON MICROWAVE THEORY AND TECHNIQUES, vol. MTT-6, pp. 195–202; April, 1958.

With the increased use of broad-band components, rapid, convenient measurements over a wide frequency band becomes increasingly important. Automatic techniques for measuring phase and amplitude were described, and the use of a magnetically-controlled ferrite attenuator for amplitude stabilization was outlined.

[225] J. B. Linker, Jr. and H. H. Grimm, "Wide-band microwave transmission measuring system," IRE TRANS. ON MICROWAVE THEORY AND TECHNIQUES, vol. MTT-6, pp. 415–418; October, 1958.
[226] Herbert A. Dropkin, "Direct reading microwave phase-meter," 1958 IRE NATIONAL CONVENTION RECORD, pt. 1, pp. 57–63.
[227] G. F. Engen, "Amplitude stabilization of a microwave signal source," IRE TRANS. ON MICROWAVE THEORY AND TECHNIQUES, vol. MTT-6, pp. 202–206; April, 1958.

Other developments in measurement techniques were presented in the following papers.

[228] G. E. Schafer and R. W. Beatty, "A method for measuring the directivity of directional couplers," IRE TRANS. ON MICROWAVE THEORY AND TECHNIQUES, vol. MTT-6, pp. 419–422; October, 1958.
[229] J. I. Gaicoya, "Tuning a probe in a slotted line," PROC. IRE, vol. 46, pp. 787–788; April, 1958.
[230] K. G. Beauchamp, "A phase sensitive detector for indicating VSWR," *Electronic Industries*, vol. 17, pp. 74–77; February, 1958.
[231] G. Richard Blair, "An ultra-precise microwave interferometer," 1958 IRE NATIONAL CONVENTION RECORD, pt. 1, pp. 48–56.

Radiometry

Recent advances in radiometry were reported in the Radio Astronomy Issue of the PROCEEDINGS OF THE IRE in January, 1958. Some of the papers of specific interest to those in microwaves are noted below.

Attention was focused on the sensitivity of the receiver, and the angular resolution of the receiving system. In highly sensitive radiometers, with temperature thresholds less than 1°K, internal receiver noise establishes an absolute limit. Other factors which limit the system sensitivity are background radiation, atmospheric absorption, and fluctuations in the characteristics of the receiving system. The most sensitive radiometers use a switching technique to compare the received noise with a known standard. An evaluation of the sensitivity of different systems was reported as well as a study of the ultimate sensitivity of superheterodyne receivers. Improvements of angular resolution by the use of interferometers were also discussed. The theory of radio interferometry was related to previous work in the optical region. An important theorem on the optimum spacing of the antennas for a given angular resolution was derived. It was shown that current practice is too conservative.

[232] P. D. Strum, "Considerations in high-sensitivity microwave radiometry," PROC. IRE, vol. 46, pp. 43–53; January, 1958.
[233] C. T. McCoy, "Microwave crystal receivers," PROC. IRE, vol. 46, pp. 61–66; January, 1958.
[234] R. N. Bracewell, "Radio interferometry of discrete sources," PROC. IRE, vol. 46, pp. 97–105; January, 1958.

Knowledge of the polarization of the received wave yields valuable information about the Faraday rotation in the ionosphere. Various techniques for measuring polarization in terms of total intensity, orientation, polarization fraction, and axial ratio, were discussed. Three systems for determining these parameters were compared: two antennas, for the measurement of intensity, phase difference, and correlation function; three antennas, with phase measurements; four antennas, with intensity measurements. The two antenna system was described in detail.

[235] M. H. Cohen, "Radio astronomy polarization measurements," PROC. IRE, vol. 46, pp. 172–183; January, 1958.
[236] M. H. Cohen, "The Cornell radio polarimeter," PROC. IRE, vol. 46, p. 183–190. January, 1958.

Specific examples of radiometric devices appeared in the following papers.

[237] F. D. Drake and H. I. Ewen, "A broad-band microwave source comparison radiometer for advanced research in radio astronomy," PROC. IRE, vol. 46, pp. 53–60; January, 1958.
[238] M. Graham, "Radiometer circuits," PROC. IRE, vol. 46, p. 1966; December, 1958.
[239] J. Goodman and M. Lebenbaum, "A dynamic spectrum analyzer for solar studies," PROC. IRE, vol. 46, pp. 132–135; January, 1958.
[240] J. P. Wild and K. V. Sheridan, "A swept-frequency interferometer for the study of high-intensity solar radiation at meter wavelengths," PROC. IRE, vol. 46, pp. 160–171; January, 1958.
[241] J. S. Hey and V. A. Hughes, "A method of calibrating centimetric radiometers using a standard noise source," PROC. IRE, vol. 46, pp. 119–121; January, 1958.

Frequency Measurements

Resonances in alkali metal vapors, oxygen, and paramagnetic materials were used for accurate stable sources and for frequency measurements.

Atomic resonances were applied to the problem of developing a convenient primary frequency standard. Low-frequency crystal oscillators were locked in frequency to an atomic transition by a servo system. It was shown that frequency stability depends upon the width of the resonance and the signal to noise ratio of the detected transition. Experiments were carried out using the magnetic hyperfine transitions in sodium and caesium. Productions units, with a guaranteed accuracy of 1 part in 10^9 and a minimum stability of 5 parts in 10^{10} were described.

[242] M. Arditi and T. R. Carver, "A gas cell 'atomic clock' using optical pumping and optical detection," 1958 IRE National Convention Record, pt. 1 pp. 3–9.
[243] A. O. McCoubry, "The atomichron—an atomic frequency standard: physical foundations," 1958 IRE National Convention Record, pt. 1, pp. 10–13.
[244] W. Mainberger and A. Orenberg, "The atomichron—an automatic frequency standard: operation and performance," 1958 IRE National Convention Record, pt. 1, pp. 14–18.

The possible use of an absorption line of oxygen for a frequency standard was also investigated.

[245] J. M. Richardson, "Experimental evaluation of the oxygen microwave absorption as a possible atomic frequency source," *J. Appl. Phys.*, vol. 29, pp. 136–145; February, 1958.

Paramagnetic resonance was combined with nuclear magnetic resonance for the calibration of a microwave cavity. The nuclear resonance was used to accurately determine the magnetic field. With a known field, the paramagnetic resonant frequency could be calculated to an accuracy of one part in 10^7.

[246] P. A. Crandell, "An accurate frequency measuring technique using paramagnetic resonance phenomena in the *X*-band region," 1958 IRE WESCON Convention Record, pt. 1, pp. 26–34.

Conclusion

Advances in Microwave Theory and Techniques in 1958 tended to center around direct interaction of microwaves and anisotropic media. Much information on masers, parametric amplifiers, and nonreciprocal and nonlinear devices was accumulated. Important improvements were also made in conventional sources, detectors, and transmission lines. The inference drawn from the recent trend is that classical approaches offer little promise for great forward steps. New concepts, new knowledge, and new approaches are necessary. A great challenge is before us.

Report of Advances in Microwave Theory and Techniques in Great Britain—1958*

JOHN BROWN†

TEM Lines

THE characteristic impedances of a coaxial type line in which the inner conductor is a flat strip and of a triplate strip line have been calculated.

J. C. Anderson, "The calculation of characteristic impedance by conformal transformation," *J. Brit. IRE*, vol. 18, pp. 49–54; January, 1958.
K. Foster, "The characteristic impedance and phase velocity of high-Q triplate line," *J. Brit. IRE*, vol. 18, pp. 715–723; December, 1958.

Further numerical work has been carried out on estimating the probability of a specified over-all reflection coefficient caused by a number of known mismatches of random spacing.

J. H. Craven, "The probability of specified losses at mismatched junctions," *J. Brit. IRE*, vol. 18, pp. 293–296; May, 1958.

Transient conditions have also been considered.

K. W. H. Foulds, "Transmission line discontinuities," *Electronic Radio Engr.*, vol. 35, pp. 263–267; July, 1958.

A study of irregularities in cable characteristic impedances has been made.

J. Allison, "Variations of characteristic impedance along short coaxial cables," *Proc. IEE*, vol. 105, pt. C, pp. 169–176; March, 1958.

Hollow Waveguides

Interest in the properties of the low-loss TE_{01} mode in circular waveguide continues and a survey of the waveguide requirements has been made.

A. E. Karbowiak, "Microwave aspects of waveguides for long-distance transmission," *Proc. IEE*, vol. 105, pt. C, pp. 360–369; September, 1958.

The use of dielectric filling has been suggested as a means of minimizing the losses at bends.

H. M. Barlow "Propagation Around Bends in Waveguides," IEE Mono. No. 113R, September, 1958; will be republished in *Proc. IEE*, vol. 106, pt. C; March, 1959.

A general treatment of helical coordinate systems can be applied to helical waveguides.

R. A. Waldron, "A helical coordinate system and its applications in electromagnetic theory," *Quart. J. Mech. and Appl. Math.*, vol. 11, pp. 438–461; November, 1958.

* Manuscript received by the PGMTT, March, 1959.
† Dept. of Elec. Engrg., University College, London, Eng.

Numerical results have been obtained for elliptic waveguides.

R. V. Harrowell, "An approximate theory for determining the characteristic impedances of elliptic waveguide," *J. Electronics and Control*, vol. 5, pp. 289–299; October, 1958.

The dispersion properties of loaded waveguides have been analyzed by Fourier series.

P. N. Robson, "A note on the Fourier series representation of the dispersion curves for circular iris-loaded waveguides," *Proc. IEE*, vol. 105, pt. B, pp. 69–72; January, 1958.

Waveguides partly filled with dielectric have been shown to support modes in which the longitudinal magnetic field is constant over the cross section.

L. G. Chambers, "The propagation of constant longitudinal magnetic waves in dielectric filled waveguide," *Quart. J. Mech. and Appl. Math.*, vol. 11, pp. 244–252; May, 1958.

Propagation along a set of transmission lines coupled together at intervals has been expressed in terms of a set of orthogonal modes and the results used to calculate the reflection at the interface between an empty guide and one filled with an artificial dielectric.

J. Brown, "Propagation in coupled transmission line systems," *Quart. J. Mech. and Appl. Math.*, vol. 11, pp. 235–243; May, 1958.
J. Brown and J. S. Seeley, "The fields associated with an interface between free space and an artificial dielectric," *Proc. IEE*, vol. 105, pt. C, pp. 472–475; September, 1958.

A series of papers dealing with loaded transmission lines and waveguides suitable for valves was presented at the International Convention on Microwave Valves, London, May, 1958, and are published in *Proc. IEE*, vol. 105, pt. B, supp. no. 11.

G. B. Walker, "Dielectric loading for microwave valves," pp. 717–718.
A. F. Pearce, "A structure using resonant coupling elements, suitable for a high power travelling-wave tube," pp. 719–726.
P. Palluel and J. Arnaud, "Results on delay lines for high power travelling-wave tubes," pp. 727–729.
F. Sellberg, "Theoretical investigation of some closed delay structures for high power travelling-wave tubes," pp. 730–736.
E. A. Ash, "A new type of slow-wave structure for millimetre wavelengths," pp. 737–745.
R. M. White, C. K. Birdsall, and R. W. Grow, "Multiple ladder circuits for millimetre wavelength tubes," p. 746.
D. T. Swift-Hook, "Dispersion curves for a helix in a glass tube," pp. 747–755.
P. A. Lindsay and K. D. Collins, "Some aspects of the design of a helical coupler for a travelling-wave tube operating in the 2 Gc/s band," pp. 756–761.
E. A. Ash and J. D. Pattenden, "Modified transmission-line couplers for helices," pp. 762–768.
B. Minakovic, "The coupling of three coaxial helices," pp. 769–779.
J. Hirano, "Characteristics of interdigital circuits and their use for amplifiers," pp. 780–785.

Theoretical and experimental work has confirmed that the reflectivity of a conductor can be increased by coating it with a low loss high permittivity dielectric.

G. B. Walker and J. T. Hyman, "The use of dielectric materials to enhance the reflectivity of a surface at microwave frequencies," *Proc. IEE*, vol. 105, pt. B, pp. 73–76; January, 1958.

Waveguide Components

The advantages to be gained by using elliptical coupling holes in directional couplers have been discussed.

J. Figanier and E. A. Ash, "Intrinsic directional coupler using elliptic coupling apertures," *Proc. IEE*, vol. 105, pt. C, pp. 432–437; September, 1958.

The design and construction of microstrip components has been discussed in detail.

J. M. C. Dukes, "Broad-band slot-coupled microstrip directional couplers," *Proc. IEE*, vol. 105, pt. B, pp. 147–154, March, 1958; "The application of printed circuit techniques to the design of microwave components," pp. 155–172; "Re-entrant transmission line filter using printed conductors," pp. 773–779.

Filters

G. Craven, "Wide-band waveguide filters with short linear tapers," *Proc. IEE*, vol. 105, pt. B, pp. 210–212; March, 1958.
M. H. N. Potok, "The design of inductive post-type microwave filters," *J. Brit. IRE*, vol. 18, pp. 263–272; May, 1958.

Ferrites

The propagation of waves in a circular waveguide with an axial ferrite rod has been examined theoretically and comprehensive tables of results prepared.

R. A. Waldron, "Electromagnetic wave propagation in cylindrical waveguides containing gyromagnetic media," *J. Brit. IRE*, vol. 18, pp. 597–612, October, 1958; pp. 677–690, November, 1958; pp. 733–746, December, 1958.

Variational methods have been used to assess the effect of ferrite obstacles in waveguides and cavities.

W. Hauser, "On the theory of anisotropic obstacles in cavities," *Quart. J. Mech. and Appl. Math.*, vol. 11, pp. 112–118; February, 1958. Also, "On the theory of anisotropic obstacles in waveguides," *Quart. J. Mech. and Appl. Math.*, vol. 11, pp. 427–438; November, 1958.

A survey of waveguide components using ferrites has appeared and new designs for low power duplexers have been given.

B. L. Humphreys, "Ferrite components in microwave systems," *Electronic Engrg.*, vol. 30, pp. 341–344; May, 1958.
R. S. Cole and W. N. Honeyman, "Two short low power ferrite duplexers," *Electronic Radio Engr.*, vol. 35, pp. 282–286; August, 1958.

Measurements

An ingenious power meter, in which the temperature rise in a transverse resistive card is measured, has been shown to be simple to construct and to be reliable in operation.

J. A. Lane, "Transverse film bolometers for the measurement of power in rectangular waveguides," *Proc. IEE*, vol. 105, pt. B, pp. 77–80; January, 1958.

A Hall effect wattmeter has been investigated at a frequency of 10gc/s.

H. E. M. Barlow and S. Kataoka, "The Hall effect and its application to power measurement at 10Gc/s," *Proc. IEE*, vol. 105, pt. B, pp. 53–60; January, 1958.

Design details for a direct reading thermistor bridge for power measurement at 2000 mc have been given.

J. K. Murray: "U.H.F. Power meter for operation in the 2000 Mc/s communication band," *Electronic Engrg.*, vol. 30, pp. 345–348; May, 1958.

Several aspects of standing wave ratio measurements have received further attention.

E. W. Collings, "Voltage standing wave ratio measurements," *Electronic Radio Engr.*, vol. 35, pp. 287–289; August, 1958.
R. S. Cole and W. N. Honeyman, "Two automatic impedance plotters," *Electronic Engrg.*, vol. 30, pp. 442–446; July, 1958.
J. Allison and F. A. Benson, "Measurement and attenuation of a cable of impedance through an arbitrary loss-free junction," *Proc. IEE*, vol. 105, pt. B, pp. 487–495; September, 1958.
N. F. McKenna, "Low loss structures in waveguides," *Electronic Radio Engr.*, vol. 35, pp. 470–473; December, 1958.

Cavity Resonators

A. E. Barrington and J. R. Rees, "A simple 3 cm Q-meter," *Proc. IEE*, vol. 105, pt. B, pp. 511–512; November, 1958.
A. E. Karbowiak, "The concept of heterogeneous surface impedance and its application to cylindrical cavity resonators," *Proc. IEE*, vol. 105, pt. C, pp. 1–12; March, 1958.
A. E. Karbowiak, "An instrument for the measurement of surface impedance at microwave frequencies," *Proc. IEE*, vol. 105, pt. B, pp. 195–203; March, 1958.

Noise Sources

A. C. Gordon-Smith and J. A. Lane, "Measurements on gas discharge noise sources at centimetre wavelengths," *Proc. IEE*, vol. 105, pt. B, pp. 545–547; November, 1958.
M. Kollanyi, "Application of gas discharge tubes as noise sources in the 1700–2300 Mc/s band," *J. Brit. IRE*, vol. 18, pp. 541–550; September, 1958.

Ferrites

C. M. Srivastava and J. Roberts, "Measurements of ferrite loss factors at 10 Gc/s," *Proc. IEE*, vol. 105, pt. B, pp. 204–209; March, 1958.

Optical Methods

J. I. Caicoya, "The optical approach in microwave measuring tech nique," *Brit. Commun. and Electronics*, vol. 5, pp. 500–507; July, 1958.
J. S. Seeley, "A spectrometer method for measuring the electrical constants of lossy materials," *Proc. IEE*, vol. 105, pt. C, pp. 18–26; March, 1958.
R. W. R. Hoisington, L. Kellner and M. J. Pentz, "Criteria determining the design and performance of a source modulated microwave cavity spectrometer," *Proc. Phys. Soc.*, vol. 72, pp. 537–544; October, 1958.

Semiconductors

Two sessions at the Microwave Valve convention were devoted to various aspects of semiconductor devices including amplifying devices. The papers are published in *Proc. IEE*, vol. 105, pt. B, suppl. no. 11; 1958.

C. Baron, "Theory of the microwave crystal mixer," pp. 662–664.
E. Rostas and F. Hulster, "Microwave amplification by means of intrinsic negative resistances," pp. 665–673.
K. W. H. Stevens, "Introduction to atomic and molecular generators," pp. 674–676.
G. Wade and H. Heffner, "Microwave parametric amplifiers and convertors," pp. 677–679.
K. K. N. Chang and S. Bloom, "A parametric amplifier using lower frequency pumping," pp. 680–682.
P. N. Butcher, "Theory of three-level paramagnetic masers," pp. 684–710.
A. E. Siegman, P. N. Butcher, J. C. Cromack, and W. S. C. Chang, "Travelling-wave solid-state masers," p. 711.
A. H. W. Beck and J. Lytollis, "Construction of a mobile caesium frequency standard," pp. 712–715.

Report of Advances in Microwave Theory and Techniques in Western Europe—1958*

GEORGES GOUDET†

1. Transmission Lines

1.1. *Hollow Waveguides*

A member of Philips Research Laboratory, Eindhoven, Holland, has used a new method to calculate the radiation impedance of a linear antenna in a waveguide of rectangular cross-section, *viz.*, Schwingers' variational principle. This new application, even when based on only a two-term Fourier expansion of the current distribution, gives better results than a sinusoidal current distribution.

F. de Ronde, "Schwingers' variational principle applied to the calculation of the radiation resistance and reactance of linear antenna in a waveguide of rectangular cross-section." *Onde Elect.*, no. 376 bis, tome 1, pp. 95–98; août, 1958. (In English.)

A general study tending to define the concept of impedance in hollow waveguides has been made.

A. Guerbilsky, "La notion d'impédance dans la théorie des guides d'ondes." *Ann. Télécommun.*, no. 5–6, pp. 114–120; mai-juin, 1958. (In French.)

* Received by the PGMTT, March, 1959.
† Laboratoire Central de Télécommunications.

Theoretical and experimental studies of microwave delay line for high power were made by the Research Institute of National Defence, Stockholm 80, Sweden.

B. T. Henoch, "Investigation of the disc-loaded and helical waveguide." *Trans. Roy. Inst. Technol., Stockholm*, Sweden, no. 129, 1958. (In English.)

The study of circular waveguides has been carried on.

After the propagation of plane waves in an infinite space, of lamellar structure, the propagation in a waveguide of the same structure has been studied, and application has been made to circular guide.

M. Jouguet, "Propagation dans les systèmes à structure discontinue et périodique et application aux guides d'ondes." *Câbles et Trans.*, no. 1, pp. 23–26; janvier, 1958. (In French.)

Calculation of phase and amplitude distortion in a TE_{01} wave transmission in a circular guide has been undertaken.

M. Jouguet, "Sur les effets de la distorsion d'amplitude et de phase dans les guides d'ondes." *Onde Elect.*, no. 376 bis, tome 1, pp. 119–123; août, 1958. (In French.)

A French firm, Les Câbles de Lyon, has checked experimentally the results obtained in the preceding calcu-

lation. They have more specially studied the propagation in waveguides with walls of helically-wound wire, the difficulties encountered when passing through the bends, and the attenuation measurements on short lengths of guides.

J. Bendayan, "Contribution à la technique future des télécommunications: Recherches effectuées sur les guides d'ondes circulaires en vue de la transmission de l'onde TE_{01}." *Onde Elect.*, no. 376 bis, tome 1, pp. 193–202; août, 1958. (In French.)
G. Comte, A. Ponthus, "Guides d'ondes éolotropes à structure filtrante continue pour la propagation du mode TE_{01}." *Onde Elect.*, no. 376 bis, tome 1, pp. 167–172; août, 1958. (In French.)
F. de Carfort, J. M. Paris, "Franchissement des coudes par des guides d'ondes circulaires utilisant le mode TE_{01}." *Onde Elect.*, no. 376 bis, tome 1, pp. 173–178; août, 1958. (In French.)
J. Bendayan, G. Comte, "Procédés de mesure de l'affaiblissement de courtes longueurs de guides d'ondes circulaires utilisant le mode TE_{01}." *Onde Elec.*, no. 376, bis tome 1, pp. 315–319; août, 1958. (In French.)

A theoretical study of the influence of undulations or diaphragms periodically introduced into a circular waveguide (H_{0n} and E_{0n} waves) has been made in Germany; this study may lead to the realization of delay lines.

G. Piefke, "Wellenausbreitung in einem Blenden—Hohlleiter und einem Gesickten Hohlleiter." *Arch. Elekt. Übertragung*, no. 1, pp. 26–34; janvier, 1958. (In German.)

The problems of clearing bends have also been analysed in Germany. The improvement which can result from the use of variable curvature waveguides has been mentioned.

M. G. Andreasen, "Ausbreitung von Grundwellen in Kreisrunden und quadratischen gebogenen Hohlleitern Konstanter Krümmung." *Arch. elekt. Übertragung*, no. 9, pp. 414–418; September, 1958. (In German.)
M. G. Andreasen, "Synthese eines gebogenen Hohlleiters mit stetigen Verlauf der Krümmung." *Arch. elekt. Übertragung*, no. 10, pp. 463–471; Oktober, 1958. (In German.)

A general formula, previously established, giving the attenuation in a circular guide with absorbent walls, has been discussed in Italy.

L. Caprioli, "L'attenuazione nelle guide circolari con paretti assorbenti." Alta Frequenza, no. 5, pp. 510–527; Ottobre, 1958. (In Italian.)

1.2. *Multiconductors Transmission Lines*

The Cie Générale de Télégraphie sans Fil has carried on the study of centimeter-wave three-plate circuits, constituted by a strip line surrounded by a hollow conductor with flattened rectangular section.

Directional couplers, filters, and hybrid junctions have been realized according to this technique.

A. Muser, "Circuits triplaques en ondes centimétriques." *Onde Élect.*, no. 376 bis, tome 1, pp. 134–139; août, 1958. (In French.)

The Research Institute of National Defence, Stockholm 80, Sweden, had studied partially-ferrite-filled stripline.

P. E. Ljung, "Phase-Shift in Partially Ferrite-filled Stripline." Rept. A 365, 12 pp.; 1958. (In Swedish.)

1.3. *Surface Waveguides*

The work done by the Research Institute of National Defence, Stockholm 80, Sweden, has comprised both cylindrical- and plane-surface waveguides and has involved measurements of certain properties, such as attenuation constant, field intensity decay, and attenuation caused by a step in the thickness of the dielectric coating.

As to cylindrical waveguides, the attenuation caused by bends has been subject to study. Further, a method for the determination of Q with losses present in the transition between a resonator and a transmission line has been developed in connection with the measurements of the attenuation constant.

As to plane-surface waveguides, a method has been developed for the calculation of the launching efficiency and the radiation pattern of a certain type of feed.

Investigations of the properties of a surface waveguide which makes a part of a circular cylinder are going on.

M. Viggh, "Investigations of Surface Waves over Conducting Surfaces." FOA 3-Rept. A 348, 78 pp.; 1958. (In Swedish.)
B. O. Ås, "Investigations of Cylindrical Surface-Wave Transmission Line." A 329, 48 pp.; 1958. (In Swedish.)

Experimentations on surface waveguides have been made in France. Studies on Goubau lines have been made by "Lignes Télégraphiques et Téléphoniques" and by L.C.T.

B. Chiron, "Les guides d'onde de surface et leur place dans l'ensemble des lignes de transmission en hyperfréquence." *Onde Elect.*, no. 376 bis, tome 1, pp. 238–244; août, 1958. (In French.)
H. Weill, "Les lignes de surface." *Onde Elect.*, no. 376 bis, tome 1, pp. 231–237; août, 1958. (In French.)

Radio Industrie has examined the means of exciting a surface wave on a conducting plane.

M. Sirel, "Ondes de surface sur un plan conducteur recouvert d'une bande diélectrique." *Onde Elect.*, no. 376 bis, tome 1, pp. 209–224; août, 1958. (In French.)

A study of the propagation in two- or three-dimensional periodical structure media has been made by Cie Générale de Télégraphie sans Fil, with application to the case of artificial crystals and to the case of traveling-wave tubes. The author shows the possibility of a discrete number or of a continuous band of modes at the same frequency.

G. Mourier, "Circuits à structure périodique à deux et trois dimensions. Applications possibles aux tubes à ondes progressives." *Onde Elect.*, no. 371, pp. 95–100; février, 1958. (In French.)

2. Linear Circuits

A device for the measurement of impedances at centimeter wave comprising a variable impedance in combination with a symmetrical hybrid T has been realized by Philips Research Laboratories, Eindhoven, Holland.

The modulus and the argument of variable impedance can be adjusted separately.

F. C. de Ronde "Dispositif de mesure d'impédances en ondes centimétriques, simple et à lecture directe." *Onde Elect.*, no. 376 bis, tome 1, pp. 294–295; août, 1958. (In French.)

Some improved microwave bridges have been realized.

R. Metivier, C. Romiguiere, "Pont multifréquence." *Onde Elect.*, no. 376 bis, tome 1, pp. 309–312; août, 1958. (In French.)
L. R. de Gopegui, "Banco de microondas." *Inst. nac. Electron. Bol. inform. Tech.*, no. 1, pp. 21–27; Enero, 1958. (In Spanish.)

A device giving the complex value of amplification or attenuation of a quadripole by means of a bright spot on a Smith chart has been studied by L. M. Ericsson, Stockholm, Sweden.

H. J. Olzanski, "Vector measurements in the microwave region." *Onde Elect.*, no. 376 bis, tome 1, pp. 302–304; août, 1958. (In English.)

A two-wire line which has been realized for the measurement of permittivities at 1000 MHz, has a very weak radiation field, requires only a small quantity of material, and is easy to manufacture.

P. Borderie, "Réalisation d'une ligne bifilaire pour la mesure des permittivités à 1000 MHz." *J. Phys. Radium*, no. 8–9, pp. 39S–40S; août–septembre, 1958. (In French.)

The principle of a new graphic method for the fast calculation of ϵ and μ of a material from impedance measurements, has been developed at Laboratoire H. F. de la Faculté des Sciences de Grenoble, France.

N. le Junter, "Méthode de calcul rapide de ϵ et μ à partir de mesures d'impédances en hyperfréquences et sa transposition graphique sur abaques." *Onde Elect.*, no. 376 bis, tome 1, pp. 305–308; août, 1958. (In French.)

The resonance curves of an empty reference cavity and of a cavity containing high-pressured gas have been compared by oscilloscopic means.

A. Battaglia, F. Bruin, A. Gozzini, "Microwave apparatus for the measurement of the refraction, dispersion and absorption of gases at relatively high pressure." *Nuovo Cim.*, Ital., no. 1, pp. 1–9; January 1, 1957. (In English.)

Various polarimeters developed for fundamental research can be used directly for circuit studies.

F. Picherit, "Analyseur polarimétrique à double sonde pour la bande des 1000 MHz." *Compt. rend. Acad. Sci.*, no. 6, pp. 911–913; 10 février, 1958. (In French.)
G. Raoult, R. Fauguin, A. Harlon, "Un polarimètre hyperfréquence." *Onde Elect.*, no. 376 bis, tome 1, pp. 327–331; août, 1958. (In French.)

A rapid and rather accurate method allowing the measurement of Q factor reaching 10^3 in the microwave field has been described.

H. Ebert, "Q Messverfahren im Microwellenbereich." *Elektron. Rundschau*, no. 6, p. 203; Juni, 1958. (In German.)

2.1. *Dipoles*

An adaptation method suitable for periodical discontinuity waveguides has been described.

I. Lucas, "Ueber Randglieder zur Anpassung von Hohlleiter Richtungskopplern periodischer Struktur." *Arch. elekt. Übertragung*, no. 2, pp. 91–96; Februar, 1958. (In German.)

A matched load for hollow waveguide has been realized with commercial film resistors.

U. von Kienlin, A. Kuerzl, "Ein Hohlleiterabschluss mit Handelsüblichen Schichtwiderständen." *Nachrichtentech. Z.* no. 3, pp. 138–141; März, 1958. (In German.)

2.2. *Reciprocal Multipoles*

The transmission in a rectangular waveguide loaded with capacitor screen had been studied in the Netherland. This study leads to the realization of compact filters for microwaves.

H. Bosma, "Two-capacitive window in a rectangular waveguide." *Appl. Sci. Res. B.* no. 2, pp. 131–144; 1958. (In English.)
F. A. W. van den Burg, "Transmission in a rectangular waveguide loaded with an arbitrary number of capacitive screens." *Appl. Sci. Res. B.*, no. 3, pp. 153–183; 1958. (In English.)

Directional couplers with longitudinal slot have been the subject of studies in Germany and in France. In the first publication, following a theoretical study, a chart is given for the approximate determination of the coupling according to dimensions. The measure results are in agreement with theory. In the second article, an analogy is shown between thin slot couplers and classical band-pass filters. The methods for the calculation of these filters can be immediately applied to couplers.

E. Schuon, "Eigenschaften und Bemessung des Langschlitz-Richtkopplers." *Arch. elekt. Übertragung*, no. 5, pp. 237–243; Mai, 1958. (In German.)
G. Broussaud, "Couplages entre guides d'ondes—Théorie des coupleurs directifs à fentes minces." *Ann. Radioélect.*, no. 53, pp. 187–199; juillet, 1958. (In French.)

A directional coupler performing the conversion between the TE_{01} mode of a rectangular waveguide and the TE_{01} mode in a circular guide has been studied in Germany. The mode selectivity has been calculated, and the mode purity has been measured.

A. Jaumann, "Ueber Richtungskoppler zur Erzeugung der H_{01}—Welle im runden Hohlleiter." *Arch. Elekt., Übertragung*, no. 10, pp. 440–446; Oktober, 1958. (In German.)

In Switzerland, the electric field in a waveguide coupled to the external medium by an aperture in its metallic wall has been calculated, by means of a new method in terms of the field tangential component in the aperture.

J. van Bladel, "Normal modes methods for boundary excited waveguides." *Z. angew. Phys.*, no. 2, pp. 193–202; 25 juillet, 1958.

It has been specified what conditions must be met by a complex square matrix so that it may be considered as an impedance, admittance, or diffusion matrix of a microwave junction which is physically realizable at a given frequency.

G. C. Corazza, G. Zoldan, "Realizzabilita fisica di una giunzione a microonde." *Note Recens. Not.*, no. 4, pp. 445–449; Luglio–Agosto, 1958. (In Italian.)

A mathematical study of the junctions of guides for elliptically-polarized waves has been made by Cie Française Thomson-Houston, by considering the elliptical waves either as two orthogonal rectilinearly-polarized waves or as two contrarotating circularly-polarized waves.

An application of this work to a circularly-polarized wave generator has been made.

A. Gosselin, "Ondes elliptiques et jonctions de guides d'ondes polarisées elliptiquement." *Onde Elect.*, no. 376, bis tome 1, pp. 76–78; août, 1958. (In French.)

A theoretical analysis has been made of the influence of an axial sheet of resistive material connected to the walls, on the transmission properties of a rectangular waveguide.

H. Buseck, C. Klages, "Das homogene Rechteckrohr mit Dämpfungsfolie." *Arch. elekt. Übertragung*, no. 4, pp. 163–168; April, 1958. (In German.)

2.3. *Nonreciprocal Multipoles*

The study of materials used for the realization of nonreciprocal multiples has been carried on.

The factor *g* and the damping coefficient of a ferrite result from resonance experiments made by placing a polycrystalline ferrite sphere into a microwave cavity with linearly-polarized magnetic field.

H. G. Beljers, "Determination of the gyromagnetic ratio and the magnetic resonance damping coefficient of ferrites." *Philips Res. Rep.*, no. 1, pp. 10–16; February, 1958.

The width variation of the absorption curve of iron-yttrium garnet, by substituting Cr^{3+} ions into Fe^{3+} ions, has been studied.

R. Vautier, A. J. Berteaud, "Variation de largeur de la courbe d'absorption du grenat d'yttrium—fer avec substitution de Cr^{3+}." *Compt. rend. Acad. Sci.*, no. 19, pp. 1574–1577; 10 novembre, 1958. (In French.)

The study of wave propagation in a guide containing a piece of ferrite has been carried on.

E. Barzilai, G. Gerosa, "Modes in rectangular guides filled with magnetized ferrite." *Il Nuovo Cimento Serie X*, Università di Roma, Facolta di Ingeneria, Cattedra di Elettronica, vol. 7, p. 685; March, 1958.

J. Soutif,-Guicherd, "Etude de l'effet Faraday paramagnétique." *Ann. Télécommun.*, no. 7–8, pp. 169–185; juillet-août, 1958. *Ann. Télécommun.*, no. 9–10, pp. 222–238; septembre–octobre, 1958. (In French.)

The Research Institute of National Defence, Stockholm 80, Sweden, had also studied waveguides with a hollow dielectric or magnetized ferrite rod inside.

P. E. Ljung, "Effective Permittivity for Hollow Dielectric Inserts in Waveguides." Rept. A 364, 7 pp.; 1958. (In Swedish.)

P. E. Ljung, "Reciprocal Phase-Shift by Means of a Magnetized Ferrite Rod in rectangular Waveguide." Rep. C 239, 10 pp.; 1958. (In Swedish.)

An additional paper on the study of gyrators has been published by "Lignes Télégraphiques et Téléphoniques."

P. M. Prache, "Relations entre les éléments du tenseur de perméabilité complexe." *Câbles et Trans.*, no. 1; 1958. (In French.)

The work done by the Research Institute of National Defence Stockholm 80, Sweden on microwave ferrite components has comprised ferrite material investigations, as well as development of components (isolators, circulators, switches, phase shifters, etc.).

B. Josephson, P. E. Ljung, "Microwave Ferrite." *Ericsson Tech.*, vol. 14, no. 1, pp. 39–70; 1958. (In English.)

P. E. Ljung, "Microwave Load Isolators and Related Components." *Elteknik*, vol. 1, no. 6, pp. 103–108; June, 1958. (In English.)

Theoretical and experimental study has been made of the propagation of 3.2 centimeter TE_{11} waves in a circular cross-section waveguide containing a concentric rod of "N° 4 ferroxcube" longitudinally magnetized by a static magnetic field. The influence of porosity on attenuation has been determined.

J. Snieder, "Ferromagnetic resonance in polycrystalline ferrites." *Appl. Sci. Res. B*, no. 3, pp. 185–232; 1958. (In English.)

A measurement process has been described which relates to the differential phase shift produced by a ferrite phase shifter in a rectangular waveguide. A laboratory phase shifter has been developed.

M. Vadnjal, "Misura dello sfasamento differenziale in sfasatori non reciproci per microonde." *Elettronicca* no. 3, pp. 108–115; 1958. (In Italian.)

3. Non Linear Circuits

An article has been published covering the general theory of nonlinear circuits to be used for frequency conversion.

S. Duinker, "General properties of frequency—converting networks." *Philips Res. Reps.* 13, 79–97 and 101–148; 1958.

4. Quantum Mechanical Amplifiers

A survey of the theory of the molecular amplifier has been published, as well as the main disclosed results.

G. Goudet, "La production et l'amplification d'oscillations radio-électriques à l'aide de transitions moléculaires ou atomiques." *Onde Elect.*, vol. 38, no. 379, pp. 671–686; octobre, 1958. (In French.)

Many firms are interested in this question, but few results have been published.

Any quantum mechanical system which permits a radiative transition between two energy levels will allow a multiple quanta transition; and, in addition, at least one of the energy levels shows a finite average of the electrical or magnetic dipole moment.

The possibility has been demonstrated of obtaining a stimulated emission at a ω frequency by a two-level system in which the difference of energy is $h\omega_0$, by applying to the system a radiation field at the frequency $\omega' = \omega_0 + \omega$.

A. Javan, "Transitions à plusieurs quanta et amplification maser dans les systèmes à deux niveaux." *J. Phys. radium*, no. 11, pp. 806–808; novembre, 1958. (In French.)

A more general study has been made of transitions involving several quanta.

J. M. Winter, "Etude théorique et expérimentale des transitions à plusieurs quanta entre les sous-niveaux Zeeman d'un atome." *J. phys. radium*, tome 19, no. 11, pp. 802–805; novembre, 1958. (In French.)

5. Noise

An article published by the Philips Research Laboratory, Eindhoven, Holland, may be of importance for noise studies with microwaves.

W. Verwey, "Probe measurements of electron temperature in the positive column of a rare gas discharge and correlation with microwave noise."

R. C. Terzo, Congr. Int. Fenomeni d'Ionizazione nei Gas Venezia, pp. 1115–1130. (In English.)

Report of Advances in Microwave Theory and Techniques in Japan—1958*

ISAO SOMEYA†

A number of papers were presented in the fields of microwave art from companies and universities. In this article, short abstracts of some selected papers will be mentioned.

Shimizu presented a method of describing the electromagnetic TE_{01} field within a curved waveguide of a constant but arbitrary section. He expressed Maxwell's equations converted into telegraphic equations and the bend problem which may be solved by using the techniques of coupled transmission lines.

Y. Shimizu, "Transmission of circular TE_{01} wave in curved circular waveguides," *J. Inst. Elect. Commun. Engrs. of Japan*, vol. 41, no. 1, pp. 29–35; 1958.

Oguchi and Kato discussed the characteristics of the TE_{01}, TM_{11}, and TE_{1m} mode waves in a curved circular waveguide taking their mutual couplings into account.

B. Oguchi and M. Kato, "The effects of the circular TE_{1m} waves on the propagation of the circular TE_{01} wave in curved waveguide," *ibid.*, vol. 41, no. 1, pp. 35–42, 1958.

Kumagaya discussed problems concerning the reflection and mode conversions of the TE_{01} mode produced at a position where the diameter of a multimode circular waveguide varied discontinuously.

S. Kumagaya and N. Kumagaya, "Discontinuity in the cylindrical waveguide," *ibid.*, vol. 41, no. 5, pp. 556–559; 1958.

Kumagaya and two coworkers discussed theoretically the electromagnetic waves in a circular waveguide to which is added a circular ferrite ring.

S. Kumagaya and N. Kumagaya, and K. Takeuchi, "Ferrite loaded nonreciprocal cylindrical waveguide for circular electrical wave," *ibid.*, vol. 41, no. 10, pp. 965–971; 1958.

Noda published a paper concerning characteristics of a delay compensator which is composed of a magic T and of a resonant circuit. He discussed several delay characteristics and loss performances for a trial set experimentally and theoretically.

K. Noda, "Microwave delay compensator," *ibid.*, vol. 41, no. 3, pp. 221–228; 1958.

Fukumitsu presented a paper concerning measuring procedures for long and symmetrical networks by the S-curve method.

T. Fukumitsu "Measuring procedure for long and symmetrical network by S-curve," *ibid.*, vol. 41, no. 12, pp. 1221–1225; 1958.

He discussed the four terminal circuit constant by the S-curve method which is formally applied only to a lossless circuit and can be extended to a lossy symmetric circuit.

Asano and two coworkers presented a paper concerning a coaxial directional coupler which is made for very wide band of 400–7000 mc.

T. Asano, J. Morishoma, and R. Koike, "Conical directional coupler," *ibid.*, vol. 41, no. 6, pp. 626–632; 1958.

Saito presented two papers on the electron beam, especially on the space charge wave on the electron beam.

S. Saito, "New method of measuring the noise parameters of the electron beam by using selective beam coupler," *ibid.*, vol. 41, no. 6, pp. 605–610; 1958.
S. Saito, "Parametric amplification of space charge waves on a thin electron beam," *ibid.*, no. 11, pp. 1113–1120; 1958.

In the former paper, the author treated the minimúm noise figure of TWT which has been a problem of great interest for some years past. He tried the measurement of beam noise by using a selective beam coupler devised by him, along an electron beam and succeeded in measuring correlation coefficient between current and velocity noises. In the latter paper, he dealt with a theory of a one-dimensional beam-type parametric amplifier with the very thin beam. He gave basic equations and applied the analysis to two cases, namely inverted and noninverted, and presented an approximate equivalent circuit comprising lumped inductances and lumped voltage-dependent capacitances.

* Manuscript received by the PGMTT, March, 1959.
† Elec. Commun. Lab., NTT, Tokyo, Japan.

A Ferrite Cutoff Switch*

R. F. SOOHOO†

Summary—The theory and operating characteristics of a new type of high performance reflective switch is given. It utilizes the cutoff phenomenon in transversely-magnetized ferrites. The insertion loss of the device is 0.4 db and over 60 db within the 8.8 to 9.5 kmc band when the ferrite is demagnetized and magnetized respectively. The reflection coefficient of the switch in the "off" state is more than 90 per cent over this same band. In contrast to most other ferrite devices, it is of the reflective rather than the absorptive type. Furthermore, it has the unique property that its operating bandwidth is determined mainly by the magnitude of the applied field. Possible applications of the device in antenna switching and as a tunable cutoff filter will be discussed.

Introduction

An extensive study of the cutoff phenomena in a longitudinally-magnetized ferrite-filled circular waveguide has been made by Suhl and Walker,[1] and the results have been summarized by Kales.[2] They have shown that there are three kinds of cutoffs. The first is similar to the cutoff which occurs if the circular waveguide is filled with a homogeneous, isotropic medium of the appropriate equivalent permeability. The second and third types were shown to occur when $\mu \pm K = 0$ and $\mu = 0$, respectively. Calculated values of the propagation constant for several special cases are given by Gamo.[3] The author[4] had also made some cutoff studies for circular waveguides partially filled with ferrite.

In a previous publication,[5] the author theoretically treated the cutoff phenomenon in transversely-magnetized ferrites. In this paper the theory will be extended and utilized in the design of a reflective switch. This switch will be shown subsequently to have an "off" to "on" attenuation ratio of over 150/1 in db over an 8 per cent band. The attenuation as a function of frequency at constant applied dc fields will be studied. The electromagnetic field configuration in the waveguide in the "on" and "off" states will also be determined to achieve a better understanding of the cutoff phenomena involved. Because of its reflective nature, the switch has many interesting applications some of which will be discussed.

The cutoff frequency ω_c of a waveguide of width L loaded by a ferrite slab of thickness δ placed against the guide wall and extended from top to bottom of the waveguide (see Fig. 1) was shown to be determined by the transcendental equation[5]

$$-\sqrt{\frac{\epsilon_0}{\rho\epsilon}} = \frac{\cot\left[\omega_c\sqrt{\mu_0\epsilon}\sqrt{\frac{1}{\rho}}\,\delta\right]}{\cot\left[\omega_c\sqrt{\mu_0\epsilon}(L-\delta)\right]} \tag{1}$$

where ϵ is the dielectric constant of the ferrite, and $1/\rho$, the equivalent permeability, is given by

$$\frac{1}{\rho} = \frac{\mu^2 - K^2}{\mu_0\mu} = \frac{(1+\chi_{xx})^2 + \chi_{xy}^2}{1+\chi_{xx}} \tag{2}$$

and

$$\chi_{xx} = \frac{4\pi M_s\gamma(\gamma H_i)}{(\gamma H_i)^2 - \omega^2}$$
$$\chi_{xy} = \frac{-j\omega\gamma 4\pi M_s}{(\gamma H_i)^2 - \omega^2} \tag{3}$$

where

$4\pi M_s$ = saturation magnetization of the ferrite
γ = gyromagnetic ratio of the electron, and
H_i = internal magnetic field in the ferrite.

Eq. (1) was derived by setting $\gamma = 0$ in the transcendental equation involving γ which in turn was obtained by solving the boundary value problem[6]

$$\frac{k_a}{\rho}\cot k_a(L-\delta) + k_m\cot(k_m\delta) = \frac{-\gamma}{\theta} \tag{4}$$

where

$$k_a^2 = \omega^2\mu_0\epsilon_0 + \gamma^2$$
$$k_m^2 = \omega^2\mu_0\epsilon\frac{1}{\rho} + \gamma^2, \text{ and}$$
$$\theta = \frac{\mu}{-jK} = \frac{1+\chi_{xx}}{\chi_{xy}}. \tag{5}$$

The cutoff frequency ω_{ca} of the dominant mode has been obtained from (1) for $L = 0.700''$, $\delta = 0.090''$, and plotted in Fig. 1. As was shown by Soohoo,[5] there are two cutoff frequencies involved in the solution of (1), one, ω_{ca}, being above and the other, ω_{cb}, being below the resonance frequency of the ferrite. Only the cutoff frequency ω_{ca} will be of concern here.

* Manuscript received by the PGMTT, November 25, 1958; revised manuscript received, February 9, 1959.

† Cascade Res. Corp., Los Gatos, Calif.; presently at M.I.T. Lincoln Lab., Lexington, Mass.

[1] H. Suhl and L. R. Walker, "Topics in guided-wave propagation through gyro-magnetic media, part I, the completely filled cylindrical guide," *Bell Sys. Tech. J.* vol. 33, pp. 579–659; May, 1954.

[2] M. L. Kales, "Topics in guided-wave propagation in magnetized ferrites," Proc. IRE, vol. 44, pp. 1404–1405; October, 1956.

[3] H. Gamo, "The Faraday rotation of waves in a circular waveguide," *J. Phys. Soc.* (*Japan*), vol. 8, pp. 176–182; March/April, 1953.

[4] R. F. Soohoo, "Higher-Order Mode Propagation in Ferrite Devices and Wide-Band Tunable Ferrite Microwave Filters," presented at the Conf. on Microwave Ferrites and Related Devices and Their Applications, 1957 Annual PGMTT meeting of the IRE, New York, N. Y.; May, 1957.

[5] R. F. Soohoo, "Cutoff phenomena in transversely magnetized ferrites," Proc. IRE, vol. 46, pp. 788–789; April, 1958.

[6] B. Lax, K. J. Button, and L. M. Roth, "Ferrite phaseshifters in rectangular waveguide," *J. Appl. Phys.*, vol. 25, pp. 1413–1421; November, 1954.

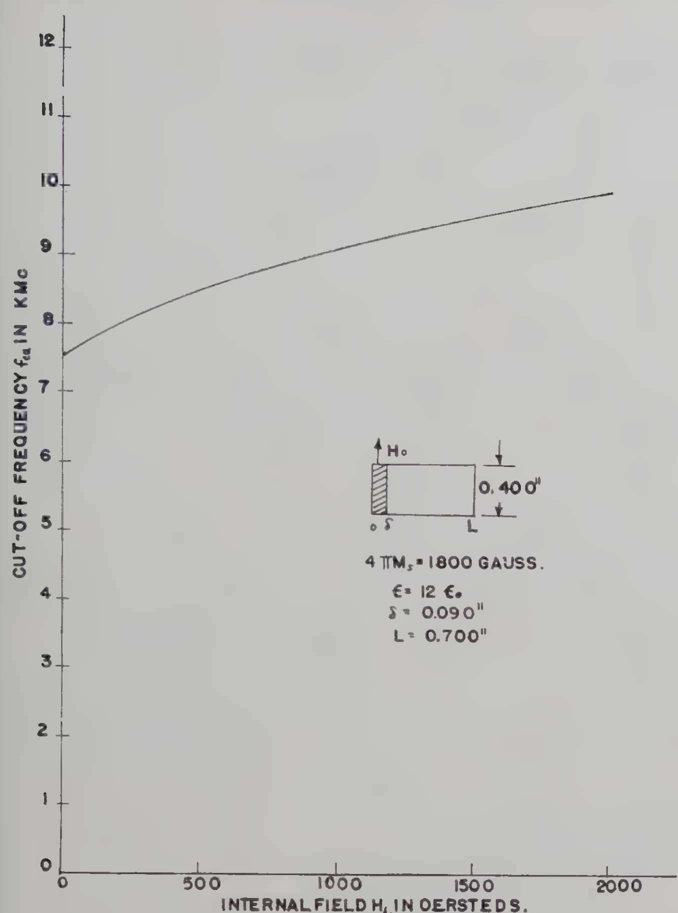

Fig. 1—Cutoff frequency of ferrite-loaded waveguide vs internal magnetic field.

From Fig. 1, it is immediately seen that if the ferrite is demagnetized, the loaded waveguide will transmit any frequency above 7.5 kmc. If an internal magnetic field of 1500 gauss, for example, is applied to the ferrite, the cutoff frequency f_{ca} of the structure will be moved up to 9.8 kmc. Thus, within the 7.5 to 9.8 kmc band, the device can be made to reject rather than transmit the incident energy by applying merely a magnetic field of the appropriate magnitude to the ferrite.

Attenuation and Reflection

The reactive attenuation below cutoff for any empty lossless waveguide could be obtained from (5). In general,

$$\gamma = \alpha + j\beta = \frac{2\pi f_c}{c}\sqrt{1 - \left(\frac{f}{f_c}\right)^2}. \qquad (6)$$

For frequencies below cutoff, $f/f_c < 1$, γ is real and we have for the reactive attenuation per unit length in db

$$\alpha = \frac{54.5 f_c}{c}\sqrt{1 - \left(\frac{f}{f_c}\right)^2}. \qquad (7)$$

Eq. (7) could be plotted as a function of frequency f with f_c as a constant parameter; when $f/f_c < 1$, α decreases continuously with increasing frequency and reaches zero when $f/f_c = 1$. When $f/f_c > 1$, α is zero for all values of f.[7]

When the waveguide is loaded by a demagnetized ferrite slab against the guide wall, α must be determined from the transcendental (4) with $\rho = 1$ and $\theta = 0$. Solving (4) and (5) simultaneously, we obtained an α vs f curve for a particular lossless ferrite-waveguide configuration ($L = 0.700''$, $\delta = 0.090''$). It can be shown that the appearance of this curve is similar to that of the empty waveguide case; the introduction of a lossless dielectric would not change the shape of the $\alpha - f$ curve.

In actual cases, the waveguide and ferrite are not lossless and the α's will always remain finite with the general occurrence of a "tail" beyond the projected cutoff frequency.[7]

When the ferrite is magnetized, $1/\rho$ deviates from unity and θ takes on finite values. The exact solution of (4) becomes rather complicated. However, experimental results (Fig. 2) have shown that the attenuation behavior of the loaded waveguide when the ferrite is magnetized is similar to that of the demagnetized state. The projected intersections (dotted) of the attenuation curves for constant dc fields with the horizontal frequency axis give approximately the cutoff frequency at the respective value of H_0 where H_0 is the applied dc magnetic field. The reflection coefficient of the device at the various dc fields are plotted in Fig. 3. It is seen that over a certain frequency band the device transmits almost all of the incident energy when the ferrite is demagnetized but rejects a large portion of it when magnetized. Thus, Figs. 2 and 3 indicate clearly that the cutoff frequency of the device is moved upward with increasing dc fields as predicted by Fig. 1.

The cutoff frequency at zero applied field is seen to be higher than the 7.5 kmc value predicted by Fig. 1. However, it must be remembered that the internal field of Fig. 1 in general is composed of the applied, demagnetizing, and anisotropy fields. Furthermore, the effective permeability of the ferrite at zero field could be appreciably different from 1;[8] the value of unity for the effective permeability has been assumed above. When comparisons are made between the experimental cutoff frequencies of Figs. 2 and 3 and the theoretical ones of Fig. 1, one must bear in mind the difference between internal and applied fields mentioned above.[5] Moreover, the ferrite is not lossless as assumed in the theoretical treatment so the idealized theory should be considered to some measure qualitative. (See "Discussion" Section.)

Field Configuration

From the expressions given for the electric field by Lax, *et al.*,[6] the electric field distribution in the guide

[7] S. Ramo and J. R. Whinnery, "Fields and Waves in Modern Radio" (1st ed.). John Wiley and Sons Inc., New York, N. Y.; p. 373; 1944.

[8] R. C. LeCraw and E. G. Spencer, "Measurement of the components of the permeability of ferrites," 1956 IRE Convention Record, pt. 5; pp. 66–74.

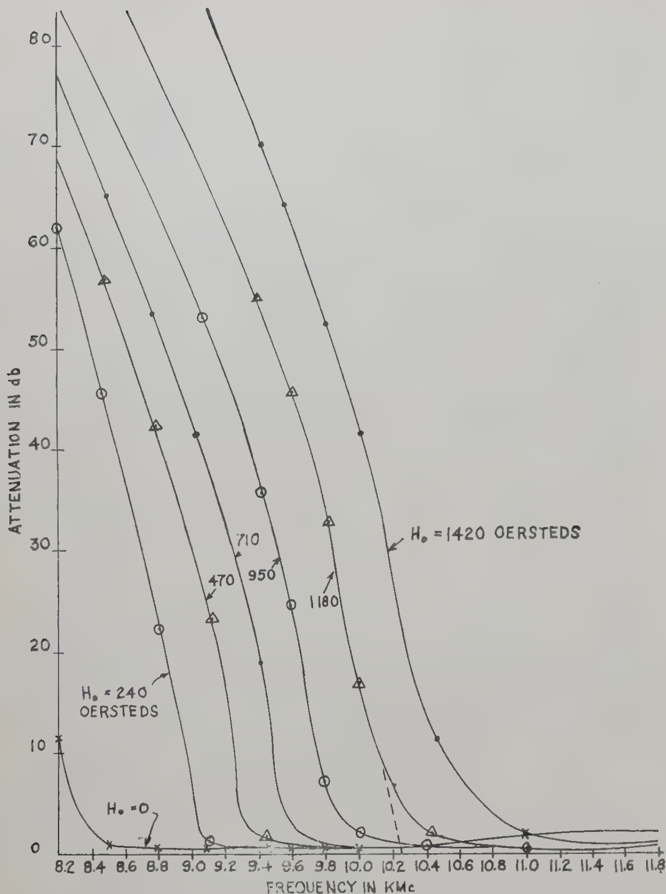

Fig. 2—Attenuation of ferrite loaded waveguide at constant applied fields vs frequency.

$$4\pi M_s = 1800 \text{ gauss}$$
$$\epsilon = 12\epsilon_0$$
$$\delta = 0.090 \text{ inch}$$
$$L = 0.700 \text{ inch}$$
Length of ferrite = 2.75 inches.

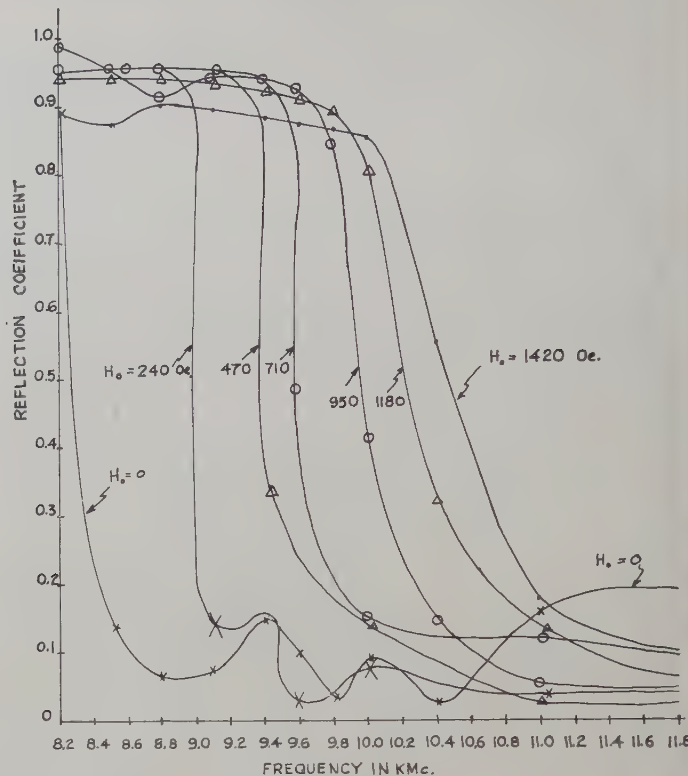

Fig. 3—Reflection coefficient of ferrite loaded waveguide at constant applied fields vs frequency.

$$4\pi M_s = 1800 \text{ gauss}$$
$$\epsilon = 12\epsilon_0$$
$$\delta = 0.090 \text{ inch}$$
$$L = 0.700 \text{ inch}$$
Length of ferrite = 2.75 inches.

cross section can be obtained. This has been done for the empty waveguide case and the ferrite loaded case with both zero field and at an internal field corresponding to cutoff at 9.1 kmc (Fig. 4); the latter is reciprocal as the device is now exactly at cutoff ($\gamma=0$). The cutoff frequency of the empty waveguide is 8.45 kmc while that of the ferrite loaded waveguide at zero field is lowered to 7.5 kmc. It is interesting to note that the electric field is pulled over to the ferrite when it is demagnetized due to dielectric loading effects while at an internal field corresponding to cutoff, the electric field is pushed out of the ferrite making the guide width effectively smaller.

The electric field intensity at the center of the waveguide, in the direction of propagation when the ferrite was demagnetized and when it was magnetized by an applied field of 1300 oersteds after a short was placed at the output end, has been monitored and plotted in Fig. 5. When the ferrite is demagnetized and the device terminated in a matched load, the VSWR is equal to 1.05; this low VSWR was achieved by tapering the ferrite at both ends. It is seen that for the zero field case, the standing wave pattern has maxima and minima of about equal spacing and respective amplitudes along the guide signifying propagation. For the $H_0=1300$ oersted case, the electric field decays rapidly and exponentially with distance with no maxima or minima observed, and this pattern remained essentially unchanged even when the short was replaced by a matched load. This supports the contention that the phenomena is predominately a cutoff one. The fact that the higher order TE_{20} mode is beyond cutoff for the experiment just described can be shown by obtaining the second root of (1).

Operating Characteristics

The attenuation and VSWR at zero field and at 1300 oersted field of an actual switch built using the principle enumerated above is plotted in Fig. 6. It is seen that from 8.8 to 9.5 kmc the attenuation at zero field is 0.4 db, while that at 1300-oersted field is over 60 db. Thus the "off" to "on" attenuation ratio is over 150 to 1 (in db) over an 8 per cent band. Similarly, a ratio of over 60 to 1 (in db) could be obtained for a 16 per cent band (8.5 to 10 kmc). The VSWR is seen to be quite high and reasonably low when the switch is in the "off" and "on" states, respectively. We observed from Figs. 2 and 3 that the bandwidth or attenuation ratio of the switch can be increased further by applying a magnetic field of higher than 1300 oersteds. Conversely, for a smaller bandwidth, a lower applied field value is re-

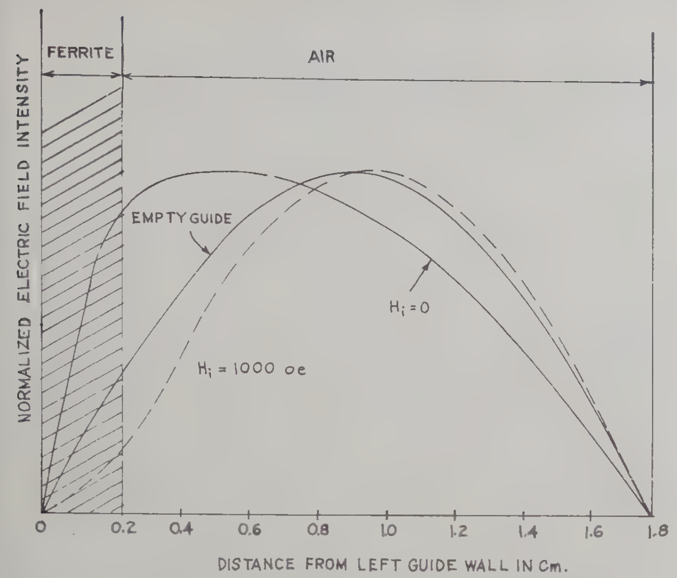

Fig. 4—Normalized electric field intensity vs distance from guide wall of ferrite loaded waveguide.

$4\pi M_s = 1800$ gauss
$\epsilon = 12\epsilon_0$
$\delta = 0.090$ inch
$L = 0.700$ inch.

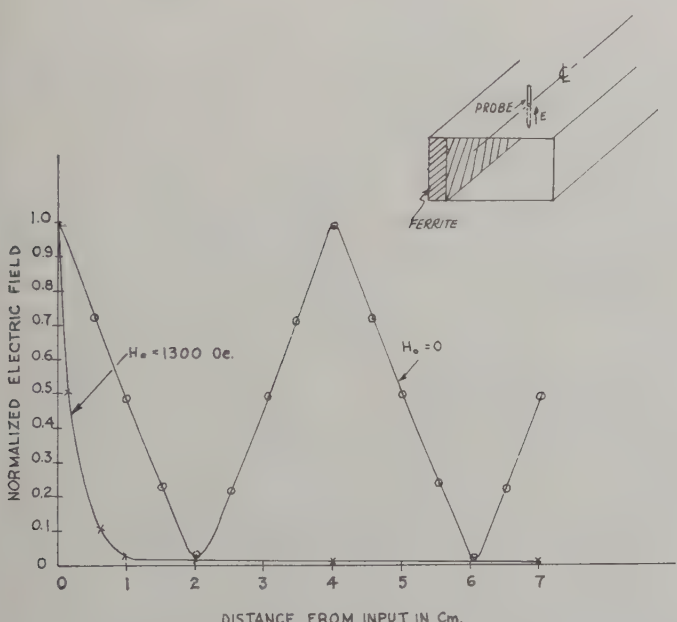

Fig. 5—Normalized electric field intensity at center of waveguide vs distance in the direction of propagation of ferrite loaded waveguide.

$4\pi M_s = 1800$ gauss
$\epsilon = 12\epsilon_0$
$\delta = 0.090$ inch
$L = 0.700$ inch.

quired. This dependence of bandwidth and attenuation ratio upon applied field magnitude is one of the novel features of this type of device.

The switching coil has a resistance of 20 ohms and an inductance of 9 mh. Thus the driving power required to give 1 ampere is rather large and switching time would be limited to the millisecond range. To reduce this power requirement, one might reduce the height of the

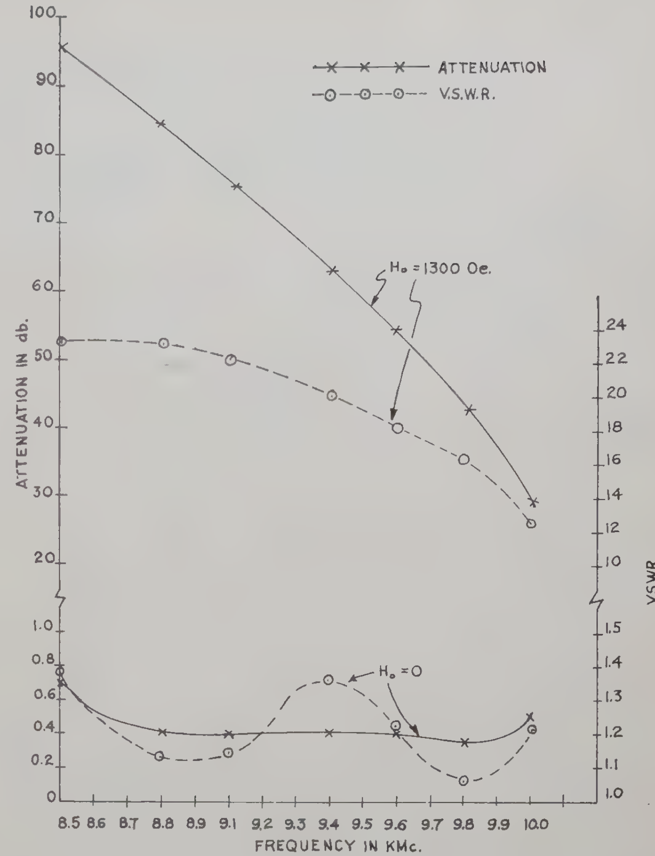

Fig. 6—Attenuation and VSWR of cutoff switch vs frequency

$4\pi M_s = 1800$ gauss
$\epsilon = 12\epsilon_0$
$\delta = 0.090$ inch
$L = 0.700$ inch
Length of ferrite = 2.75 inches.

waveguide. To minimize eddy current effects produced when a transverse magnetic field is applied from top to bottom of the waveguide, a ferrite rectangular ring magnetized by a single turn of wire arranged as shown in Fig. 7 may be used.[9,10] The legs of the ferrite ring that is against the top and bottom guide wall are used to close the magnetic circuit to reduce the required field for switching. Cutoff phenomena can be shown to occur with a slab against each side wall as well as with a slab against only one side wall. The waveguide may be made of nonmetallic material such as phenolic and coated on the inside with about 0.0005 inch of silver to lower eddy current losses still further. Preliminary results show that this is a very promising approach; it has been found that whereas a high current is required because of the single turn of wire used, the required switching voltage is very small, and the result is a considerable reduction in switching power. Using this method it is expected that switching times of the order of μs could be obtained.

It should be noted again here that if the switch were to operate over a very narrow bandwidth the magnetic

[9] B. N. Enander, "A new ferrite isolator," Proc. IRE, vol. 44, pp. 1421–1430; October, 1956.

[10] L. M. Silber and M. A. Treuhaft, "Low-Energy Ferrite Switch," presented at the Annual PGMTT Meeting at Stanford, Calif.; May, 1958.

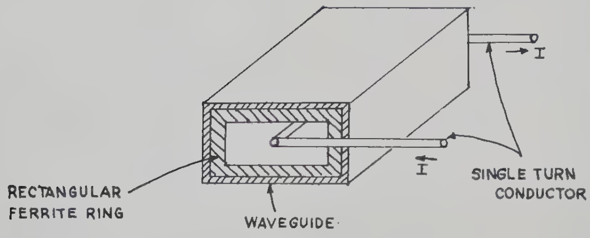

Fig. 7—A scheme for rapid switching of cutoff attenuator.

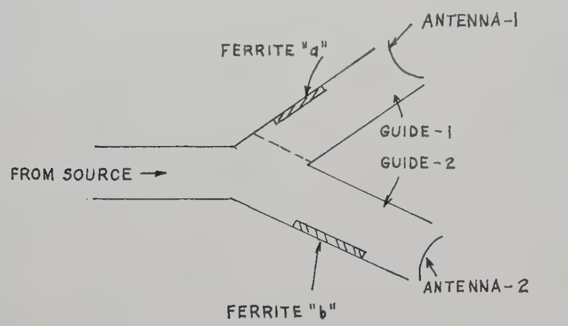

Fig. 8—Application of cutoff attenuator in antenna switching.

field requirement would be small and switching power required would be much reduced. If the location of the frequency band is to be changed, the guide width may be adjusted so that the loaded guide at zero field just cuts off at the low end of the operating band to reduce switching field requirement.

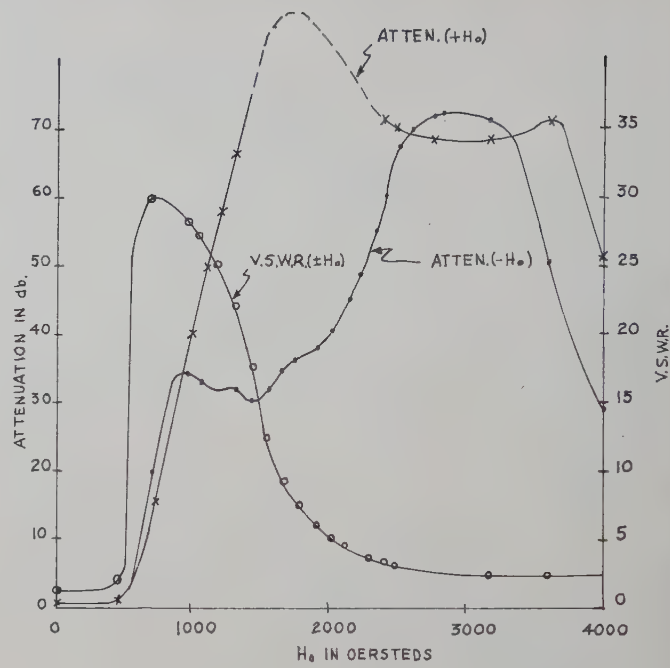

Fig. 9—Attenuation and VSWR of cutoff switch vs applied field.

$4\pi M_s = 1800$ gauss

$\epsilon = 12\epsilon_0$

$\delta = 0.090$ inch

$L = 0.700$ inch

Length of ferrite $= 2.75$ inches

$= 9.1$ kmc.

Applications

This switch can obviously be used as a tunable cutoff filter. It is seen from Fig. 2 that the attenuation varies almost linearly with frequency over a substantial bandwidth.

The switch could be used to switch from one antenna to the other as shown in Fig. 8.[11] When ferrite "a" is magnetized, waveguide 1 is cut off presenting an apparrent short at the dotted plane while waveguide 2 whose ferrite "b" is demagnetized transmits and therefore energy is radiated out of antenna 2. If now ferrite "b" is magnetized while ferrite "a" is demagnetized, energy will go out antenna 1. Experiments have shown that a transmission loss of about 1 db for the "on" antenna and an attenuation of over 60 db for the "off" antenna over about 8 per cent band is possible.

Since the attenuation of the switch goes from a constant low value up to the high value rather linearly, it can be used in an AGC system for high stability (see Fig. 9).

[11] Whereas there is a physical resemblance of this switch to the Tee and Y circulator, the power in this device does not "circulate." For example, if energy is fed in at the source arm when ferrite "a" is appropriately magnetized, it will go out of antenna 2. On the other hand, energy cannot pass freely from antenna 1 to the source due to the cutoff phenomena in the waveguide containing ferrite "a." For reference on Tee and Y circulators, see W. E. Swanson and G. J. Wheeler, "Tee circulator," WESCON CONVENTION RECORD, vol. 2, pt. 1, pp. 151–156, 1958; and H. Chait and T. Curry, "The Y Circulator," Fourth Conf. on Magnetism and Magnetic Materials, Philadelphia, Pa.; November 17–20, 1958.

Discussion

The attenuation and reflection coefficients of the switch at 9.1 kmc are plotted for the two different directions of applied field in Fig. 9. There are several interesting features shown. First of all, the reflection coefficient and therefore the reflected power is almost the same for the two directions of magnetic field. However, the attenuation may be quite different for the opposite field orientations. This may be due in part to the fact that the RF magnetic field is in general elliptically polarized at the ferrite and that one sense of polarization should exhibit resonance while the other sense should not. It is noted also that the VSWR remains high in the region of H_0 between 500 and 2000 oersteds signifying cutoff but decreases to a relatively low value for a value of H_0 above 2000 signifying absorption. This band rejection characteristic and its relationship to ferromagnetic resonance has been previously discussed by the author.[5]

The reflection coefficient data of Fig. 3 could account for only part of the high attenuation depicted by Fig. 2. The total attenuation is due to a combination of cutoff and its resultant reactive attenuation as well as a resistive type of attenuation in the ferrite.

Acknowledgement

The author wishes to thank D. Chang and M. Gan who aided with the calculations and measurements for this paper.

Propagation Constants of Circular Cylindrical Waveguides Containing Ferrites*

H. K. F. SEVERIN†

Summary—**The paper describes some results of a theoretical and experimental investigation of the propagation behavior of circular cylindrical waveguides containing longitudinally magnetized ferrite rods. As long as no concentration of the RF-magnetic field in the ferrite occurs, theoretical expressions for the propagation constants can be given by applying first-order perturbation method. Faraday rotation measurements have been made between 5000 and 7600-mcs using commercially available ferrites. Reasonable agreement between theoretical and experimental results has been found for a thin axial ferrite rod in an air-filled guide in both cases of saturated and nonsaturated ferrites. Energy concentration in the ferrite determines the propagation behavior in the partially filled waveguide. This effect can be enhanced by surrounding the ferrite rod with a dielectric tube. For a given rod diameter and permittivity of the tube there is an optimum outer diameter of the tube for which the Faraday-rotation becomes maximum.**

Introduction

THE first microwave applications of ferrites used a round waveguide containing an axial ferrite pencil in an axial magnetic field. The microwave Faraday effect was demonstrated by Hogan[1] in 1952, and a number of waveguide components have been developed which utilize this phenomenon. Such Faraday rotation devices continue to be of great practical importance.

In this paper some results are described of a theoretical and experimental investigation of circular waveguides containing longitudinally magnetized ferrites. One aim is to provide an improved and more quantitative understanding of the propagation behavior of this type of waveguide structure and thereby aid the design of Faraday rotation wave guide components.

Another aim is to find out how such devices can be optimized; *e.g.*, for high-speed switches or modulators the main problem is to obtain rapid build-up and decay of magnetizing current. To achieve this, it is necessary to use a minimum number of turns on the magnetizing coil. Furthermore the demagnetizing field should be kept as small as possible. The application of long thin ferrite rods having small demagnetization factors leads necessarily to longitudinal field structures, *i.e.* Faraday rotation devices. To get along with low magnetizing current the Faraday rotation for a given magnetic field intensity should be optimum.

The special cases of

1) a circular waveguide filled with ferrite,
2) a circular waveguide filled with an axial ferrite rod or tube and dielectric of the same permittivity as the ferrite, and
3) a circular waveguide filled with a thin axial ferrite rod or tube and dielectric of different permittivity

are investigated in detail, because these are the only cases where explicit theoretical expressions for the angle of rotation can be obtained so far. By means of these results the general case of the partially filled waveguide can also be understood and its behavior estimated within certain limits of accuracy sufficient for many practical cases. These considerations are confirmed by experimental results, where the angle of rotation as function of the rod diameter is measured for magnetized and saturated ferrites.

For a partially ferrite-loaded guide, the surrounding medium of dielectric can effect both an increase and a decrease of the angle of rotation depending on the diameter of the ferrite rod, the dimensions of the surrounding dielectric tube and its permittivity. In a detailed experimental investigation the influence of these parameters has been studied. For a certain ferrite rod and a certain permittivity of the surrounding dielectric tube there is always an optimum diameter for the tube.

Longitudinally Magnetized Ferrites in Circular Waveguides

The fact that the permeability is a scalar quantity for circularly polarized fields in an infinite ferrite medium means that the normal modes of propagation along the direction of magnetization are right and left circularly polarized waves. For the considerably more complicated structure of a round rod of ferrite enclosed axially by a circular waveguide carrying the dominant wave, it may still be true that circularly polarized waves are the normal modes.

The waveguide Faraday effect consists of the rotation of the whole field pattern of the "linearly polarized" TE_{11}-wave, where the diametral plane of maximum electric field intensity is defined as plane of polarization. Faraday rotation of an angle θ means a rotation of the plane of polarization and consequently of the whole field pattern by that angle. In the round guide two linearly polarized TE_{11}-waves can exist in independent states of polarization, those planes being perpendicular to each other. Because of this twofold degeneracy there are also circularly polarized TE_{11}-waves possible.

For a circular waveguide containing an axial ferrite rod of arbitrary radius and magnetization an extensive

* Received by the PGMTT, March 30, 1959. The work on this paper was performed at RCA Labs., Princeton, N. J., in 1956, during a leave of absence from the University of Goettingen.

† Philips Laboratories, Hamburg, Germany.

[1] C. L. Hogan, "The microwave gyrator," *Bell Sys. Tech. J.*, vol. 31, pp. 1–31; 1952.

analysis of the propagation behavior has been made by van Trier[2] and by Suhl and Walker.[3] These investigations show that wave forms with vanishing longitudinal component of E or H do not exist. Far from ferromagnetic resonance, however, this sixth field component is one order of magnitude smaller than the other components. Therefore, the mode spectrum may be divided into two groups, namely quasi-TE- and quasi-TM-modes, which become TE- and TM-waves when the anisotropy is gradually removed. For the dominant mode the following picture of Faraday rotation can be given. Suppose a circular cylinder of gyromagnetic medium extends along the axis of the guide for $z>0$ and a linearly polarized TE_{11}-wave is incident from $z=-\infty$. This wave may be decomposed mathematically into right and left circularly polarized TE_{11}-waves of equal amplitudes and propagation constants. The wave transmitted through the anisotropic medium will consist of two circularly polarized quasi-TE_{11}-waves. As long as the anisotropy is small, the amplitudes of the two components will be nearly the same, and the slight difference in the imaginary parts of the propagation constants will result in a Faraday rotation of the transmitted linearly polarized quasi-TE_{11}-wave. In the case of large anisotropies, however, real and imaginary parts of the propagation constants are different for the two circularly polarized waves, and therefore transmitted and reflected waves are no longer linearly polarized. By measuring the ellipticity of the transmitted wave it can be checked experimentally, whether the presumptions of the calculation are fulfilled by the ferrite loaded waveguide section under test.

Although the authors cited above[2,3] have obtained the general solution to the problem in form of its characteristic equation, owing to the complexity of this transcendental equation, no explicit expression for the propagation constants can be given. In order to avoid lengthy computing programs one may resort to techniques of approximation, *e.g.*, to a perturbation method. That takes as a starting point a situation, the propagation problem of which is solved, and the change in propagation constant due to a slight change in the original state of the system is calculated. For the problems under discussion here, the small change of the state means a slight modification of the permeability or permittivity within certain regions of the system. Such modifications may be caused by the weak magnetization of an originally unmagnetized ferrite filling the waveguide, or by the introduction of a slender pencil into the originally empty guide. The propagation constant for a magnetized ferrite rod of arbitrary radius, coaxial with a circular waveguide, the space between guide wall and rod being filled with an isotropic dielectric of the same permittivity as the ferrite, can also be calculated by means of perturbation theory. The discussion of these problems opens the understanding for the practically more important case of a ferrite rod of any radius in an air-filled guide.

Consider a waveguide with perfectly conducting walls enclosing a lossless medium of the tensor permeability $[\mu]$ and permittivity $[\epsilon]$. Let the cutoff frequency be ω_c and let the electromagnetic field of the corresponding mode be characterized by the vectors $\boldsymbol{e}$ and $\boldsymbol{h}$. Provided that the cutoff frequencies of other modes are not too close to ω_c a modification of the material constants $[\Delta\epsilon]\ll[\epsilon]$ and $(\Delta\mu]\ll[\mu]$ leads in first-order approximation to the change of cutoff frequency given by the expression[4,5]

$$-\frac{\Delta\omega_c}{\omega_c}\quad\frac{1}{2}\,\frac{\displaystyle\int_F\!\!\int\left\{[\Delta\epsilon]ee^* + Z^2[\Delta\mu]hh^*\right\}df}{\displaystyle Z^2\int_F\!\!\int [\mu]hh^*df}, \tag{1}$$

which follows from the equality of the time averages of stored electrical and magnetic energy. The integration is performed over the cross section F of the guide, and Z stands for the characteristic impedance of free space.

$$Z = \sqrt{\frac{\mu_0}{\epsilon_0}} = 377 \text{ [ohms]}.^6$$

Throughout this paper it is presumed that the circular waveguide fully or partially loaded with a coaxial ferrite rod will not propagate higher order modes, but carries only the dominant mode. For the unperturbed guide the components of the magnetic field of the circularly polarized TE_{11}-waves are

$$\left.\begin{aligned} h_z &= h_0 J_1\left(s_{11}\frac{r}{a}\right)\exp\left(i\omega t - kz \pm \phi\right)\\ h_r &= \mp\, ih_0\frac{\lambda_c}{\lambda_G}J_1'\left(s_{11}\frac{r}{a}\right)\exp\left(i\omega t - kz \pm \phi\right)\\ h_\phi &= h_0\frac{1}{2\pi}\frac{\lambda_c^2}{\lambda_G r}J_1\left(s_{11}\frac{r}{a}\right)\exp\left(i\omega t - kz \pm \phi\right)\end{aligned}\right\} \tag{2}$$

where the two different signs characterize the right or left circularly polarized wave, respectively. r, ϕ, z are right circular cylindrical coordinates and a is the radius of the waveguide. Furthermore, J_1 is the Bessel function of first order, $s_{11}=1.841$ equals the first root of its derivation J_1'. Guide wavelength λ_G, cutoff wavelength λ_c and vacuum wavelength λ are connected by

[2] A. A. T. M. van Trier, "Guided electromagnetic waves in anisotropic media," *Appl. Sci. Res.*, vol. 3 (B), pp. 305–371; 1953.

[3] H. Suhl and L. R. Walker, "Topics in guided wave propagation through gyromagnetic media," *Bell Sys. Tech. J.*, vol. 33, pp. 575–659, 939–986 and 1133–1194; 1954.

[4] J. O. Artman and P. E. Tannenwald, "Measurement of susceptibility tensor in ferrites, *J. Appl. Phys.*, vol. 26, pp. 1124–1132; 1955.

[5] H. Severin, "Effectiveness and limits of a first-order perturbation method for waveguides," to be published.

[6] The rationalized mks or Giorgi system of units is used throughout this paper.

$= 1.256\ 10^{-6}$ Vs/Am

$$\lambda_G = \frac{\lambda}{\sqrt{\epsilon\mu - \left(\frac{\lambda}{\lambda_c}\right)^2}}, \tag{3}$$

where for the TE_{11}-mode

$$\lambda_c = 3.412a.$$

For a circular waveguide filled with ferrite, (2) is correct as long as the ferrite is not magnetized and therefore behaves like an isotropic dielectric. With a dc-magnetic field applied longitudinally such that the occurring anisotropy is kept small, the slightly different propagation constants of the two circularly polarized quasi-TE_{11}-waves may be calculated in first order approximation using (1) and the unperturbed field (2).

When the ferrite is uniformly magnetized and saturated by a dc magnetic field H_z applied along the positive z-axis and subjected to an RF-field

$$h_x, h_y, h_z \ll H_z; \tag{4}$$

the permeability tensor $[\mu]$ relating the flux density $\boldsymbol{b}$ and the magnetic field intensity $\boldsymbol{h}$ according to

$$\boldsymbol{b} = \mu_0[\mu]\boldsymbol{h}$$

has the form[7]

$$[\mu] = \begin{bmatrix} \mu_1 & -i\kappa & 0 \\ i\kappa & \mu_1 & 0 \\ 0 & 0 & 0 \end{bmatrix} \tag{5}$$

where the tensor components μ_1 and κ are in general complex quantities because of the magnetic losses of the material. For right circular cylindrical coordinates the permeability tensor (5) is identical with that in Cartesian coordinates. This can be seen by applying rotation operators to the matrix equation (4) in Cartesian space and obtaining (4) in cylindrical coordinates. If the originally unmagnetized ferrite becomes weakly anisotropic by magnetization, then

$$[\Delta\mu]hh^* = (\mu_1 - 1)(|h_r|^2 + |h_\phi|^2) + 2_k\mathrm{Im}(h_r^* h_\phi)$$

and with (2)

$$[\Delta\mu]hh^*$$

$$= h_0^2\left(\frac{\lambda_c}{\lambda_G}\right)^2 \left\{ (\mu_1 - 1)\left[F_1'^2\left(s_{11}\frac{r}{a}\right) + \frac{J_1^2\left(s_{11}\frac{r}{a}\right)}{\left(s_{11}\frac{r}{a}\right)^2} \right] \pm \right.$$

$$\left. \pm\, 2\kappa J_1'\left(s_{11}\frac{r}{a}\right)\frac{J_1\left(s_{11}\frac{r}{a}\right)}{s_{11}\frac{r}{a}} \right\}. \tag{6}$$

[7] D. Polder, "On the theory of ferromagnetic resonance," *Phil. Mag.*, vol. 40, pp. 99–115; 1949.

The integrals occurring in (1) can be computed elementary. With the results given in Appendix I and

$$\frac{\Delta k_G}{k_G} = -\epsilon\mu\left(\frac{k}{k_G}\right)^2 \frac{\Delta\omega_c}{\omega_c},$$

from (3) it follows in first order approximation that

$$\frac{\Delta k_G}{k_G} = \frac{1}{2\pi}\left(\frac{k_c}{k_G}\right)^2\left(\frac{s_{11}}{a}\right)^2 \frac{1}{(s_{11}^2 - 1)J_1^2(s_{11})}$$

$$\frac{1}{h_0^2}\cdot\iint[\Delta\mu]hh^* df \tag{7}$$

where the integration has to be performed over the cross section of the ferrite.

The angle of Faraday rotation is given by the difference in the phase velocities of the two circularly polarized components and the path length through the ferrite medium according to

$$\theta = \frac{l}{2}(k_G^- - k_G^+). \tag{8}$$

Together with (6) and (7) one gets

$$\theta = \frac{2\kappa}{(s_{11}^2 - 1)J_1^2(s_{11})} k_G l$$

$$\cdot \int J_1\left(s_{11}\frac{r}{a}\right) J_1'\left(s_{11}\frac{r}{a}\right) d\left(s_{11}\frac{r}{a}\right). \tag{9}$$

Therefore in first order approximation Faraday rotation does not depend on the main diagonal component μ_1 of the permeability tensor but only on its off-diagonal component κ.

Various Ferrite Configurations in Circular Waveguides

The problems mentioned in the introduction will be treated in the following. It is supposed that the ferrite is magnetized longitudinally and saturated, and the operating frequency is far away from ferromagnetic resonance. Then the anisotropy is small enough to apply the perturbation method for calculating the change of propagation constants or the Faraday rotation, respectively, in first order approximation.

The angle of Faraday rotation, according to (8), may be found as the difference of the propagation constants k_G^- and k_G^+, given in Appendix II, or more directly by using (9). From it for the waveguide filled with ferrite it follows immediately that

$$\theta_0 = \frac{\kappa}{s_{11}^2 - 1} k_G l. \tag{10}$$

For plane electromagnetic waves in an unbound ferrite medium one has in the same approximation

$$\theta_\infty = \tfrac{1}{2}\kappa\sqrt{\epsilon}kl,$$

and therefore

$$\frac{\theta_0}{\theta_\infty} = \frac{2}{s_{11}^2 - 1} \frac{\lambda/\sqrt{\epsilon}}{\lambda_G} = 0.83 \frac{\lambda/\sqrt{\epsilon}}{\lambda_G},$$

which result is identical with that found by Suhl and Walker[8] in a more rigorous way. θ_0 is smaller than θ_∞ as to be expected, because the field is not circularly polarized at every point of the guide cross section. Furthermore with respect to the plane wave case the waveguide causes additional dispersion.

Another problem of some interest is that of an axial ferrite rod or tube of arbitrary radius and infinite length in a round waveguide, where the remainder of the waveguide is filled with a nonmagnetic dielectric, whose permittivity is equal to that of the ferrite. Although this problem may be not of immediate practical significance its solution will be helpful in treating the practically more important case of a ferrite rod in an air-filled guide. Because the field (2) is exact in the unmagnetized case, there is no restriction on the diameter of the ferrite rod. From (9) it follows that

$$\frac{\theta}{\theta_0} = \frac{J_1^2\left(s_{11}\frac{\rho}{a}\right)}{J_1^2(s_{11})} \tag{11}$$

for a ferrite rod of the diameter 2ρ, and

$$\frac{\theta}{\theta_0} = 1 - \frac{J_1^2\left(s_{11}\frac{\rho}{a}\right)}{J_1^2(s_{11})} \tag{12}$$

for the complementary tube of the inner diameter 2ρ and the outer diameter $2a$. Considering the rod, for the two limiting cases of very small or large diameter, respectively, from (11) one gets

$$\rho \ll a: \frac{\theta}{\theta_0} = \frac{1}{4} \frac{s_{11}^2}{J_1^2(s_{11})} \left(\frac{\rho}{a}\right)^2 \tag{11a}$$

$$\rho \approx a: \frac{\theta}{\theta_0} = 1 - (s_{11}^2 - 1)\left(\frac{a-\rho}{a}\right)^2. \tag{11b}$$

As regards the tube for very small or large wall thickness result (12) simplifies to

$$\rho \approx a: \frac{\theta}{\theta_0} = (s_{11}^2 - 1)\left(\frac{a-\rho}{a}\right)^2 \tag{12a}$$

$$\rho \ll a: \frac{\theta}{\theta_0} = 1 - \frac{1}{4} \frac{s_{11}^2}{J_1^2(s_{11})} \left(\frac{\rho}{a}\right)^2. \tag{12b}$$

In Figs. 1 and 2 the Faraday rotation computed according to (11) and (12) has been drawn as function of the diameter or wall thickness of the ferrite rod or tube, respectively. For comparing these two cases in Fig. 3

[8] H. Suhl and L. R. Walker, "Faraday rotation of guided waves," *Phys. Rev.*, vol. 86, pp. 122–123; 1952.

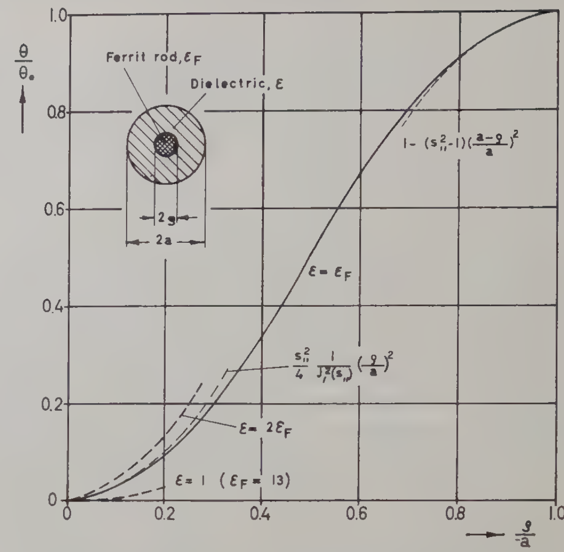

Fig. 1—Faraday rotation of a TE_{11}-wave propagating through a round waveguide containing an axial rod of ferrite embedded in a dielectric of the permittivity ϵ.

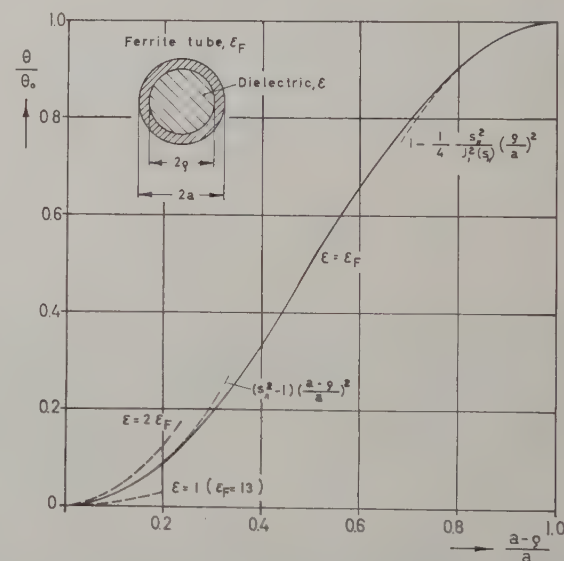

Fig. 2—Faraday rotation of a TE_{11}-wave propagating through a round waveguide containing a ferrite tube at its wall and a dielectric filler of the permittivity ϵ.

the angle of rotation has been plotted vs the area occupied by the ferrite. With equal areas (quantities) of ferrite the axial rod gives considerably larger rotation than the tube as to be expected from the h-field configuration of the TE_{11}-mode (Fig. 4).

The practically most important problem is that of a thin axial ferrite rod inserted axially into an air-filled guide. Because of the high permittivity of the ferrites (between 10 and 15) relative to that of air, rather severe restrictions are put on the diameter of the rods to which a perturbation method is applicable. This limitation would be substantially relaxed if exact solutions for dielectric rods of high permittivity introduced axially into round guides would be available, which could be used as the basis for magnetic perturbation calculation. Unfortunately, since such solutions are not known so

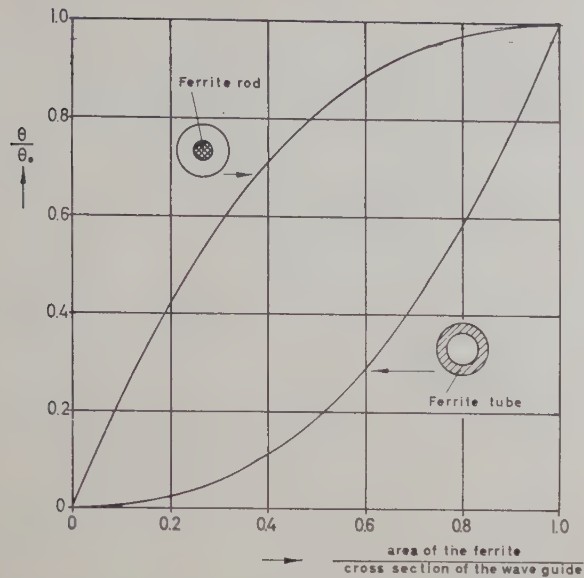

Fig. 3—Comparison of the Faraday rotation of a TE_{11}-wave propagating through a round waveguide containing an axial rod of ferrite with the rotation for a ferrite tube at the wall of the guide. The remaining part of the cross-section is filled with a dielectric of the same permittivity as the ferrite.

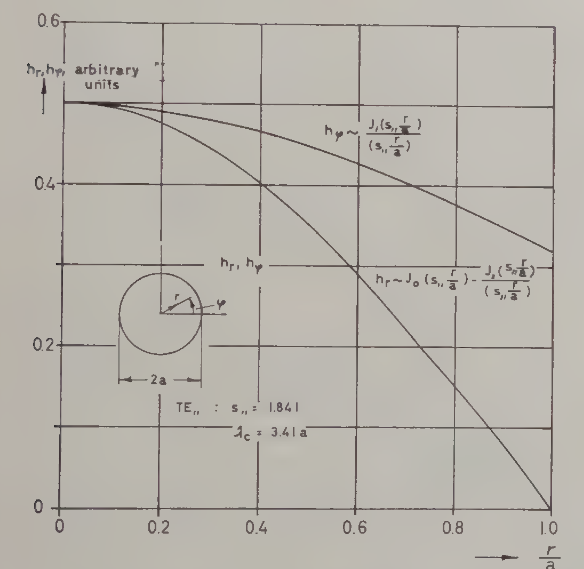

Fig. 4—Transverse components of the magnetic field of a circularly polarized TE_{11}-wave in a round waveguide. The same field distribution holds for a linearly polarized TE_{11}-wave along the diameter characterized by $\phi=\pi/4$.

far, the "unperturbed," *i.e.*, unmagnetized case of the dielectrically loaded guide may be treated independent of the magnetic perturbation also by first-order perturbation method.

As before, the radius of the guide is a and that of the ferrite rod is $\rho \ll a$. Its permittivity is ϵ_F, and we consider the more general case, that the remainder of the waveguide is filled with a dielectric of the permittivity ϵ. For $s_{11}(r/a) \ll 1$

$$J_1\left(s_{11}\frac{r}{a}\right) \approx \frac{1}{2}\, s_{11}\frac{r}{a}, \qquad J_1'\left(s_{11}\frac{r}{a}\right) \approx \frac{1}{2}$$

and from (9) it follows that

$$\theta = \frac{\kappa}{4}\,\frac{s_{11}^2}{(s_{11}^2-1)J_1^2(s_{11})}\, l k_G^{(\epsilon)} \left(\frac{\rho}{a}\right)^2$$

and together with (10) one has

$$\frac{\theta}{\theta_0} = \frac{1}{4}\,\frac{s_{11}^2}{J_1^2(s_{11})}\,\frac{k_G^{(\epsilon)}}{k_G^{(\epsilon_F)}}\left(\frac{\rho}{a}\right)^2. \tag{13}$$

As to be expected, this result becomes identical with (11a) if $\epsilon=\epsilon_F$. $k_G^{(\epsilon)}$ and $k_G^{(\epsilon_F)}$ are the propagation constants of the round waveguide filled with a dielectric of the permittivity ϵ or with an unmagnetized ferrite of the permittivity ϵ_F, respectively. Instead of $k_G^{(\epsilon)}$ one would expect the propagation constant k_G of the unmagnetized structure of ferrite rod and surrounding dielectric. A first order approximation of k_G has been given in Appendix II. In (13) from k_G only $k_G^{(\epsilon)}$ remains because terms of higher than quadratic order have to be neglected in this approximation.

If on the other hand the radius of the ferrite rod approaches the radius of the guide, *i.e.*, $s_{11}(r/a) \approx s_{11}$, with

$$J_1\left(s_{11}\frac{r}{a}\right) \approx J_1(s_{11}) - \frac{s_{11}^2-1}{2}\,J_1(s_{11})\left(\frac{a-r}{a}\right)^2$$

$$J_1'\left(s_{11}\frac{r}{a}\right) \approx \frac{s_{11}^2-1}{s_{11}}\,J_1(s_{11})\,\frac{a-r}{a} + \frac{1}{2}\,\frac{s_{11}^2-3}{s_{11}}\,J_1(s_{11})\left(\frac{a-r}{a}\right)^2$$

from (9) the result (11b) is obtained. The permittivity of the thin walled dielectric tube representing the perturbation in the waveguide otherwise filled with ferrite does not influence the Faraday rotation in first order approximation.

Finally, also for the two structures complementary to those treated above the Faraday rotation can be computed by first-order perturbation method. If the waveguide contains a thin-walled ferrite tube adjoining the wall of the guide and the remainder is filled with a dielectric of the permittivity ϵ, one finds

$$\frac{\theta}{\theta_0} = (s_{11}^2-1)\,\frac{k_G^{(\epsilon)}}{k_G^{(\epsilon_F)}}\left(\frac{a-\rho}{a}\right). \tag{14}$$

For the waveguide filled with ferrite and an axial dielectric rod of small radius $\rho \ll a$ and permittivity ϵ one obtains result (12b). Again the permittivity of the dielectric perturbation does not influence the Faraday rotation in first order approximation.

For the cases that the dielectric is air ($\epsilon=1$) or its permittivity is twice as high as that of the ferrite ($\epsilon_F=13$), the results (13) and (14) are drawn in Figs. 1 and 2 for comparison with the case where ferrite and dielectric have equal permittivities.

Experimental Results

The Faraday rotation of a few ferrites has been measured using a similar equipment as described by Hogan.[1]

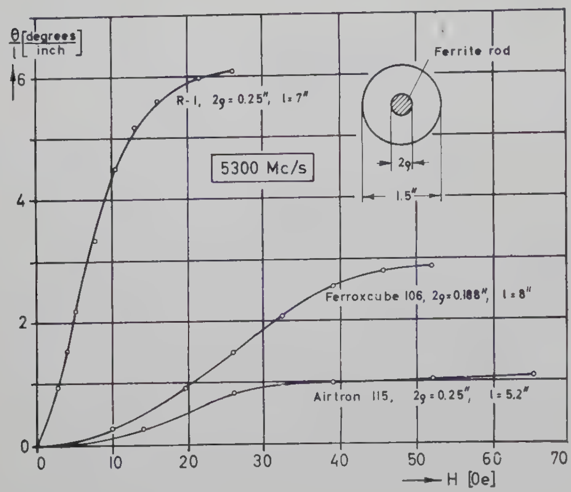

Fig. 5—Faraday rotation per unit length of a TE_{11}-wave propagating at a frequency of 5300 mc through a round waveguide containing an axial ferrite rod, as function of the applied longitudinal dc magnetic field.

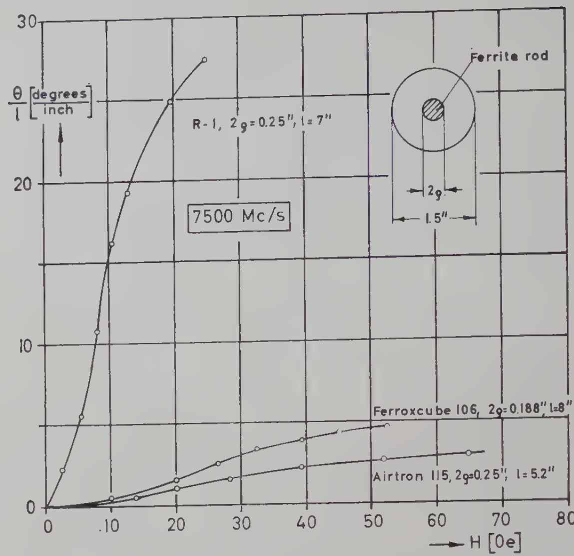

Fig. 6—Faraday rotation per unit length of a TE_{11}-wave propagating at a frequency of 7500 mc through a round waveguide containing an axial ferrite rod, as function of the applied longitudinal dc magnetic field.

The ferrite samples are supported by two polyfoam discs and placed along the axis of a circularly cylindrical waveguide carrying the dominant TE_{11}-mode. This section is fed from a rectangular waveguide by means of a proper nonreflective transition. On the opposite end of the circular waveguide the analyzer consisting of another nonreflective transition and a rectangular waveguide with detector mouth is supported, so that it can be rotated around the longitudinal axis of the system. The circular guide is placed in a specially constructed coil system[9] producing an axial magnetic field of constant intensity along the length of the ferrite rod.

Measurements have been made at frequencies between 5 and 7.6 kmc on the following ferrite materials available to us in form of thin long rods:

General Ceramics	$R-1$	$(M_s=2150\text{ G})$
Ferroxcube	106	$(M_s=3300\text{ G})$
Airtron	115	$(M_s=1850\text{ G})$.

From Kittel's formula for the ferromagnetic resonance in a finite body[10] it follows that for a long thin pencil approximately

$$f_{\text{res}} = \frac{\gamma}{2\pi}\left(H_z + \frac{1}{2}\frac{M_s}{\mu_0}\right) \tag{15}$$

holds, where

$$\frac{\gamma}{2\pi} = 2.8\left(\frac{Mc/s}{Oe}\right).$$

Long thin specimens of soft ferrite materials magnetized longitudinally saturate at applied fields of about 10 to 50 oersteds. Therefore in (15) H_z may be neglected against $\frac{1}{2}M_s/\mu_0$, and the resonance frequency is deter-

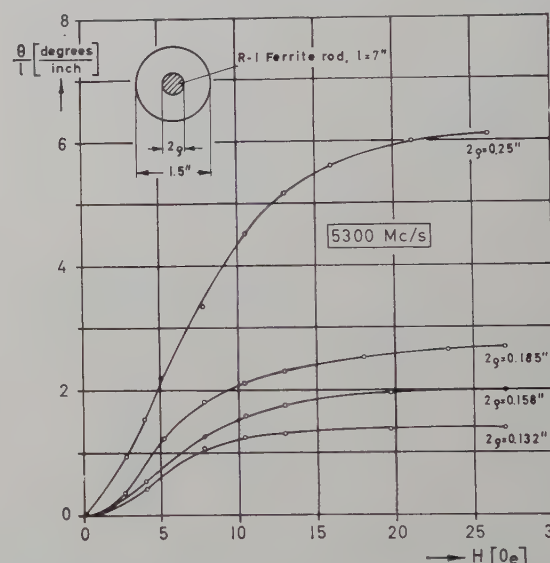

Fig. 7—Faraday rotation per unit length of a TE_{11}-wave propagating at a frequency of 5300 mc through a round waveguide containing an axial $R-1$ ferrite rod, as function of the applied longitudinal dc magnetic field for various diameters of the ferrite rod.

mined by the saturation magnetization. For the materials under investigation ferromagnetic resonance must be expected at frequencies of 3, 4.6 or 2.6 mc, so that in any case the operating frequency was above ferromagnetic resonance.

For the various ferrites, Figs. 5–7 show the Faraday rotation measured as function of the applied field with rod diameter and frequency as parameters. The curves look very similar to the curve of magnetization vs applied field, as to be expected and observed by others.[1,2,11] According to (10) and (13) for the cases of

[9] H. Severin, "A coil system producing a uniform magnetic field along its axis," to be published.

[10] C. Kittel, "On the theory of ferromagnetic resonance absorption," *Phys. Rev.*, vol. 73, pp. 155–161; 1948.

[11] P. J. B. Clarricoats, A. G. Hayes and A. F. Harvey, "A survey of the theory and applications of ferrites at microwave frequencies," *Proc. IEE*, vol. 104, B Suppl., pp. 267–282; 1957.

the ferrite filled guide and slender axial ferrite pencils the rotation per unit path length is proportional to the off-diagonal component κ of the permeability tensor (5). This may be true in first order approximation also for rods of arbitrary diameter. Because of

$$\kappa = \frac{\gamma \dfrac{M_s}{\mu_0} \omega}{\omega^2 - \omega^2_{\text{res}}} \approx \frac{\gamma}{\mu_0} \frac{M_s}{\omega} \tag{16}$$

for $\omega \gg \omega_{\text{res}}$, the Faraday rotation in a saturated medium is proportional to the saturation magnetization. In the case of an unsaturated medium Rado[12] has shown that (16) remains valid when therein the saturation magnetization M_s is replaced by the magnetization M. In

$$M = \mu_0(\mu - 1)H_i$$

the internal field H_i may be replaced approximately by the applied field H_z for rods being long enough to keep the demagnetizing field negligibly small. Therefore the curve of Faraday-rotation as function of the applied magnetic field is very similar to the curve of magnetization vs applied field. Comparing corresponding curves in Figs. 5 and 6 one sees that the rotation increases with increasing frequency. For a waveguide partially loaded with ferrite, because of the difference in permittivities an increase in frequency causes the electromagnetic energy to become concentrated more and more in the ferrite rod, thus resulting in an increase of rotation. An increase of the rod diameter should have the same effect on the energy concentration in the ferrite, and this is confirmed by the measuring results shown in Fig. 7.

Those effects of energy concentration are of course not taken into account by the first-order perturbation method, which is based on the unperturbed fields of the empty guide. The results of the perturbation method must therefore be insufficient, if with increasing frequency or diameter of the ferrite rod energy concentration occurs. Its influence can clearly be seen from Fig. 8 by comparing the curves of Faraday rotation vs frequency for rods of different diameters. Such measurements indicate up to which rod diameter the application of first-order perturbation method may be possible. In the case of Fig. 8 this limit is $d = 0.132$ inch, possibly $d = 0.158$ inch for frequencies below 6000 mc. Fig. 9 indicates a remarkable agreement between measurements and calculation for rod diameters $d = 0.1$ inch and 0.125 inch. For an infinite medium the plane wave theory shows that Faraday-rotation is independent of frequency if the operating frequency is much higher than the ferromagnetic resonance frequency.[7] The frequency dependence of Faraday rotation shown in Fig. 9 is determined by two effects. First the guide wavelength is not linearly related to the vacuum wavelength as can be seen from Fig. 10. Secondly Fig. 11 shows that for a ferrite rod of the material $R-1$ the measuring frequencies are too close to ferromagnetic resonance as to neglect $\omega_{\text{res}} \ll \omega$ and apply the approximation (16). With reference to Fig. 9 the results found for the nonsaturated Airtron-ferrite confirm Rado's theory on nonsaturated materials.[12,13]

With increasing diameter of the ferrite rod the elec-

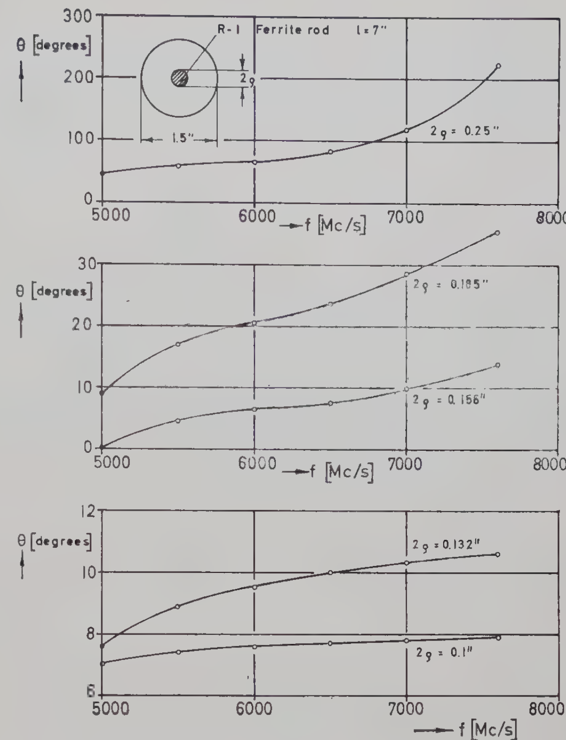

Fig. 8—Faraday rotation of a TE_{11}-wave propagating through a round waveguide containing an axial $R-1$ ferrite rod, as function of the frequency for various diameters of the ferrite rod. $H_{dc} = 26$ oersteds.

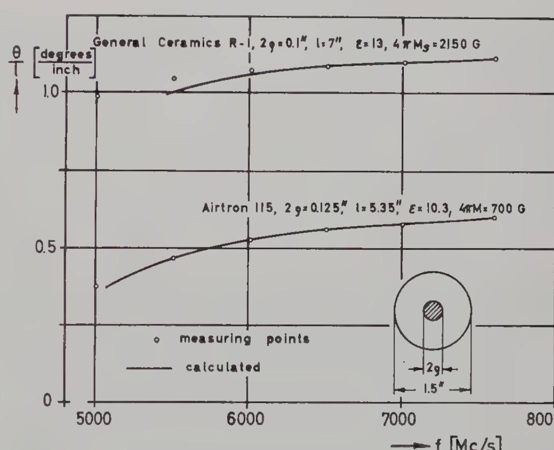

Fig. 9—Faraday rotation per unit length of a TE_{11}-wave propagating through a round waveguide containing a thin axial ferrite rod, as function of the frequency, measured and calculated by first-order perturbation method.

[12] G. T. Rado, "Theory on the microwave permeability tensor and Faraday effect in non-saturated ferromagnetic materials," *Phys. Rev.*, vol. 89, p. 529; 1953.

[13] R. C. LeCraw and E. G. Spencer, "Tensor permeabilities of ferrites below magnetic saturation," 1956 IRE CONVENTION RECORD, pt. 5, pp. 66–74.

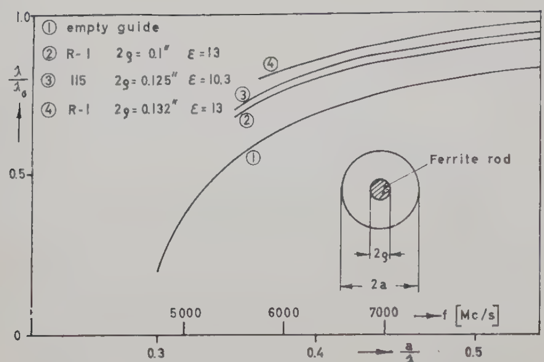

Fig. 10—Guide wavelength of the TE_{11}-wave in a round guide containing an axial dielectric rod, calculated by first-order perturbation method. λ=wavelength in free space. (Frequency scale for a waveguide diameter $2a=1.5$ inches.)

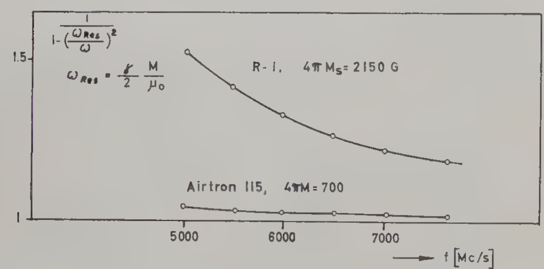

Fig. 11—Frequency dependence of the off-diagonal component K for General Ceramics $R-1$ ferrite and Airtron 155 ferrite.

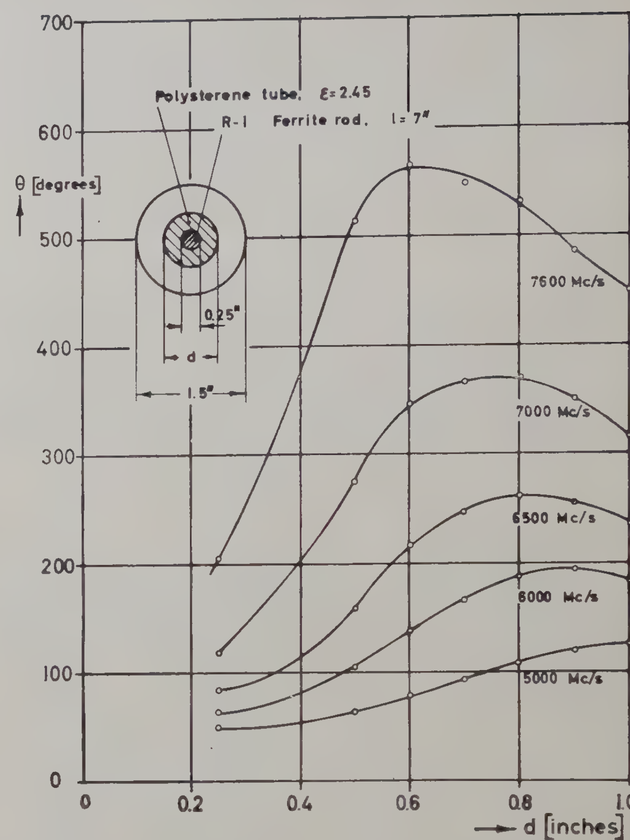

Fig. 12—Faraday rotation of a TE_{11}-wave propagating at various frequencies through a round waveguide containing an axial $R-1$ ferrite rod embedded in a polysterene tube, as function of the tube diameter. $H_{dc}=25$ oersteds.

tromagnetic field becomes concentrated in the ferrite, as described above. This effect may be enlarged by surrounding the ferrite with a suitable dielectric tube. Achieving optimum Faraday rotation is of some practical importance if the magnetizing field cannot be strengthened without considerable expense, *e.g.*, as with high-speed steering elements. Furthermore, in this case one is restricted to long thin rods of ferrite in order to keep the demagnetization factor as small as possible.

Rowen[14] observed an enhancement of the Faraday-rotation for a partially ferrite loaded guide if the remainder of the guide is filled with a medium of high permittivity. For ferrite rods of small diameters this is confirmed by the result of our perturbation calculations (Fig. 1). According to observations of Fox, Miller and Weiss,[15] the rotation increases or decreases with increasing permittivity of the surrounding medium depending on the diameter of the ferrite rod. For larger diameters most of the electromagnetic energy is concentrated in the ferrite. Therefore, with increasing permittivity of the surrounding medium the ratio of energy in the ferrite to the total guide energy decreases and this may result in a decrease of rotation. Analogous considerations should hold if the ferrite rod is embedded in dielectric tubes of various outer diameters. For a given permittivity and frequency, the ratio of energy in the ferrite to the guide energy, and therefore, the rotation, are expected to increase up to a certain tube diameter and to decrease again if the tube diameter increases further. This is confirmed by corresponding measurements reproduced in Fig. 12. The results indicate that there is always an optimum tube diameter for which the rotation is maximum. For higher frequencies this maximum shifts to smaller tube diameters. For polysterene tubes ($\epsilon=2.45$) a factor 2 · · · 3 in rotation could be won.

In Fig. 13 the optimum values of Fig. 12 have been compared with the mathematically treatable case that the ferrite rod is embedded in a dielectric of the same permittivity filling the waveguide. In this case no RF-energy is concentrated in the ferrite, because the permittivities are equal and the permeabilities differ only slightly. The comparison with the optimum rotation values of the partially loaded guide (Fig. 12), which are up to three times larger, indicates the enormous influence of the field concentration in the ferrite. The important result for practical applications is the fact that with a dielectric tube of suitable diameter, even with the relatively small permittivity $\epsilon=2.4$, higher values of rotation can be achieved than with a dielectric of the permittivity 13 filling the cross section of the waveguide. Finally one may consider also the impedance match problem, which is much simpler to overcome in the first case.

[14] J. H. Rowen, "Ferrites in microwave applications," *Bell Sys. Tech. J.*, vol. 32, pp. 1133–1369; 1953.

[15] A. G. Fox, S. E. Miller, and M. T. Weiss, "Behavior and applications of ferrites in the microwave region," *Bell Sys. Tech. J.*, vol. 34, pp. 5–103; 1955.

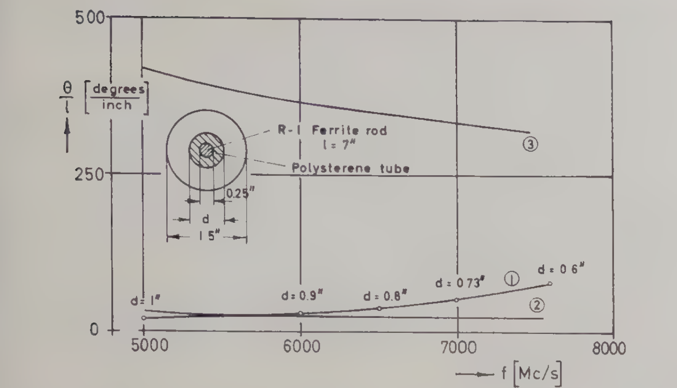

Fig. 13—Faraday rotation per unit length of a TE_{11}-wave propagating through a round waveguide
1) containing an axial ferrite rod surrounded by a dielectric tube of optimum diameter (see Fig. 12).
2) for the same ferrite rod embedded in a dielectric of equal permittivity filling the waveguide.
3) filled with ferrite.

Appendix I

If one introduces the field components (2) into formula (1) the following integrals result, which can be evaluated elementarily:

$$\int J_1^2\left(s_{11}\frac{r}{a}\right) r\,dr$$

$$= \frac{1}{2}\left(\frac{a}{s_{11}}\right)^2 x^2\{J_1^2(x) - J_0(x)J_2(x)\}\Big|_{x=s_{11}(r/a)}$$

$$= \frac{1}{2}\left(\frac{a}{s_{11}}\right)^2 \{(x^2-1)J_1^2(x) + x^2J_1'^2(x)\}\Big|_{x=s_{11}(r/a)}$$

$$\int J_1^1\left(s_{11}\frac{r}{a}\right)\frac{J_1\left(s_{11}\frac{r}{a}\right)}{s_{11}\frac{r}{a}} r\,dr = \frac{1}{2}\left(\frac{a}{s_{11}}\right)^2 J_1^2\left(s_{11}\frac{r}{a}\right)$$

$$\int \left\{\frac{J_1^2\left(s_{11}\frac{r}{a}\right)}{\left(s_{11}\frac{r}{a}\right)^2} + J_1'^2\left(s_{11}\frac{r}{a}\right)\right\} r\,dr$$

$$= \int J_0^2\left(s_{11}\frac{r}{a}\right) r\,dr - 2\frac{a}{s_{11}}\int J_1\left(s_{11}\frac{r}{a}\right)J_1'\left(s_{11}\frac{r}{a}\right)dr$$

$$= \frac{1}{2}\left(\frac{a}{s_{11}}\right)^2\{(x^2-2)J_1^2(x) + x^2J_0^2(x)\}\Big|_{x=s_{11}(r/a)}$$

$$= \frac{1}{2}\left(\frac{a}{s_{11}}\right)^2\{(x^2-1)J_1^2(x) + x^2J_1'^2(x) + 2xJ_1(x)J_1'(x)\}\Big|_{x=s_{11}(r/a)}.$$

Appendix II

The propagation constants k_G^- and k_G^+ of the two circularly polarized waves traveling through the ferrite loaded waveguide section

$$k_G^{\mp} = k_G\left(1 + \frac{\Delta k_G^{\mp}}{k_G}\right) \tag{17}$$

can be calculated from (7) in first order approximation with the aid of the integrals given in Appendix I. In the following, the results are collated for the structures treated above.

First for the ferrite filled guide one gets

$$\frac{\Delta k_G^{\mp}}{k_G} = \frac{1}{2}(\mu_1 - 1) \pm \frac{1}{s_{11}^2 - 1}\kappa. \tag{18}$$

In the second case of an axial ferrite rod of the radius ρ embedded in a dielectric of equal permittivity one has

$$\frac{\Delta k_G^{\mp}}{k_G} = \frac{1}{2}\frac{1}{(s_{11}^2-1)J_1^2(s_{11})} \cdot \{(\mu_1 - 1)[(x^2-1)J_1^2(x) + x^2J_1'^2(x) + 2xJ_1(x)J_1'(x)] \pm 2\kappa J_1^2(x)\}_{x=s_{11}(\rho/a)} \tag{19}$$

which result is identical with that found by Suhl and Walker[3]; it simplifies for $\rho \ll a$ to

$$\frac{\Delta k_G^{\mp}}{k_G} = \frac{1}{4}\frac{s_{11}^2}{(s_{11}^2-1)J_1^2(s_{11})}\left(\frac{\rho}{a}\right)^2\{(\mu_1 - 1) \pm \kappa\} \tag{20}$$

and for $\rho \approx a$ to

$$\frac{\Delta k_G^{\mp}}{k_G} = \frac{1}{2}(\mu_1 - 1) \pm \frac{1}{s_{11}^2-1}\kappa - \frac{1}{s_{11}^2-1}(\mu_1 - 1) \cdot \left\{\frac{a-\rho}{a} + \frac{1}{2}\left(\frac{a-\rho}{a}\right)^2\right\} \mp \kappa\left(\frac{a-\rho}{a}\right)^2. \tag{21}$$

The result has been written in the form

$$\left(\frac{\Delta k_G}{k_G}\right)_{\substack{\text{ferrite}\\\text{tube}}} = \left(\frac{\Delta k_G}{k_G}\right)_{\substack{\text{ferrite filled}\\\text{wave guide}}} - \left(\frac{\Delta k_G}{k_G}\right)_{\substack{\text{ferrite}\\\text{rod}}}. \tag{22}$$

Because of this relation the above results also include the complementary problem of a ferrite tube adjoining the wall of the guide, the remainder of which is filled with a dielectric of the same permittivity as the ferrite. The corresponding limiting cases of ferrite tubes of very small or large wall thickness are covered by the formulas given above.

If the ferrite and the surrounding dielectric have different permittivities ϵ_F and ϵ, the application of the first-order perturbation method is restricted to small or large diameters of the ferrite rod or dielectric rod, respectively. For a thin ferrite pencil ($\rho \ll a$) from (7) one again gets (20). In (17) the propagation constant k_G of the unmagnetized structure can be found also by

first order perturbation method[5] as

$$k_G = k_G^{(\epsilon)}\left\{1 + \frac{1}{4}\frac{s_{11}^2}{(s_{11}^2 - 1)J_1^2(s_{11})}\right.$$

$$\left.(\epsilon_F - \epsilon)\left(\frac{k}{k_G^{(\epsilon)}}\right)^2\left(\frac{\rho}{a}\right)^2\right\}. \quad (23)$$

Specializing (20) and (23) to $\epsilon = 1$ and combining them with (17) we obtain the same result as Suhl and Walker[3] [(11) p. 1142] who treated the problem of a thin ferrite rod in an air-filled guide in a more general way. Clarricoats[16] has completed the result by considering the case of a ferrite with loss in first order approximation.

If on the other hand the radius of the ferrite rod approaches the radius of the guide, (21) holds with[5]

$$k_G = k_G^{(\epsilon_F)}\left\{1 - \frac{1}{s_{11}^2 - 1}(\epsilon_F - \epsilon)\left(\frac{k}{k_G^{(\epsilon_F)}}\right)^2\frac{a-\rho}{a}\right\}.$$

Finally the two complementary cases can be treated.

[16] P. I. B. Clarricoats, "Some properties of circular wave guides containing ferrites," *Proc. IEE*, vol. 104, B Suppl., pp. 286–295; 1957.

For the thin walled ferrite tube ($\rho \approx a$) adjoining the guide one gets

$$\frac{\Delta k_G^{\mp}}{k_G} = \frac{1}{s_{11}^2 - 1}(\mu_1 - 1)\frac{a-\rho}{\rho} \pm \kappa\left(\frac{a-\rho}{a}\right)^2$$

with

$$k_G = k_G^{(\epsilon)}\left\{1 - \frac{1}{s_{11}^2 - 1}(\epsilon - \epsilon_F)\left(\frac{k}{k_G^{(\epsilon)}}\right)^2\frac{a-\rho}{a}\right\}$$

and for the wave guide filled with ferrite and an axial dielectric rod ($\rho \ll a$)

$$\frac{\Delta k_G^{\mp}}{k_G} = \frac{1}{2}(\mu_1 - 1) \pm \frac{1}{s_{11}^2 - 1}\kappa$$

$$- \frac{1}{4}\frac{s_{11}^2}{(s_{11}^2 - 1)J_1^2(s_{11})}\{(\mu_1 - 1) \pm \kappa\}\left(\frac{\rho}{a}\right)^2$$

with

$$k_G = k_G^{(\epsilon_F)}\left\{1 + \frac{1}{4}\frac{s_{11}^2}{(s_{11}^2 - 1)J_1^2(s_{11})}\right.$$

$$\left.\cdot(\epsilon - \epsilon_F)\left(\frac{k}{k_G^{(\epsilon_F)}}\right)^2\left(\frac{\rho}{a}\right)^2\right\}.$$

Magnified and Squared VSWR Responses for Microwave Reflection Coefficient Measurements*

R. W. BEATTY†

Summary—**In conventional microwave impedance measuring instruments, the measured ratio of maximum to minimum detector signal level is ideally equal to the voltage standing-wave ratio (VSWR) of the termination. In this paper, it is shown how radically different types of response are obtainable in which the observed ratio may approximately equal the square of the VSWR or may be magnified any desired amount. Theory is given enabling accurate measurements by interesting techniques. Accuracies of 0.1 per cent in VSWR to 2.0 have been achieved using magnified response techniques.**

Introduction

In most microwave impedance measuring instruments, such as the idealized slotted line, the resonance line, and rotary standing-wave indicators, the ratio of the maximum to the minimum amplitude of the output to the detector is ideally equal to the voltage standing-wave ratio (VSWR) of the termination subjected to measurement.

* Manuscript received by the PGMTT, February 20, 1959.
† Radio Standards Lab., Nat. Bur. of Standards, Boulder, Colo.

Other radically different types of response are obtainable. The two responses to be discussed in this paper have been called magnified and squared VSWR responses for reasons which will become apparent.

A simplified explanation will first be given, followed by a more complete mathematical description.

The differences among responses are shown in Fig. 1, three response curves calculated for the same termination.

Simplified Explanations

Squared VSWR Response

A simplified explanation can be given for one system yielding squared VSWR response. Other systems which have been devised apparently do not permit simplified explanations and will not be thoroughly analyzed. Enough theory will be given however, to permit their use as measurement systems.

The system shown in the diagram in Fig. 2 consists

of a straight section of uniform lossless waveguide (which may be either coaxial line or rectangular waveguide, for example) with oppositely located coupling probes for generator and detector. A short circuit which may be adjusted in position terminates one end of the uniform waveguide section while the other end is terminated in the sliding load to be measured. In this system it is necessary to vary the phase of the load by sliding it inside the waveguide, but in other systems to be described, this is not always required.

Referring to the simplified model of Fig. 2(b),

$$E = e\frac{Z_p}{Z_G + Z_p} \approx i_G Z_p = i_G \frac{1}{\dfrac{1}{Z_s'} + \dfrac{1}{Z_L'}}. \qquad (1)$$

If the short circuit is located $\lambda_G/4$ from the probes, $Z'_s = \infty$, and

$$E \approx i_G Z_L' = i_G \frac{1 + \Gamma_L e^{-j2\beta l}}{1 - \Gamma_L e^{-j2\beta l}}. \qquad (2)$$

As l varies, $|E|$ goes through maxima and minima. The ratio σ_A of the maxima to minima is

$$\sigma_A = \left(\frac{1 + |\Gamma_L|}{1 - |\Gamma_L|}\right)^2 = \sigma_L^2. \qquad (3)$$

Where σ_L is the VSWR of the load. The meaning of other symbols used above should become clear upon reference to Fig. 2(b).

Magnified Response

A system yielding magnified response is shown in Fig. 3. A directional coupler is connected to respond mainly to the wave reflected from a phasable or sliding termination whose VSWR is to be measured. For simplicity, it is assumed that the generator and detector do not produce reflections ($\Gamma_G = \Gamma_D = 0$), and that no reflections are produced in arm 2 by the directional coupler ($S_{22} = 0$).

The signal coupled to the detector has two components. One is fixed and exists because the directivity is not infinite. The other is from the load reflection and varies in phase as the load is slid inside the waveguide. As the relative phase of the two components vary, the magnitude of the resultant varies. If the components are of approximately equal magnitudes, the range of variation of the resultant may be large even though the reflection from the termination may be small.

Inspection of the diagram of Fig. 3 leads to the following equations describing the response.[1]

$$b_3 \approx b_G(S_{31} + S_{21}S_{32}\Gamma_L e^{-j2\beta l}) = b_G S_{31}(1 + K\Gamma_L e^{-j2\beta l}). \quad (4)$$

The response is of the same form as that of the idealized slotted line (see Fig. 1) excepting that Γ_L is multiplied by the factor K. Since $|K|$ may be very large (it

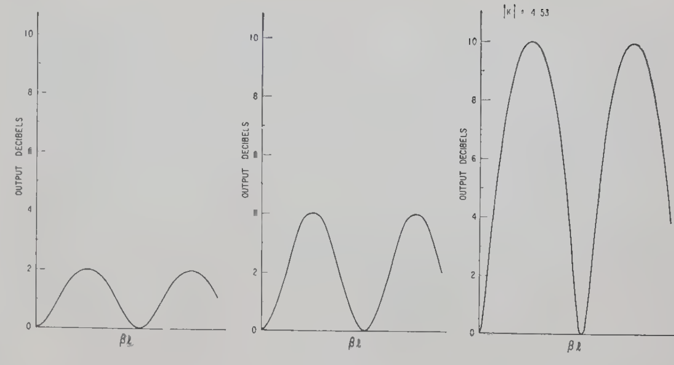

(a) (b) (c)

Fig. 1—Response curves of three measurement systems with termination having a VSWR of 1.26;

(a) idealized slotted line,

$$d = c[1 + K\Gamma_1 e^{-j2\beta l}]$$

(b) squared VSWR response,

$$d = c'\left[\frac{1 + \Gamma_L e^{-j2\beta l}}{1 - \Gamma_L e^{-j2\beta l}}\right],$$

(c) magnified response,

$$d = c''[1 + K\Gamma_L e^{-j2\beta l}].$$

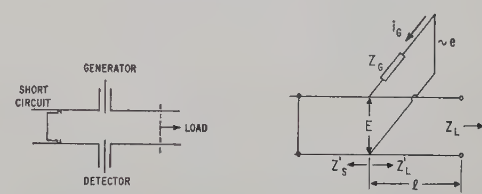

(a) (b)

Fig. 2—Diagram and simplified model of one system yielding squared VSWR response; (a) diagram of system, (b) simplified model.

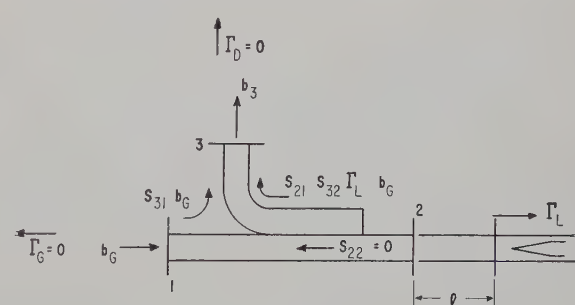

Fig. 3—Diagram of simplified system to illustrate magnified response.

approximately equals the directivity ratio of the directional coupler), one may consider Γ_L to be magnified by the factor $|K|$, leading to the term magnified response. It should be noted however that the response variation will increase as one increases $|K|$ up to the point where $|K\Gamma_L| = 1$, and then will decrease with further increase in $|K|$.

Analysis

Both magnified and squared VSWR responses may be analyzed by considering the generalized treatment[2]

[1] In this equation, b represents a wave amplitude, S a scattering coefficient of the directional coupler, and Γ_L the voltage reflection coefficient of the load.

[2] A. C. MacPherson and D. M. Kerns, "A new technique for the measurement of microwave standing-wave ratios," Proc. IRE, vol. 44, pp. 1024–1030, August, 1956.

of MacPherson and Kerns of a 3-arm junction measurement system for phasable loads. Such a junction is shown in Fig. 4. where it has been assumed for convenience that the necessary variation in phase is obtained by changing the length l of uniform, lossless waveguide.

Instead of using the gathering coefficients employed by MacPherson and Kerns, the solution[3] for b_3 is obtained in terms of the more familiar scattering coefficients and may be expressed as follows:

$$b_3 = C \frac{1 + K\Gamma_L e^{-j2\beta l}}{1 - \Gamma_{2i}\Gamma_L e^{-j2\beta l}} = CK\Gamma_L e^{-j2\beta l} \frac{1 + \dfrac{1}{K\Gamma_L} e^{j2\beta l}}{1 - \Gamma_{2i}\Gamma_L e^{-j2\beta l}} \tag{5}$$

where

$$C = \frac{b_G S_{31}}{\begin{vmatrix} (1 - S_{11}\Gamma_G) & S_{13}\Gamma_D \\ S_{31}\Gamma_G & (1 - S_{33}\Gamma_D) \end{vmatrix}},$$

$$K = \frac{S_{21}S_{32}}{S_{31}} - S_{22},$$

and

$$\Gamma_{2i} = \frac{\begin{vmatrix} (1 - S_{11}\Gamma_G) & S_{12} & -S_{13}\Gamma_D \\ -S_{21}\Gamma_G & S_{22} & -S_{23}\Gamma_D \\ -S_{31}\Gamma_G & S_{32} & (1 - S_{33}\Gamma_D) \end{vmatrix}}{\begin{vmatrix} (1 - S_{11}\Gamma_G) & S_{13}\Gamma_D \\ S_{31}\Gamma_G & (1 - S_{33}\Gamma_D) \end{vmatrix}}.$$

In the above expressions, the component of the emergent wave amplitude supplied by the generator is $b_G = a_1 - b_1\Gamma_G$, where a_1 represents the amplitude of the wave incident on the junction in arm 1. Symbols of the form $S_{m,n}$ are the scattering coefficients of the junction, and Γ_G, Γ_D, and Γ_L are the voltage reflection coefficients of the generator, detector, and load, respectively, as indicated in Fig. 4.

The reflection coefficient Γ_{2i} is that which would be obtained "looking into" arm 2 if the generator was turned off and its impedance (as observed at T_1) was unchanged in so doing.

The variation in $|b_3|$ as we vary the phase (ψ_L) of Γ_L is defined to be the response of the systems represented by Fig. 4, and is determined by (5).

The properties of (5) will be examined in an effort to classify types of responses obtainable. It is evident that the parameter C affects only the level of the response, while the form of the response curve ($|b_3|$ vs ψ_L) is affected by the parameters K and Γ_{2i}.

We may consider the response for the conditions $\Gamma_{2i}=0$, $|K|=1$, the usual or normal type of response,

[3] G. E. Schafer and R. W. Beatty, "A method for measuring the directivity of directional couplers," IRE Trans. on Microwave Theory and Techniques, vol. MTT-6, pp. 419–422; October, 1958.

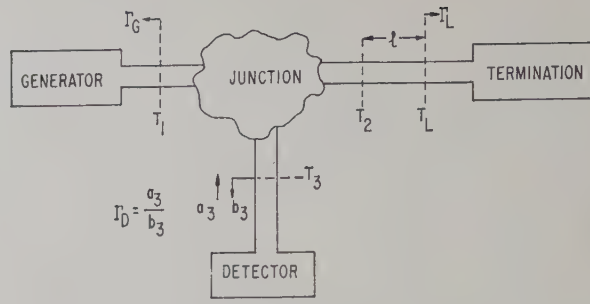

Fig. 4—Three-arm junction with phasable load.

since it leads to the form obtained in the case of an idealized slotted line.

The response form previously referred to as magnified response is obtained when $\Gamma_{2i}=0$, and $|K|$ is unrestricted. However values of $|K|$ may range from zero to infinity, and it is possible to have a magnification factor $|K|$ greater or less than unity. The case where $|K|$ is less than one is of dubious interest, but the possibility of $|K|$ greater than unity appears especially attractive for the measurement of small reflections.

If Γ_{2i} differs from zero, it will cause distortion in the response curve, which is considered undesirable. However, a distinctly different type of response may be obtained if $|\Gamma_{2i}| \approx 1$, and if the phases of $|K|$ and $|\Gamma_{2i}|$ are equal. This leads to squared VSWR response if $|K| \approx 1$. This type of response is not only curious, but may prove useful in some measurement applications.

Actually $|\Gamma_{2i}|$ is less than unity in actual (not lossless) systems, so that the ideal squared VSWR response may be closely approached with an actual system, but never quite reached.

A fourth type of response is obtained if the phases of K and Γ_{2i} are the same, $|\Gamma_{2i}| \approx 1$, and $|K|$ is unrestricted. The ratio of maximum to minimum detector signal level corresponding to (3) is

$$\sigma_A = \frac{1 + |K\Gamma_L|}{1 - |K\Gamma_L|} \sigma_L. \tag{6}$$

It seems appropriate to call this a magnified squared VSWR response, and it may have applications in the measurement of large VSWR.

This completes the classification of responses, since conditions other than those mentioned may be regarded as causing distortions of the types described above.

Means of Obtaining Various Responses

Examples have already been given (Figs. 2 and 3) of junctions permitting magnified and squared VSWR responses. However other types of arrangements are possible and offer a variety of measurement systems, each with its possible advantages and disadvantages.

In order to closely approach squared VSWR response ($|\Gamma_{2i}| \approx 1$, $|K| \approx 1$) it becomes evident that the 3-arm junction should have low loss and low coupling to the load. (This may be shown from a consideration of the conditions imposed upon the scattering coefficients by

losslessness.) These conditions are not sufficient however, as one may conclude after trying junctions which satisfy only these conditions. It is necessary for K and Γ_{2i} to have the same phase, and this is obtained by some tuning device, such as the adjustable short-circuit in Fig. 2. There may be some difficulty in obtaining the desired response in some cases, because it is not always possible to obtain the correct phase relationship, but the junction forms represented in Fig. 5(a) to (d) have all been found experimentally to permit a close approach to squared VSWR response by proper adjustment of the tuner. The arrangement of 5(e) should also permit squared VSWR response, but has not been constructed or tested.

Magnified Response occurs upon making $|K|$ greater than unity while $\Gamma_{2i}=0$. It evidently cannot be obtained with a lossless junction, for then $|K|=1$. If it is assumed that we can always make $\Gamma_G=0$, then Γ_{2i} would equal S_{22}, and this would vanish, so that $K=S_{21}S_{32}/S_{31}$. The directional coupler connected as shown in Fig. 3 evidently permits magnified response since $|S_{32}/S_{31}|$ is the directivity ratio and may be quite large while $|S_{21}|$ is usually between 0.7 and 1.0. The use of auxiliary tuners[4] with a directional coupler permits greater versatility since one may adjust the directivity ratio upwards or downwards with one tuner, then adjust the other tuner to make $\Gamma_{2i}=0$. These adjustments are independent only if made in the order described. Referring to Fig. 6, the tuner in arm 2 is adjusted first in order to obtain the desired value of $|K|$, then the tuner in arm 1 is adjusted to make $\Gamma_{2i}=0$.

Measurements Using Squared VSWR Response

Any of the junctions of Fig. 5 or their equivalents may be used if the unknown is phasable. This requirement is satisfied if the unknown termination slides inside the waveguide. In principle, a phase shifter or line stretcher may also be used to provide the phase variation, but in practice, they are less than perfect, leading to additional errors in measurement. If the unknown termination does not slide within the waveguide, the arrangements of Fig. 5(d) and (e) may be used. Either flexible cables must be used to couple the generator and detector to the moving junction, or the generator and detector may be arranged to move with the junction. If the termination is not too large, it and the waveguide section could be moved, keeping everything else fixed. The arrangement shown for rectangular waveguide is not readily adaptable to operation with coaxial lines. However the arrangement of Fig. 5(e) should be satisfactory for operation with coaxial line.

The correct adjustment of the tuner is made with $\Gamma_L=0$ and corresponds to maximum detector output for Figs. 2 and 5(a) and to minimum detector output for the others shown. When the correct adjustment has been made, the response curves will be symmetrical about the maxima and minima.

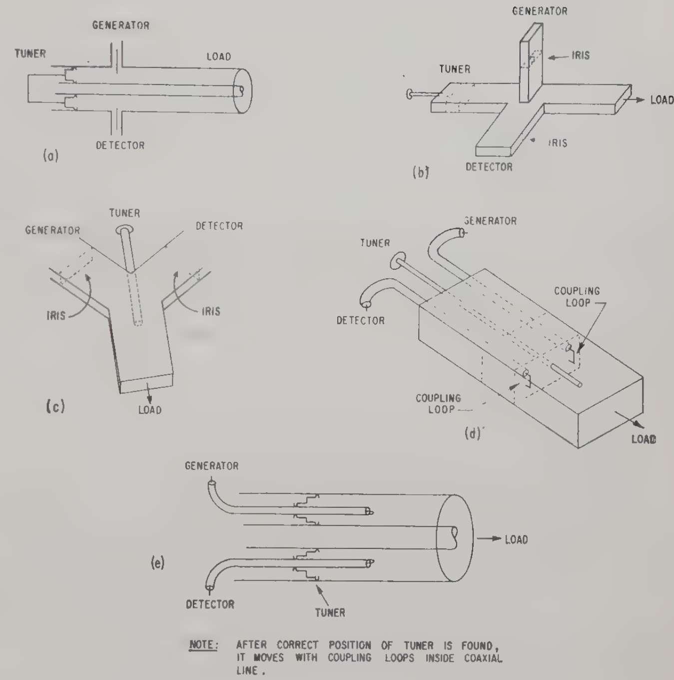

Fig. 5—Schematic drawings of junctions permitting squared VSWR response. (a), (b), (c), (d), (e).

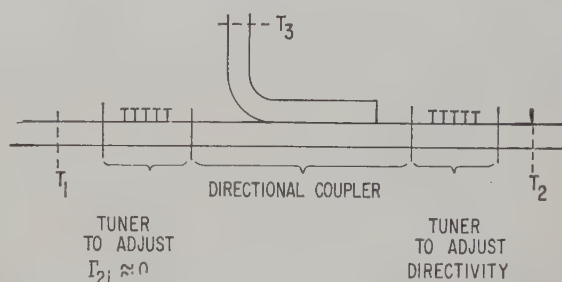

Fig. 6—Directional coupler with auxiliary tuners.

A correction may be made for deviations from the ideal conditions $|K| \approx 1$, $|\Gamma_{2i}| \approx 1$, using the methods indicated[2] by MacPherson and Kerns. Instead of analyzing the response curve to obtain the parameter y required for the correction, a shorter method is as follows. Only the real part (g) of y is needed for a correction to the VSWR. It can be shown that to a good approximation (to the first order in g and b),

$$\sigma_I = \frac{1 + |K\Gamma_L|}{1 - |K\Gamma_L|} = \sqrt{\sigma_A} + \tfrac{1}{2}(g+1)(\sigma_A - 1), \quad (7)$$

where

$$(g+1) \approx \frac{|b_3|\,(\Gamma_L = 0)}{|b_3|_{\max}(|\Gamma_L| = 1)}.$$

It is still necessary to determine $|K|$ in order to obtain $|\Gamma_L|$ or σ_L. This may be done by measuring σ_I when a termination of known $|\Gamma_L|$ is connected.

[4] G. F. Engen and R. W. Beatty, "Microwave Reflectometer Techniques," this issue, p. 351.

Measurements Using Magnified Response

The arrangement of Fig. 6 may be used to measure the voltage reflection coefficient Γ_U of an unknown termination. Two basic methods[4,5] will be outlined.

In the first method, the auxiliary tuners are adjusted for the conditions $\Gamma_{2i}=0$ and $K=\infty$. Inspection of (5) shows that $|b_3|$, the magnitude of the detector arm wave amplitude will then be proportional to $|\Gamma_L|$. One then measures the ratio r of the $|b_3|$ values obtained when the load is first unknown (Γ_U), then a standard of known reflection coefficient magnitude $|\Gamma_S|$. Then

$$|\Gamma_U| = r|\Gamma_S|. \tag{8}$$

The adjustments of the tuners preceding the measurement is as follows.[4] One adjusts the tuner in arm 2 until no variation is observed in $|b_3|$ as one slides a termination of low reflection inside the output waveguide. Then the tuner in arm 1 is adjusted until no variation in $|b_3|$ is observed as one slides a termination of high reflection inside the output waveguide. If necessary, the above operations are repeated in sequence until no variation in $|b_3|$ is observed as either termination is slid.

In the second method, the tuner in arm 2 is adjusted (with the unknown connected to arm 2) until the detector output is zero. Then $K\Gamma_U=-1$. The tuner in arm 1 is then adjusted until $\Gamma_{2i}=0$. A reflection standard of known $|\Gamma_S|$ is then connected to arm 2, and the phase of Γ_S is varied. Substitution of the above conditions into (5) leads to

$$\sigma_A = \frac{|b_3|_{\max}}{|b_3|_{\min}} = \frac{|\Gamma_U| + |\Gamma_S|}{||\Gamma_U| - |\Gamma_S||}. \tag{9}$$

In the event that $|\Gamma_S| \approx 1$, (approximately true for a sliding short-circuit), then $\sigma_A=\sigma_U$.

Note that it is unnecessary to vary the phase of Γ_U, the reflection coefficient of the unknown termination in either method. In the second method one needs to vary the phase of Γ_S, but this is easily done if a sliding short-circuit is used.

Alternatively a fixed reflection standard may be used if a suitable line stretcher is incorporated into arm 2 of the measuring instrument.

[5] R. W. Beatty and D. M. Kerns, "Recently developed microwave impedance standards and methods of measurement," IRE Trans. on Instrumentation, vol. I-7, pp. 319–321; December, 1958.

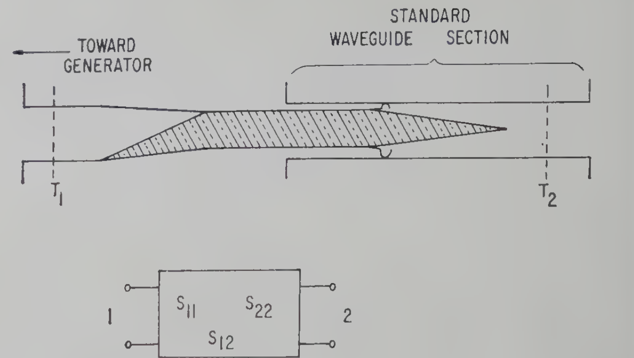

Fig. 7—Line stretcher and scattering coefficient representation.

Because of the special condition $\Gamma_{2i}=0$, the line stretcher need not be of the constant impedance type, since reflections that it may introduce may be cancelled by reflections from the tuner in arm 1. Also, the reference plane for arm 2 may be located in the uniform waveguide section of the line stretcher between the source of its reflections and the load. As shown in Fig. 7, the reference plane T_2 remains fixed although the output waveguide and load move. The line stretcher must be stable however, so that the parameters S_{11}, S_{12}, and S_{22} with respect to the reference planes T_1 and T_2 do not vary as it operates.

With the addition of the line stretcher, the second method described above may be called a magnified difference method, since the smaller the difference between $|\Gamma_S|$ and $|\Gamma_U|$, the greater the variation in $|b_3|$ as the phase is changed (9).

Evaluation

It is too early to make a conclusive evaluation of the worth of the responses described above and their applications in measurement systems. However, the techniques employing magnified response give promise of increased accuracy in the measurement of low and intermediate VSWR. Accuracies of approximately 0.1 per cent in VSWR to 2.0 have been achieved, and perhaps an order of magnitude better than that is possible.

Acknowledgment

Dr. D. M. Kerns made many helpful suggestions, including the junction of Fig. 5(b), and W. J. Anson and E. Niesen made measurements to verify the techniques described above.

Microwave Reflectometer Techniques*

G. F. ENGEN† AND R. W. BEATTY†

Summary—A rigorous analysis of the microwave reflectometer is presented for what is believed to be the first time. By means of this analysis, the correct adjustment of auxiliary tuners is described, and the errors resulting from incorrect adjustments are treated in a quantitative manner.

It is shown how the reflectometer technique may be further simplified while preserving the accuracy of measurement. A convenient method of adjusting the auxiliary tuners is described, sources of error are discussed, and an example is given of the calculation of error limits.

Introduction

THE microwave reflectometer in its usual form consists of a pair of directional couplers so arranged that one couples to the forward, and the other to the reverse wave. The ratio of the sidearm outputs is, in the ideal case, equal or at least proportional to the magnitude of the reflection coefficient of the termination, from which one can calculate the standing wave ratio.

In practice, this relationship is only approximately realized because of imperfections in the directional couplers and other factors. However, directional couplers having high directivity (40 db or more) and low main guide VSWR (less than 1.05) are commercially available which permit good accuracy to be realized over a large (1.5 to 1) frequency range, while at a given frequency, further improvements may be realized by the use of auxiliary tuning.[1]

The use of auxiliary tuners has not been fully exploited or completely treated however, and in this paper a more general and rigorous analysis of the microwave reflectometer will be presented leading to the introduction of additional tuning elements. Procedures for the adjustment of these transformers will be described and a particularly simple form of the reflectometer developed. A quantitative treatment of the errors in these techniques will be presented.

General Theory

The basic form of the reflectometer is shown in Fig. 1. If b_3 and b_4 represent the voltage amplitudes of the signals at the respective detectors, the desired response is

$$\left|\frac{b_3}{b_4}\right| = |\Gamma_l| \quad \text{or} \quad \left|\frac{b_3}{b_4}\right| = K|\Gamma_l|$$

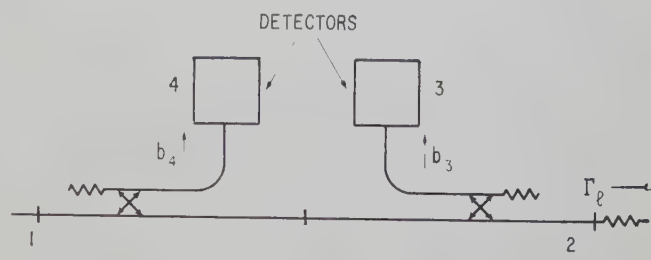

Fig. 1—Basic reflectometer.

where Γ_l is the voltage reflection coefficient of the termination on arm 2, and K is a constant whose value must be determined.

A mathematical treatment of the four arm junction and detectors shows (assuming linearity) that the response will in general be of the form:

$$\frac{b_3}{b_4} = \frac{A\Gamma_l + B}{C\Gamma_l + D} \tag{1}$$

where the A, B, C, and D are functions of the parameters of the four arm junction and detectors.

A particularly simple and convenient group of expressions for the terms A, B, C and D, may be obtained by the following procedure. The performance of the reflectometer of Fig. 1 is characterized by the functional relationships imposed upon the terminal variables a_1, b_1, a_2, and b_2, which represent the incident and emergent voltage wave amplitudes at arms 1 and 2 respectively and the responses of the detection systems (usually power) employed at arms 3 and 4. The main interest is in the relationship between the detector responses and the ratio

$$\frac{a_2}{b_2} = \Gamma_l$$

as given in (1). A variety of equivalent circuit representations may be substituted for that shown in Fig. 1 provided the relationships of interest among the terminal variables are preserved. A convenient choice for the present purpose is as follows:

Assuming that the detector impedance is constant (as will be true for example of a barretter operated at a constant resistance) mathematical models for the detectors may be constructed of lossless and matched detectors preceded by lossy fourpoles of the required parameters to produce the externally observed behavior. Reference planes in arms 3 and 4 are then chosen between these ideal detectors and the lossy discontinuities such that the latter become part of the four arm junc-

* Manuscript received by the PGMTT, January 13, 1959; revised manuscript received, February 20, 1959.

† Radio Standards Lab., Nat. Bur. of Standards, Boulder, Colo.

[1] J. K. Hunton and N. L. Pappas, "The *hp* microwave reflectometers," *Hewlett-Packard J.*, vol. 6; September–October, 1954.

tion as shown in Fig. 2. The remainder of the system may be represented in the usual manner. This permits one to analyze the general behavior of the reflectometer as a four arm junction under the materially simplifying assumption of matched detectors on arms 3 and 4.

The main effects of this type of formulation are those of modifying the values of the scattering coefficients from those which would obtain were the reference planes in arms 3 and 4 chosen to coincide with the physical junction between the detector mounts and the associated four arm junction; and of placing the reference planes in arms 3 and 4 in a physically inaccessible position, but this is of no concern since the subsequent measurements or adjustments of the four arm junction to be described do not require access to these planes. In addition, as noted, the detector impedance is assumed to be constant. There is no further loss in generality.

An analysis of the reflectometer of Fig. 2 yields:

$$A = S_{21}S_{32} - S_{31}S_{22}$$
$$B = S_{31}$$
$$C = S_{21}S_{42} - S_{41}S_{22}$$
$$D = S_{41} \tag{2}$$

where the $S_{m,n}$ are the scattering coefficients of the four arm junction comprised of the directional couplers and lossy fourpoles.

It is evident that the desired response will be realized if $B=C=0$. For ideal couplers of infinite directivity and a main guide VSWR of unity (and matched detectors) the terms S_{31}, S_{42}, and S_{22} are all zero, and

$$\left|\frac{b_3}{b_4}\right| = \left|\frac{A}{D}\Gamma_l\right|$$

as required.

In practice, the failure of the directional couplers and detectors to meet these criteria may be compensated or corrected for by the introduction of tuners at positions X and Y as shown in Fig. 3 (the tuner at Z serves an auxiliary role to be described later). The adjustment of T_X and T_Y to produce the conditions $B=C=0$ may be carried out in a variety of ways, two of which will be described. The first of these tuning procedures perhaps gives one a better feel for the conditions under which the adjustments may be physically realized, and is included for the sake of completeness, while the second method, the one which is recommended, is more convenient and potentially more accurate.

Adjustment of Tuners

In the first method, arm 2 is terminated in a matched load and T_X adjusted for a null in arm 3 (with arm 1 connected to the generator). This produces the condition $S_{31}=0$ (by definition of the scattering coefficient). The generator is then connected to arm 2; a load (not necessarily matched) connected to arm 1, and T_Z adjusted to produce a null in arm 4. If T_Y is now adjusted such that the reflection coefficient

$$\Gamma_{2i} = \frac{b_2}{a_2}$$

observed at arm 2 vanishes, it can be shown[2] that

$$S_{21}S_{42} - S_{41}S_{22} = 0,$$

and the desired operating conditions have been realized.[3]

It will be noted[2] that the first adjustment (of T_X) is independent of the second, while the converse is not true, thus the adjustments should be made in the order indicated. In addition, while T_Z is employed in the second tuning operation, once the proper adjustment of T_Y has been realized, T_Z may be readjusted (as will subsequently prove desirable) without affecting this result obtained by adjustment of T_Y.[4]

The alternative procedure will now be described. Referring again to (1), it will be evident that even before the introduction of tuning transformers, the terms B and C (for a reflectometer assembled from commercial

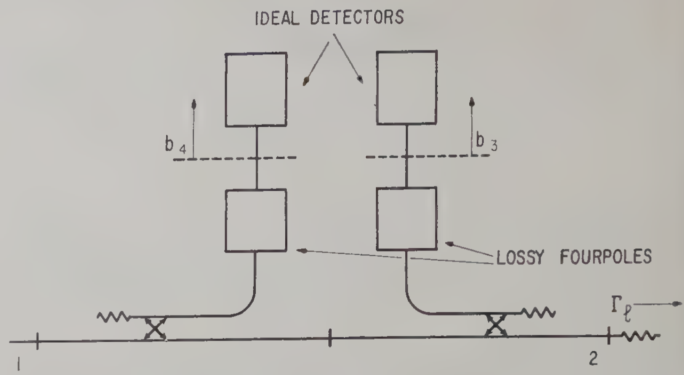

Fig. 2—Equivalent reflectometer.

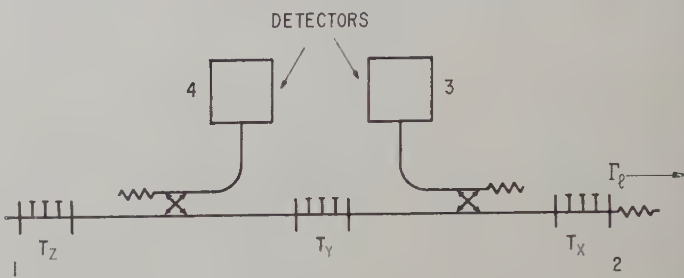

Fig. 3—Reflectometer with auxiliary tuners.

[2] The proof of this statement and several of those to follow may be effected by solving the scattering equations for the indicated quantities under the stated conditions, or by obtaining the scattering parameters of the individual components, *i.e.*, tuners and directional couplers. The proofs are generally straightforward but tedious.

[3] The minimum requirements which must be satisfied by the two couplers in order that these adjustments may be physically realized have not been determined at the time of this writing, but would appear to be well satisfied by commercially available components.

[4] The expression ($S_{21}S_{42}-S_{41}S_{22}$) may also be written

$$S_{41}\left(\frac{S_{21}S_{42}}{S_{41}} - S_{22}\right).$$

It can be shown (see note 2) that the second factor is invariant to the adjustment of tuner T_Z.

components) are quite small with regard to A and D respectively. Consider the system response to a phasable or sliding load of such magnitude that $|A\Gamma_l| \approx |B|$. From inspection it is evident that the numerator of (1) will undergo marked changes in amplitude, while the denominator remains relatively constant as the phase of the load is varied; and if T_X is adjusted to minimize the variation in the ratio

$$\left|\frac{b_3}{b_4}\right|$$

as the phase of Γ_l is varied, the condition $S_{31}=0$ will be approximately realized. The sliding load of low VSWR is then replaced by one of large VSWR (a sliding short). Variations in output as the position of the short is changed will now be predominantly due to variations in the denominator, and if T_Y is adjusted such that $|b_3/b_4|$ is again constant, the condition $S_{21}S_{42}-S_{41}S_{22}=0$ will also be very nearly realized.

A more complete mathematical treatment of the above procedure yields three solutions for a constant magnitude of b_3/b_4 as the phase of Γ_l is varied. The first solution, $A/C=B/D$ is trivial since it gives for b_3/b_4 a value which is entirely independent of Γ_l. The second solution, the one of interest, is:

$$\frac{B}{A} = \left(\frac{C}{D}\right)^* |\Gamma_l|^2 \tag{3}$$

where (*) denotes the complex conjugate.

In practice, A and D are nominally of the same order of magnitude so when (3) is satisfied, $|B|$ is of the order of $|C\Gamma_l^2|$. Thus if the sliding load has a VSWR of 1.02 ($|\Gamma_l|=0.01$), it is evident that the first tuning operation will make $|B|$ smaller than $|C|$ by a factor of approximately 10^4, while the second operation ($|\Gamma_l|\approx 1$) will reduce $|C|$ to the nominal size of $|B|$. Thus a series of these operations rapidly converges to the desired conditions $B=C=0$.

The third solution referred to above is the limiting one of a matched load ($\Gamma_l=0$) which also yields a constant ratio of b_3/b_4. The ideal or perfect match is, of course, never achieved in practice, while the closest approach to this ideal is usually by means of a variable sliding load which is adjusted to produce the minimum change of signal in an appropriate associated measuring system as the position of the load is varied. If a matched load is available, it is only necessary to adjust T_X until the output at arm 3 vanishes, while if an adjustable sliding load is used, it is convenient to carry out the operations as required to make Γ_l and b^3 vanish simultaneously. The technique described earlier, however, does not require a matched (reflection free) sliding load, but only that its reflection coefficient be small.

If the initial conditions are such that $|B| \gg |A\Gamma_l|$, the variation in the ratio

$$\left|\frac{b_3}{b_4}\right|$$

would be quite small, so as a first step (where only the phase of Γ_l is adjustable), it is usually desirable to first adjust for a null in arm 3 for an arbitrary position of the load and then adjust for a constant ratio

$$\left|\frac{b_3}{b_4}\right|$$

as the phase is varied. It will be noted that the magnitude of b_3/b_4 depends upon the magnitude of Γ_l.

It is thus of interest to note that the technique requires neither a perfectly matched load or ideal short, but only two phasable loads of different reflection coefficient magnitudes. The more closely these ideals are realized however, the more rapidly will a series of these operations converge to the desired conditions, which in practice can usually be realized to the required accuracy by only one adjustment each of T_X and T_Y. It is also of interest to note that if a perfectly matched load ($\Gamma_l=0$), an ideal sliding short ($\Gamma_l=e^{j\theta}$), and a dissipation free transformer at X are assumed, the two tuning operations, in this method, are completely independent of one another. That is, the adjustment of T_X to yield the condition $B=0$, as noted earlier, is independent of the adjustment of T_Y, while the adjustment of T_Y for the condition $B/A=(C/D)^*$ is independent of T_X.[5]

Having completed these adjustments, the response becomes:

$$\left|\frac{b_3}{b_4}\right| = \left|\frac{A}{D}\Gamma_l\right|.$$

The magnitude of the ratio A/D may be conveniently determined by observing the response to a load of known reflection, a convenient example being a fixed short for which Γ_l has the nominal magnitude 1. Thus if the response to the short is

$$\left|\frac{b_3}{b_4}\right|_s$$

one has for the unknown reflection coefficient Γ_u.

$$|\Gamma_u| = \frac{\left|\frac{b_3}{b_4}\right|_u}{\left|\frac{b_3}{b_4}\right|_s}. \tag{4}$$

Once the reflection coefficient has been determined, the VSWR may, of course, be obtained by the usual formula

$$\sigma_u = \frac{1+|\Gamma_u|}{1-|\Gamma_u|}.$$

[5] A formal proof of this statement is somewhat lengthy, but may be recognized intuitively in the following way. An ideal sliding short preceded by a dissipation free transformer still appears as a load of $|\Gamma_l|=1$ and variable phase angle, thus the condition $B/A=(C/D)^*$ is invariant to the addition (or removal) of a lossless tuning transformer at arm 2.

A variety of techniques are available for measuring the ratio

$$\left|\frac{b_3}{b_4}\right|.$$

In general, both b_3 and b_4 will change with generator output and load impedance, requiring a ratio type meter such that

$$\left|\frac{b_3}{b_4}\right|$$

is indicated directly, or a pair of instruments to determine $|b_3|$ and $|b_4|$ individually. Alternatively, a feedback servo loop may be employed to keep $|b_4|$ constant, requiring only the observations of the values of $|b_3|$.

The functional dependence of b_4 upon the load impedance may be substantially eliminated by adjusting transformer T_Z such that the value of $|b_4|$ is independent of a sliding short at arm 2. This will reduce the amount of correction required of the servo loop, if one is employed, or the signal b_4 might be then applied to the automatic gain control channel if a standing wave amplifier were employed to measure $|b_3|$. These are only several of a number of possibilities.

If the adjustment to make $|b_4|$ independent of the load impedance has been made with sufficient care, $|b_4|$ will depend only upon the generator level, and if the generator is sufficiently stable, the signal $|b_4|$ will be constant and thus no longer contain any useful information. This first coupler with its associated detector and transformer T_Z may then be eliminated, resulting in a simplified system. This particular case appears to be enough of interest to warrant separate treatment.

A Modified Form of Reflectometer

Referring to the three arm junction of Fig. 4, the wave amplitude b_3 incident upon the detector in arm 3 can be written:

$$b_3 = b_g \frac{E\Gamma_l + F}{G\Gamma_l + H}, \tag{5}$$

where

$$E = \begin{vmatrix} S_{21} & S_{22} \\ S_{31} & S_{32} \end{vmatrix},$$

$$F = S_{31},$$

$$G = -\begin{vmatrix} -(1 - S_{11}\Gamma_g) & S_{12} & S_{13}\Gamma_d \\ S_{21}\Gamma_g & S_{22} & S_{23}\Gamma_d \\ S_{31}\Gamma_g & S_{32} & -(1 - S_{33}\Gamma_d) \end{vmatrix},$$

$$H = \begin{vmatrix} (1 - S_{11}\Gamma_g) & S_{13}\Gamma_d \\ S_{31}\Gamma_g & (1 - S_{33}\Gamma_d) \end{vmatrix},$$

b_g is the equivalent generator voltage wave amplitude, and Γ_g and Γ_d are the generator and detector reflection coefficients at reference planes 1 and 3 respectively. It will be noted that the reference planes have been chosen to coincide with the terminal surfaces of the directional coupler, thus exhibiting the dependence on the detector impedance explicitly.

Eq. (5) is of the same form as (1) and the adjustment of T_X' and T_Y' to make F and G vanish may be carried out in the manner already described except that in step two of the first method $\Gamma_{2i} = b_2/a_2$ is made to vanish by adjustment of T_Y' with arm 1 terminated in the generator impedance, instead of the procedure described earlier.

Measurement of the ratio

$$r = \frac{|b_3|_u}{|b_3|_s} = \frac{|\Gamma_u|}{|\Gamma_s|}$$

and a knowledge of $|\Gamma_s|$ again permits the calculation of $|\Gamma_u|$ or σ_u and again, a variety of techniques such as power, audio, or heterodyne detection may be employed, or a calibrated standard attenuator may be placed in the system and the changes in attenuation required to keep $|b_3|$ constant observed.

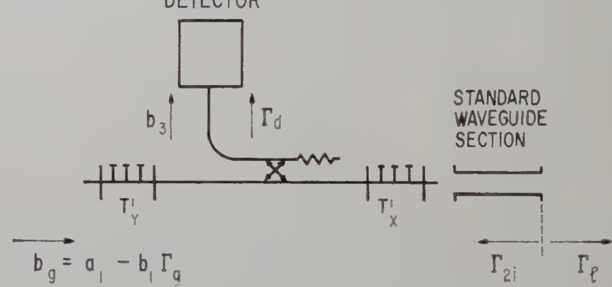

Fig. 4—Modified reflectometer.

The modified technique thus provides a reduction in the complexity of both the waveguide plumbing and associated detection equipment, but requires a signal source of stable amplitude, while the more conventional system is ideally independent of the generator level. Both systems are adaptable to either rectangular waveguide or coaxial systems, and may usually be assembled from commercially available components although it is desirable to use a precision waveguide section to terminate arm 2 in which the sliding loads may be inserted, as shown in Fig. 4. The importance of good flanges or connectors at arm 2 should also be recognized.

Analysis of Errors[6]

The sources of error, in determining $|\Gamma_u|$ and σ_u by these methods to be discussed in this section include: a) incorrect measurement of r, and uncertainty in value of $|\Gamma_s|$, and b) improper adjustment of the tuners, such that B and C do not vanish.

The consideration of other sources of error is outside the scope of this present paper, but will be treated more

[6] The analysis also applies to the modified reflectometer if the quantities E, F, G, H are substituted for A, B, C, D.

fully in a subsequent paper (in preparation) on the application of the technique to measurement of bolometer mount efficiency.

The error due to a) may be determined by inspection. If the equation for $|\Gamma_u|$ is written in the form:

$$|\Gamma_u| = |\Gamma_s| \frac{\left|\dfrac{b_3}{b_4}\right|_u}{\left|\dfrac{b_3}{b_4}\right|_s} = |\Gamma_s|\, r, \tag{6}$$

it is evident that the fractional error in $|\Gamma_u|$ will equal the sum of the fractional errors in $|\Gamma_s|$ and r if the latter are small.

With regard to the second item b) it will be recalled that the condition for constant output as the phase of the load is varied is:

$$\frac{B}{A} = \left(\frac{C}{D}\right)^* |\Gamma_l|^2,$$

which establishes a theoretical upper limit to the accuracy with which a particular tuning adjustment may be made.

In practice, however, the limitation usually stems from improper adjustment of the tuning transformers such that the output variations are not completely eliminated. In the discussion to follow it will be assumed that such is the case, that is, it is assumed that B and C have been reduced to the point where the variations in the expression

$$\left|\frac{b_3}{b_4}\right| = \frac{|A\Gamma_l + B|}{|C\Gamma_l + D|}$$

are due entirely to variations in the numerator or denominator as the loads of small and large VSWR are employed respectively.

A first order correction to (6) may be written as follows:

$$|\Gamma_u| = |\Gamma_s| \frac{|b_3|_u}{|b_3|_s} \left| 1 + \frac{B}{A} \frac{\Gamma_s - \Gamma_u}{\Gamma_s \Gamma_u} + \frac{C}{D}(\Gamma_s - \Gamma_u) + \cdots \right|. \tag{7}$$

The ratios $|B/A|$ and $|C/D|$ may be determined from the expressions:

$$K_1 = 20 \log \left[1 + 2 \left| \frac{B}{A\Gamma_l} \right| \right]$$

and

$$K_2 = 20 \log \left[1 + 2 \left| \frac{C}{D} \right| \right]$$

where K_1 and K_2 are the ratios in decibels of the maximum to minimum outputs with the sliding loads of small and large VSWR respectively, $|\Gamma_l|$ is the reflection coefficient of the load of small VSWR, and a reflection coefficient of unity has been assumed for the load of large VSWR.

Except for the presence of the factor Γ_l, these equations for K_1 and K_2 are of the same form, and values for $|B/A|$ and $|C/D|$ may be obtained from Fig. 5 where the value of $|C/D|$ is taken from the line $|\Gamma_l| = 1$. It will be noted that the evaluation of the right hand side of (7) further presupposes a knowledge of Γ_u but for the present purpose of assigning a limit of error, an accurate value is not required.

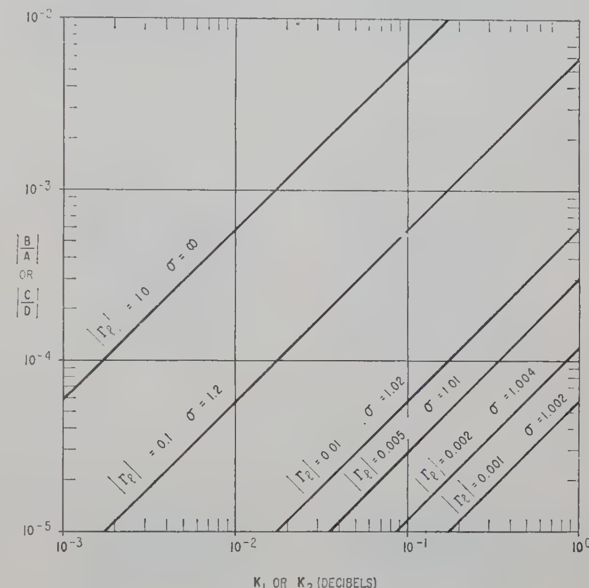

Fig. 5—Graph for the determination of $|B/A|$ and $|C/D|$.

As an example, if a sliding load of VSWR = 1.005 is employed in the first tuning operation, and the variation in output is reduced to 1 db, $|B/A|$ will have a value of approximately 1.6×10^{-4}. If the variation in the second step with the sliding short is reduced to 0.02 db, the value for $|C/D|$ will be approximately 1.2×10^{-3}. Assuming that the unknown load has a value $|\Gamma_u| \approx 0.2$, $(\sigma \approx 1.5)$, $|\Gamma_s| = 1.000$ (corresponding to a short-circuit) and assuming the terms in the right hand factor of (7) combine in the worst phase, values of 6 and 1.2 for

$$\left| \frac{\Gamma_s - \Gamma_u}{\Gamma_s \Gamma_u} \right|$$

and $|\Gamma_s - \Gamma_u|$ obtain respectively, for a total error of $\pm(1.6 \times 10^{-4} \times 6 + 1.2 \times 10^{-3} \times 1.2) \approx \pm 2.4 \times 10^{-3}$, or ± 0.24 per cent.

Acknowledgment

The authors extend their thanks to David F. Wait who contributed to the error analysis, to Dr. David M. Kerns for his helpful suggestions in reviewing the manuscript, and to Wilbur J. Anson and Edward Niesen who provided experimental demonstrations of the techniques described.

Application of a Backward-Wave Amplifier to Microwave Autodyne Reception*

J. K. PULFER†

Summary—A microwave receiver using a single-circuit backward-wave amplifier as a combination radio-frequency amplifier and homodyne local oscillator is described. The amplifier tube is operated at a value of beam current just above that required to maintain oscillation. It is shown that in this way, the high gain and narrow bandwidth of the single-circuit backward-wave amplifier may be utilized in an electronically tunable microwave receiver. The resultant sensitivity is 10 to 15 db worse than that obtainable from a good superheterodyne. The loss in sensitivity is due entirely to the high noise figure of the backward-wave amplifier, which can theoretically be reduced to a value comparable with that of a superheterodyne. The advantages of the receiver are its simplicity and its lack of image difficulties. Rejection of off-frequency signals is such that they are attenuated by at least 50 db.

Introduction

In many fields, a microwave spectrum analyzer is desirable which can display a band of frequencies of 25 to 50 per cent while at the same time maintaining a resolution of one in 10,000 or better. The resolution can easily be obtained by using a superheterodyne system, but the wide display bandwidth requires either a high first intermediate frequency or a zero intermediate frequency (homodyne) system in order to avoid images.

In principle the microwave homodyne receiver is simple and straightforward. The image problem inherent in superheterodyne receivers is no longer present. In attempting to build a practical receiver, however, one encounters the following difficulties:

1) The noise output from the mixer, which usually limits the sensitivity of the homodyne, is inversely proportional to frequency in the video range, and so is much larger for homodyne than superheterodyne operation.

2) The noise output of the local oscillator is also concentrated in a narrow spectrum around the oscillator frequency, and may contribute to the overall receiver noise figure.

3) Very high gain broadband video amplifiers are subject to hum, stray pickup, and microphonics, and so must have a limited lower-cutoff frequency.

4) For the video bandwidths usually required, the observable minimum signal for homodyne detection is usually only 20 to 25 db less than that for direct video detection, so that unless some filtering is included ahead of the detector, off-frequency signal rejection is very poor.

* Received by the PGMTT, January 21, 1959.
† Defense II Sect., Natl. Res. Council, Ottawa, Can.

Backward-Wave Amplifier Autodyne

It is evident that many of the disadvantages of the homodyne system would be removed by providing a high-gain narrow-band filter ahead of the mixer. This would eliminate the mixer as a source of noise, reduce the effects of local oscillator noise, hum, and microphonics, and improve off-frequency signal rejection. It raises the further problem, however, of keeping the filter and the local oscillator tracking in frequency.

The autodyne detector[1] used in the early days of radio consisted of a triode regenerative amplifier operating just above the oscillation threshold resulting in very high gain and coherent detection for a Morse code CW signal.

In the system to be described, a single-circuit backward-wave amplifier (BWA), which behaves as a high-gain narrow-band electronically-tunable filter, is allowed to oscillate. The filter and the local oscillator, therefore, track automatically in frequency, and can be tuned electronically. As in the conventional triode autodyne detector, simultaneous amplification and oscillation occur in the tube just above starting current. The output of the backward-wave tube is then fed into a crystal detector at high level, and thence to a video amplifier. It is also possible to recover the video voltage directly from the electron beam by means of a suitable collector. With presently available tubes, the latter method has not been too successful.

In order to understand the operation of the BWA Autodyne properly, it is necessary to study the effect of simultaneous application of two signals to a backward-wave amplifier.

In a recent publication, Laico, McDowell, and Moster[2] have shown that saturation of the beam in a conventional forward-wave traveling wave tube results in reduction of amplitude variations in the sum of two simultaneously applied signals, while preserving the phase changes. Behavior of signals in a backward-wave amplifier is similar provided that they are sufficiently close in frequency to be amplified simultaneously.

Results and Discussion

The above reasoning has been verified by measurements on an experimental homodyne receiver constructed from a Varian VAD-161 backward-wave am-

[1] F. E. Terman, "Radio Engineering," 2nd ed., McGraw-Hill Book Co., New York, N. Y., p. 453; 1937.

[2] J. P. Laico, H. L. McDowell, and C. R. Moster, "Medium power traveling wave tube for 6000 mc radio relay," *Bell Sys. Tech. J.*, vol. 35, pp. 1285–1346; November, 1956.

plifier.[3] The VAD-161 is a modification of the VA-161 oscillator in which the collector end of the helix is brought out to allow insertion of radio-frequency signals. The frequency range is 8.0 to 12.4 kmc.

A block diagram of the receiver and measuring equipment is given in Fig. 1. Two types of display were used. A spectrum analyzer was used with a CW signal generator to determine the frequency response of the amplifier. To measure signal discernibility, a pulsed input signal from 1 to 10 μsec long was used, and the output displayed on an oscilloscope.

Measurements were made at a fixed frequency of 10.4 kmc (approximately the center of the band). Attenuators were placed in both the input and output circuits of the amplifier to avoid any errors caused by external reflections.

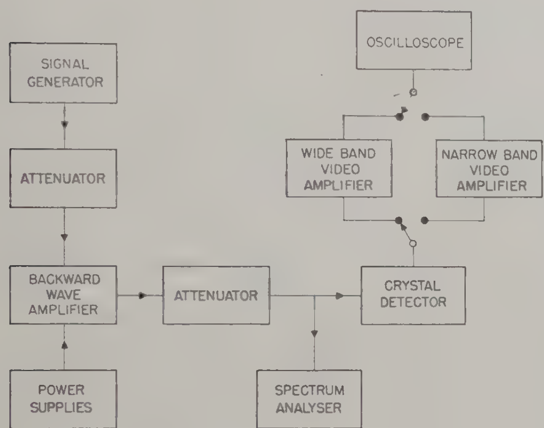

Fig. 1—Block diagram of the experimental receiver and measuring equipment.

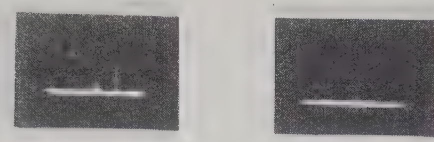

(a) (b)

Fig. 2—Amplifier and detector output when beam current is 99.5 per cent of starting current.

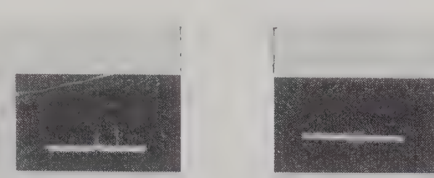

(a) (b)

Fig. 3—Amplifier and detector output for a beam current 100.3 per cent of starting current.

(a) (b)

Fig. 4—Amplifier and detector output for a beam current 100.6 per cent of starting current.

(a) (b)

Fig. 5—Amplifier and detector output for a beam current 107 per cent of starting current.

Operation of the receiver is best illustrated by Figs. 2–5. These show both the output spectra of the backward-wave tube for CW input, and the corresponding video output pulse (10 μsec long), for values of beam current of the backward-wave oscillator near starting current. The center frequency of the backward-wave amplifier response is on the center of the spectrum in Fig. 2(a). The width of the display is 4 mc and a CW signal at -80 dbm and 1 mc from the center frequency has resulted in a "pip" on the right-hand side of the spectrum. Fig. 2(a) illustrates the case where the beam current is just 99.5 per cent of starting current. The noise output from the amplifier can be seen at the center of the spectrum. The corresponding video output for a 10-μsec pulsed signal is shown in Fig. 2(b). As the lower cutoff frequency of the video amplifier was 20 kc, the pulse has been differentiated.

In Fig. 3(a) the beam current has been increased to 100.3 per cent of starting current, and the oscillator output occupies the center of the spectrum. There has been no significant change in the amplified signal at 1 mc away from the frequency of oscillation. The pulsed video output as displayed in Fig. 3(b) has become bipolar, and so is passed by the video amplifier.

In Fig. 4(a) the beam current has been increased to 100.6 per cent of starting current. At this point, the oscillator output has increased to a level which results in almost complete bunching of the electron beam. The tendency to saturation which results produces a third spectral component separated from the signal by 2 mc and on the opposite side of the oscillator frequency. As can be seen from the corresponding pulsed output displayed in Fig. 4(b) saturation of the beam current has not reduced the output pulse a significant amount.

In order to produce a noticeable change in the output the beam current was increased to 107 per cent of starting current giving the results illustrated in Fig. 5. Since the oscillator output was much greater than the signal at this beam current, almost complete saturation has taken place, and the two sidebands corresponding to the signal and its image reflected in the oscillator are approximately equal in amplitude. The resultant suppression also produces a reduction of amplitude of the output pulse as in Fig. 5(b).

[3] This tube was developed by Varian of Canada Ltd., Georgetown, Ont., under the auspices of the Defence Research Board, Can. (Electronic Components Res. and Dev. Committee).

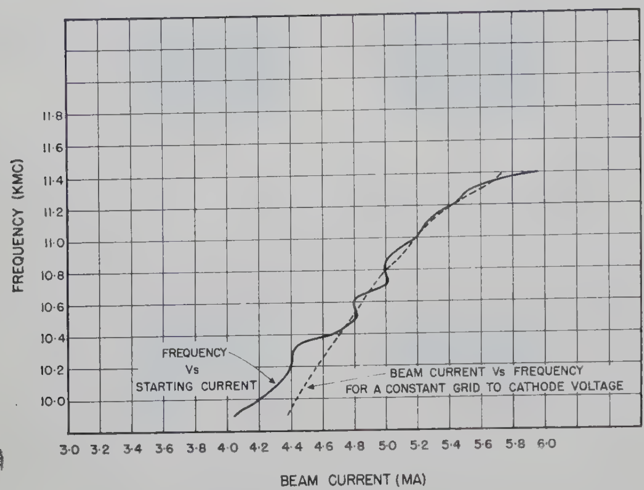

Fig. 6—Graph of frequency vs starting current, compared with frequency vs beam current at a constant grid voltage.

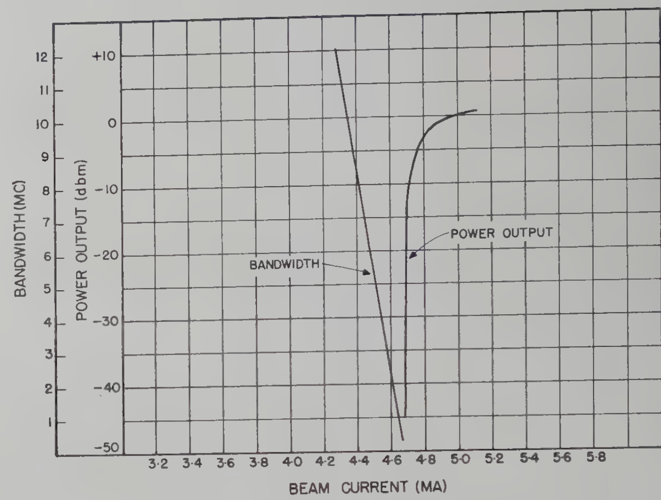

Fig. 7—Graph illustrating the variation of amplifier bandwidth and oscillator output with beam current in the vicinity of starting current.

It can be seen, therefore, that ratio of beam current to starting current must be maintained between 1 and 1.01 for maximum gain. This is not as difficult as would first appear, since a small change in beam current results in a relatively large change in oscillator output which may be regulated by a feedback system. Another factor which should be considered is the change of beam current, as frequency is changed (by varying the delay line voltage). Fig. 6 shows a plot of starting current vs frequency, and also a plot of beam current vs frequency for a constant grid voltage. It can be seen that operation over the entire range from 10.4 to 11.4 kmc results in a variation of only ± 2 per cent of beam current relative to starting current.

If the sensitivity of the backward-wave amplifier is constant over a wide band of frequencies, one other factor affects the wide-band operation of the over-all receiver. This is the variation in sensitivity of the crystal detector with frequency. It is difficult to find a video crystal mount with sensitivity constant within one or two db over a wide frequency range, particularly at frequencies above 10,000 mc. Usually the variation in crystal sensitivity at high level (-20 dbm or higher) is not as pronounced as the variation in minimum detectable signal, but can still be troublesome.

Fig. 7 illustrates the rate of change of amplifier bandwidth below oscillation starting current, and the way in which the output changes at currents above the starting current. Bandwidth measurements above the oscillation threshold are not possible because it is very difficult to measure the value of amplified signal at the center frequency in the presence of an oscillation at that frequency, which is much larger in magnitude. Some idea of the gains and signal levels involved in the operation of the amplifier can be obtained from Fig. 8. Curve (a) illustrates how the gain of the amplifier increases with beam current. This gain was measured by applying a CW signal to the amplifier and comparing the outputs at different values of beam current.

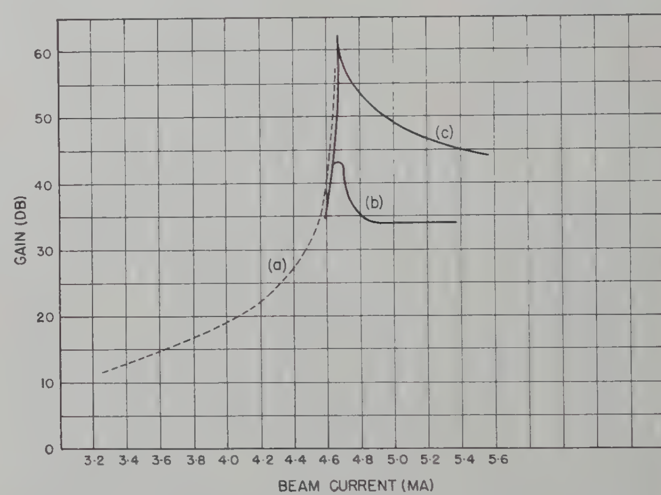

Fig. 8—Gain vs beam current for the type VAD-161-2 backward wave amplifier for three different input signals.

As the beam current reaches starting current, the regenerative gain increases indefinitely. Curve (b) illustrates gain at a frequency 1 mc higher than oscillation frequency.

Curve (c), which is a plot of sensitivity to a pulsed signal, shows that pulse sensitivity continues to fall well above the oscillation threshold, owing to saturation of the beam as described above.

In Fig. 9(a), a 1-μsec and a 10-μsec pulse at -70 dbm are illustrated. A wideband video amplifier was used, and the increased rise time of the pulses was caused by the narrow-band radio-frequency amplification. By using a pulse stretcher followed by a narrow-band video amplifier, the output can be made unipolar, and the sensitivity improved for longer pulses as illustrated in Fig. 9(b), where 1-μsec and 10-μsec pulses at -80 dbm are illustrated.

Fig. 10 is a typical plot of the sensitivity of the receiver vs frequency for a fixed delay line voltage. As can be seen, off-frequency signals are rejected by at least 50

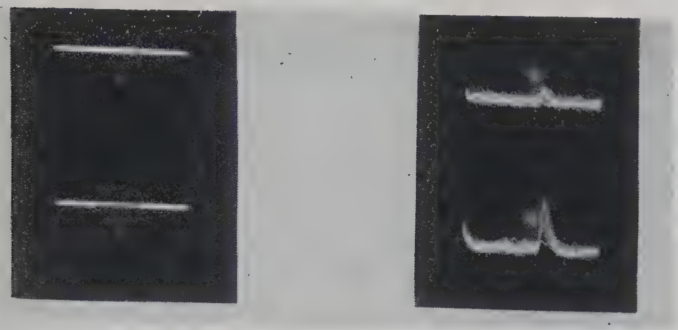

(a) (b)

Fig. 9—(a) Output pulses from a 1.5 mc video amplifier for 1-μsec and 10-μsec inputs at a level of -70 dbm. (b) Output pulses from a 1 mc video amplifier and pulse stretcher for 1-μsec and 10-μsec inputs at -80 dbm.

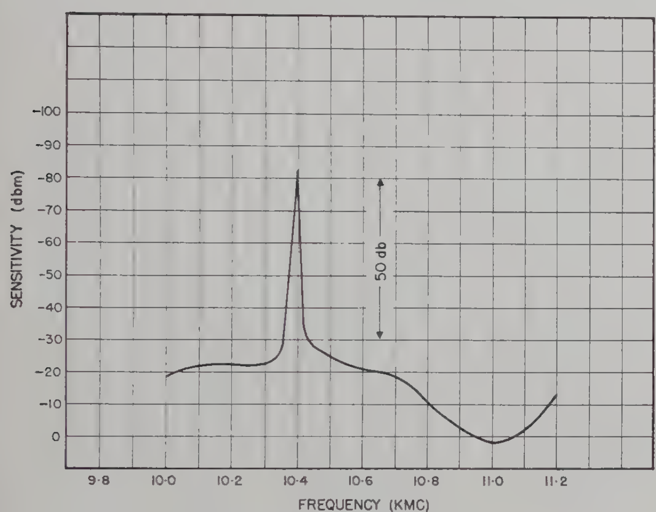

Fig. 10—Receiver sensitivity vs frequency for a fixed line voltage.

db. Bandwidth at the 3 db points is approximately 1 megacycle.

Where fixed frequency operation with good long-term stability is required, dc is used on the filaments, and a supply with a regulation of $<.025$ per cent is used for grid and cathode voltages. When the tube is used as a sweeping receiver for spectrum analysis, the requirements on power supply regulation, and ripple are an order less important.

Fig. 11 illustrates the over-all dynamic range of the receiver. This range is limited for large signals by saturation of the video amplifier and is not limited by the oscillator tube.

Minimum detectable 1-μsec pulsed signal is of the order of -90 dbm, with all voltages optimized. Minimum detectable CW signal is of the order of -105 dbm. If the output is fed to a pair of earphones, a 400-cycle square-wave modulated signal can be heard at -105 dbm. These values of sensitivity correspond to an over-all noise figure of about 22 db. This noise is generated in the backward-wave amplifier and could possibly be reduced considerably by proper gun design.[4]

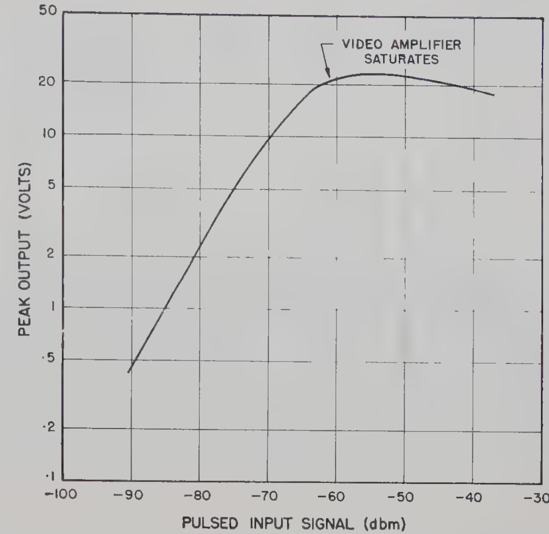

Fig. 11—Dynamic range of receiver.

Conclusion

A receiver can be constructed using a single backward-wave amplifier, crystal detector, and video amplifier. While this receiver is not a true homodyne, it operates with a locally generated voltage mixing in a crystal with an incoming signal. The oscillation is essential to operation of the receiver since maximum gain occurs just above oscillation starting point. The receiver has the following advantages:

1) It can be tuned over relatively wide bands electronically without complicated circuitry and power supplies.

2) It does not have image difficulties, as does a superheterodyne.

3) The unwanted signal rejection is at least 50 db, which is considerably better than that of the homodyne.

4) Bandwidth may be increased if sensitivity can be sacrificed.

Acknowledgment

The author is indebted to H. W. Poapst, who constructed the experimental receiver and assisted with the measurements, and to many of his colleagues for helpful suggestions given during the experimental work and preparation of this report.

[4] M. R. Currie and D. C. Forster, "Low noise tunable preamplifiers for microwave receivers," Proc. IRE, vol. 46, pp. 570–579; March, 1958.

Mode Theory of Lossless Periodically Distributed Parametric Amplifiers*

K. KUROKAWA† AND J. HAMASAKI†

Summary—In this paper, an operator $T\theta$ is introduced for the analysis of the periodically distributed parametric amplifier. The operator is the product of a diagonal matrix expressing the pumping phase relation and the T matrix of the basic section of the amplifier. The eigenvectors of $T\theta$ are called the "modes" of the amplifier. The orthogonality properties of the modes are proved in a similar way as for the conventional mode theory. Finally, an expression is derived for the power gain of the amplifier as an application of the theory.

I. Introduction

Considerable attention has been given recently to the parametric amplifier mainly because of the possibility of low-noise characteristics. The limitation of bandwidth[1] has been removed by the proposal of the traveling wave parametric amplifier; this proposal has been made by Miyakawa[2] and by Tien and Suhl[3] independently. The loss of available ferrites, however, requires a large amount of pumping power for the traveling wave ferromagnetic amplifier. In this regard, the traveling wave parametric amplifier with semiconductor diodes, as the active elements periodically loaded in the transmission line is more promising. As a matter of fact, some successful results already have been reported.[4] The term "periodically distributed parametric amplifier" will be used in this paper for the amplifier of this type to distinguish it from the one with uniformly distributed variable reactances. The theoretical study of the periodically distributed parametric amplifier was first undertaken by Saito. It is shown that the growing and decreasing waves can propagate in the lossless transmission line periodically loaded with the variable capacitors, of which the invariant parts are effectively cancelled out. These growing and decreasing waves are, naturally, very similar to those of the traveling wave amplifier discussed by Miyakawa, Tien, and Suhl. The extension of Saito's work leads to the eigenvalue problem of an operator $T\theta$, the product of a diagonal matrix expressing the pumping phase relation, and the T matrix of the basic section of the amplifier. The eigenvectors of the operator $T\theta$ may be called the modes of the periodically distributed amplifier. Presentation of the theory of these modes is the aim of this paper. The orthogonality relations between the modes are proved in a similar way as for the conventional mode theory.[5] Finally, the first approximation of the gain of the amplifier is derived as an application of the theory.

* Manuscript received by the PGMTT, February 16, 1959; revised paper received, March 23, 1959.

† Inst. of Indus. Sci., Univ. of Tokyo, Chiba City, Japan.

[1] H. Heffner and G. Wade, "Gain, bandwidth, and noise characteristics of the variable-parameter amplifier," *J. Appl. Phys.*, vol. 29, pp. 1321–1331; September, 1958.

[2] H. Miyakawa, "Amplification and frequency conversion in propagating circuits," *Inst. Elec. Comm. Engrs., Japan Nat'l. Convention Record*, p. 8; November, 1957 (in Japanese).

[3] P. K. Tien and H. Suhl, "A traveling wave ferromagnetic amplifier," Proc. IRE, vol. 46, pp. 700–706; April, 1958.

[4] R. S. Engelbrecht, "A low-noise nonlinear reactance traveling wave amplifier," Proc. IRE, vol. 46, p. 1655; September, 1958.

II. Introduction of the Operator $T\theta$

For the sake of simplicity, we shall consider the lossless two terminal pair networks with a variable capacitor as illustrated in Fig. 1. Fig. 1 (a) and (b) are identical two-terminal pair networks. The invariant part of the variable capacitor is divided into two parts, each of which is included in (a) and (b). Z_0 is the image impedance of (a) or (b) looking into the outside terminal, and Z_0' is the impedance looking into the inside terminal. (The prime notation indicates the value of the inside terminals.) In this section we shall indicate whether a quantity refers to the angular frequency ω_1 or ω_2 by the last subscript 1 or 2, respectively. We often omit this last subscript if the equation holds for both frequencies.

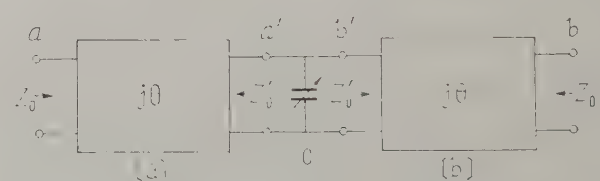

Fig. 1—Basic section of the amplifier.

The voltage and current at each terminal in Fig. 1 are, in terms of the incident waves (subscript i) and the reflected waves (subscript r),

$$V_a = \sqrt{Z_0}(a_i + a_r) \qquad V_a' = \sqrt{Z_0'}(a_i e^{-j\theta} + a_r e^{j\theta})$$

$$I_a = \frac{1}{\sqrt{Z_0}}(a_i - a_r) \qquad I_a' = \frac{1}{\sqrt{Z_0'}}(a_i e^{-j\theta} - a_r e^{j\theta}) \tag{1}$$

$$V_b = \sqrt{Z_0}(b_i + b_r) \qquad V_b' = \sqrt{Z_0'}(b_i e^{j\theta} + b_r e^{-j\theta})$$

$$I_b = \frac{1}{\sqrt{Z_0}}(b_i - b_r) \qquad I_b' = \frac{1}{\sqrt{Z_0'}}(b_i e^{j\theta} - b_r e^{-j\theta}). \tag{2}$$

[5] H. A. Haus, "Coupling of modes of propagation," M.I.T. Rep. (unpublished).

Since the voltages at the c-terminals must be equal,

$$V_a' = V_b'.$$

For ω_1, the above equation becomes

$$a_{i1}e^{-j\theta_1} + a_{r1}e^{j\theta_1} = b_{i1}e^{j\theta_1} + b_{r1}e^{-j\theta_1}. \tag{3}$$

The equation of continuity is

$$I_a' = I_b' + I_c \tag{4}$$

where I_c is the current through C. I_c is related to the voltage across C. If the pumping angular frequency ω_p is equal to the sum of ω_1 and ω_2, that is, if

$$\omega_1 + \omega_2 = \omega_p, \tag{5}$$

the relation is[6]

$$I_c = \begin{pmatrix} I_1 \\ I_2^* \end{pmatrix} = \begin{bmatrix} 0 & j\omega_1 \dfrac{c}{2} \\ -j\omega_2 \dfrac{c^*}{2} & 0 \end{bmatrix} \begin{pmatrix} V_1 \\ V_2^* \end{pmatrix} \tag{6}$$

where the asterisk denotes the complex conjugate. Using (1), (2), (3), and (6), we rewrite (4) in the form

$$a_{i1}e^{-j\theta_1} - a_{r1}e^{j\theta_1} - j\omega_1 \frac{c}{2}\sqrt{Z_{01}'Z_{02}'^*}(a_{i2}^*e^{j\theta_2} + a_{r2}^*e^{-j\theta_2}) = b_{i1}e^{j\theta_1} - b_{r1}e^{-j\theta_1}. \tag{7}$$

From (3) and (7), we have

$$b_{i1} = a_{i1}e^{-2j\theta_1} - j\omega_1 \frac{c}{4}\sqrt{Z_{01}'Z_{02}'^*}(a_{i2}^*e^{j(\theta_2-\theta_1)} + a_{r2}^*e^{-j(\theta_1+\theta_2)}). \tag{8}$$

Similarly, all the b's can be expressed in terms of the a's. The result is, in the matrix form,

$$B = TA \tag{9}$$

where

$$T = \left[\begin{array}{cc|cc} e^{-2j\theta_1} & 0 & -j\omega_1 c\dfrac{\sqrt{Z_{01}'Z_{02}'^*}}{4}e^{j(\theta_2-\theta_1)} & -j\omega_1 c\dfrac{\sqrt{Z_{01}'Z_{02}'^*}}{4}e^{-j(\theta_1+\theta_2)} \\ C & e^{2j\theta_1} & j\omega_1 c\dfrac{\sqrt{Z_{01}'Z_{02}'^*}}{4}e^{j(\theta_1+\theta_2)}, & j\omega_1 c\dfrac{\sqrt{Z_{01}'Z_{02}'^*}}{4}e^{j(\theta_1-\theta_2)} \\ \hline j\omega_2 c^*\dfrac{\sqrt{Z_{01}'Z_{02}'^*}}{4}e^{j(\theta_2-\theta_1)}, & j\omega_2 c^*\dfrac{\sqrt{Z_{01}'Z_{02}'^*}}{4}e^{j(\theta_1+\theta_2)} & e^{2j\theta_2} & 0 \\ -j\omega_2 c^*\dfrac{\sqrt{Z_{01}'Z_{02}'^*}}{4}e^{-j(\theta_1+\theta_2)}, & -j\omega_2 c^*\dfrac{\sqrt{Z_{01}'Z_{02}'^*}}{4}e^{j(\theta_1-\theta_2)} & 0 & e^{-2j\theta_2} \end{array}\right]$$

$$A = \begin{pmatrix} a_{i1} \\ a_{r1} \\ \hline a_{i2}^* \\ a_{r2}^* \end{pmatrix} \qquad B = \begin{pmatrix} b_{i1} \\ b_{r1} \\ \hline b_{i2}^* \\ b_{r2}^* \end{pmatrix}. \tag{10}$$

The vector A expresses the waves at the input and the vector B at the output of the basic circuit. The circuit in Fig. 1 is represented by the square matrix T, which transforms A into B.

Next we shall consider the n similar circuits connected in cascade. The variable capacitor of each circuit has the pumping phase lagged by $2\theta_p$ from that of the preceding one. These circuits are represented by the similar matrices to T, but they have $ce^{-2j\theta_p}$, $ce^{-4j\theta_p}$, $\cdots$ $ce^{-2(n-1)j\theta_p}$ in place of c.

For the analysis of the cascade connections of the same circuits, it is well known that the solutions of the eigenvalue problem of T are of great help: the circuits as a whole transform each eigenvector to the same eigenvector multiplied by (the eigenvalue)^n. The circuits under consideration are, however, different from each other, and the solutions of the eigenvalue problem of T are of no advantages at all.

Here we assume that T transforms the ω_1 components a_1 and the ω_2 components a_2 of A to $\gamma_1 a_1$ and $\gamma_2 a_2$, respectively, where γ_1 and γ_2 are scalers.

If we write T in the form

$$T = \left(\begin{array}{c|c} t_1 & cm_1 \\ \hline c^*m_2 & t_2 \end{array}\right), \tag{11}$$

(9) becomes

$$\begin{pmatrix} b_1 \\ \hline b_2^* \end{pmatrix} = \left(\begin{array}{c|c} t_1 & cm_1 \\ \hline c^*m_2 & t_2 \end{array}\right)\begin{pmatrix} a_1 \\ \hline a_2^* \end{pmatrix} = \begin{pmatrix} \gamma_1 a_1 \\ \hline \gamma_2^* a_2^* \end{pmatrix}. \tag{12}$$

The operator of the second section is

$$\left(\begin{array}{c|c} t_1 & ce^{-2j\theta_p}m_1 \\ \hline c^*e^{2j\theta_p}m_2 & t_2 \end{array}\right).$$

[6] H. E. Rowe, "Some general properties of nonlinear elements. II. Small signal theory," Proc. IRE, vol. 46, pp. 850–860; May, 1958.

From (12), we have

$$\left(\begin{array}{c|c} t_1 & ce^{-2j\theta_p}m_1 \\ \hline c^*e^{2j\theta_p}m_2 & t_2 \end{array}\right)\left(\begin{array}{c} a_1 \\ \hline a_2^*e^{2j\theta_p} \end{array}\right) = \left(\begin{array}{c} \gamma_1 a_1 \\ \hline \gamma_2^* a_2^* e^{2j\theta_p} \end{array}\right). \quad (13)$$

Hence, if we assume the relevance

$$\gamma_2^* = \gamma_1 e^{2j\theta_p}, \quad (14)$$

the output of the second section becomes

$$\left(\begin{array}{c|c} t_1 & ce^{-2j\theta_p}m_1 \\ \hline c^*e^{2j\theta_p}m_2 & t_2 \end{array}\right)\left(\begin{array}{c|c} t_1 & cm_1 \\ \hline c^*m_2 & t_2 \end{array}\right)\left(\begin{array}{c} a_1 \\ \hline a_2^* \end{array}\right)$$

$$= \left(\begin{array}{c|c} t_1 & ce^{-2j\theta_p}m_1 \\ \hline c^*e^{2j\theta_p}m_2 & t_2 \end{array}\right)\left(\begin{array}{c} \gamma_1 a_1 \\ \hline \gamma_2^* a_2^* \end{array}\right) = \left(\begin{array}{c} \gamma_1^2 a_1 \\ \hline \gamma_2^{*2} a_2^* \end{array}\right). \quad (15)$$

Similarly, the output of the nth section is

$$\left(\begin{array}{c|c} t_1 & ce^{-2(n-1)j\theta_p}m_1 \\ \hline c^*e^{2(n-1)j\theta_p}m_2 & t_2 \end{array}\right) \cdots$$

$$\cdot \left(\begin{array}{c|c} t_1 & ce^{-2j\theta_p}m_1 \\ \hline c^*e^{2j\theta_p}m_2 & t_2 \end{array}\right)\left(\begin{array}{c|c} t_1 & cm_1 \\ \hline c^*m_2 & t_2 \end{array}\right)\left(\begin{array}{c} a_1 \\ \hline a_2^* \end{array}\right)$$

$$= \left(\begin{array}{c} \gamma_1^n a_1 \\ \hline \gamma_2^{*n} a_2^* \end{array}\right). \quad (16)$$

This is a very simple relation. Thus we have shown that the solutions of (12) may play an important part in our analysis.

If we put

$$\gamma_1 = \lambda e^{-j\theta_p}, \qquad \gamma_2^* = \lambda e^{j\theta_p}, \quad (17)$$

then (14) is satisfied. We now rewrite (12) in the form

$$(T - \lambda I_\theta)A = 0 \quad (18)$$

where

$$I_\theta = \begin{bmatrix} e^{-j\theta_p} & 0 & 0 & 0 \\ 0 & e^{-j\theta_p} & 0 & 0 \\ 0 & 0 & e^{j\theta_p} & 0 \\ 0 & 0 & 0 & e^{j\theta_p} \end{bmatrix}. \quad (19)$$

The vector A satisfying (18) is transformed into $\lambda^n I_\theta^n A$ by the transformation of the left hand side of (16). Multiplying (18) by I_θ^{-1} from the left, we obtain

$$(T_\theta - \lambda I)A = 0 \quad (20)$$

where I is the unit matrix and

$$T_\theta = T_\theta^{-1}T = I_\theta^* T. \quad (21)$$

Eq. (20) has just the conventional form of the eigenvalue problems. As is well known, there are four independent eigenvectors (m eigenvectors in case of m dimensional space) and an arbitrary vector can be expressed as a linear combination of them. Each eigenvector A_k is independently transformed by the amplifier into $\lambda_k^n I_\theta^n A_k$, where λ_k is the eigenvalue of the eigenvector A_k. For this reason, the eigenvectors of T_θ may be called the modes of the periodically distributed parametric amplifier.

III. The Orthogonality Properties of the Modes

The eigenvectors of T_θ have certain properties of orthogonality which are important when we wish to express a vector as the sum of the eigenvectors. The orthogonality theorems take, of course, different forms from the conventional circuits. The theorems hold in a more general case than the particular amplifier discussed in Section II. We shall prove them in the general case, using one of the Manley-Rowe relations.[7]

For the lossless parametric circuit with ω_p satisfying (5), the Manley-Rowe relation is

$$\frac{W_1}{\omega_1} - \frac{W_2}{\omega_2} = 0 \quad (22)$$

where W_1 and W_2 represent the real powers flowing into the circuit at the angular frequencies ω_1 and ω_2, respectively.

If ω_1 and ω_2 are both in the pass-band of the two-terminal pair network, using (1) and (2), from (22) we obtain

$$\frac{1}{\omega_1}\,\mathrm{Re}\,(V_{a1}I_{a1}^* - V_{b1}I_{b1}^*) - \frac{1}{\omega_2}\,\mathrm{Re}\,(V_{a2}I_{a2}^* - V_{b2}I_{b2}^*)$$

$$= \frac{1}{\omega_1}(|a_{i1}|^2 - |a_{r1}|^2 - |b_{i1}|^2 + |b_{r1}|^2)$$

$$- \frac{1}{\omega_2}(|a_{i2}|^2 - |a_{r2}|^2 - |b_{i2}|^2 + |b_{r2}|^2)$$

$$= A^+\Omega^{-1}A - B^+\Omega^{-1}B$$

$$= A^+(\Omega^{-1} - T^+\Omega^{-1}T)A = 0 \quad (23)$$

where the symbol $^+$ denotes the complex conjugate transposed matrix and

$$\Omega^{-1} = \begin{bmatrix} \frac{1}{\omega_1} & 0 & 0 & 0 \\ 0 & -\frac{1}{\omega_1} & 0 & 0 \\ 0 & 0 & -\frac{1}{\omega_2} & 0 \\ 0 & 0 & 0 & \frac{1}{\omega_2} \end{bmatrix}. \quad (24)$$

Since (23) must hold for every A,

$$\Omega^{-1} = T^+\Omega^{-1}T. \quad (25)$$

This is the condition which T of all the parametric circuits should satisfy. (See Appendix, Section A.)

[7] J. M. Manley and H. E. Rowe, "Some general properties of nonlinear elements—part I. General energy relations," Proc. IRE, vol. 44, pp. 904–913; July, 1956.

If two T's, T_a and T_b, satisfy (25), then

$$(T_aT_b)^+\Omega^{-1}(T_aT_b) = T_b^+T_a^+\Omega^{-1}T_aT_b = T_b^+\Omega^{-1}T_b = \Omega^{-1}. \quad (26)$$

Eq. (26) shows that the product of two T's, (T_aT_b), again satisfies (25). It is worth noting that the unit matrices I and T of the conventional circuits also satisfy (25). Since I_θ^{-1} satisfies (25), T_θ also satisfies (25):

$$\Omega^{-1} = T_\theta^+\Omega^{-1}T_\theta. \quad (27)$$

If λ_k is an eigenvalue of T_θ, the determinant of $(T_\theta-\lambda_k I)$ vanishes:

$$\det\,(T_\theta - \lambda_k I) = 0. \quad (28)$$

Taking the complex conjugate transpose of (28), we have

$$\det\,(T_\theta^+ - \lambda_k^* I) = 0.$$

Since $\det\,(T_\theta)\neq 0$, $\lambda_k\neq 0$. From these relations, we have

$$\begin{aligned}\det\,(T_\theta^+ - \lambda_k^* I)\,\det\,(\Omega^{-1}T_\theta) &= \det\,(T_\theta^+\Omega^{-1}T_\theta - \lambda_k^*\Omega^{-1}T_\theta)\\ &= \det\,(\Omega^{-1} - \lambda_k^*\Omega^{-1}T_\theta)\\ &= \det\,(\Omega^{-1}\lambda_k^*)\,\det\left(\frac{1}{\lambda_k^*}I - T_\theta\right) = 0.\end{aligned}$$

The final result is

$$\det\left(T_\theta - \frac{1}{\lambda_k^*}I\right) = 0. \quad (29)$$

It says, if λ_k is an eigenvalue then $1/\lambda_k^*$ is also an eigenvalue of T_θ. In other words, when $|\lambda_k|\neq 1$, the eigenvalues λ_k and $1/\lambda_k^*$ appear always in pairs. When $|\lambda_k|=1$, $1/\lambda_k^*$ is equal to λ_k, and the result is trivial.

If λ_k and λ_l are the two eigenvalues of T_θ,

$$T_\theta A_k = \lambda_k A_k. \quad (30)$$

$$T_\theta A_l = \lambda_l A_l. \quad (31)$$

From (31), we have

$$\frac{1}{\lambda_l^*}(T_\theta A_l)^+ = \frac{1}{\lambda_l^*}A_l^+T_\theta^+ = A_l^+.$$

Multiplying by $\Omega^{-1}T_\theta A_k$ from the right and using (27), we have

$$\frac{1}{\lambda_l^*}A_l^+\Omega^{-1}A_k = A_l^+\Omega^{-1}T_\theta A_k.$$

Multiplying (30) by $A_l^+\Omega^{-1}$ from the left and substituting in the above equation, we obtain

$$\left(\lambda_k - \frac{1}{\lambda_l^*}\right)A_l^+\Omega^{-1}A_k = 0. \quad (32)$$

If $\lambda_k\neq 1/\lambda_l^*$, from (32), we have

$$A_l^+\Omega^{-1}A_k = 0. \quad (33)$$

In case $|\lambda_k|\neq 1$, since $\lambda_k\neq 1/\lambda_k^*$, we can set $l=k$ in (33); that is,

$$A_k^+\Omega^{-1}A_k = 0 \qquad (|\lambda_k|\neq 1). \quad (34)$$

Next, we expand ΩA_k in terms of the modes in the form

$$\Omega A_k = \sum_j \alpha_j A_j.$$

Multiplying by $A_k^+\Omega^{-1}$ from the left, we have

$$A_k^+A_k = \sum_j \alpha_j A_k^+\Omega^{-1}A_j \neq 0. \quad (35)$$

Assuming that λ_k is not degenerate and using (33), when $|\lambda_k|=1$, we obtain

$$A_k^+\Omega^{-1}A_k \neq 0 \qquad (|\lambda_k| = 1). \quad (36)$$

If $|\lambda_k|\neq 1$, there is always the eigenvector A_l corresponding to the eigenvalue $1/\lambda_k^*$. In this case, (35) becomes

$$A_k^+\Omega^{-1}A_l \neq 0$$

which can be rewritten in the form

$$A_l^+\Omega^{-1}A_k \neq 0. \quad (37)$$

Here, we define $\tilde{A}_k$ by

$$\tilde{A}_k = A_k^+ \qquad \text{if } |\lambda_k| = 1 \quad (38)$$

$$\tilde{A}_k = A_l^+ \qquad \text{if } |\lambda_k| \neq 1 \quad (39)$$

where A_l is the eigenvector corresponding to the eigenvalue $1/\lambda_k^*$. Then, (33), (34), (36), and (37) become

$$\begin{aligned}\tilde{A}_l\Omega^{-1}A_k &= 0 \qquad (l\neq k)\\ \tilde{A}_k\Omega^{-1}A_k &\neq 0.\end{aligned} \quad (40)$$

These are the orthogonality theorems which we wished to prove.

In the case of degeneracy, the above proof does not necessarily hold. It is, however, always possible to introduce the eigenvectors in such a way as to secure the orthogonality, and we are justified in assuming (40) even in case of degeneracy. (See Appendix, Section B.)

IV. Power Gain of the Amplifier

In this section, we shall derive an expression for the power gain of the periodically distributed parametric amplifier.

We need the solutions of the eigenvalue problem (20). In the preceding sections, we have imposed no conditions on θ_p. Here we shall confine ourselves to the case of synchronous pumping:

$$\theta_p = \theta_1 + \theta_2. \quad (41)$$

All the eigenvalues and the corresponding eigenvectors can be obtained by the standard method of algebra, or by the method of perturbation. To the first order of approximation, they are

$$\lambda_1 = (1+\delta)e^{j(\theta_2-\theta_1)}$$

$$A_1 = \begin{pmatrix} 1 \\ -j\dfrac{\delta}{2\sin 2\theta_1} \\ j\sqrt{\dfrac{\omega_2}{\omega_1}}\,\dfrac{c^*}{|c|}\,e^{-j\theta_p} \\ -\sqrt{\dfrac{\omega_2}{\omega_1}}\,\dfrac{c^*}{|c|}\,\dfrac{\delta e^{-j\theta_p}}{2\sin 2\theta_2} \end{pmatrix}$$

$$\lambda_2 = e^{j(3\theta_1+\theta_2)}$$

$$A_2 = \begin{pmatrix} 0 \\ 1 \\ \sqrt{\dfrac{\omega_2}{\omega_1}}\,\dfrac{c^*}{|c|}\,\dfrac{\delta e^{-j\theta_p}}{2\sin 2\theta_1} \\ -\sqrt{\dfrac{\omega_2}{\omega_1}}\,\dfrac{c^*}{|c|}\,\dfrac{\delta e^{-j\theta_p}}{2\sin 2\theta_p} \end{pmatrix}$$

$$\lambda_3 = (1-\delta)e^{j(\theta_2-\theta_1)}$$

$$A_3 = \begin{pmatrix} 1 \\ j\dfrac{\delta}{2\sin 2\theta_1} \\ -j\sqrt{\dfrac{\omega_2}{\omega_1}}\,\dfrac{c^*}{|c|}\,e^{-j\theta_p} \\ -\sqrt{\dfrac{\omega_2}{\omega_1}}\,\dfrac{c^*}{|c|}\,\dfrac{\delta e^{-j\theta_p}}{2\sin 2\theta_2} \end{pmatrix}$$

$$\lambda_4 = e^{-j(\theta_1+3\theta_2)}$$

$$A_4 = \begin{pmatrix} \sqrt{\dfrac{\omega_1}{\omega_2}}\,\dfrac{c}{|c|}\,\dfrac{\delta e^{j\theta_p}}{2\sin 2\theta_2} \\ -\sqrt{\dfrac{\omega_1}{\omega_2}}\,\dfrac{c}{|c|}\,\dfrac{\delta e^{j\theta_p}}{2\sin 2\theta_p} \\ 0 \\ 1 \end{pmatrix} \tag{42}$$

where

$$\delta = \sqrt{\omega_1\omega_2}\,|c|\,\frac{\sqrt{Z_{01}'Z_{02}'^*}}{4}. \tag{43}$$

If ω_1 and ω_2 are in the pass-band, as we have assumed, δ is real and we have $\lambda_1 = 1/\lambda_3^*$ which we proved in Section III. A_1 and A_3 represent the growing and decreasing waves, for $|\lambda_1|$ is greater than unity and $|\lambda_3|$ is smaller than unity. It is worth noting that they are almost the incident waves. A_2 and A_4 are the reflected waves, of which the propagation constants do not change in this approximation. The orthogonality theorems (40) are satisfied to the same order of approximation.

For the calculation of the power gain, we first express the input vector A as the sum of the eigenvectors in the form

$$A = \sum_k \alpha_k A_k. \tag{44}$$

A_k is transformed into $\lambda_k^n I_\theta^n A_k$ by the amplifier. Hence, for the output vector B, we have

$$B = \sum_k \alpha_k \lambda_k^n I_\theta^n A_k. \tag{45}$$

Multiplying by $\tilde{A}_k\Omega^{-1}I_\theta^{-n}$ from the left, because of the orthogonality properties of the modes, we obtain

$$\tilde{A}_k\Omega^{-1}I_\theta^{-n}B = \alpha_k\lambda_k^n\tilde{A}_k\Omega^{-1}A_k.$$

Therefore

$$\alpha_k = \frac{\tilde{A}_k\Omega^{-1}I_\theta^{-n}B}{\lambda_k^n\tilde{A}_k\Omega^{-1}A_k}. \tag{46}$$

For simplicity, we assume that the output is terminated with Z_0: $b_{r1} = b_{r2}^* = 0$. Then, from (42), (44), and (46), we have

$$A = \begin{vmatrix} \dfrac{1}{2e^{-jn(\theta_1-\theta_2)}}\left(b_{i1}e^{jn\theta_p}\left\{\dfrac{1}{(1+\delta)^n} + \dfrac{1}{(1-\delta)^n}\right\} \underbrace{-j\sqrt{\dfrac{\omega_1}{\omega_2}}\,\dfrac{c}{|c|}\,b_{i2}^*e^{-j(n-1)\theta_p}\left\{\dfrac{1}{(1+\delta)^n} - \dfrac{1}{(1-\delta)^n}\right\}}_{\text{the order of }\delta}\right) \\ j\sqrt{\dfrac{\omega_2}{\omega_1}}\,\dfrac{c^*}{|c|}\,\dfrac{e^{-j\theta_p}}{2e^{-jn(\theta_1-\theta_2)}}\left(\underbrace{b_{i1}e^{jn\theta_p}\left\{\dfrac{1}{(1+\delta)^n} - \dfrac{1}{(1-\delta^n)}\right\}}_{\text{the order of }\delta} - j\sqrt{\dfrac{\omega_1}{\omega_2}}\,\dfrac{c}{|c|}\,b_{i2}^*e^{-j(n-1)\theta_p}\left\{\dfrac{1}{(1+\delta)^n} + \dfrac{1}{(1-\delta)^n}\right\}\right) \end{vmatrix}. \tag{47}$$

We further assume that the input is also terminated with Z_{02} at ω_2:

$$V_2 = -Z_{02}I_2.$$

This means

$$a_{i2} = 0. \tag{48}$$

From (47) and (48), we have

$$b_{i1}e^{jn\theta_p}\left\{\frac{1}{(1+\delta)^n} - \frac{1}{(1-\delta)^n}\right\} = j\sqrt{\frac{\omega_1}{\omega_2}}\,\frac{c}{|c|}\,b_{i2}^*e^{-j(n-1)\theta_p}\left\{\frac{1}{(1+\delta)^n} + \frac{1}{(1-\delta)^n}\right\}. \tag{49}$$

Substituting in a_{i1} in (47), we obtain

$$a_{i1} = \frac{1}{e^{-jn(\theta_1-\theta_2)}} b_{i1} e^{jn\theta_p} \left\{ \frac{2}{(1+\delta)^n + (1-\delta)^n} \right\}. \quad (50)$$

The power gain is the ratio of the output power $|b_{i1}|^2$ to the input power $|a_{i1}|^2$. Thus we find

$$G = \frac{|b_{i1}|^2}{|a_{i1}|^2} = \left\{ \frac{(1+\delta)^n + (1-\delta)^n}{2} \right\}^2 = \cosh^2 n\delta. \quad (51)^8$$

We took $|a_{i1}|^2$ as the input power instead of $|a_{i1}|^2 - |a_{r1}|^2$. The reason for this choice is that the net input power $|a_{i1}|^2 - |a_{r1}|^2$ may become negative because, from (47), a_{r1} is of the order of δ and a_{i1} becomes of the order of δ if G is of the order of $1/\delta^2$. In this case a circulator can be employed to secure the stability.

Appendix

A. The Form of Ω^{-1}

In case ω_2 is in the stop-band (Z_{02} is pure imaginary) while ω_1 remains in the pass-band, the same manipulation as (23) leads to

$$\Omega^{-1} = \begin{bmatrix} \frac{1}{\omega_1} & 0 & 0 & 0 \\ 0 & -\frac{1}{\omega_1} & 0 & 0 \\ 0 & 0 & 0 & \pm j\frac{1}{\omega_2} \\ 0 & 0 & \mp j\frac{1}{\omega_2} & 0 \end{bmatrix} \quad (52)$$

where the upper signs in the matrix refer to the inductive Z_{02} and the lower signs to the capacitive Z_{02}. With this Ω^{-1} in place of (24), the orthogonality theorems can be proved without alteration.

B. The Orthogonality in the Case of Degeneracy

We shall consider the case of double degeneracy. Let A_1 and A_2 be the independent degenerate eigenvectors with $|\lambda_1| \neq 1$. Because of the degeneracy, we have

$$\frac{d}{d\lambda_1} \det (T_\theta - \lambda_1 I) = 0. \quad (53)$$

In a similar way as for (29), we obtain

$$\frac{d}{d\left(\frac{1}{\lambda^*_1}\right)} \det \left(T_\theta - \frac{1}{\lambda^*_1} I\right) = 0 \quad (54)$$

proving that $1/\lambda_1^*$ is also two fold. We denote the two independent eigenvectors corresponding to the eigenvalue $1/\lambda_1^*$ by A_{-1} and A_{-2}. In terms of the modes, ΩA_1 and ΩA_2 are

$$\Omega A_1 = \sum_k \alpha_k A_k$$
$$\Omega A_2 = \sum_k \beta_k A_k. \quad (55)$$

If we put

$$A_a = A_1 + aA_2$$
$$A_b = A_1 - aA_2, \quad (56)$$

then, using (33) and (55), we have

$$0 \neq A_a^+ A_a = A_a^+(A_1 + aA_2)$$
$$= A_a^+ \Omega^{-1}(\alpha_{-1}A_{-1} + \alpha_{-2}A_{-2} + a\beta_{-1}A_{-1} + a\beta_{-2}A_{-2})$$
$$0 \neq A_b^+ A_b = A_b^+(A_1 - aA_2)$$
$$= A_b^+ \Omega^{-1}(\alpha_{-1}A_{-1} + \alpha_{-2}A_{-2} - a\beta_{-1}A_{-1} - a\beta_{-2}A_{-2}).$$

Hence, if we define A_{-a} and A_{-b} by

$$A_{-a} = \alpha_{-1}A_{-1} + \alpha_{-2}A_{-2} + a\beta_{-1}A_{-1} + a\beta_{-2}A_{-2}$$
$$A_{-b} = \alpha_{-1}A_{-1} + \alpha_{-2}A_{-2} - a\beta_{-1}A_{-1} - a\beta_{-2}A_{-2}, \quad (57)$$

the above equations become

$$A_a^+\Omega^{-1}A_{-a} \neq 0 \qquad A_b^+\Omega^{-1}A_{-b} \neq 0. \quad (58)$$

In order to obtain the relations

$$A_a^+\Omega^{-1}A_{-b} = A_1^+A_1 - aA_1^+A_2 + a^*A_2^+A_1 - |a|^2 A_2^+A_2 = 0$$
$$A_b^+\Omega^{-1}A_{-a} = A_1^+A_1 + aA_1^+A_2 - a^*A_2^+A_1 - |a|^2 A_2^+A_2 = 0 \quad (59)$$

we need only to put

$$|a| = \sqrt{\frac{A_1^+A_1}{A_2^+A_2}}, \qquad \angle a = -\angle A_1^+A_2. \quad (60)$$

Since $a \neq 0$, A_a, A_b, A_{-a} and A_{-b} thus defined are independent to each other and they satisfy the orthogonality theorems. In case $|\lambda_1| = 1$, similarly the modes can be introduced so as to secure the orthogonality. The generalization of the above discussion to the case of multiple degeneracy is not difficult.

V. Acknowledgment

The authors wish to thank Prof. S. Saito for his guidance and many valuable suggestions. The continued support and encouragement of Profs. M. Hoshiai and N. Takagi have been greatly appreciated.

[8] Eq. (41) requires transmission lines without a cutoff effect. The effect of cutoff would be

$$\theta_p = \theta_1 + \theta_2 + \Delta\theta.$$

In this case, (51) becomes

$$G \doteq \cosh^2 n\delta' + \left(\frac{\Delta\theta}{\delta'}\right)^2 \sinh^2 n\delta', \quad \text{where} \quad \delta' = \sqrt{\delta^2 - (\Delta\theta)^2}.$$

O-Guide and X-Guide: An Advanced Surface Wave Transmission Concept*

M. SUGI† AND T. NAKAHARA†

Summary—**This paper describes the O-guide and X-guide which are proposed by the authors and are the advanced surface waveguides composed of thin dielectric sheets. The results of an analysis of the TE fundamental mode in the O-guide are described, and the theoretical characteristics as a transmission line are discussed. The practical guides are suitable especially for the SHF region and guides can be obtained which have lower attenuation constants than coaxial lines, G-lines, and rectangular waveguides.**

Introduction

It is the principle of surface wave transmission to convey an electromagnetic wave along the boundary surface of a medium which is located in free space and in which the propagation velocity of the wave is lower than in free space. This is accomplished by making the wave concentrate in the vicinity of the surface of this medium. The G-line[1] which was proposed by G. Goubau in 1950 is a typical surface wave transmission line, and is very convenient because of its simple construction; it also has several defects as a transmission line, namely, large conductor loss, small concentration efficiency of the wave, and interference from the external field.

Here the authors propose "Thin Dielectric Sheet Waveguides" as more advanced surface wave transmission lines. Two examples are described below, and they are called respectively "O-guide" and "X-guide" and designed according to the principle that a thin dielectric plate placed parallel to the electric field has a more effective concentrating action than one located perpendicularly; in the case of a thin magnetic plate such as a ferrite, the relationship is just the opposite. It is quite the same in principle to use magnetic substances, but unfortunately there are very few practical materials available.

The waveguides mentioned above have two merits: they have no conductor loss and excellent efficiency of concentration: better results can be realized by shielding the above lines with metal because interference from the external field will in this manner be eliminated.

Plane Wave

In this paper the rationalized MKS system of units is used throughout.

Let us first consider the plane wave. Suppose a thin dielectric plate having a thickness of $2t$, and a dielectric constant $\epsilon^*\epsilon_0$, where ϵ^* is a relative dielectric constant and ϵ_0 is the constant of the free space, is placed in the y-z plane in the infinite free space as shown in Fig. 1. We shall also suppose that an electromagnetic plane wave is propagating along the dielectric plane in the z-direction; and that in the case of Fig. 1(a) the electric field has only a y-component; in the case of Fig. 1(b), the magnetic field has only a y-component. Accordingly, the mode of the wave in Fig. 1(a) is regarded as a TE mode and the one in Fig. 1(b) as a TM mode.

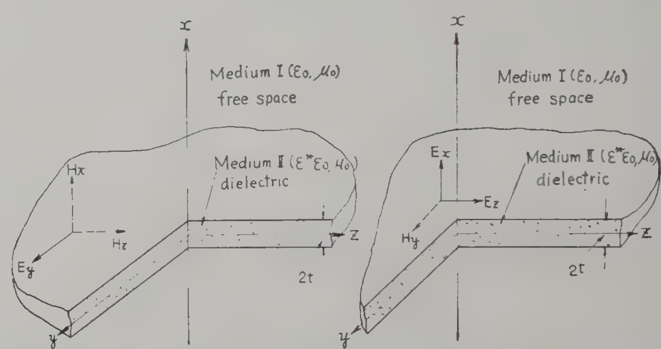

Fig. 1—(a) TE mode, (b) TM mode.

Now we shall observe the field in the medium I, because the one in the medium II is not important in our case. Let us consider the field component equations in the medium I as a function of x, where x is the distance from y-z plane. Here all field quantities are understood to contain the common factors which are independent of x.

Solving the equations analytically, we can obtain the following equations for Fig. 1(a):

$$E_y \simeq E_{y0}e^{-\alpha_a x}, \tag{1}$$

where E_{y0} is a constant and α_a can be expressed as follows provided that t is very small in comparison with the wavelength,

$$\alpha_a \simeq k^2 t(\epsilon^* - 1), \tag{2}$$

where k is the free space propagation constant and can be expressed as

$$k = \omega\sqrt{\epsilon_0\mu_0} = \frac{2\pi}{\lambda_0}, \tag{3}$$

where ω is angular frequency, μ_0 is the permeability of the free space and λ_0 is the wavelength in free space.

* Manuscript received by the PGMTT, December 8, 1958; revised manuscript received, March 2, 1959.

† Sumitomo Electric Industries, Ltd., Osaka, Japan.

[1] G. Goubau, "Surface waves and their application to transmission line," *J. Appl. Phys.*, vol. 21, pp. 1119–1128; November, 1950. See also Goubau, "Single-conductor surface-wave transmission line," Proc. IRE, vol. 39, pp. 619–624; June, 1951.

For Fig. 1(b) we obtain the following:

$$H_y \simeq H_{y0} e^{-\alpha_b x}, \tag{4}$$

where H_{y0} is a constant and α_b can be expressed as follows under the same condition as for (1):

$$\alpha_b \simeq k^2 t \frac{\epsilon^* - 1}{\epsilon^*}. \tag{5}$$

Comparing (2) with (5), it can be concluded that the thin dielectric plate in the case of Fig. 1(a) is more effective on the concentration of the wave than the one in the case of Fig. 1(b), namely, a thin dielectric plate placed parallel to the electric field has a more effective concentrating action than one located perpendicularly.

By the above reasoning, the G-line has a poorer efficiency of concentration, as stated in the introduction of this paper.

Now, let us pay attention only to the former type and consider a physically realizable construction of the transmission line because the construction discussed above is that of the infinite plane and is physically unobtainable. We can easily find two types of the practical lines which are illustrated in Fig. 2(a) and Fig. 2(b).

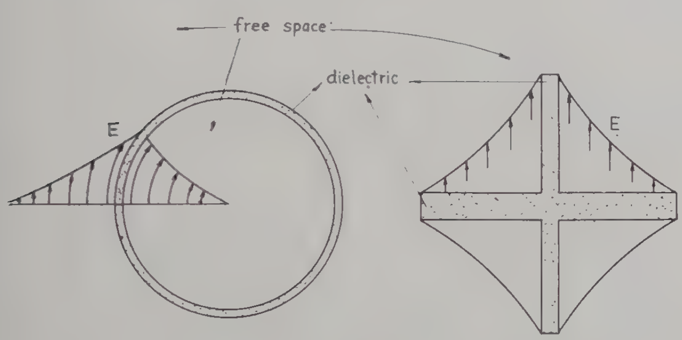

Fig. 2—(a) O-guide cross section, (b) X-guide cross section.

We can obtain the construction shown in Fig. 2(a) by transforming the whole system in Fig. 1(a) to cylindrical co-ordinates and the construction shown in Fig. 2(b) by combining the plate in y-z plane with the one in z-x plane to form a two-dimensional concentrating action.

Since the H-guide[2] which was similar to these lines was reported previously, let us call these lines "O-guide" in the case of Fig. 2(a) and "X-guide" in the case of Fig. 2(b).

The transmission mode that should be noted in the O-guide is the TE mode and in the X-guide the hybrid mode in which the wave has both the electric and magnetic components in the z-direction.

In the X-guide shown in Fig. 2(b), the horizontal dielectric plate must have $\epsilon^* t$ of a larger value than that of the vertical one, as is clearly indicated in the same figure, for the reason shown in Fig. 1.

[2] F. J. Tischer, "H-guide, A new microwave concept," *Tele-Tech.*, vol. 15, pp. 50, 51, 130, 134, 136; November, 1956.

O-Guide

Now let us suppose that there is a dielectric cylinder having a thin wall of a thickness T, a radius a, and a dielectric constant $\epsilon^*\epsilon_0$ in the infinite free space as shown in Fig. 3. We assume a wave of TE mode is propagating along the z-axis.

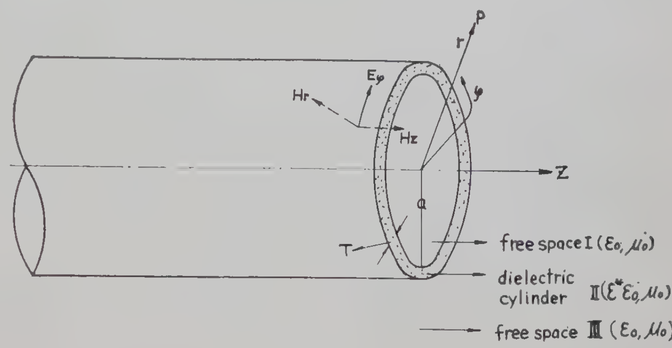

Fig. 3.

Starting from Maxwell's equations and using the cylindrical co-ordinates as shown in Fig. 3, we obtain the following sets of equations for the field components; if the thickness T is very small compared with the radius a and the wavelength λ and all the field quantities are understood to contain the common factors $\exp\{j(\omega t - B_z Z)\}$, where j is $\sqrt{-1}$, t is time, and other notations as defined below:

$$\left.\begin{aligned} E_\phi^{\mathrm{I}} &= \frac{-j\omega\mu_0}{\alpha_r} A I_1(\alpha_r r), \\ H_r^{\mathrm{I}} &= \frac{j\beta_z}{\alpha_r} A I_1(\alpha_r r), \\ H_z^{\mathrm{I}} &= A I_0(\alpha_r r), \end{aligned}\right\} \tag{6}$$

$$\left.\begin{aligned} E_\phi^{\mathrm{III}} &= \frac{j\omega\mu_0}{\alpha_r} B K_1(\alpha_r r), \\ H_r^{\mathrm{III}} &= \frac{-j\beta_z}{\alpha_r} B K_1(\alpha_r r), \\ H_z^{\mathrm{III}} &= B K_0(\alpha_r r) \end{aligned}\right\}. \tag{7}$$

Here A and B are the arbitrary constants. Both are related by the boundary condition, and I_n and K_n are respectively the first and second kind of the modified Bessel functions. The meanings of other notations are as follows:

The lower suffix denotes co-ordinate.
The upper suffix denotes the medium.

ω = angular frequency,
α_r = propagation constant in r-direction,
β_z = propagation constant in z-direction.

The following equation is given by the relation among α_r, β_z, and k;

$$\beta_z^2 = k^2 + \alpha_r^2. \tag{8}$$

Substituting (6) and (7) in the equations of the boundary condition at $r=a$, we get following two relations:

$$\frac{A}{B} = -\frac{K_1(\alpha_r a)}{I_1(\alpha_r a)}, \tag{9}$$

$$\{I_1(\alpha_r a)K_1(\alpha_r a)\}^{-1} = (\epsilon^* - 1)Tak^2 \equiv Y. \tag{10}$$

Eq. (10) is called the "characteristic equation." From this equation, the constant α_r which shows the concentration can be determined if the value of $Y \equiv (\epsilon^* - 1)Tak^2$ is given, where Y is decided by the construction.

In the case of Fig. 1(a) there is no cut-off phenomenon, but in the case of Fig. 3, namely that of a cylinder, there occurs a phenomenon resembling "cut-off." This means that the surface wave cannot exist at the frequency lower than the cut-off frequency.

The cut-off wavelength λ_c can be expressed through (10), since $I_1(x)K_1(x) \leqq 0.5$ for real number x,

$$\lambda_c = \pi\sqrt{2(\epsilon^* - 1)Ta}. \tag{11}$$

The attenuation of this guide is caused only by the dielectric loss and of course no loss is caused by the conductor loss. After calculating the transmitted power and the dielectric loss, we obtain the following expression as the attenuation constant $\bar{\alpha}_z$;

$$\bar{\alpha}_z = \frac{\alpha_r \epsilon^* Tk^2 \tan\delta}{\beta_z} A(X), \tag{12}$$

where

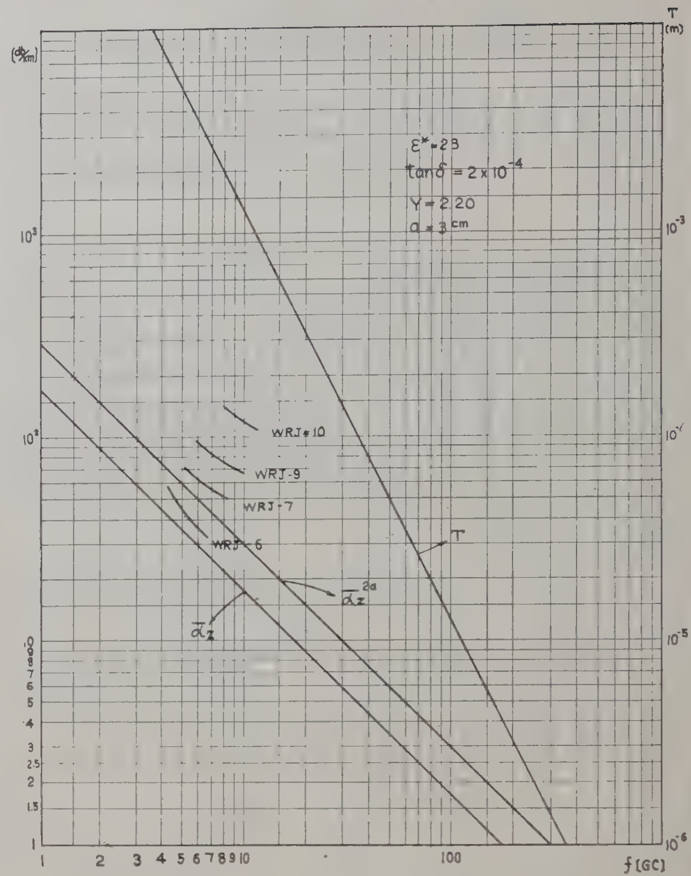

Fig. 4.

$$A(X) = \frac{\{K_1(X)\}^2}{(\mu+1)X\left(\frac{1}{4}\{K_0(X)+K_2(X)\}^2 - \left(1+\frac{1}{X^2}\right)\{K_1(X)\}^2\right)} \tag{13}$$

$$\mu = \mu(X) = \frac{\{K_1(X)\}^2\left(\left(1+\frac{1}{X^2}\right)\{I_1(X)\}^2 - \frac{1}{4}\{I_0(X)+I_2(X)\}^2\right)}{\{I_1(X)\}^2\left(\frac{1}{4}\{K_0(X)+K_2(X)\}^2 - \left(1+\frac{1}{X^2}\right)\{K_1(X)\}^2\right)} \tag{14}$$

$$X = \alpha_r a,$$

$\tan\delta$ = loss factor of the dielectric.

It can be concluded from these equations that the attenuation constant is proportional to $\tan\delta$, and approximately proportional to the third power of frequency. And if the concentrating action is constant, *i.e.*, if Y is constant, it can be shown that the attenuation constant is inversely proportional to $\epsilon^*/\epsilon^* - 1$. On account of the above, dielectric materials of higher ϵ^* and smaller $\tan\delta$ are better suited for the purpose.

Fig. 4 shows the frequency characteristic of a polyethylene cylinder, with a diameter of 3 cm, supposing $Y = 2.20$, $\epsilon^* = 2.3$, and $\tan\delta = 2\times10^{-4}$. In this figure, the curve denoted T shows the necessary thickness required to keep $Y = 2.20$. And the curve denoted $\bar{\alpha}_z$ shows the attenuation characteristic mentioned above. It should be noted that $\bar{\alpha}_z$ decreases as the frequency increases.

$\bar{\alpha}_z^{2a}$ means the attenuation constant when the transmitted power through the space outside the cylinder of a radius $2a$ is completely neglected. Consequently if the shield be placed at the position of the radius $2a$, the attenuation constant should not exceed $\bar{\alpha}_z^{2a}$. The curves designated WRJ-6, 7, 9, and 10 in the same figure show the attenuation constants for the rectangular wave guides WRJ-6, 7, 9, and 10 which correspond to respectively WR 159, 137, 112, and 90 specified in RETMA Standards. These curves are shown for comparison. Comparing these curves shows that this guide has much lower loss than conventional rectangular waveguides.

Miscellaneous

From the point of view of the practical application, the SHF region may be most suitable for these guides, but some problems in the shielding, supports, bends, and launching must be solved in order to use this waveguide in practice. The authors have some ideas for solving these problems, but no experiments have yet been done.

Conclusion

The advanced surface wave transmission lines composed of thin dielectric sheets are suitable, especially for SHF region, and have lower loss than the coaxial lines, G-lines, H-guides, and rectangular waveguides.

Corrections

H. A. Wheeler and H. L. Bachman, authors of "Evacuated Waveguide Filter for Suppressing Spurious Transmission from High-Power S-Band Radar," which appeared on pages 154–162 of the January, 1959 issue of these TRANSACTIONS, have submitted the following corrections;

Table I, just above (7) and (8), is changed to read:

At f_1 and f_2:

Table II, (10), is changed to read:

$$f_4^2 = f_7^2 + \frac{f_8^2 - f_7^2}{1 + \frac{f_7^2}{f_8^2}\left(\frac{f_8^2 - f_5^2}{f_7^2 - f_5^2}\right)^2}.$$

Page 160, at the end of second column, "The reflection loss" is deleted.

Page 161, at the beginning of first column, "by about 0.2 db. The sum of these effects holds the dissipation loss" is deleted. Insert these words after the third line below the short table (Metal walls, etc.).

J. F. Cline and B. M. Schiffman wish to call attention to a typographic error in an equation in their article "Tunable Passive Milticouplers Employing Minimum-Loss Filters," which appeared on pages 121–127 of the January, 1959 issue of these TRANSACTIONS. The error occurs in (11) on page 125. The radical sign should terminate at the end of the binomial and before the final -1. The equation should read as follows:

$$\frac{Q_T}{Q_U} = \frac{3}{2}\left(\sqrt{1 + \frac{8}{9}\,(10^{L_0/20} - 1)} - 1\right). \quad (11)$$

The Transmission of TE_{01} Wave in Helix Waveguides*

TOSHIO HOSONO† AND SHISHU KOHNO‡

Summary—**Relations are investigated between the transmission characteristics of a helix waveguide and its surface impedance in regions where any simple approximate formulas are not available because of the magnitude of the surface impedance. The numerical calculations show that, for any given value of the surface impedance and the angular mode index, there exist an infinite number of different modes which are distinguishable from each other by different values of the radial propagation content.**

Selecting a mode with minimum attenuation for each given surface impedance, we can draw the equiattenuation lines, connecting these points of equal attenuation on the complex surface impedance plane. At some point on the complex surface impedance plane, a maximum value of the minimum attenuation is found. For the TM_0 mode supported by a helix waveguide 50 mm in diameter, used at a frequency of 50 kmc, this minimax value of the attenuation constant is about 8 neper per meter, and the corresponding value of the surface impedance is about 57.6−j28.8 ohms. The attenuation constants of all the TM_0 modes corresponding to this optimum value of the surface impedance cannot be smaller than this minimax value.

The same kind of calculations are also performed for the two lowest hybrid modes. Physical structures giving the best value of the surface impedance are also suggested.

Introduction

FOR the TE_{01} wave transmitted inside the cylindrical metallic waveguide, attenuation is very small and therefore transmission over a long distance is possible. However, because economic requirements limit the size of the waveguide which can be put to practical use to the same extent as is the ordinary telephone cable size, it is necessary to use a frequency in the millimeter wave range in order to realize the small attenuation.

For a guide with a two inch diameter such that the TE_{01} wave can be transmitted at an attenuation of two db/mile at the frequency 50 kmc, approximately 200 unwanted modes can also be transmitted. Therefore any deviation of the waveguide from a straight circular cylinder gives rise not only to an increase in attenuation due to mode conversion but also to signal distortions by mode conversion and reconversion into the original TE_{01} wave.[1]

The principal problem of the TE_{01} wave transmission is the elimination of the transformation between the TE_{01} mode and unwanted modes. Several ways of combating mode conversion effects have been proposed.[2–8] Among these, use of the spaced-ring and helical structures as a waveguide or a mode filter is most attractive.

Analyses of these structures have been done by several authors. Morgan and Young[2] have studied the transmission characteristics of a special type of helix waveguide which is composed of a sheath helix with a lossy jacket. They performed extensive numerical calculations and gave sufficient basis for a design of this type of helix waveguide. Recently, Unger[9] studied helix waveguides with a multilayer jacket and stated the numerical results for some guide dimensions and material properties. There remains, however, a possibility that other types of helix waveguides may have better characteristics. A way of studying this possibility is to analyze the helix waveguide as one having an anisotropic surface impedance. This approach of analysis is very general because any special helix structure can be characterized by a surface impedance properly assumed. Formal equations expressing the relations between the t-transmission characteristics and the surface impedance have already been obtained by Karbowiak[10] Hosono[3] and Piefke.[4] Unfortunately these equations cannot be used directly, especially when the magnitude of the surface impedance is large.

The object of the present paper is to show by numerical calculation, the direct relationship between t-transmission characteristics and surface impedance in regions where the simple approximate formulas are not available.

Characteristic Equation for a Zero-Pitch Helix Waveguide

The helix waveguide of radius a and pitch angle Ψ is

* Manuscript received by the PGMTT, November 26, 1958; revised manuscript received, February 3, 1959.

† Elec. Eng. Dept., Nippon Univ., Kanda-Surugadai, Tokyo, Japan.

‡ The Furukawa Electric Co. Ltd., Tokyo, Japan.

[1] S. E. Miller, "Waveguide as a communication medium," *Bell Sys. Tech. J.*, vol. 33, p. 1209; November, 1954.

[2] S. P. Morgan and J. A. Young, "Helix waveguide," *Bell Sys. Tech. J.*, vol. 35, pp. 1347–1384; November, 1956.

[3] T. Hosono, "Helix waveguide," Inst. Elect. Commun. Engs. of Japan, Session of Microwave Transmission; February, 1957.

[4] G. Piefke, "Wellenausbreitung in der Sheiben-Leitung," *Arch. elekt. Übertragung*, vol. 11, pp. 49–59; February, 1957.

[5] Enrique A. Marcatili, "Heat loss in grooved metallic surface," Proc. IRE, vol. 45, pp. 1134–1139; August, 1957.

[6] T. Hosono and S. Kohno, "The transmission of TE_{01} wave in corrugated waveguides," *Congres Internationale, Circuits et Antennes Hyperfrequences*, Paris, France, Session 9, 54. vol. 1, p. 253; October, 1957.

[7] J. A. Morrison, "Heat loss of circular electric waves in helix waveguides," IRE Trans. on Microwave Theory and Techniques, vol. MTT-6, pp. 173–177; April, 1958.

[8] D. Marcuse, "Attenuation of TE_{01} wave within the curved helix waveguide, *Bell Sys. Tech. J.*, vol. 37, p. 1599; November, 1958.

[9] H.-G. Unger, "Helix waveguide theory and applications," *Bell Sys. Tech. J.*, vol. 37, p. 1649; November, 1958.

[10] A. E. Karbowiak, "Theory of imperfect waveguides: the effect of wall impedance," *J. Inst. Elec. Engr.*, vol. 102, pp. 698–708; September, 1955.

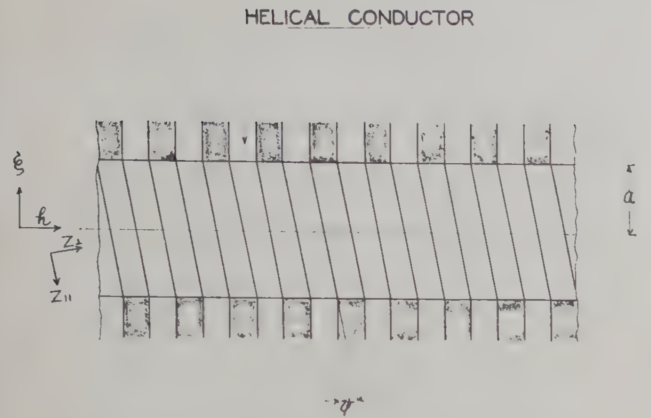

Fig. 1—The longitudinal section of a helix waveguide.

shown in Fig. 1. The characteristic equation for this type of helix waveguide is given by the following formula.[3,6]

$$\frac{\left(1-\frac{nh}{\xi^2 a}\cot\Psi+\frac{Z_\parallel}{Z_0}\,\frac{jkaJ'n(\xi a)}{\xi aJn(\xi a)}\right)\left(\frac{jkaJ'n(\xi a)}{\xi aJn(\xi a)}+\frac{Z_\perp}{Z_0}\left(1-\frac{nh}{\xi^2 a}\cot\Psi\right)\right)}{\left(1+\frac{nh}{\xi^2 a}\tan\Psi+\frac{Z_\perp}{Z_0}\,\frac{jkaJ'n(\xi a)}{\xi aJn(\xi a)}\right)\left(\frac{jkaJ'n(\xi a)}{\xi aJn(\xi a)}+\frac{Z_\parallel}{Z_0}\left(1+\frac{nh}{\xi^2 a}\tan\Psi\right)\right)}=\cot^2\Psi \qquad (1)$$

where

propagation factor $\exp\,(jhz+jn\theta-j\omega t)$ is assumed and
a = inner radius of waveguide
h = axial propagation constant
$k=\omega\sqrt{\mu_0\epsilon_0}$ = propagation constant in free space
n = angular mode index
$Z_0=\sqrt{\mu_0/\epsilon_0}$ wave impedance of free space
$Z_\parallel$ = surface impedance parallel to the helix direction
$Z_\perp$ = surface impedance perpendicular to the helix
Ψ = pitch angle of helix
$\xi=\sqrt{k^2-h^2}$ = radial propagation constant.

When the pitch angle is very small (1) is reduced to

$$\left(\frac{kaJ'n(\xi a)}{\xi aJn(\xi a)}-j\frac{Z_\parallel}{Z_0}\right)\left(\frac{kaJ'n(\xi a)}{\xi aJn(\xi a)}-j\frac{Z_0}{Z_\perp}\right)=\left(\frac{nha}{\xi^2a^2}\right)^2. \qquad (2)$$

This is the characteristic equation for a zero-pitch helix waveguide.[3,4,6] For $n=0$ (2) can be factored into two factors, and the solutions are

$$ka\frac{Z_0}{Z_\parallel}=-j\,\frac{(\xi a)J_0(\xi a)}{J_1(\xi a)} \qquad (3)$$

for the TE_0 modes,

$$ka\frac{Z_\perp}{Z_0}=-j\,\frac{(\xi a)J_0(\xi a)}{J_1(\xi a)} \qquad (4)$$

for the TM_0 modes.

These two modes are the only pure TE and TM modes that can exist in a zero-pitch helix waveguide. The TE_0 modes present low loss, and the TM_0 modes high loss. All other modes ($n\neq 0$) are mixed modes that cannot be separated into the pure TE or TM modes, so they are called hybrid modes, *i.e.*, HY_n modes. All the hybrid modes might also have high loss. For these modes, assuming $Z_\parallel/Z_0\ll 1$, we get the following formulas from (5):

$$\frac{ka}{\xi a}\,\frac{J'n(\xi a)}{Jn(\xi a)}\left(\frac{ka}{\xi a}\,\frac{J'n(\xi a)}{Jn(\xi a)}-j\frac{Z_0}{Z_\perp}\right)=\left(\frac{nha}{\xi^2a^2}\right)^2. \qquad (5)$$

When the function is

$$\frac{\dot{x}J_0(\dot{x})}{J_1(\dot{x})}\equiv F(\dot{x}), \qquad (6)$$

then the following relations can be obtained.

$$\frac{\dot{x}J_1'(\dot{x})}{J_1(\dot{x})}=F(\dot{x})-1 \qquad (7)$$

$$\frac{J_2'(\dot{x})}{\dot{x}J_2(\dot{x})}\equiv\frac{1}{2-F(\dot{x})}-\frac{2}{\dot{x}^2}\,. \qquad (8)$$

Using this $F(\dot{x})$ function, the characteristic equations for the first three lossy modes, TM_0, HY_1 and HY_2 series are written as:

$$TM_0:\ ka\frac{Z_\perp}{Z_0}=-jF(\dot{x}) \qquad (9)$$

$$HY_1:\ ka\frac{Z_\perp}{Z_0}=j\left(\frac{1}{(\dot{x})^2}\{F(\dot{x})-1\}+\frac{1}{F(\dot{x})-1}\left\{\frac{1}{(ka)^2}-\frac{1}{(\dot{x})^2}\right\}\right)^{-1} \qquad (10)$$

$$HY_2:\ ka\frac{Z_\perp}{Z_0}=j\left(\frac{1}{2-F(\dot{x})}-\frac{2}{(\dot{x})}+\frac{2}{\dfrac{(\dot{x})^2}{2\{2-F(\dot{x})\}}-1}\left\{\frac{1}{(ka)^2}-\frac{1}{(\dot{x})^2}\right\}\right)^{-1}. \qquad (11)$$

Numerical Calculations

Although there are large numbers of unwanted modes in the practical TE_{01} transmission line, it has been found that only modes having a smaller value of angular mode index can have a relatively large coupling to the TE_{01} mode.[1] Thus the numerical calculations have been performed only for the TM_0, HY_1, and HY_2 modes using a Fuji 128 relay computer.

As a first step the values of $F(\dot{x})$ are determined in the region $0\leq\rho\leq 10$ for 0°, 5°, 10°, 15°, 20°, and 25° respectively, where

$$\dot{x}\equiv\xi a\equiv\rho e^{-j\phi}. \qquad (12)$$

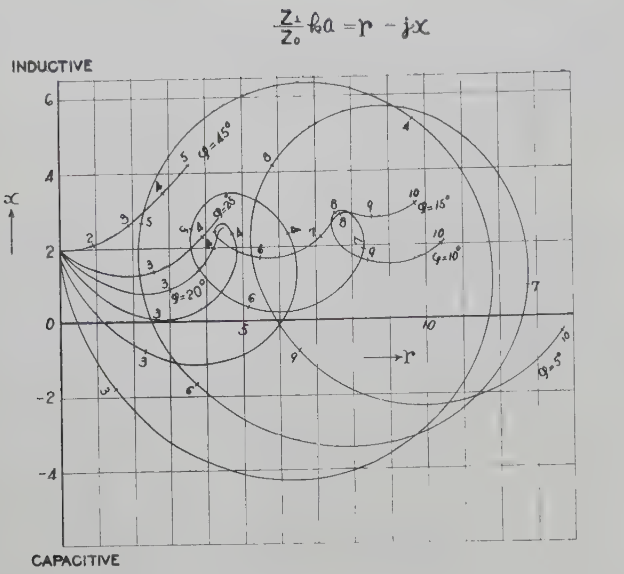

Fig. 2—Surface impedance. The curves show equi-φ lines and the numbers along this line show ρ values.

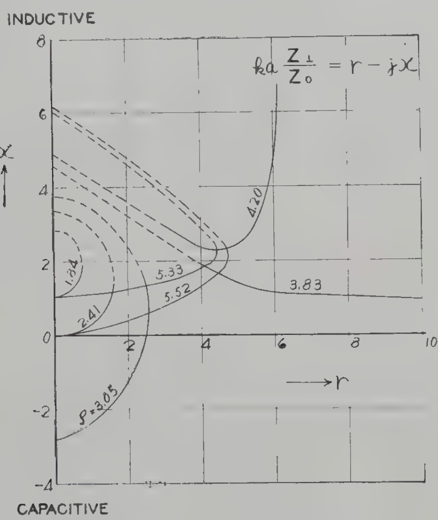

Fig. 3—Surface impedance vs the equiamplitude ρ lines.

These results lead to the normalized surface impedance $kaZ_\perp/Z_0$ for the TM_0 modes. The vector diagrams are shown in the following two figures, that is, the equiphase lines in Fig. 2 (the constant ϕ lines), and the equiamplitude lines in Fig. 3 (the constant ρ lines). As a second step, the propagation constants

$$ha = \beta a + j\alpha a = \sqrt{(ka)^2 - (\xi a)^2} \tag{13}$$

are calculated for the same amplitudes ρ and angles ϕ. The curves of αa vs ρ with the parameter ϕ are given in Fig. 4.

By eliminating the parameter ξa from the above two figures, the relation between the normalized surface impedance $ka\ Z_1/Z_0$ and the attenuation factor αa is found. The results show that there is a large number of TM_0 modes corresponding to any special surface impedance. In order to distinguish them, it is convenient to use the value of the radial propagation constant itself.

In general, unwanted modes with lower attenuation may be more harmful than ones with higher attenuation. Therefore we choose the one mode which shows

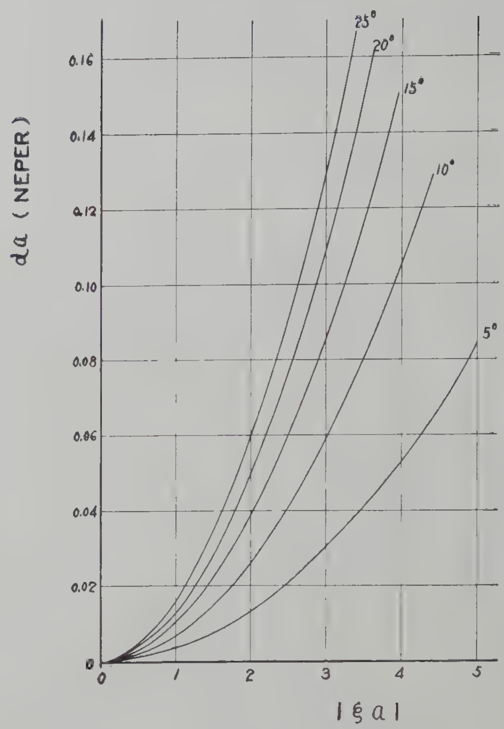

Fig. 4—$|\xi a| \equiv \rho$ vs αa at $ka = 26.2$.

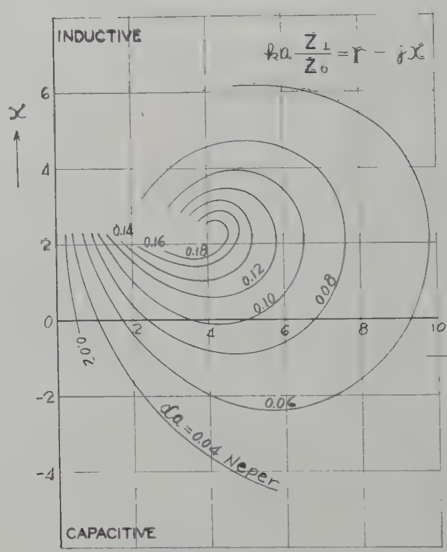

Fig. 5—Relations between surface impedance and attenuation constants of TM_0 waves $ka = 26.2$ (diameter 50 mm, frequency 50 kmc).

minimum attenuation in the infinite series of TM_0 modes corresponding to each given surface impedance. The equiattenuation lines in the $ka\ Z_\perp/Z_0$ plane, as shown in Fig. 5, is plotted for the case of $ka = 26.2$ which corresponds to $2a = 5$ cm and $f = 50$ kmc. In Fig. 5, the attenuation factor αa takes a maximum value 0.2 neper at $ka\ Z_\perp/Z_0 = 4 - j2$. Therefore if a helix waveguide having this optimum value of surface impedance is designed no TM_0 modes in the guide can have an attenuation factor smaller than 0.2 neper, the minimax value of the attenuation factor.

In the same way, for HY_1 and HY_2 modes, we get the relations between $ka\ Z_\perp/Z_0$ and ξ from (8), (9), and (11), which are shown in Figs. 6 and 7 for the case of $ka = 26.2$. The best values of the surface impedance for

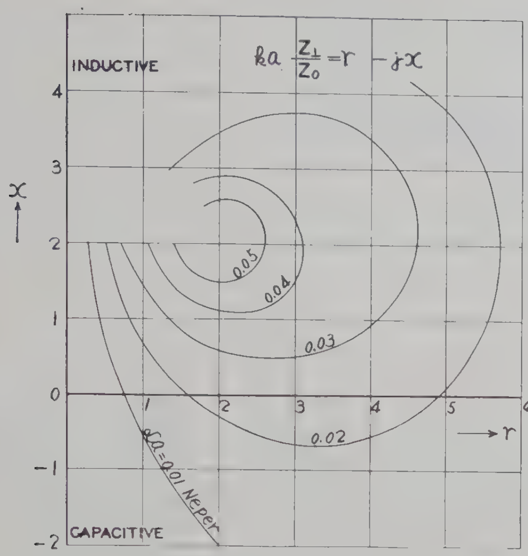

Fig. 6—Relations between surface impedance and attenuation constants of HY_1 waves, $ka=26.2$, (diameter 50 mm, frequency 50 kmc).

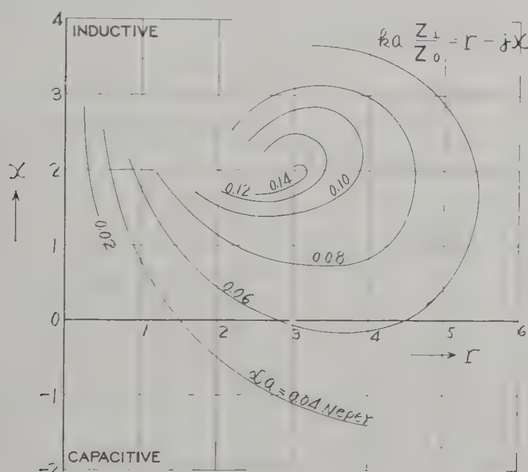

Fig. 7—Relations between surface impedance and attenuation constants of HY_2 waves, $ka=26.2$, (diameter 50 mm, frequency 50 kmc).

TABLE I

THE BEST VALUE OF SURFACE IMPEDANCE AND THE MINIMAX VALUE OF ATTENUATION CONSTANT FOR A HELIX WAVEGUIDE (50 mm ID, at 50 kmc)

Mode	Best Value of Z_1	Minimax Value of α
TM_0	57.6−j28.8 (ohms)	8.0 (nep/meter)
HY_1	28.8−j28.8	2.4
HY_2	43.2−j28.8	6.0

a mode-filter for HY_1 and HY_2 modes may be found from these curves.

Thus we have the best value, as is shown in Table I.

WAVEGUIDE STRUCTURES

In the previous section, the best value of the surface impedance $Z_\perp$ for the mode filter was found. There remains, however, the problem of designing the physical structures corresponding to this optimum surface impedance. Although this problem has not yet been solved completely, two possible structures are suggested.

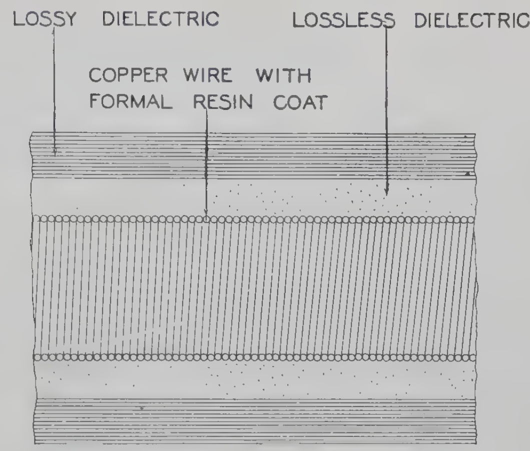

Fig. 8—The longitudinal section of a helix waveguide.

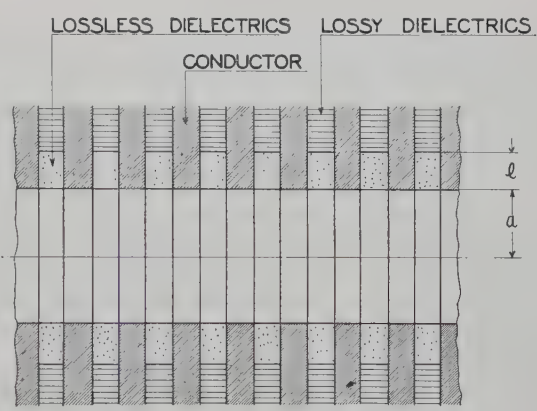

Fig. 9—The longitudinal section of a spaced-ring waveguide.

The first is a sheath helix structure with multilayer jacket, as indicated in Unger's paper.[9] In Fig. 8, the simplest one of this type is shown. The inner layer is lossless dielectrics while the outer jacket is lossy material. Both the thickness of the inner layer and the electrical properties of the outer jacket are varied so as to realize the best value of surface impedance.

Another example is the spaced-ring structure shown in Fig. 9. Here also the depth l of the lossless dielectrics and the lossy material are varied to obtain the best condition. In this case, the radial transmission line calculations can be used to design the surface impedance.

CONCLUSION

The characteristics of a helix waveguide as a mode-filter has been theoretically examined. The relations between the anisotropic surface impedance and the attenuation constant were investigated to determine the best value of the above impedance for a mode filter. The best values were obtained numerically for the TM_0, HY_1, and HY_2 modes. Two examples of helix structure which have possibility of giving the best value of the surface impedance were also proposed.

ACKNOWLEDGEMENT

The authors express sincere gratitude for the numerical calculation of the above formulas to S. Miyazaki and H. Ishikawa of the Furukawa Electric Co. Ltd.

Design of Linear Double Tapers in Rectangular Waveguides*

R. C. JOHNSON†

Summary—This paper considers the problem of a taper connecting two uniform waveguides of arbitrary dimensions and propagating a single mode; an approximate expression for the reflection coefficient is derived. The special case of a linear double taper in rectangular waveguide is examined in detail for propagation in the TE_{10} mode. Approximate expressions for the reflection coefficient and voltage standing wave ratio as functions of the taper dimensions and free space wavelength are derived and experimentally verified.

Introduction

Tapered sections of waveguides are useful impedance matching devices with wide bandwidth characteristics. Of particular interest is the linear taper because of its ease of fabrication.

Several theoretical papers on reflections in nonuniform transmission lines are available in the literature. Matsumaru[1] recently analyzed linear and sinusoidal E-plane tapers in rectangular waveguides, supporting his theory with experimental evidence. He also pointed out that linear tapers perform almost as well as exponential tapers and better than shorter hyperbolic tapers. Quite often, however, it is necessary to design a double taper, *i.e.*, one that tapers simultaneously in both the E-plane and H-plane. Therefore, the microwave circuit engineer needs a method which enables him to design a linear taper which will match two uniform waveguides of arbitrary dimensions. This paper provides such a method for designing linear, single or double tapers in rectangular waveguide employing propagation in the TE_{10} mode. A similar analysis can be applied to other cases.

Reflection Coefficient of Tapered Waveguide

The exact theory of reflection in waveguides is quite complicated, particularly when the dimensions of the discontinuities are not small compared to a wavelength. For a small step discontinuity between guides of impedances Z_a and Z_b, the following well-known expression for the reflection coefficient can be used:[2]

$$\Gamma = \frac{Z_b - Z_a}{Z_b + Z_a}. \tag{1}$$

Consider a tapered waveguide of length L which connects two uniform waveguides of impedances Z_0 and Z_1 as shown in Fig. 1. Let x be the distance from the end of the taper where the impedance is Z_0 and assume that the impedance in the taper is a smooth function of x such that $Z(0) = Z_0$ and $Z(L) = Z_1$. Partition the interval $0 \leq x \leq L$ into N equal subintervals, and replace the taper with N uniform waveguides, each having a length of $\Delta x = L/N$. Let the impedance of the nth segment be $z_n = Z(x_n)$.

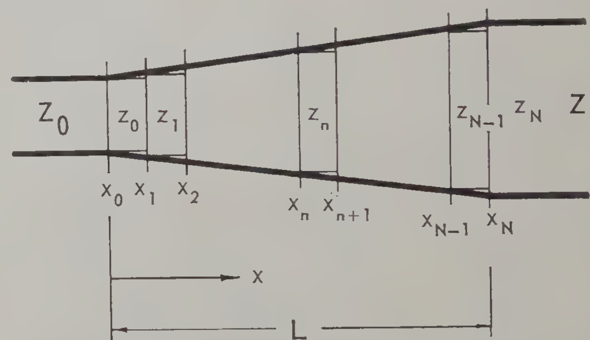

Fig. 1—Tapered waveguide of length L connecting uniform waveguides of impedances Z_0 and Z_1.

The total reflection coefficient is now a function of the N small reflections from the discontinuities at x_1, x_2, $\cdots$, x_N. If N is large, the reflection at each discontinuity becomes very small. Neglecting multiple reflections and the excitation of higher order modes, the N small reflections can be summed as complex vectors in the following manner;

$$\Gamma \approx \Gamma_1 \exp[-2\gamma_0\Delta x] + \Gamma_2 \exp[-2\gamma_0\Delta x - 2\gamma_1\Delta x] + \cdots + \Gamma_N \exp\left[-2\sum_{m=0}^{N-1}\gamma_m\Delta x\right],$$

or

$$\Gamma \approx \sum_{n=1}^{N}\Gamma_n \exp\left[-2\sum_{m=0}^{n-1}\gamma_m\Delta x\right], \tag{2}$$

where γ_n is the propagation constant in the nth segment, and

$$\Gamma_n = \frac{z_n - z_{n-1}}{z_n + z_{n-1}}$$

* Manuscript received by the PGMTT, February 24, 1959.
This work was supported by the U.S. Army Signal Engineering Lab., Fort Monmouth, N. J., under contract DA 36-039 SC-74870; the Diamond Ordnance Fuze Lab., Washington, D. C., under contract DA 49-186-502 ORD-709; and the Engineering Experiment Station, Georgia Inst. Tech., Atlanta, Ga.
† Engineering Experiment Station, Georgia Institute of Technology, Atlanta, Ga.
[1] K. Matsumaru, "Reflection coefficient of E-plane tapered waveguides," IRE Trans. on Microwave Theory and Techniques, vol. MTT-6, pp. 143–149; April, 1958.
[2] J. C. Slater, "Microwave Transmission," McGraw-Hill Book Co. Inc., New York, N. Y., p. 59; 1942.
S. A. Schelkunoff, "Electromagnetic Waves," D. Van Nostrand Co., Inc., New York, N. Y., pp. 319–320; 1943.

is the reflection coefficient at the nth discontinuity. Eq. (2) can be written as

$$\Gamma \approx \sum_{n=1}^{N} \frac{(z_n - z_{n-1})/\Delta x}{z_n + z_{n-1}} \exp\left[-2\sum_{m=0}^{n-1} \gamma_m \Delta x\right] \Delta x.$$

Letting N approach infinity, the total reflection coefficient for the taper can be expressed by the integral

$$\Gamma = \int_0^L \frac{Z'(x)}{2Z(x)} \exp\left[-2\int_0^x \gamma(\tau)d\tau\right] dx \tag{3}$$

or

$$\Gamma = \int_0^L \frac{1}{2}\left(\frac{d}{dx}\ln Z\right) \exp\left[-2\int_0^x \gamma d\tau\right] dx, \tag{4}$$

where the prime denotes differentiation with respect to x.

The right side of (4) is a summation of infinitesimal vectors of slowly varying phase; Γ is equal to the resultant. In optics, a summation of this type is commonly called a vibration curve. A graphical representation of (4) is shown in Fig. 2(a). Integrating (4) by parts, the reflection coefficient becomes

$$\Gamma = \frac{1}{4\gamma_0}\left(\frac{d}{dx}\ln Z\right)_0 - \frac{1}{4\gamma_1}\left(\frac{d}{dx}\ln Z\right)_1 \exp\left[-2\int_0^L \gamma dx\right]$$
$$+ \int_0^L \frac{d}{dx}\left(\frac{1}{4\gamma}\frac{d}{dx}\ln Z\right) \exp\left[-2\int_0^x \gamma d\tau\right] dx. \tag{5}$$

The right side of (5) is the sum of two vectors (terms 1 and 2) and a small vibration curve (term 3) somewhat similar in form to the vibration curve of (4). A graphical representation of (5) is shown in Fig. 2(b).

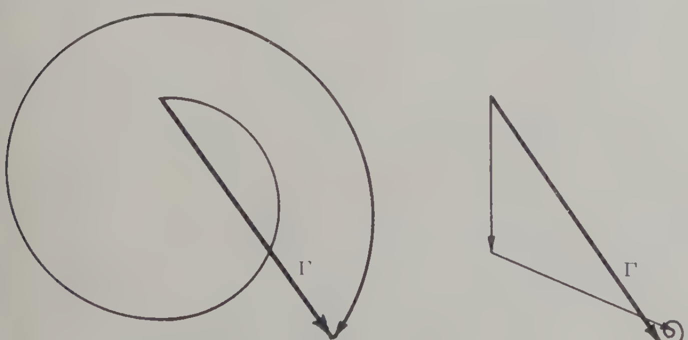

(a) (b)

Fig. 2—(a) Graphical representation of (4), (b) Graphical representation of (5).

Eqs. (4) and (5) are expressions for the reflection coefficient from a tapered section of transmission line or waveguide. The procedure from here depends upon the particular type of taper and waveguide under consideration. Eq. (5) yields a particularly simple result for an exponential taper in which γ is not a function of x. In this case the vibration curve term is zero and the reflection coefficient becomes

$$\Gamma = \frac{1}{4\gamma L}\ln\frac{Z_1}{Z_0}\left[1 - \exp(-2\gamma L)\right],$$

which is the same expression as that given by Ragan.[3]

Linear Taper in Rectangular Waveguide

The taper which will be examined in this paper is that of a linear double taper in rectangular waveguide employing the TE_{10} mode. Except for the phase factor, the integrand in the vibration curve (term 3) of (5) is the derivative of the product $1/2\gamma$ times the integrand of (4). Except where the frequency of operation is in the region near cutoff, γ and Z are slowly varying functions, and the vibration curve term in (5) is assumed to be negligible (See Appendix). This leaves the approximation,

$$\Gamma = \frac{1}{4\gamma_0}\left(\frac{d}{dx}\ln Z\right)_0$$
$$- \frac{1}{4\gamma_1}\left(\frac{d}{dx}\ln Z\right)_1 \exp\left[-2\int_0^L \gamma dx\right], \tag{6}$$

which is identical with the expression derived by Frank[4] using approximate solutions of the tapered transmission line equations. It should be noted that the logarithmic derivative is discontinuous at the ends of the taper; the values to be used are those just inside the tapered portion.

Fig. 3 illustrates the general configuration of a linear taper of length L connecting rectangular waveguides of impedances Z_0 and Z_1. In the taper section a and/or b are linear functions of x of the form

$$a = a(x) = a_0 + \frac{a_1 - a_0}{L}x$$

$$b = b(x) = b_0 + \frac{b_1 - b_0}{x}x.$$

To interpret (6) in terms of the TE_{10} mode in rectangular waveguide in free space dielectric, the integrated characteristic impedance defined on a voltage-current basis[5] is used. Thus, let

$$Z = \frac{\pi\eta_0}{2}\frac{b}{a\sqrt{1-(\lambda/2a)^2}} \tag{7}$$

and

$$\gamma = i\frac{2\pi}{\lambda_g} = i\frac{2\pi}{\lambda}\sqrt{1-(\lambda/2a)^2}, \tag{8}$$

where a and b are the width and height of the guide, respectively, λ is the free space wavelength, and λ_g is the guide wavelength. The logarithmic derivative in the taper is then found to be

[3] G. I. Ragan, "Microwave Transmission Circuits," Rad. Lab. Series, vol. 9, McGraw-Hill Book Co., Inc., New York, N. Y., p. 307; 1948.

[4] N. H. Frank, "Reflections from Sections of Tapered Transmission Lines and Wave Guides," Rad. Lab. Rep. No. 189; January 6, 1943.

[5] Schelkunoff, *op. cit.*, p. 319; Slater, *op. cit.*, pp. 183–185.

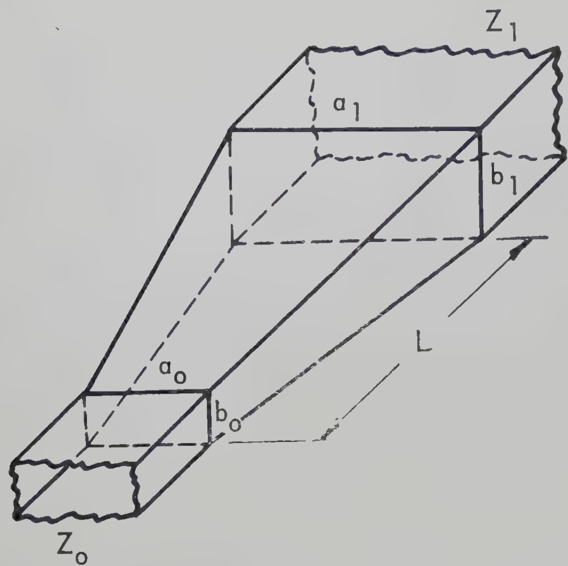

Fig. 3—Linear taper of length L connecting rectangular waveguides of impedances Z_0 and Z_1.

$$\frac{d}{dx}\ln Z = \frac{1}{L}\left[\frac{b_1 - b_0}{b} - \frac{(a_1 - a_0)/a}{1 - (\lambda/2a)^2}\right]. \tag{9}$$

The exponent in (6) can be written in the form

$$-2\int_0^L \gamma dx = -i4\pi\int_0^L \frac{dx}{\lambda_g}, \tag{10}$$

which is recognized as $-i4\pi$ times the number of guide wavelengths in the taper.

Substitution of (8), (9), and (10) into (6) yields the following expression for reflection coefficient,

$$\Gamma = \frac{i}{8\pi L/\lambda}\left[K_1 \exp(-i4\pi l) - K_0\right] \tag{11}$$

where

$$K_0 = \frac{(b_1 - b_0)/b_0 - [(a_1 - a_0)/a_0]/[1 - (\lambda/2a_0)^2]}{[1 - (\lambda/2a_0)^2]^{1/2}} \cdot \tag{12}$$

$$K_1 = \frac{(b_1 - b_0)/b_1 - [(a_1 - a_0)/a_1]/[1 - (\lambda/2a_1)^2]}{[1 - (\lambda/2a_1)^2]^{1/2}} \tag{13}$$

$$l = \int_0^L \frac{dx}{\lambda_g} = \frac{1}{\lambda}\int_0^L \sqrt{1 - (\lambda/2a)^2}\,dx. \tag{14}$$

Eq. (14) may be evaluated by using a series expansion of the radical and integrating term by term. The result is

$$l = \frac{L}{\lambda}\left\{1 + \sum_{n=1}^{\infty}(-1)^n \frac{\frac{1}{2}\left(\frac{-1}{2}\right)\left(\frac{-3}{2}\right)\cdots\left(\frac{-2n+3}{2}\right)}{n!(2n-1)} \cdot\left(\frac{\lambda}{2a_1 - 2a_0}\right)\left[\left(\frac{\lambda}{2a_0}\right)^{2n-1} - \left(\frac{\lambda}{2a_1}\right)^{2n-1}\right]\right\}. \tag{15}$$

Within the recommended operating range of standard waveguides, the first two terms of the series are sufficient; however, for frequencies near cutoff, additional terms should be used.

The absolute magnitude of the reflection coefficient is

$$|\Gamma| = \frac{1}{L/\lambda}\left[\frac{K_0^2 + K_1^2}{64\pi^2} - \frac{K_0K_1}{32\pi^2}\cos(4\pi l)\right]^{1/2}. \tag{16}$$

Using the relation

$$\text{VSWR} = \frac{1 + |\Gamma|}{1 - |\Gamma|}, \tag{17}$$

the dominant mode voltage standing wave ratio (VSWR) can be calculated as a function of taper length and frequency for a linear taper connecting two specified waveguides. It is easy to calculate VSWR versus taper length for a fixed frequency since K_0 and K_1 are independent of length and l is proportional to length. To calculate VSWR versus frequency for a fixed taper length, the three constants must be evaluated for each frequency; however, the calculations are simple.

Linear E-Plane Taper in Rectangular Guide

In the special case of an E-plane taper an expression which is simpler than (16) can be derived for the absolute magnitude of the reflection coefficient. Since the guide width is constant, γ is not a function of x; therefore,

$$l = \int_0^L \frac{dx}{\lambda_g} = \frac{L}{\lambda_g}\cdot \tag{18}$$

Substituting (12), (13), and (18) into (11), the expression for the reflection coefficient becomes

$$\Gamma = \frac{i}{8\pi L/\lambda_g}\left[\frac{b_1 - b_0}{b_1}\exp(-4\pi L/\lambda_g) - \frac{b_1 - b_0}{b_0}\right]. \tag{19}$$

The absolute magnitude of the reflection coefficient is then

$$|\Gamma| = \frac{1}{8\pi L/\lambda_g}\left|1 - \frac{b_0}{b_1}\right|\left[1 + \left(\frac{b_1}{b_0}\right)^2 - 2\left(\frac{b_1}{b_0}\right)\cos(4\pi L/\lambda_g)\right]^{1/2}, \tag{20}$$

and the VSWR can be calculated from (17).

Eq. (19) is considerably different from the expression for reflection coefficient derived by Matsumaru;[6] however, the calculated VSWR's agree well for impedance ratios as great as $Z_1/Z_0 = 2$. With an impedance ratio of $Z_1/Z_0 = 2.8$ (20) predicts a slightly higher VSWR than that predicted by Matsumaru as illustrated in Fig. 4.

Eq. (20) was used to calculate the curve of VSWR vs taper length in Fig. 5 for an impedance ratio of

[6] Matsumaru, *op. cit.*, Eq. (8).

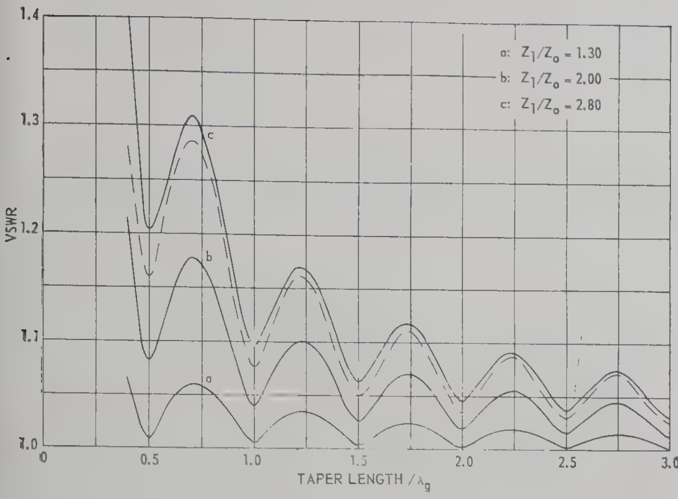

Fig. 4—VSWR of linear E-plane tapers. The solid curves were calculated from (20) and the dashed curve was calculated by Matsumaru.

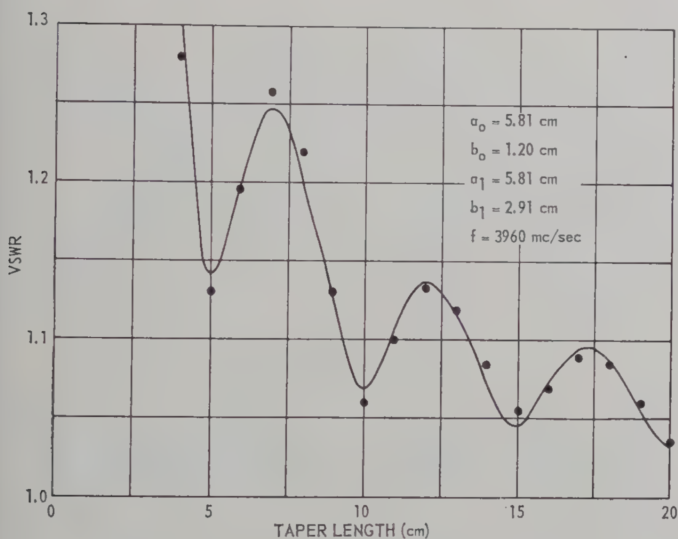

Fig. 5—VSWR versus taper length calculated from (20). The experimental points were reported by Matsumaru.

$Z_1/Z_0 = 2.42$. The experimental points were reported by Matsumaru[7] and used to verify his theoretical expression. It is seen that they can also serve to verify (20).

Experimental Investigation

In the experimental phase, a linear double taper was electroformed and tested over a wide band of frequencies. It was desirable to have the low end of the test frequency band near cutoff since the approximation of (6) does not hold there. A design frequency of 9500 mc was selected and the taper was fabricated to connect guides with dimensions of 0.900 inch$\times$0.400 inch and 0.750 inch$\times$0.600 inch; the latter has a cutoff frequency of 7869 mc. Based on (7) these waveguides have an impedance ratio of 2.33 at the design frequency. Measuring the VSWR from this taper gave an indication of

[7] *Ibid.*, Fig. 5.

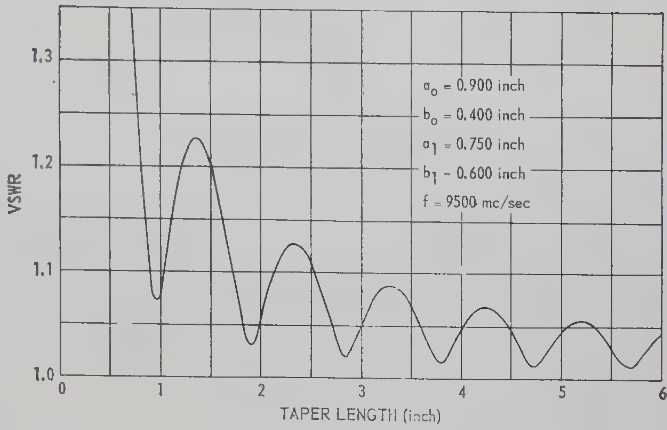

Fig. 6—Theoretical VSWR versus taper length for a linear double taper.

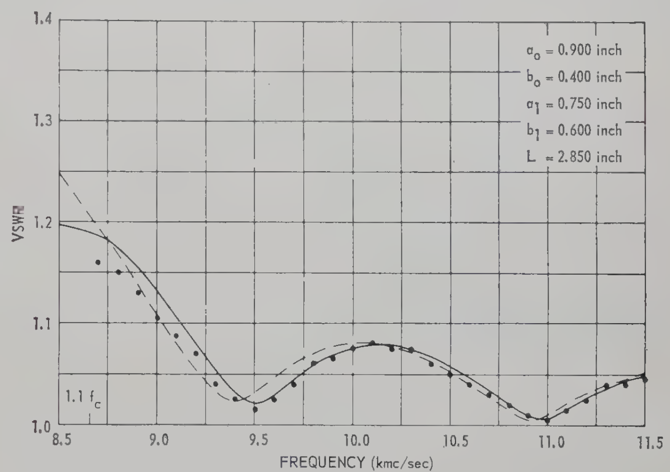

Fig. 7—VSWR versus frequency for a linear double taper. The curves were calculated from (16); the value of l was obtained from (15) using the first four terms of the series for the solid curve and the first two terms for the dashed curve. The points are experimental measurements.

the validity of (6) in the region near cutoff.

The curve of VSWR versus taper length shown in Fig. 6 was calculated using (16). The value of l was obtained from (15) using the first four terms of the series. A taper length of 2.850 inches was chosen, and curves of VSWR versus frequency were calculated from (16) for two values of l. Both curves are shown in Fig. 7.

The 0.750 inch$\times$0.600 inch guide was terminated by a sliding load, and the VSWR was measured at several frequencies with a standard X-band slotted line at the 0.900 inch$\times$0.400 inch end of the taper. The experimental points are also shown in Fig. 7. The agreement between the measured and theoretical VSWR is satisfactory at 10 per cent above cutoff; it becomes increasingly better at higher frequencies. Since the low end of the recommended operating bands for standard waveguides generally is 23 to 36 per cent above cutoff, (16) can be used to predict the VSWR from linear tapers for most practical applications.

Conclusion

The approximate expression for the absolute magnitude of the reflection coefficient in (16) enables the microwave circuit engineer to design linear, double or single tapers which will match rectangular waveguides of arbitrary dimensions employing the TE_{10} mode. The VSWR can be predicted as a function of the taper dimensions and the free space wavelength. In the experimental phase the measured VSWR agreed satisfactorily with the calculated value at 10 per cent above cutoff; the agreement became increasingly better for higher frequencies.

Appendix

It is desirable to estimate the resultant of the vibration curve, term 3 of (5),

$$\int_0^L \frac{d}{dx}\left(\frac{1}{4\gamma}\frac{d}{dx}\ln Z\right)\exp\left[-2\int_0^x \gamma d\tau\right]dx.$$

The length T of the curve can be found by neglecting the phase factor in the integrand;

$$T = \left|\int_0^L \frac{d}{dx}\left(\frac{\lambda_g}{8\pi}\frac{d}{dx}\ln Z\right)dx\right|. \tag{21}$$

Integrating and substituting from (12) and (13), the length of the vibration curve is found to be

$$T = \left|\frac{K_1 - K_0}{8\pi L/\lambda}\right|. \tag{22}$$

The magnitude of the error in the approximation (6) must be less than T, and under normal circumstances, it will be considerably smaller than T since the vibration curve is a spiral through $4\pi l$ radians.

A better estimate of the magnitude of the error in (6) can be made by assuming a circular vibration curve of length T turning through $4\pi l$ radians as illustrated in Fig. 8(b). Then, the maximum magnitude of the error is approximately the diameter d of the circular path, where

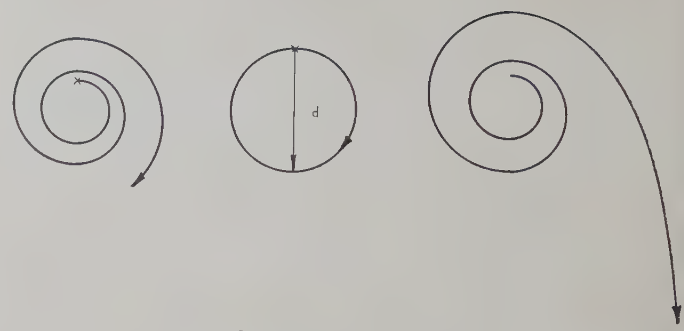

Fig. 8—Illustrations of (a) a typical vibration curve, (b) a circular vibration curve, and (c) a typical vibration curve from a taper having one end near cutoff.

$$d = \frac{T}{2\pi l} = \left|\frac{K_1 - K_0}{16\pi^2 l L/\lambda}\right|. \tag{23}$$

For most applications, d is very small and (16) can be used with confidence. One must be cautious, however, at a frequency close to cutoff. If the width of one end of the taper is near the cutoff dimension, the phase shift per unit length will be very small at this end, and a vibration curve similar to that in Fig. 8(c) will result. In this case, the magnitude of the error may be larger than d but must still be smaller than T.

Acknowledgement

The author is indebted to J. S. Hollis for his many suggestions and helpful criticism and to Elizabeth Bone for her assistance in the calculations and microwave measurements.

Spurious Mode Generation in Nonuniform Waveguide*

L. SOLYMAR†

Summary—This paper deals with the problem of a nonuniform waveguide joining two uniform ones and the spurious modes generated by it when a pure mode is incident in one of the uniform waveguides.

The generalised telegraphist's equations are stated and transformed into a set of differential equations for the amplitudes of the forward and backward travelling waves. The expressions for the coupling coefficients between the various modes are given and analysed.

By making certain assumptions, the differential equations are solved and the amplitudes of the modes are given in a closed form.

Subject to these same assumptions, it is proved that the power in the spurious modes may be kept below any predetermined level, provided the nonuniform waveguide is sufficiently gradual.

I. Introduction

WAVEGUIDES whose cross sections change along the axis have been frequently investigated. A general solution was first given by Stevenson,[1] who expanded the field intensities into a series of the cross sectional wave functions. Using the same approach generalised telegraphist's equations were derived independently at the same time by Schelkunoff,[2] Reiter,[3] and Katzenelenbaum.[4] Since then, these methods were used successfully for solving a large number of problems.[5–13]

In the present paper, the amplitudes of the spurious modes, due to a nonuniform waveguide section, are determined. In Section II, Reiter's equations are transformed into a differential equation system in terms of forward and backward travelling waves. In Section III, the coefficients of this differential equation system are computed, and a few general conclusions are drawn. The differential equation system is simplified and solved by using a few approximations in Section IV, while in Section V, a theorem on sufficiently gradual nonuniform waveguides is proved. Section VI deals with two practical examples illustrating the application of the formulae derived.

II. The Generalised Telegraphist's Equations

Let the uniform waveguide G_1 extend from $z=-\infty$ to $z=0$, and the uniform waveguide G_2 from $z=L$ to $z=\infty$ (Fig. 1.). Let us connect them by a nonuniform waveguide which has the following properties: the equation of the surface is $F(x, y, z)=0$, which is differentiable as a function of z. A plane perpendicular to the z axis cuts this surface in a single, closed curve; the cross-section of the nonuniform waveguide. The interior of any cross section is denoted by $S(z)$, and its boundary by $C(z)$. The cross-sections at $z=0$ and $z=L$ correspond to those of the uniform waveguides G_1 and G_2 respectively.

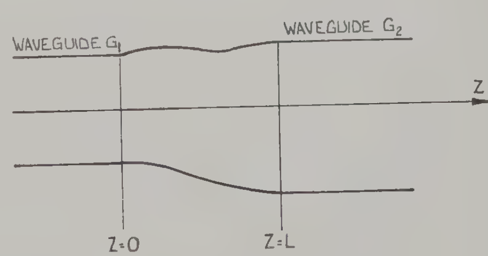

Fig. 1—A nonuniform waveguide section.

Our purpose is to determine the spurious modes in waveguide G_2, if waveguide G_1 is fed by a pure mode (subsequently called the main mode).

The nonuniform waveguide may be regarded as a system of coupled transmission lines, where the coupling coefficients are functions of z. The field intensities in the nonuniform waveguide may be represented by equivalent voltages and currents. The differential equation system for these voltages and currents is known as the generalised telegraphist's equation. Neglecting losses, we can use the following form as derived by Reiter:[14]

* Manuscript received by the PGMTT, January 21, 1959; revised manuscript received, March 20, 1959.

† Standard Telecommunication Labs., Ltd., Enfield, Middlesex, Eng.

[1] A. F. Stevenson, "General theory of electromagnetic horns," *J. Appl. Phys.*, vol. 22, pp. 1447–1454; December, 1951.

[2] S. A. Schelkunoff, "Conversion of Maxwell's equations into generalised telegraphist's equations," *Bell Sys. Tech. J.*, vol. 34, pp. 995–1044; September, 1955.

[3] G. Reiter, "Connection of two waveguides by a waveguide of variable cross-section," (In Hungarian) thesis from applied mathematics, University Eotvos Lorand, Budapest; June, 1955.

[4] B. Z. Katzenelenbaum, "Nonuniform waveguides with slowly changing parameters," (In Russian) *Dokl. Akad. Nauk, USSR*, vol. 12, pp. 711–714; 1955.

[5] B. Z. Katzenelenbaum, "Long symmetrical waveguide taper for H_{01} wave," (In Russian) *Radiotek. Elek.*, vol. 2, pp. 531–538; May, 1957.

[6] S. P. Morgan, "Theory of curved circular waveguide containing an inhomogeneous dielectric," *Bell Sys. Tech. J.*, vol. 36, pp. 1209–1252; September, 1957.

[7] Y. Shimizu, "Theory of transmitting circular electric wave around bends," Congres Internatl. Circuits et Antennes Hyperfrequences, Paris, France; October, 1957.

[8] B. Oguchi and M. Kato, "The effects of circular TE_{1m} waves on the propagation of circular TE_{01} wave in a curved waveguide," Congres Internatl. Circuits et Antennes Hyperfrequences, Paris, France; October, 1957.

[9] H. G. Unger, "Circular electric wave transmission through serpentine bends," *Bell Sys. Tech. J.*, vol. 36, pp. 1279–1291; September, 1957.

[10] H. G. Unger, "Normal mode bends for circular electric waves," *Bell Sys. Tech. J.*, vol. 36, pp. 1292–1307; September, 1957.

[11] B. Z. Katzenelenbaum, "On the general theory of nonuniform waveguides," (In Russian) *Dokl. Akad. Nauk, USSR*, vol. 116, pp. 203–206; 1957.

[12] B. Z. Katzenelenbaum, "On the theory of nonuniform waveguides with slowly changing parameters," Congres Internatl. Circuits et Antennes Hyperfrequences, Paris, France; October, 1957.

[13] H. G. Unger, "Circular waveguide taper of improved design," *Bell Sys. Tech. J.*, vol. 37, p. 899; July, 1958.

[14] G. Reiter, "Generalised telegraphist's equation for waveguides of varying cross-section," presented at the Convention on Long Distance Transmission by Waveguide," London, Eng., 1959; January 29–30.

$$-\frac{dV_i}{dz} = j\beta_i K_i I_i - \sum_p T_{pi} V_p$$
$$-\frac{dI_i}{dz} = j\frac{\beta_i}{K_i} V_i + \sum_p T_{ip} I_p \tag{1}$$

where i and p denote arbitrary modes (for the time being there is no need to discriminate the E and H modes). V_i and I_i are the equivalent voltages and currents for the mode i. β_i is the propagation coefficient, and K_i is the wave impedance. T_{pi} and T_{ip} represent the voltage and current transfer coefficients.

We point out that there is no mutual impedance between the voltages and currents of *different* modes, and there is a simple connection between the current and voltage transfer coefficients.

The transfer coefficient T_{pi} may be expressed as follows;

$$T_{pi} = \int_{S(z)} \bar{e}_p \frac{\partial \bar{e}_i}{\partial z} dS \tag{2}$$

where $\bar{e}_p$ and $\bar{e}_i$ are the mode vector functions[15] of the corresponding modes, which satisfy the normalisation conditions,

$$\int_{S(z)} |\bar{e}_p|^2 dS = 1. \tag{3}$$

For writing the mode vector functions, we must differentiate between E and H modes. For E modes, (subscripts in parentheses)

$$\bar{\mathbf{e}}_{(p)} = -\nabla_t \psi_{(p)}. \tag{4}$$

For H modes, (subscripts in brackets)

$$\bar{\mathbf{e}}_{[p]} = \bar{\mathbf{z}}_0 x \nabla_t \psi_{[p]} \tag{5}$$

where

∇_t = the gradient operator transverse to the z axis
z_0 = the unit vector in the direction of the z axis.

The $\psi_{(p)}$ and $\psi_{[p]}$ functions satisfy the differential equations

$$\nabla_t^2 \psi_{(p)} + h_{(p)}^2 \psi_{(p)} = 0$$
$$\psi_{(p)} = 0 \text{ on } C(z) \tag{6}$$

and

$$\nabla_t^2 \psi_{[p]} + h_{[p]}^2 \psi_{[p]} = 0$$
$$\frac{\partial \psi_{[p]}}{\partial n} = 0 \text{ on } C(z) \tag{7}$$

where

$$h_{[p]} = (k^2 - \beta_{[p]}^2)^{1/2}$$
$$h_{(p)} = (k^2 - \beta_{(p)}^2)^{1/2}$$
$$k = 2\pi/\lambda.$$

[15] N. Marcuritz, "Waveguide Handbook," McGraw-Hill Book Co., Inc., New York, N. Y., p. 4; 1951.

For the description of a wave phenomenon, the representation in terms of forward and backward travelling waves seems to be more suitable. Therefore, assuming that

$$K_i \neq 0 \quad \text{and} \quad K_i \neq \infty, \tag{7a}$$

we introduce as new variables the amplitudes of the forward and backward travelling waves, A_i^+ and A_i^-, by the relations

$$V_i = K_i^{1/2}(A_i^+ + A_i^-)$$
$$I_i = K_i^{-1/2}(A_i^- + A_i^-). \tag{8}$$

Substituting (8) into (1) we obtain the following differential equations for coupled travelling waves;

$$\frac{dA_i^+}{dz} = -j\beta_i A_i^+ - \frac{1}{2}\frac{d(\ln K_i)}{dz} A_i^- + \sum_p (S_{ip}^+ A_p^+ + S_{ip}^- A_p^-)$$
$$\frac{dA_i^-}{dz} = -\frac{1}{2}\frac{d(\ln K_i)}{dz} A_i^+ + j\beta_i A_i^- + \sum_p (S_{ip}^- A_p^+ + S_{ip}^+ A_p^-) \tag{9}$$

where S_{ip}^+ is the forward and S_{ip}^- the backward coupling coefficient. Both may be expressed in terms of the transfer coefficients as follows:

$$S_{ip}^{\pm} = \frac{1}{2}\left[\frac{K_p^{1/2}}{K_i^{1/2}} T_{pi} \mp \frac{K_i^{1/2}}{K_p^{1/2}} T_{ip}\right]. \tag{10}$$

If the waveguide G_1 is fed by a mode m, the boundary conditions for the differential equation system are as follows;

$$A_m^+(0) = A_0, \qquad A_m^-(L) = 0$$
$$A_i^+(0) = 0 \qquad A_i^-(L) = 0 \qquad (i \neq m). \tag{11}$$

III. The Transfer and Coupling Coefficients

Substituting the mode vector functions into (2), using Green's and Stokes' theorems, the relations

$$K_{[i]} = \frac{\omega\mu}{\beta_{(i)}}, \qquad K_{(i)} = \frac{\beta_{(i)}}{\omega\epsilon}, \qquad k^2 = \omega^2\mu\epsilon \tag{12}$$

and the identities

$$\frac{\partial \psi_{(i)}}{\partial z} \equiv -\frac{\partial \psi_{(i)}}{\partial n} \tan\theta;$$
$$\frac{\partial}{\partial z}\frac{\partial \psi_{[i]}}{\partial n} \equiv -\frac{\partial^2 \psi_{[i]}}{\partial n^2} \tan\theta \text{ on } C(z), \tag{13}$$

the transfer and coupling coefficients may be expressed by line integrals as follows;[16]

[16] Similar expressions can be derived for the cases when $h_{(i)} = h_{(p)}$ and $h_{[i]} = h_{[p]}$.

$$T_{(i)(p)} = \frac{h_{(p)}^2}{h_{(i)}^2 - h_{(p)}^2} \oint_{C(z)} \tan\theta \frac{\partial \psi_{(i)}}{\partial n} \frac{\sigma \psi_{(p)}}{\partial n} ds; \qquad h_{(i)} \neq h_{(p)} \tag{14}$$

$$T_{(i)[p]} = 0, \tag{15}$$

$$T_{[i](p)} = -\oint_{C(z)} \tan\theta \frac{\partial \psi_{[i]}}{\partial s} \frac{\partial \psi_{(p)}}{\partial n} ds \tag{16}$$

$$T_{[i][p]} = \frac{h_{[i]}^2}{h_{[p]}^2 - h_{[i]}^2} \oint_{C(z)} \tan\theta \psi_{[i]} \frac{\partial^2 \psi_{[p]}}{\partial n^2} ds; \qquad h_{[i]} \neq h_{[p]} \tag{17}$$

$$T_{(i)(i)} = S^{-}_{(i)(i)} = -\frac{1}{2} \oint_{C(z)} \tan\theta \left(\frac{\partial \psi_{(i)}}{\partial n}\right)^2 ds \tag{18}$$

$$T_{[i][i]} = S^{-}_{[i][i]} = -\frac{1}{2} \oint_{C(z)} \tan\theta \left(\frac{\partial \psi_{[i]}}{\partial s}\right)^2 ds \tag{19}$$

$$S^{+}_{(i)(i)} = S^{+}_{[i][i]} = 0 \tag{20}$$

$$S^{\pm}_{(i)(p)} = \frac{\beta_{(i)} h_{(p)}^2 \pm \beta_{(p)} h_{(i)}^2}{2\sqrt{\beta_{(i)}\beta_{(p)}}(h_{(i)}^2 - h_{(p)}^2)} \oint_{C(z)} \tan\theta \frac{\partial \psi_{(i)}}{\partial n} \frac{\partial \psi_{(p)}}{\partial n} ds; \qquad h_{(i)} \neq h_{(p)} \tag{21}$$

$$S^{\pm}_{(i)[p]} = \frac{k}{2\sqrt{\beta_{(i)}\beta_{[p]}}} \oint_{C(z)} \tan\theta \frac{\partial \psi_{(i)}}{\partial n} \frac{\partial \psi_{[p]}}{\partial s} ds \tag{22}$$

$$S^{\pm}_{[i][p]} = \frac{\beta_{[i]} h_{[p]}^2 \oint_{C(z)} \tan\theta \psi_{[p]} \frac{\partial^2 \psi_{[i]}}{\partial n^2} ds \pm \beta_{[p]} h_{[i]}^2 \oint_{C(z)} \tan\theta \psi_{[i]} \frac{\partial^2 \psi_{[p]}}{\partial n^2} ds}{2\sqrt{\beta_{[i]}\beta_{[p]}}(h_{[i]}^2 - h_{[p]}^2)} \tag{23}$$

where

ω = angular frequency
μ = permeability
ϵ = dielectric constant
θ = angle between the outward normal to $C(z)$ and the normal to the nonuniform waveguide (Fig. 2)
ds = an element of the $C(z)$ curve.

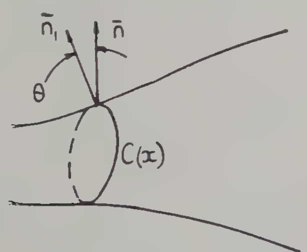

Fig. 2—Parameters used for the description of the nonuniform waveguide. $\bar{n}$—the outward normal to the boundary curve, $\bar{n}_1$—the outward normal to the nonuniform waveguide.

A few interesting conclusions may be drawn from the above Equations.

1) The transfer voltage coefficient from an E mode to an H mode is zero (15).

2) The transfer current coefficient from an H mode to an E mode is zero (15).

3) The S^+ matrix is skew-symmetric (10).

4) The S^- matrix is symmetric (10).

5) The backward coupling coefficient into the same mode is frequency independent (18), (19).

6) The coupling coefficients change very little with frequency, if it is not too near to the cut-off frequency (21)–(23).

7) The absolute values of the forward and backward coupling coefficients from an H mode into an E mode (or from an E mode into an H mode) are identical (22).

8) If on $C(z)$ either $\tan\theta$, or $\partial\psi_{[p]}/\partial s$ equal zero, there is no coupling between the H_p mode and any of the E modes. (For example no E modes are generated by changing the dimensions of the broad side of a rectangular waveguide, which supports an H_{0n} mode) (22).

9) The coupling of any one H mode to another (or any E mode to another) is larger the nearer their corresponding cut-off numbers are. This is only a rough rule, because the effect of the line integrals in (21) and (23) is not taken into account.

IV. An Approximate Solution of the Differential Equation System

We shall consider only such nonuniform waveguides in which the expected power conversion into the spurious modes is small by comparison with the power in the main mode. For gradual transitions, this is generally true. An exception arises however when a spurious mode has the same cut-off number as the main mode at each cross section. Excluding the latter case, we may assume that neither the spurious modes nor the reflection in the main mode have any effect on the forward propagation of the main mode. (This assumption was frequently

used in nonuniform transmission line theory[17] and led to the linearisation of the Riccatti differential equation.)

Thus we have to solve for $A_m^+(z)$ the following simple differential equation;

$$\frac{dA_m^+}{dz} = -j\beta_m A_m^+, \qquad A_m^+(0) = A_0, \tag{24}$$

whence

$$A_m^+(z) = A_0 \exp\left[-j\int_0^z \beta_m dz\right]. \tag{25}$$

We assume further that the backward traveling main mode and both the forward and backward travelling spurious modes are excited only by the main mode; *i.e.*, we neglect the interaction of the different spurious modes among themselves, and the interaction between a forward and backward travelling spurious mode. Because of the restriction (7a) the solution will be valid only for those modes which are above cut-off *everywhere* in the nonuniform waveguide.

Subject to the above approximations, the following differential equations can be written

$$\begin{aligned} &\frac{dA_m^-}{dz} - j\beta_m A_m^- = \left(S_{mm}^- - \frac{1}{2}\frac{d(\ln K_m)}{dz}\right)A_m^+ \\ &\frac{dA_i^+}{dz} + j\beta_i A_i^+ = S_{im}^+ A_m^+ \\ &\frac{dA_i^-}{dz} - j\beta_i A_i^- = S_{im}^- A_m^+. \end{aligned} \tag{26}$$

Taking into account the boundary conditions (11), the solutions of the differential equations are as follows;

$$A_m^-(0) = -\exp\left[-j\int_0^L \beta_m dz\right]\int_0^L \left(S_{mm}^- - \frac{1}{2}\frac{d(\ln K_m)}{dz}\right)\exp\left[-j2\int_0^z \beta_m dz\right]dz \tag{27}$$

$$\left.\begin{matrix} A_i^+(L) \\ A_i^-(0) \end{matrix}\right\} = \pm\exp\left[-j\int_0^L \beta_i dz\right]\int_0^L S_{im}^\pm \exp\left[-j\int_0^z (\beta_m \mp \beta_i)dz\right]dz. \tag{28}$$

The amplitudes of the forward and backward converted spurious modes have been computed recently by Katzenelenbaum,[11,12] using a different approach. The equations given in this paper are believed to be more accurate because no approximations were used in the determination of the coupling coefficients.

V. A Theorem on Sufficiently Gradual Tapers

If the equation of the surface of the nonuniform waveguide, $F(x, y, z) = 0$, is given, the functions $S_{im}^\pm(z)$, $\beta_i(z)$, $\beta_m(z)$ may be determined. Then subject to the validity of the approximations used in the previous Section, the amplitudes of the forward and backward travelling spurious mode i may be obtained from (28). Let us investigate how these amplitudes will change if the nonuniform waveguide is lengthened by a factor σ while its other dimensions are retained. The equation of the new nonuniform wave guide is

$$F\left(x, y, \frac{z}{\sigma}\right) = 0, \tag{29}$$

the coupling coefficient is

$$\frac{1}{\sigma} S_i^{m\pm}\left(\frac{z}{\sigma}\right), \tag{30}$$

the propagation coefficients are

$$\beta_i\left(\frac{z}{\sigma}\right) \quad \text{and} \quad \beta_m\left(\frac{z}{\sigma}\right), \tag{31}$$

and the amplitude of the spurious mode i is given as follows;

$$\left.\begin{matrix} |A_i^+(\sigma L)| \\ |A_i^-(0)| \end{matrix}\right\} = \left|\int_0^L S_{im}^\pm(t) \cdot \exp\left\{-j\sigma\int_0^t [\beta_m(t) \mp \beta_i(t)]dt\right\}dt\right|, \tag{32}$$

where $t = z/\sigma$ and L is the length of the original nonuniform waveguide.

Using a transformed form of the Riemann lemma, it may be easily shown that the amplitude of any spurious mode may be held below any predetermined level by choosing σ sufficiently large.[18] Hence, if a pure mode is incident at the input, the mode at the output may be made arbitrarily pure. Thus a sufficiently gradual nonuniform waveguide may be represented by a single nonuniform transmission line.

[17] F. Bolinder, "Fourier transforms in the theory of inhomogeneous transmission lines," *Trans. Roy. Inst. Tech.*, Stockholm, Sweden, no. 48, p. 84; 1951.

[18] This does not mean that by making the nonuniform waveguide longer it will be necessarily better.

Examples

For the first example, let us take a rectangular waveguide, with b its narrow wall a function of z, and compute the reflection of the H_{01} mode. Then

$$\frac{d(\ln K_{[01]})}{dz} = 0 \tag{33}$$

$$S^{-}_{[01][01]} = -\frac{1}{2}\frac{d(\ln b)}{dz} \tag{34}$$

where

$$A^{-}_{[01]} = \exp j\beta_{[01]}L \int_0^L \frac{d(\ln b)}{dz} \exp\left[-j2\beta_{[01]}z\right]dz. \tag{35}$$

Eq. (35) agrees with the result derived by ordinary transmission line theory, but an essential difference is implied.

By classical transmission line theory, the *only* reason for reflection is a change in impedance, and for that reason it has been assumed that the characteristic impedance of the rectangular waveguide (excited in the dominant mode) is proportional to its height. This assumption certainly led to a correct result, but it had to introduce the concept of characteristic impedance, which has a very limited scope in dealing with waveguides.

However, approaching the rectangular waveguide from the viewpoint of general nonuniform waveguide theory, it is obvious from (27) that even in first order approximation—reflections are due to *two* reasons: 1) change in wave impedance, and 2) backward coupling into the same mode.

Thus—in our interpretation—the reflection in the above rectangular waveguide is due to a backward coupling and not a change in impedance.

Let us take for the second example a circularly symmetrical taper, which connects two circular waveguides of different diameters. We shall compute the amplitude of the spurious modes H_{MN}, E_{MN} in waveguides G_1 and G_2, when waveguide G_1 is fed by an H_{mn} mode. The calculation applies only to modes above cut-off at every cross-section of the taper.

Substituting the necessary expressions into (28), we get the amplitudes of the spurious modes in the following form;

$$\left.\begin{matrix} A^{+}_{[MN]}(L) \\ A^{-}_{[MN]}(0) \end{matrix}\right\} = 0 \qquad \text{if } M \neq m. \tag{36}$$

$$\left.\begin{matrix} A^{+}_{[mN]}(L) \\ A^{-}_{[mN]}(0) \end{matrix}\right\} = \pm \exp\left[\mp j\int_0^L \beta_{[mN]}dz\right]\int_0^L S^{\pm}_{[mN][mn]} \cdot \exp\left[-j\int_0^z (\beta_{[mn]} \mp \beta_{[mN]})dz\right)dz; \quad n \neq N \tag{37}$$

where

$$S^{\pm}_{[mN][mn]} = \frac{\beta_{[mN]}\chi^2_{[mn]}(\chi^2_{[mN]} - m^2) \pm \beta_{[mn]}\chi^2_{[mN]}(\chi^2_{[mn]} - m^2)}{\beta_{[mN]}\beta_{[mn]}(\chi^2_{[mN]} - \chi^2_{[mn]})} \frac{d(\ln a)}{dz}. \tag{38}$$

$\chi_{[mn]}$—the nth root of the Bessel function $j_M'(x)$, a—the radius of the cross-section at z.

$$\left.\begin{matrix} A^{+}_{(MN)}(L) \\ A^{-}_{(MN)}(0) \end{matrix}\right\} = 0 \qquad \text{if } M \neq m \tag{39}$$

$$\left.\begin{matrix} A^{+}_{(mN)}(L) \\ A^{-}_{(mN)}(0) \end{matrix}\right\} = \pm \exp\left[\mp j\int_0^L \beta_{(mN)}dz\right]\int_0^L S^{\pm}_{(mN)[mn]} \cdot \exp\left[-j\int_0^z (\beta_{[mn]} \mp \beta_{(mN)})dz\right]dz \tag{40}$$

where

$$S^{\pm}_{(mN)[mn]} = \frac{k}{\sqrt{\beta_{[mn]}\beta_{(mH)}}} \frac{m}{\sqrt{\chi_{[mn]} - m^2}} \frac{d(\ln a)}{dz}. \tag{41}$$

The amplitudes of the forward and backward H_{mn} and E_{mn} modes are given in terms of integrals which can be evaluated by any one of the approximate integration methods when the shape of the taper is given.

VI. Conclusions

A differential equation system in terms of forward and backward traveling waves has been obtained for a general nonunform waveguide. The forward and backward coupling coefficients between the different modes have been given and some general conclusions have been drawn about their properties. Assuming that all the investigated modes are above cut-off at every cross-section of the nonuniform waveguide, and the change in axial direction is gradual, the differential equation system has been solved. The amplitudes of the spurious modes at the beginning and at the end of the nonuniform waveguide have been given in a closed form.

It has been proved that by making the nonuniform waveguide more and more gradual, the amplitudes of all the spurious modes tend to zero. Thus—assuming a pure incident mode—a sufficiently gradual nonuniform waveguide may be represented by a single nonuniform transmission line.

VII. Acknowledgment

The author wishes to thank Standard Telecommunication Laboratories Ltd. for permission to publish this paper.

A High Power Diplexing Filter*

LEO YOUNG† AND JOHN Q. OWEN‡

Summary—An L-band diplexing filter has been constructed with an estimated power-carrying capacity of 5 megw at atmospheric pressure (for a power safety factor of nearly four to one) and an insertion loss of less than 0.1 db.

The filter consists of two hybrid junctions and two high pass waveguide sections, which are arranged as in a balanced duplexer, with the "TR-tubes" replaced by the high-pass sections.

In the upper frequency band, the input VSWR is better than 1.10 over a seven and one-half per cent bandwidth, but deteriorates only slightly over a larger bandwidth. In the lower frequency band, the input VSWR is better than 1.32 over a 13 per cent bandwidth. The separation interval between these two bands is approximately 10 per cent between their nearest frequencies.

Introduction

DIPLEXING filters do not usually require high power handling capacity, since applications are more numerous in communication than in radar systems. Thus, in one such filter[1] in 2 by 1-inch waveguide, voltage breakdown was expected to occur at a power level somewhere in excess of 500 watts.

The *L*-band filter reported on here was required to pass up to 5 megw at atmospheric pressure in the upper passband (1250 to 1350 mc), but only relatively low power (up to 20 kw) in the lower passband (990 to 1130 mc), although the design method could readily be extended to handle much higher powers in the lower passband also. The filter insertion loss was less than 0.1 db. The other principal performance characteristics are summarized below.

VSWR at upper passband input:	1.10 maximum
VSWR at lower passband input:	1.32 maximum
Cross-coupling in upper passband:	36 db minimum
Cross-coupling in lower passband:	at least 60 db.

The cross-coupling figures were measured using a matched termination at the common output; the effect of a mismatched termination on the cross-coupling is described in a later section.

Design Considerations

The high power capacity, low VSWR, and low insertion loss requirements led to the choice of the "balanced" or "branching"[2] filter structure shown schematically in Fig. 1. This depends on the properties of the two hybrid junctions and the two high pass waveguides.[3,4] The principle of operation is similar to that of a balanced duplexer, with the high pass waveguides replacing the TR-tubes. The performance is determined largely by the match of the two magic tee hybrids and the four identical matching transformers into and out of the two high pass waveguides.

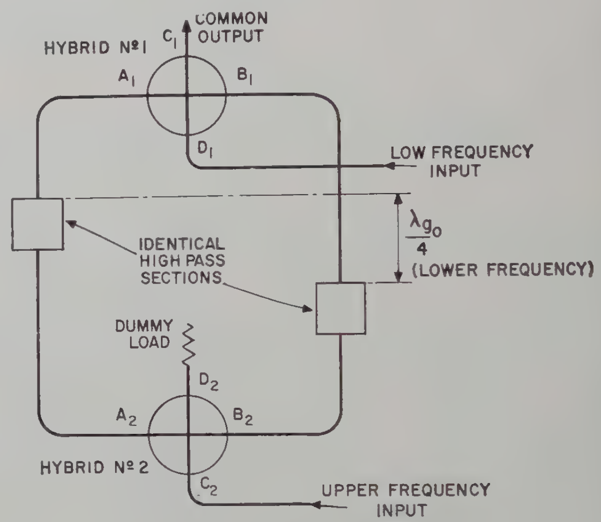

Fig. 1—Filter schematic.

Operation of the Filter

The operation of the filter is readily understood when certain assumptions are made:

1) The hybrid junctions are perfectly matched and balanced.
2) The identical high pass waveguides and associated transformers are perfect and lossless.

In the upper frequency band, a signal incident in arm C_2 of hybrid 2 (Fig. 1) divides equally between arms A_2 and B_2, passes through the perfect filters, and recombines in the hybrid 1, emerging from arm C_1. In this particular case, the operation would be the same from either end of the filter.

In the lower frequency band, a signal incident in arm D_1 of the hybrid 1 divides equally between arms A_1 and B_1. If the separation of the now cut-off waveguides were exactly one quarter wavelength at this frequency, then one component after reflection would travel one-half wavelength further than the other. This relative

* Manuscript received by the PGMTT, January 23, 1959; revised manuscript received March 31, 1959. This work was part of a project sponsored by the Rome Air Development Center.

† Westinghouse Electric Corp., Electronics Div., Baltimore, Md.
‡ Raytheon Mfg. Co. Waltham, Mass.

[1] M. E. Breese and S. B. Cohn, "Diplexing filters," 1954 IRE Convention Record, vol. 2, pt. 8, Communications and Microwave, pp. 125–133.

[2] W. D. Lewis and L. C. Tillotson, "A Non-reflecting branching filter for microwaves," *Bell Sys. Tech. J.*, vol. 27, pp. 83–95; January, 1948. (Bell Telephone System Monograph B-1520.)

[3] Compare G. L. Ragan, "Microwave Transmission Circuits," McGraw-Hill Book Co., Inc., New York, N. Y., M.I.T. Rad. Lab. Series, vol. 9, p. 644 and p. 706; 1948.

[4] A different application of the cut-off effect to filters is described by P. A. Rizzi, "Microwave filters utilizing the cut-off effect," IRE Trans. on Microwave Theory and Techniques, vol. MTT-4, pp. 36–40; January, 1956.

phase change of 180° is such that the signal now emerges from arm C_1. Thus with perfect components, there is no cross-coupling between input[5] ports C_2 and D_1.

Practical Limitations

In practice, however, the hybrids are not perfectly matched or balanced, nor are the high-pass sections perfectly matched in the upper frequency band. Such reflections contribute directly to cross-coupling from the upper to the lower frequency band. Consider again a signal in the upper band, incident in arm C_2. There is now some reflection from the high pass sections and, as the spacing is no longer a quarter wavelength at this frequency, the phase difference is no longer 180°. The reflected waves then couple to both arms C_2 and D_2, as well as being partially reflected back again into the imperfectly matched arms A_2 and B_2. Most of the power is coupled into arm D_2, where it would be completely absorbed if the dummy load on that arm were perfect; in practice, there is further reflection. The reflected waves are finally transmitted to the (lower frequency band) input arm D_1 with little further attenuation, causing cross-coupling between the two inputs at frequencies in the upper band.[6]

The cross-coupling in the lower frequency band presents few problems as the attenuation obtained from the 5 by 3-inch high pass (and now cut-off) waveguide is 40 db at 1130 mc, and is greater at lower frequencies. In addition, because of the symmetry of the filter, there is little direct coupling of the residual energy passing through the cut-off waveguides.

Description of the Filter

A cross-section of the filter is shown in Fig. 2. There are three terminal ports. The common output is 8 by 2-inch waveguide; the higher frequency, higher power input is $6\frac{1}{2}$ by $3\frac{1}{4}$-inch waveguide, and the lower frequency, lower power, input is $\frac{7}{8}$-inch rigid coaxial line. All waveguide parts are made of aluminum.

High Pass Waveguide Section

The choice of five inch-wide rectangular waveguide for the filter, having a cut-off frequency of 1180 mc, ensures adequate attenuation at 1130 megacycles. A length of 26 inches gives 40 db at this frequency and a cross-section of 5 by 3 inches is adequate to transmit the peak power. The most difficult part of the development was the design of transformers effecting a good impedance match between the 5 by 3-inch waveguide and the 8 by 2-inch waveguide of the hybrids (Fig. 2) in the transmission band. The characteristic impedance of the 5 by 3-inch waveguide is appreciably larger than that of the 8 by 2-inch waveguide and the impedance ratio increases rapidly as cut-off is approached in the 5 by 3-inch waveguide.

The transformer was designed in two parts. One was an E-plane two-section quarter-wave transformer[7–10] and the other was a linear taper with cross-sections of constant aspect ratio. The E-plane quarter wave transformer takes the waveguide from 8 by 2-inch to 8 by 4.8-inch cross section; the maximum measured VSWR in the required passband was 1.03, which is close to the measuring accuracy of the test equipment.[11] The linear taper from 8 by 4.8-inch to 5 by 3-inch cross section was made 18 inches long and uses one inductive matching post at the narrow end; its VSWR over the transmission band is better than 1.18. This completes the transformation from 8 by 2-inch to 5 by 3-inch waveguide.

The complete high pass section, consisting of the 5 by 3-inch waveguide and associated transformers into 8 by 2-inch waveguides at each end, had a VSWR of better than 1.22 over the transmission band.

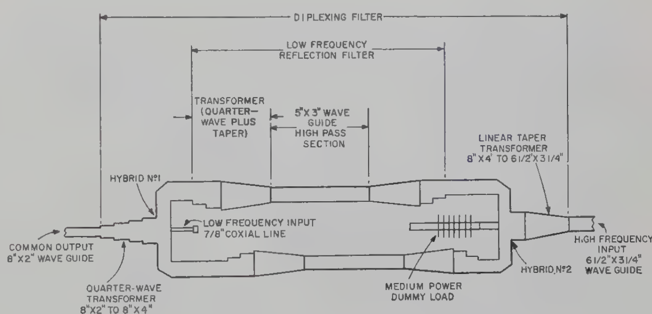

Fig. 2—*E*-plane section of diplexing filter.

Hybrids

The hybrids need not be exactly alike as their electrical requirements differ. Hybrid 1 must be well matched to the 8 by 2-inch transmission line leading to the common output arm C_1. Arm D_1, however, need only be well matched in the lower frequency band. The balance must be as good as possible in both bands. Hybrid 2 must be well matched to the $6\frac{1}{2}$ by $3\frac{1}{4}$-inch waveguide in the upper frequency band, and its arm D_2 requires good matching in the upper band. Both hybrids consist of

[5] The two separate frequency ports will be referred to as inputs, for convenience. The combination port will therefore be referred to as the output. Obviously the terms input and output could be interchanged.

[6] It should be possible to reduce this cross-coupling by using a mismatched load on arm D_2, which would cause destructive interference between these waves. This, however, was not attempted.

[7] S. B. Cohn, "Optimum design of stepped transmission-line transformers," IRE Trans. on Microwave Theory and Techniques, vol. MTT-3, pp. 179–185; April, 1955.

[8] R. E. Collin, "Theory and design of wide-band multisection quarter-wave transformers," Proc. IRE, vol. 43, pp. 179–185; February, 1955.

[9] H. J. Riblet, "General synthesis of quarter-wave impedance transformers," IRE Trans. on Microwave Theory and Techniques, vol. MTT-5, pp. 36–43; January, 1957.

[10] Leo Young, "Tables for cascaded homogeneous transformers," IRE Trans. on Microwave Theory and Techniques, vol. MTT-7, pp. 233–237; April, 1959.

[11] It can be shown theoretically that the VSWR of a two-section quarter-wave transformer of impedance ratio 2.4:1 can be made better than 1.01 over a bandwidth of up to 20 per cent.

the same basic unit, an E-plane T-junction with an 8 by 4-inch series arm, and two 8 by 2-inch colinear arms (Fig. 3). By a suitable choice of the height h of the wedge, a good match was obtained from arm C to arms A and B over both bands. The shunt arm is introduced through a hole in the center of the wedge in the form of a probe coupling to a $\frac{7}{8}$-inch rigid coaxial line.

This type of hybrid was chosen because of the inherent balance given by mechanical symmetry and because the impedance matching parameters of the series and shunt arms are almost independent. The cross bar was introduced primarily to give adequate mechanical support and to ensure alignment of the probe.

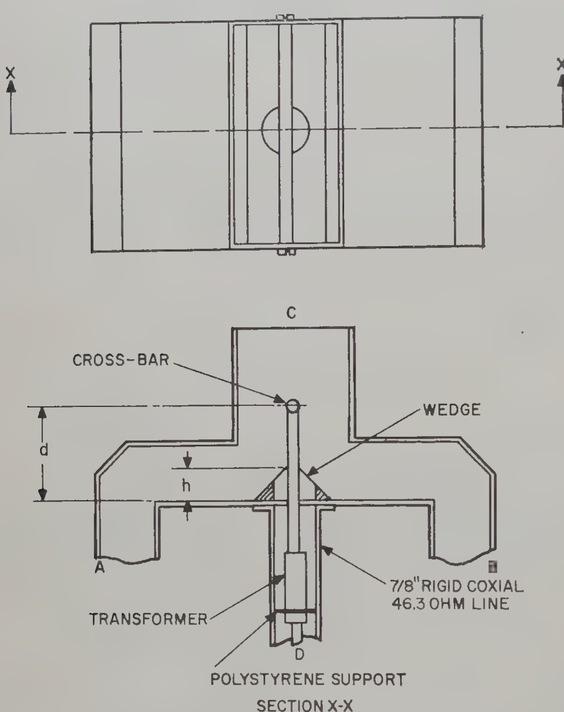

Fig. 3—Hybrid junction.

The VSWR into arm C of each hybrid is better than 1.02 over the lower frequency band, and better than 1.08 over the upper frequency band.

Arm D_1 was matched in the lower frequency band. A single quarter-wave transformer in the $\frac{7}{8}$-inch coaxial line (Fig. 3) and the height d of the probe were adjusted alternately to give a final VSWR better than 1.41.

Arm D_2 was matched in the upper frequency band. It is required to transmit efficiently to the dummy load that portion of the power which after reflection from the imperfectly matched high pass sections does not couple to arm C_2. Therefore the transformer in the coaxial line and the height d of the probe were together adjusted to give a low VSWR in the upper band looking into arm D_2, with matched dummy loads in arms A_2 and B_2. This VSWR was better than 1.62.

Terminal Transformers

A good transformer was required to match the 8 by 2-inch line to the 8 by 4-inch input to hybrid 1. In terms of guide wavelength, the bandwidth was 57 per cent, as both frequency bands use this transformer. A theoretical design[7–10] was calculated using a three-section quarter-wave transformer. The measured VSWR did not exceed 1.03 in the combined band.[12]

At input arm C_2 of the filter, a linear taper, 9.2 inches long, was used from 8 by 4-inch to $6\frac{1}{2}$ by $3\frac{1}{4}$-inch waveguide. The VSWR did not exceed 1.02 in the upper frequency band.

VSWR of Dummy Load

The medium high power dummy load on arm D_2 had a VSWR not exceeding 1.18 in the upper frequency band.

Over-all Performance

The principal performance characteristics of the filter have already been summarized in the Introduction.

VSWR

Fig. 4 shows VSWR against frequency plots at the two separate frequency inputs, with a matched termination on the common output.

Cross-coupling

Fig. 5 shows the cross-coupling in the upper frequency band as a function of frequency. A similar curve for the lower band could not be plotted as the measuring equipment readings were at the noise level, which indicated better than 60 db cross-coupling.

The effect of load mismatch on cross-coupling was investigated at 1260, 1290, and 1320 mc. Various sliding mismatches up to 2.1 in VSWR were connected to the output arm, and the worst cross-coupling at these frequencies remained better than 30 db (compared with 36 db for a matched load, shown in Fig. 5).

Insertion Loss

The insertion loss was too small to measure exactly. It is probably less than 0.05 db over most of the upper frequency band, and probably only slightly more in the lower frequency band.

High Power Carrying Capacity

No high power tests were conducted owing to lack of adequate test equipment. In the upper frequency band, the weakest section is probably the 5 by 3-inch waveguide which cuts off at 1180 mc. Assuming a maximum voltage[13] of 30,000 volts/cm, and a frequency of 1250

[12] The theoretical optimum design for a three-section quarter-wave transformer of impedance ratio 2:1 and of 57 per cent bandwidth yields a maximum VSWR of 1.02.

[13] G. L. Ragan, *loc. cit.*, p. 191.

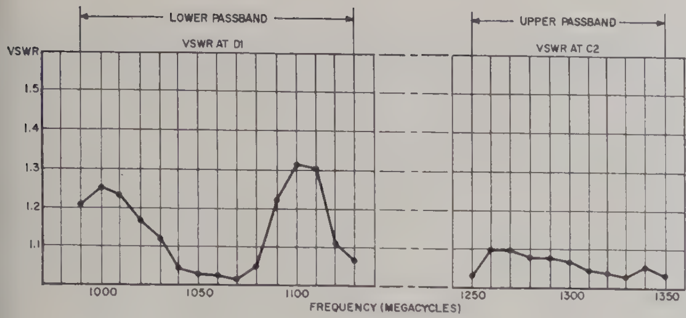

Fig. 4—Input VSWR of filter.

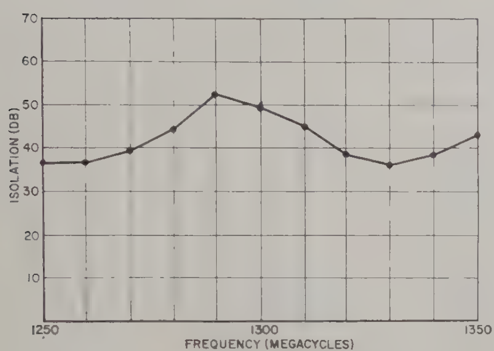

Fig. 5—Isolation in upper frequency band.

mc, the maximum power before voltage breakdown occurs at atmospheric pressure would be 18 megw. With a power safety factor of four to one, the maximum safe power is then $4\frac{1}{2}$ megw.

In the lower frequency band, the maximum power is determined by the $\frac{7}{8}$-inch coaxial line and connector; it should be over 40 kw in the present design, which uses a polystyrene bead support. If there were a requirement for high power capacity, an H-plane waveguide arm[14] could be used in place of the coaxial line, or the magic tee could be replaced by a short-slot[15] or a multi-slot[16] or a branch-guide directional coupler.[17,18]

[14] Patricia A. Loth, "Recent advances in waveguide hybrid junctions," IRE Trans. on Microwave Theory and Techniques, vol. MTT-4, pp. 268–271; October, 1956.

[15] H. J. Riblet, "Short slot hybrid junction," Proc. IRE, vol. 40, pp. 180–184; February, 1952.

[16] H. J. Riblet and T. S. Saad, "A new type of waveguide directional coupler," Proc. IRE, vol. 36, pp. 61–64; January, 1948.

[17] Leo Young, "Branch guide directional couplers," *Proc. Natl. Elec. Conf.*, vol. 12, pp. 723–732; Chicago, 1956.

[18] P. D. Lomer and J. W. Crompton, "A new form of hybrid junction for microwave frequencies," *Proc. IEE*, vol. 104, pt. B, pp. 261–263; May, 1957, and *Proc. IEE*, vol. 104, pt. B, p. 586; November, 1957.

VSWR Over Extended Band

The input VSWR was also measured from 1230 to 1370 mc and found to be better than 1.15. The performance of the filter may be expected to deteriorate only slightly over this extended band. The VSWR was found to remain below 1.20 up to 1400 mc, and below 1.45 up to 1560 mc, which suggests that it is an inherently more broad-band device than the present application calls for.

Conclusion

A diplexing filter with high power capacity, low insertion loss, and low VSWR, has been described. The isolation in the lower frequency band can be made as large as desired by making the cut-off waveguide sections sufficiently long.

Improved performance over conventional filters has been obtained by the use of a "balanced" filter, which is a relatively bulky and heavy structure, and incorporates a dummy load to reduce cross-coupling. A photograph of the filter is reproduced in Fig. 6.

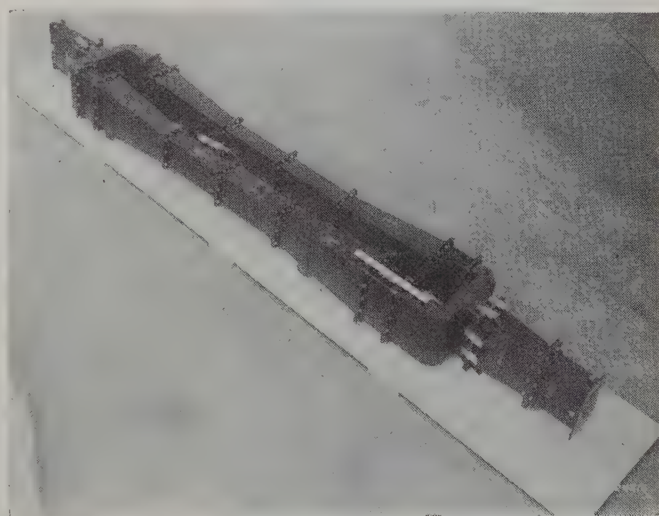
Fig. 6—Over-all view of the filter, with 12-inch rule in lower right.

Acknowledgment

This type of filter was originally proposed by C. C. Jones in 1952. The authors also wish to acknowledge the assistance of G. Valenzuela, who carried out many of the measurements and design calculations.

Correspondence

End Plate Modification of X-Band TE_{011} Cavity Resonators*

In the application of microwave refractometers,[1,2] the sampling cavity consists of a right circular cylinder whose parallel faces are partially opened to permit air flow (See Fig. 1). The ambient air is aspirated through the cavity, and the instrument measures a weighted average of the index of the air contained at any time within the cavity.

Fig. 1—Right cylindrical resonant cavity with open end plates.

In the interests of rapid response and simplification of turbulence considerations, attempts have been made to determine the effects of opening up the sampling cavity end plates. This has the immediate effect of reducing response time, but also impairs the electrical characteristics of the cavity by reducing its Q. This correspondence describes some experiments into the effects of different end plate configurations on the Q. Some earlier work on this problem has been reported by Adey.[3]

The general design of the end plates constructed is shown in Fig. 2, and they were used on a right cylindrical cavity barrel (number 1, Table I) of dimensions which gave it, with solid end plates, a resonant frequency of about 9,340 mc and a Q of 11,000. Five such sets of end plates of different ring radii and ring thickness were used, the total end plate area removed being about 90 per cent in each instance. All had the ring offset into the cavity barrel. With none of these end plate patterns was a Q greater than 5000 achieved.

To try to reduce the excessive fringing losses which seemed to be indicated by these very low Q values, another series of end plates was made having the ring flush with the inside surface of the end plate and extending *outward* from the barrel. It was believed that these protruding rings, acting as circular guides below cutoff, would diminish the losses due to external fields. To maintain the resonant frequency at about the same level, a new barrel was constructed, (number 2, Table I) dimensionally changed to keep the frequency at 9,350 mc in spite of the effective lengthening which resulted from inversion of the ring position, and three new sets of end plates of differing ring radii and ring length were tried thereon. To investigate the effect of ring length, each ring of these sets was originally made 0.75 inch long. They were then shortened in 0.05 inch steps and the Q and frequency noted during the shortening process. The frequency varied only a few mc throughout, but the Q, after showing little variation during the reduction of ring length from 0.75 inch to 0.5 inch fell rapidly as the ring length was reduced below 0.5 inch. On this barrel, the open end plates with the longer rings gave Q values for the cavity ranging from 7000 to 9000.

The data obtained from the second cavity, described in the preceding paragraph, indicated that a loss of about 100 mc in the calculated frequency was inherent in the use of the open type of end plate. Consequently, a third barrel (number 3, Table I) was fabricated of brass, the dimensions of which, using this criterion, would give it a resonant frequency of about 9,400 mc. It was further altered by adjusting the value of radius to

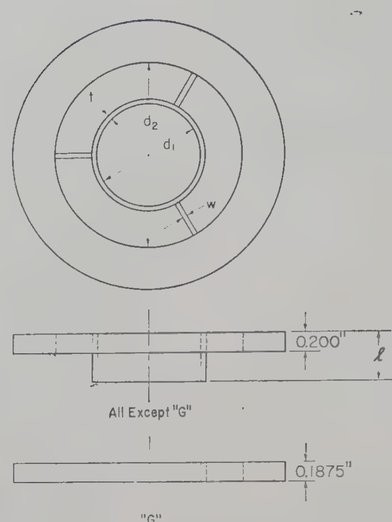

Fig. 2—General drawing of open end plates; end view at top, side views at bottom.

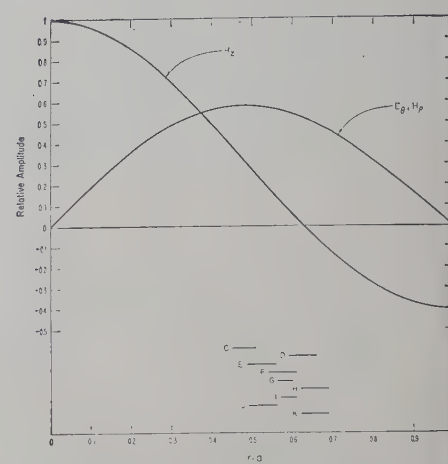

Fig. 3—Relative radial location of boundary surfaces of central ring of end plate in experimental open cavities.

TABLE I

CAVITY BARREL DIMENSIONS (INCHES)

Barrel number	a Inside diameter	b Length	c Outside diameter	d Iris thickness (At thinnest point)	e Depth of counter bores	f Iris diameter
1	1.905	1.653	2.750	0.030	round 0.135 rectangular 0.142	0.25
2	1.670	1.625	2.750	0.030	0.242 0.244	0.25
3	1.635	1.650	2.410	0.060	0	0.25

TABLE II

DIMENSIONS, FREQUENCY AND Q OF VARIOUS EXPERIMENTAL END PLATE PATTERNS

Code Designation	Dimensions (inches) See Figure 2: t width central ring	d_1 I.D. central ring	w width of struts	d_2 I.D. sup ring	l length central ring	Cavity barrel number	f_0 mc	Q	Per cent end area open
C	1/16	0.852	1/16	1.90	0.5	1	8,951	3,000	90.6
D	1/16	1.125	1/16	1.90	0.5	1	8,953	4,080	89.6
E	1/16	0.935	1/16	1.90	0.5	1	9,021	4,920	90.3
F	1/16	1.030	1/16	1.90	0.5	1	8,977	4,688	90.0
G	1/32	0.935	1/16	1.67	0.188	2	9,237	2,340	92.6
H	1/16	1.031	1/16	1.67	0.5	2	9,233	8,817	88
I	1/32	1.094	1/16	1.90	0.5	1	8,961	3,815	93.6
J	1/16	0.814	1/16	1.67	0.55	2	9,254	7,416	89
K	1/16	1.007	1/16	1.635	0.448	3	9,381	7,720	92.6
109 A and B	∼0.5	0.500	∼1/4	1.82	A = 0.487 B = 0.456	1	8,974	9,031	21.4
Solid	—	—	—	—	—	2	9,345	11,000	0

* Received by the PGMTT, September 22, 1958; revised manuscript received, January 27, 1959.

[1] G. Birnbaum, "A recording microwave refractometer," *Rev. Sci. Instr.*, vol. 6, pp. 169–171; February, 1950.

[2] C. M. Crain, "An airborne microwave refractometer," *Rev. Sci. Instr.*, vol. 23, pp. 143–151; April, 1952.

[3] A. W. Adey, "Microwave refractometer cavity design," *Can. J. Tech.*, vol. 34, pp. 519–521; March, 1957.

length ratio to about 0.5 (optimum Q for a closed cavity) and by changing the exterior design to eliminate the usual counterbores through which the coupling irises were drilled, by grinding off the parallel flats till the iris lips at their thinnest points were only 0.60 inch thick. The final gross dimensions selected were:

Outside diameter	2.410 inches
Length	1.650 inches
Inside diameter	1.635 inches.

The conductivity of this cavity was improved with a rubbed-on silver solution, and a set of open end plates was fabricated for it, similar in design to the series used on the second barrel described above, but with the pertinent dimensions so changed as to locate the central ring in the same region of the fields of the new cavity as was used to obtain the highest Q in cavity number 2. The length of each ring was 0.448 inch, and they left the cavity end 92.6 per cent open to air flow. Tested on the new cavity barrel, the resonant frequency was about 9400 mc and the Q about 7700.

To summarize, the series of experiments outlined above show that right cylindrical resonant cavities may be constructed having values of Q of about 8000 when more than 92 per cent of the area of the parallel boundaries has been removed.

The conducting surfaces of these open end plates must be located with some accuracy if the best results are to be achieved. For those consisting of a central ring which is offset into the cavity barrel, the optimum Q is obtained when the ring is slightly larger than the locus (in a closed cavity) of maximum intensity of the E_θ component of the electromagnetic field; for those consisting of a central ring extending outward from the cavity, the location of the ring at the zero intensity locus (in a closed cavity) of the H_z component of the field yields the maximum Q. These results are summarized graphically in Fig. 3 and Table II.

M. C. Thompson, Jr.
F. E. Freethey
D. M. Waters
Radio Prop. Engrg. Div.
Nat. Bur. of Standards
Boulder, Colo.

Design of Open-Ended Microwave Resonant Cavities*

This paper summarizes a Ph.D. dissertation[1] on the design and analysis of open-ended microwave cavities. The study was motivated by the need for a cavity with a high measure of quality, Q, through which an unobstructed flow of gases or particulate matter could be obtained. Used in connection with the Crain refractometer, instantaneous measurements of the refractive index of the material in the cavity can be made. Measurements utilizing his technique but with other types of cavities have previously been made in order to study the dielectric properties of smoke and other aerosols.[2]

In the atmospheric refractometers developed by Crain[3,4] and Birnbaum,[5] provisions were made for permitting the flow of air and other gases through the sampling cavities by means of holes drilled in the end plates. The holes were located in regions of small current flow. Adey[6] and Thompson and Freethey[7] have extended this study and have obtained a considerable increase in the size of openings in the end walls of cylindrical cavities.

In the research described in this paper, cavities are terminated in short sections partitioned so that each subdivision is a waveguide operating at a frequency below cut-off. Although this technique may in some cases result in field configurations somewhat similar to those existing with the perforations located on the basis of current minima, it offers a fresh approach to the design of the cavities.

Two cavities have been considered. One is made from a rectangular waveguide with a thin dividing strip across the narrow dimension of the guide. The other is a cylinder terminated with sections which have thin dividing strips both concentric to the cylinder and radially outward.

The purpose of this research was to examine the basic principles involved and not to produce a finished cavity. For this reason, the prototypes were made from the most readily available materials. Improvement in the temperature characteristics could be obtained by other choices of materials.

To eliminate the end plates of a cavity as a physical barrier to free passage of material, it is required that they be replaced by some other type of termination which will satisfactorily perform the same function. Initial experiments used tuned stubs that were intended to cause a totally reflecting termination. This scheme was abandoned, however, because the problems of tuning the stubs, and at the same time having them correctly separated, were such as to make proper operation very difficult. Instead, terminations were used which involved very thin sheets of conducting material placed parallel to the axis of the cavity. These terminations present very little interruption to the smooth flow of material through the cavity.

The terminations used are so designed that they divide the waveguide which forms the body of the cavity into two or more smaller waveguides such that these smaller waveguides are "beyond cutoff" for the frequency of operation of the cavity. Two such terminations, placed approximately an integral number of half-wavelengths apart, serve the same function as the shorting end plates normally used. Actually, since the terminations are not short circuits but rather are reactive devices, they must be placed slightly closer together than would solid end plates for operation at the same frequency.

Two types of cavities using the general type of termination described in the previous section have been fabricated and tested. The first of these, rectangular in cross section, is shown in Fig. 1. It consists of a short piece of standard size brass waveguide (WR90) approximately one-half wavelength long between terminations. The terminations are made of 0.015 inch brass sheet material. The second, cylindrical in cross section, is shown in Fig. 2. It consists of commercial size brass tubing and, like the rectangular, is approximately one-half wavelength between terminations. The terminations are fabricated from a combination of 0.015 inch brass sheet material and approximately 1 inch tubing with 0.032 inch wall thickness. It is believed that the thickness of all of these terminations could be reduced without seriously affecting the electrical characteristics of the cavities if fabrication could be conveniently accomplished. However, since all parts are silver plated, all

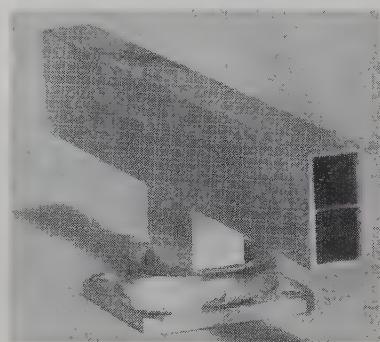

Fig. 1—Photograph of rectangular cavity.

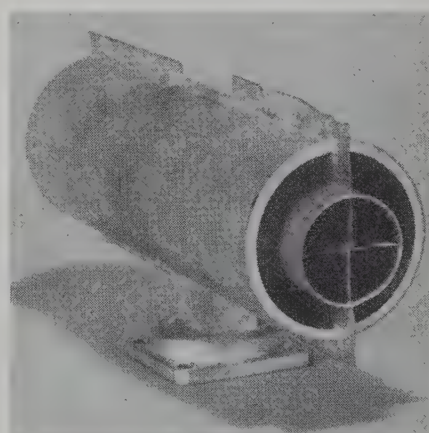

Fig. 2—Photograph of cylindrical cavity.

* Received by the PGMTT, December 8, 1958; revised manuscript received February 9, 1959.

[1] Donald C. Thorn, "Design of open-ended resonant cavity," Ph.D. dissertation, The University of Texas, Austin; August, 1958 (available from University Microfilms, Inc., Ann Arbor, Mich.).

[2] C. M. Crain, J. E. Boggs, and D. C. Thorn, "Refractive index measurements of smokes and aerosols," IRE Trans. on Instrumentation, vol. I-6, pp. 246–251; December, 1957.

[3] C. M. Crain, "Dielectric constants at water vapor and atmospheric air at a frequency of 9,340 megacycles," *Phys. Rev.*, vol. 74, pp. 691–693, September, 1948.

[4] C. M. Crain, "Apparatus for recording fluctuations in the refraction index of the atmosphere," *Rev. Sci. Instr.*, vol. 24, pp. 456–457; May, 1950.

[5] G. Birnbaum, "A recording microwave refractometer," pp. 169–176; February, 1950.

[6] Albert W. Adey, "Microwave refractometer cavity design," pp. 519–521; 1957.

[7] M. C. Thompson and F. E. Freethey, "Effects of End-Plate Modification on Q at X-Band Cylindrical TE_{011} Resonant Cavities," Natl. Bur. of Standards, Rep. No. 5049. Boulder, Colo.

junctions are made with silver solder. The temperature necessary for silver soldering limits the thinness of material to be worked. In both type cavities, the sections with the terminations were chosen long enough so that the fields in these sections of "beyond cutoff" waveguide will be attenuated adequately and hence will not radiate. Some radiation from the cylindrical cavity occurred because the number of cross-plates was insufficient to prevent the propagation of modes in the outer portion.

Each of the cavities of both types considered was originally fabricated with the terminations left unsoldered and held in place only by friction (increased by adding external clamps). This was done so that the cavities might be tuned to a reasonable frequency by sliding the terminations in and out. The frequency of each design was near 9435 mcps, the nominal frequency of Crain refractometer measuring cavities.

After the terminations were properly placed and soldered, measurements of the voltage standing wave ratio (VSWR) due to cavity input impedance were made as a function of frequency. Since there is no convenient means of calculating the size of feed hole which gives critical coupling, feed holes were cut small and gradually enlarged until the plot of VSWR vs frequency showed a minimum value near unity.

Following the technique given by Montgomery,[8] the unloaded Q of these cavities was calculated to be 3420 for the rectangular cavity and 2310 for the cylindrical cavity.

The next pertinent test was to determine the relation between cavity Q and the axial length of the terminations. When the length of termination sections on the rectangular cavities was decreased by increments, it was found that the Q was essentially constant for terminating section lengths greater than two inches but dropped rapidly as the length of the stub was decreased below two inches.

Since physical dimensions, as well as index of refraction, determine the resonant frequency of a cavity, the coefficient of thermal expansion of the material of the cavity will cause an erroneous indication of change in index unless the proper temperature correction is known. A possible means of temperature compensation involves the use of a material with a larger temperature coefficient for the divider in the terminating stub than for the material in the body of the cavity, but extensive efforts in this direction were not carried out.

The rectangular cavity must be considered a satisfactory, working piece of equipment with sufficiently good characteristics to make it acceptable for its designed function as a governing cavity for a Pound oscillator. The cross sectional obstruction due to the termination is only 1.66 per cent of the waveguide cross section area. With sufficient effort, it should be possible to temperature compensate such a cavity to any degree required.

D. C. Thorn
A. W. Straiton
Elec. Eng. Res. Lab.
Univ. of Texas
Austin, Tex.

[8] C. G. Montgomery, ed., "Technique of Microwave Measurements," Mass. Inst. Tech., vol. 11, McGraw-Hill Book Co., Inc., New York, N. Y.

Transverse Electric Field Distributions in Ferrite Loaded Waveguides*

The transverse electric field distribution in dielectric and ferrite loaded waveguides has been measured by several investigators.[1,2] Knowledge of the actual field distribution within the waveguide is needed in the design of field displacement isolators, phase-shifters, and similar microwave devices. In making such measurements, care must be taken to choose lengths of samples of ferrites or dielectrics sufficiently long enough so that the distribution in one transverse plane will be the same (except for an attenuation effect) as in another transverse plane.

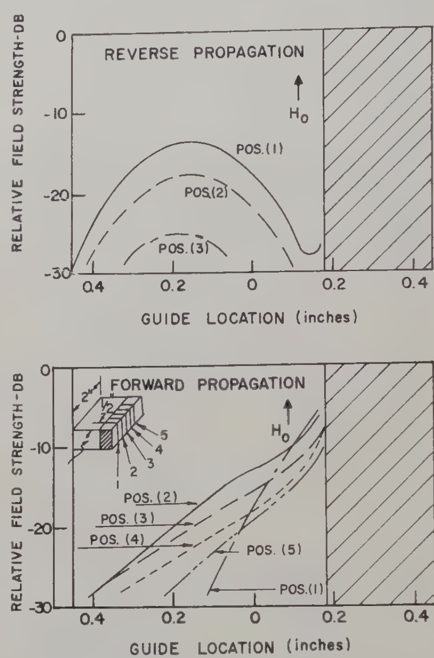

Fig. 1—Electric field distribution at 0.250 inch intervals along ferrite slab 0.259 inch thick with an external dc field of 2000 gauss.

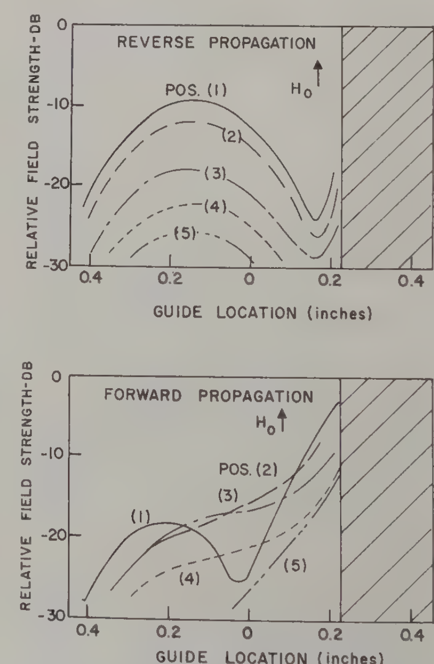

Fig. 2—Electric field distribution at 0.250 inch intervals along ferrite slab 0.227 inch thick with $H_0=2000$ gauss.

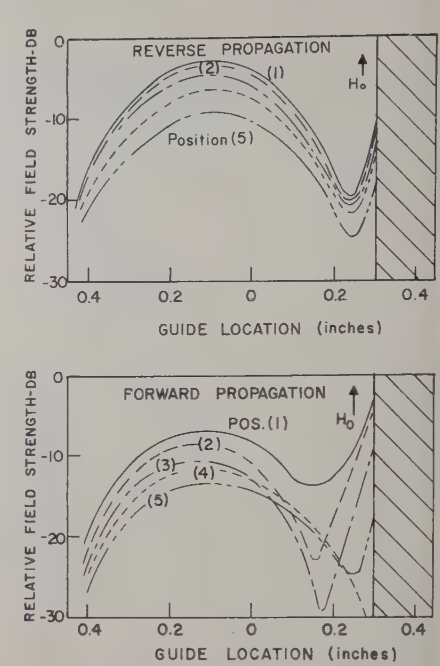

Fig. 3—Electric field distribution at 0.250 inch intervals along ferrite slab 0.145 inch thick with $H_0=2000$ gauss.

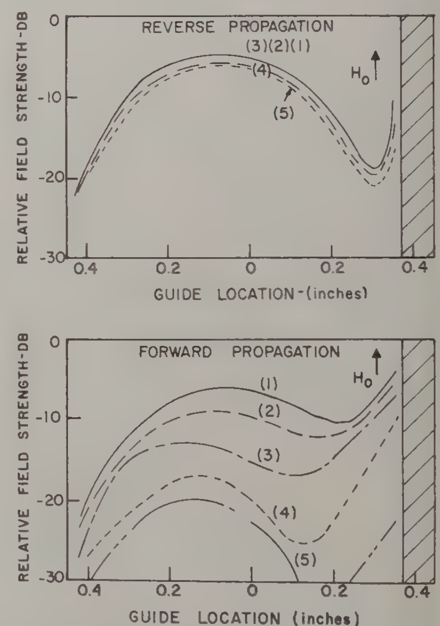

Fig. 4—Electric field distribution at 0.250 inch interval along ferrite slab 0.081 inch thick with $H_0=2000$ gauss.

To show that variations in distribution are indeed present, measurements were made with a transverse electric field detector[1,2] at various positions along a ferrite slab (see the sketch in the lower half of Fig. 1). As the incident wave penetrates from

* Received by the PGMTT, February 13, 1959. This work was supported in part by the Office of Naval Research under Contract No. N7onr-29529.

[1] R. L. Comstock, D. J. Angelakos and A. Johnson. "Determination of Fields in a Ferrite-Loaded Waveguide," Elec. Res. Lab., Univ. of California, Series 60, Issue 186; 1957.

[2] T. M. Straus, 1958 IRE Wescon Convention Record, pt. I.

the empty waveguide into the ferrite loaded region of the waveguide, its transverse electric field distribution becomes different. In particular, Fig. 2 illustrates the effect of a finite sample. The transverse electric field distribution measured a short distance after the incident wave has entered the ferrite section (marked Position 1) indicates one mode-type or combination of modes whereas further on along the sample, the transverse electric field distribution (marked Position 2) is of another mode-type. Figs. 1–4 are for various thicknesses of ferrite slab. The frequency is 9.275 kmc.

D. J. Angelakos
Elec. Engrg. Dept.
Univ. of Calif.
Berkeley 4, Calif.

Feeding RF Power From a Self-Excited, Pulsed Source into a High-Q Resonant Load*

A problem frequently arising in microwave electronics is the feeding of pulsed power from a self-excited source into a high-Q resonant load. A typical example is the one of feeding power from a pulsed magnetron into a high-Q microwave cavity[1] such as that used in a linear accelerator. In the past, it has been customary to use a stabilizing load in a series tee system[2] which results in approximately half the magnetron power being fed into the high-Q cavity.

In this letter, a high-power ferrite isolator system is described which is capable of feeding 78 per cent of the available power from a 5586, S-band megawatt magnetron into a microwave cavity having an unloaded Q of 14,400. The performance of this ferrite system is compared to the series tee and shown to result in 38 per cent increase in power with no reduction in stability characteristics.

The experimental setup used is shown in Fig. 1. The microwave power from the 5586, S-band magnetron is fed through a coax-to-waveguide transition, then through a Cascade S-159 isolator and phase shifter into a TM_{010} mode cavity. The cavity was resonant at 2840 mc. It had an unloaded Q of 14,400, a shunt resistance of 3.32 megohms, and a VSWR on resonance of 1.2 (coupling greater than critical).

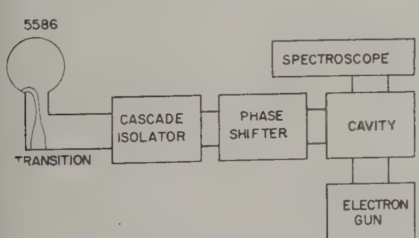

Fig. 1.

The power delivered by the magnetron to the cavity was determined by accelerating a 20 kv electron beam injected into the system by means of an electron gun and then measuring the exit electron momentum with a spectroscope. The electron momentum is determined by the peak axial field which in turn is determined by the power delivered to the cavity.

Input power to the magnetron was adjusted so that, for a magnetic field of 2650 gauss, 50 amperes peak anode current was delivered for each of the load conditions. The voltage pulse was obtained from a 3-μsec line-type modulator operating at 60 cps repetition rate.

For tee stabilization, the required voltage input was 26 kv peak or 1.30 megw peak input power. For this case, the loaded VSWR was 1.8 resulting in an output power of 453 kw peak of which 233 kw peak, or 51.4 per cent, was delivered to the cavity. The peak axial electric field was 311 kv/cm as determined from a measured exit momentum of 3940 gauss-cm.

For isolator stabilization, the required voltage input was 25.8 kv peak or 1.29 megw peak input power. For this case, the loaded VSWR was 1.11 resulting in an output power of 410 kw peak of which 321 kw peak, or 78.3 per cent, was delivered to the cavity. The peak axial electric field was 365 kv/cm as determined from a measured exit momentum of 4550 gauss-cm.

Thus, relative to the power delivered to the cavity by the tee-stabilized system, isolator stabilization permitted an increase in cavity power of 37.8 per cent with no deterioration of stability in performance. This increase was possible even though the shift in operating point caused by the mismatch of the tee required a higher power output from the magnetron. Hence the increase in cavity power was obtained along with an improvement in operating conditions resulting from the lower VSWR.

H. A. Spuhler
R. J. Kenyon
P. D. Coleman
Dept. of Elec. Engrg.
Univ. of Illinois
Urbana, Ill.

* Received by the PGMTT, February 27, 1959.

[1] G. B. Collins, "Microwave Magnetrons," Rad. Lab. Series, vol. 6, pp. 638–639; McGraw-Hill Book Co., Inc., New York, N. Y.; 1958.

[2] I. Kaufman and P. D. Coleman, *J. Appl. Phys.*, vol. 28, pp. 936–944; September, 1957.

An Image Line Coupler*

For many microwave transmission systems, it is possible to make use of high-conductivity "image planes" as ground planes or as shields. Strip transmission lines, image plane lines, and dielectric image lines are examples of such systems. In order to make use of both sides of the ground plane, energy can be coupled from one side of the plane to the other by means of holes in the metal plate. Obviously, many existing coupling devices can be redesigned for such use. One such application is the directional coupler. In this paper, it is applied to the dielectric image line.

The dielectric image line[1-3] has been used for certain applications.[4,5] This line consists of a half round dielectric rod mounted on an image plane, (see Fig. 1).

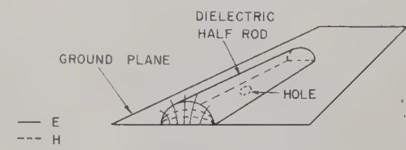

Fig. 1—Dielectric image line.

Now if a hole is made between the two sides of the image plane, coupling exists between the two sides. The purpose of this paper is to indicate what effect this coupling produces. According to H. A. Bethe,[6] the coupling may be determined approximately by considering it as arising from coupling by two dipoles. The electric field on the secondary side of the plane (near the hole) is similar to that generated by an oscillating electric dipole, with its dipole moment parallel to the electric field of the incident wave (near the hole) on the primary side of the plane. The magnetic field behaves as if the hole contained a magnetic dipole moment parallel to the incident magnetic field but in the opposite direction. Making the usual approximations as to aperture size, thickness, and extent of the image plane the following equations can be obtained:

Coupling:

$$C = 20 \log_{10} \frac{\pi h^3}{12\lambda_0 S}\left[\frac{1}{\eta} E_n^2 \frac{F_e(t)}{F_H(t)} + 2\eta H_t^2 \cos\theta\right] F_H(t) \text{ db.}$$

Directivity:

$$D = 20 \log_{10} \frac{\left[2\eta H_t^2 \cos\theta + \frac{1}{\eta} E_n^2 \frac{F_e(t)}{F_H(t)}\right]}{\left[2\eta H_t^2 \cos\theta - \frac{1}{\eta} E_n^2 \frac{F_e(t)}{F_H(t)}\right]} \text{ db.}$$

For maximum directivity:

$$\cos\theta = \frac{E_n^2}{2\eta^2 H_t^2} \cdot \frac{F_e(t)}{F_H(t)} \cdot$$

Here, $F_e(t)$ and $F_H(t)$ are attenuation factors for the electric and magnetic fields, respectively in propagating through the circular

* Received February 13, 1959; revised manuscript received March 12, 1959. This work was supported in part by the Office of Naval Research under Contract No. N7-onr-29529.

[1] D. D. King, "Circuit components in dielectric image lines," IRE Trans. on Microwave Theory and Techniques," vol. MTT-3, pp. 35–39; December, 1955.

[2] D. D. King, "Properties of dielectric image lines," IRE Trans. on Microwave Theory and Techniques," vol. MTT-3, pp. 75–81; March, 1955.

[3] S. P. Schlesinger and D. D. King, "Dielectric image lines," IRE Trans. on Microwave Theory and Techniques, vol. MTT-6, pp. 291–299; July, 1958.

[4] H. W. Cooper, M. Hoffman, and S. Isacson, "Image line surface wave antenna," 1958 IRE National Convention Record, pt. 1.

[5] B. Packer and D. L. Angelakos, "An Image Line Coupler," Univ. of Calif., Berkeley, Inst. of Engrg. Res., Rep. No. 188, series no. 60; July, 1957.

[6] H. A. Bethe, "Lumped Constants for Small Irises," Mass. Inst. Tech., Cambridge, Rad. Lab. Rep. No. 43-22; March, 1943.

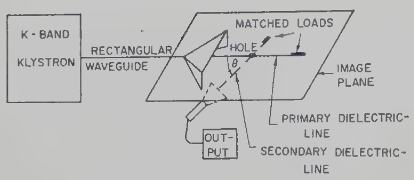

Fig. 2—Experimental set-up.

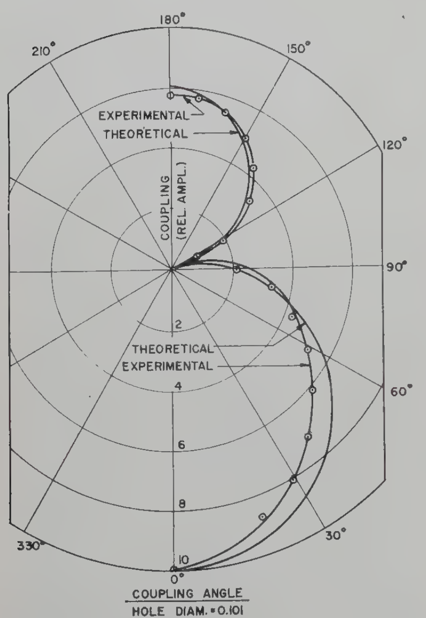

Fig. 3—Coupling as a function of angle θ.

hole acting as a waveguide beyond cut-off. E_n is the normal component of the electric field and H_t is the transverse component of the magnetic field both in the dielectric guide at the coupling hole. The longitudinal component of the magnetic field H_z is neglected. S is a power normalizing factor, h is the diameter of the hole, λ_0 is the free-space wavelength, and η is the specific impedance of free space. Fig. 2 defines the angle θ. If t, the thickness of the plane, is very small, the ratio $F_e(t)/F_H(t) \sim 1$ and the equations further simplify

$$C = T[1 + g \cos \theta]$$

and

$$D = \frac{1 + g \cos \theta}{1 - g \cos \theta}.$$

C and D are given in relative values, T is a constant of proportionality, and g is approximately the ratio of magnetic to electric coupling.

An experimental dielectric image line coupler was investigated at 24.4 kmcps. Fig. 2 illustrates the arrangement of the experiment. The ground plane thickness was 0.026 inch and the hole size was 0.101 inch in diameter. For these dimensions, $F_H(t)$ was 1.112 and $F_e(t)$ was 0.827. The ratio $F_e(t)/F_H(t)$ then is 0.742 and should be used (instead of 1.00) if greater accuracy is called for. Fig. 3 shows the variation of the coupling as a function of the angle θ. Plotted in the same figure is a curve called "Theoretical" which is of the form: $C = T(1 + g \cos \theta)$. The factor g is approximately equal to 4, the ratio of magnetic to electric coupling. The magnitude of the coupling is normalized so that at $\theta = 0°$, $C = 10$. Similar data were taken for hole diameters of 0.078, 0.082, 0.093, 0.111, 0.128 inch with no substantial differences apparent.

Fig. 4 illustrates how this arrangement may be used as a directional coupler. The

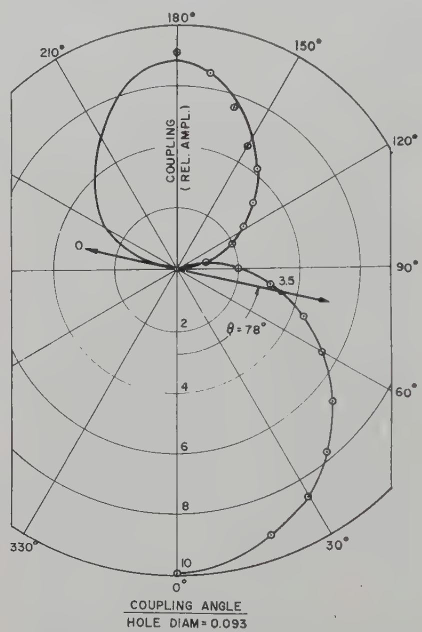

Fig. 4—Direct coupling.

solid line at $\theta = 78°$ represents the orientation of the secondary guide with respect to the primary guide. In one direction, the coupling is approximately zero whereas in the other direction it is 3.5 relative units.

Many other possible arrangements of holes and slots may be used to produce equivalent results or to improve the coupling and directivity behavior.

D. J. Angelakos
Elec. Engrg. Dept.
Univ. of Calif.
Berkeley 4, Calif.

An Extension of the Concept of Stop and Pass Bands of a Zobel Type Filter to a General Reciprocal Two Port Network Which has a Nonloxodromic Transformation*

The conventional treatment[1] of the Zobel filter starts with symmetrical T or π sections of pure reactances and then develops the iterative measures of the network; the fixed points and the propagation constant. It is shown that the propagation constant is either pure real (stop band)[2] or pure imaginary (pass band). These iterative measures can be worked out for the general T section. Fig. 1 shows the nomenclature used for the symmetrical T section and the general two port.

* Received by the PGMTT, March 9, 1959.

[1] W. L. Everitt and G. E. Anner, "Communication Engineering," McGraw-Hill Book Co., Inc., New York, N. Y.; 1956.

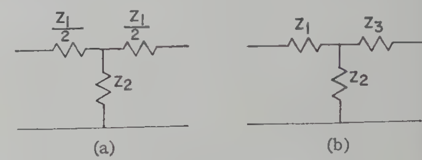

Fig. 1—(a) The symmetrical T section, (b) the asymmetrical T section.

TABLE I

(a) The symmetrical T section

$$\cosh \gamma = 1 + \frac{Z_1}{2Z_2}$$

$$Z_{it} = Z_0 = \pm \sqrt{Z_1 Z_2 + \frac{Z_1^2}{4}}$$

(b) The asymmetrical T section

$$\cosh \gamma = 1 + \frac{Z_1 + Z_3}{2Z_2}$$

$$Z_{it} = Z_1 - Z_3 \pm \sqrt{\left(\frac{Z_1 + Z_3}{2}\right)^2 + (Z_1 + Z_3)Z_2}$$

Table 1 lists the equations for the fixed points and the propagation constant for both networks. The network properties can also be developed as a bilinear transformation,[3] and the network can be classified by its type of transformation. For the two port, the input impedance is related to the output impedance by

$$Z' = \frac{\dfrac{(Z_1+Z_2)Z}{Z_2} + \dfrac{Z_1Z_2+Z_2Z_3+Z_3Z_1}{Z_2}}{\dfrac{1}{Z_2}Z + \dfrac{Z_2+Z_3}{Z_2}}.$$

The trace of the normalized transformation is $2 + (Z_1+Z_3)/Z_2$ which is twice $\cosh \gamma$. For the transformation to be nonloxodromic the trace must be real, hence the sum of the two series impedance phasors is either in phase or 180° out of phase with the phasor impedance of the shunt arm. It has been shown[4] that it is always possible in a microwave two port, to find reference planes at which the transformation is nonloxodromic. Thusly for any microwave network, reference planes can be found where $\cosh \gamma$ is real. If the transformation is hyperbolic $(|a+d| > 2)\gamma$ will be real. If the transformation is elliptic $(|a+d| < 2)\gamma$ will be imagi-

[2] With the exception of a possible 180° phase reversal.

[3] E. F. Bolinder, "Impedance and polarization-ratio transformations by a graphical method using isometric circles," IRE Trans. on Microwave Theory and Techniques, vol. MTT-4, pp. 176–180; July, 1956.

[4] D. J. R. Stock and L. J. Kaplan, "The analogy between the Weissfloch transformer and the ideal attenuator (reflection coefficient transformer) and an extension to include the general lossy two port," IRE Trans. on Microwave Theory and Techniques, to be published.

nary and $a+d=\pm 2$ the cut off conditions will be obtained. The cut off may be either between loss and phase shift as in a Zobel filter or between gain and phase shift because the cosine is an even function; therefore, it cannot perceive if the hyperbolic transformation is due to gain (negative resistance) or loss.

If the impedance plane is mapped onto the Riemann sphere, the criterion for determining whether the network is in the stop or pass band will depend on whether the Pascal line[5] cuts or does not cut the Riemann sphere (the parabolic transformation occurs at tangency). These transformation characteristics have been used by Bolinder[6] to show the analogy of the exponential line to the high pass filter and can be used to denote the difference between lossy and lossless uniform transmission lines. This classification can be used for any device, as waveguide, which has cut off phenomena or accounts for losses in any transmission device.

Thus it is seen that it is always possible to find reference terminals for a given network at which the resultant is either pure gain or pure loss or pure phase shift in the Zobel sense. Of course the insertion loss will depend on the termination as well as the properties of the two port.

D. J. R. Stock
L. J. Kaplan
Elec. Engrg. Dept.
New York Univ., N. Y.

[5] E. F. Bolinder, "Impedance transformations by extension of the isometric circle method to the three dimensional hyperbolic space," *J. Math. Phys.*, vol. 36, pp. 49–61; April, 1957.
[6] E. F. Bolinder, "Study of the exponential line by the isometric circle method and hyperbolic geometry," *Acta Pol.*, Elec. Engrg. Series, vol. 7, no. 8; 1957.

Characteristic Impedance of Split Coaxial Line*

A few years ago, the balun was studied at our laboratory and it is important to know the characteristic impedances of the line. There are several papers[1–3] concerning this characteristic impedance. The cross section of the transmission lines is shown in Fig. 1 and the characteristic impedances are calculated in these papers. Last year, a paper was published in the IRE Trans. on Microwave Theory and Technique on this problem, using similar methods described below. I wish to describe my approach and show a disparity.

* Received by the PGMTT, December 9, 1958.
[1] H. Kogō and K. Morita, "Electrode capacity of slit-coaxial cylinder," *J. Inst. Elec. Commun. Eng., Japan*, vol. 38, pp. 548–552; July, 1955.
[2] H. Kogō and K. Morita, "Electrode capacity of slit-coaxial cylinder," (supplement) *J. Inst. Elec. Commun. Eng., Japan*, vol. 39, pp. 33–36; January, 1956.
[3] J. Smolarska, "Characteristic impedance of the slotted coaxial line," IRE Trans. on Microwave Theory and Techniques, vol. MTT-6, pp. 161–164; April, 1958.

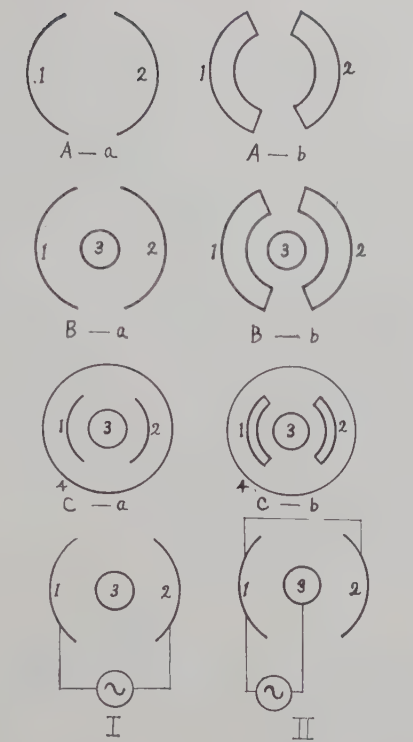

Fig. 1—Cross section of the transmission lines and line construction. A) Split cylinder, B) split coaxial, C) split coaxial with outer pipe; a) thin outer wall, b) thick outer wall; I) line composed of sides 1, 2, II) line composed of sides 1, 2 and central conductor 3.

The characteristic impedance of the split coaxial line shown in Fig. 1 can be classified physically and mathematically as follows:

A) The split cylinder
   a) the thin outer wall
   b) the thick outer wall
B) The split coaxial line
   a) the thin outer wall
   b) the thick outer wall
C) The split coaxial with outer pipe.

There are two cases. In the first case, the split two sides 1 and 2, compose the transmission line (I) and, in the second case, the split two side 1 and 2, and a central conductor 3 form the transmission line (II) shown in Fig. 1. The mathematical treatment of these cases are difficult because of the thickness of the outer conductors, *A-a*, *A-b*, and *B-a* in the above table are described in a previous treatise.[1,2] The same results were obtained by J. Smolarska by using a similar method. For the remaining problems *B-b*, one must rely on an approximate solution, the accurate solution being much too difficult.

The characteristic impedance of *B-b* with regard to the split coaxial shown in Fig. 2, is acquired from the accurate solution by using the accurate values of the characteristic impedances of the split cylinder considering wall thickness and the split coaxial with thin outer wall.

The characteristic impedance composed of the outer and a central conductor of *B-b* is almost equal to that compared with the case of a zero thickness since the width of the split is narrow and the disturbance of the split portion shown in Fig. 3 differs slightly by the existence of the thickness.

Fig. 2—Relation of the split coaxial line and its decomposite construction.

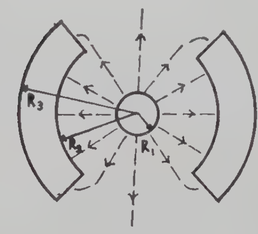

Fig. 3—Disturbance by the thick outer wall.

The curved lines in Fig. 4 show the results of the experiment using a water tank, and these are almost equal to the computed value using the approximate theory. A treatise similar to Smolarska's[3] has already been published. Our approach used almost the same transformation equation as found in treatise, but in detail, small differences are found in the papers. For example, Compare A[3] with B.[1]

1) The next formulas are adopted to transform the original figure into the orthogonal line coordinates.

   A) $\omega = \log Z$ (Transformation).

   B) $\mu = R_1 e^Z$ (Transformation).

2) The *S-C* transformation is common in both *A* and *B*, but the corresponding points differ.
   A) Corresponds with three unknown constants α, β, and γ for the singular point.
   B) Corresponds with two unknown constants α, β, for the character of the elliptic function.
3) The enumeration method of unknown constants.
   A) This uses the definite integral, namely a definite integral is used for the distance between each singular point.
   B) This uses the indefinite integral and substitutes to acquire the value of the corresponding in its consequent equation.
4) The numerical computation.
   A) The numerical computation used the approximate calculating equation as follows: $\beta \gg 1$, $\beta \gg \gamma$, and $\beta \gg \alpha$. These relations are useful only to the case of the particular split angle. However, the errors are not investigated.
   B) The approximate calculating equation is not in use and accordingly the split width is extended to the whole range.
5) The numerical compution of the characteristic impedance is calculated in the following cases.

   Line I).

   A) $R/r = 2.3, 2.6, 2.72, 3.37$.

   B) $Z_0 = 25\Omega, 50\Omega, 150\Omega$, (for the no splits).

   Line (II).

   A) $R/r = 2.72$.

   B) $Z_0 = 25\Omega, 50\Omega, 150\Omega$, (for the no splits).

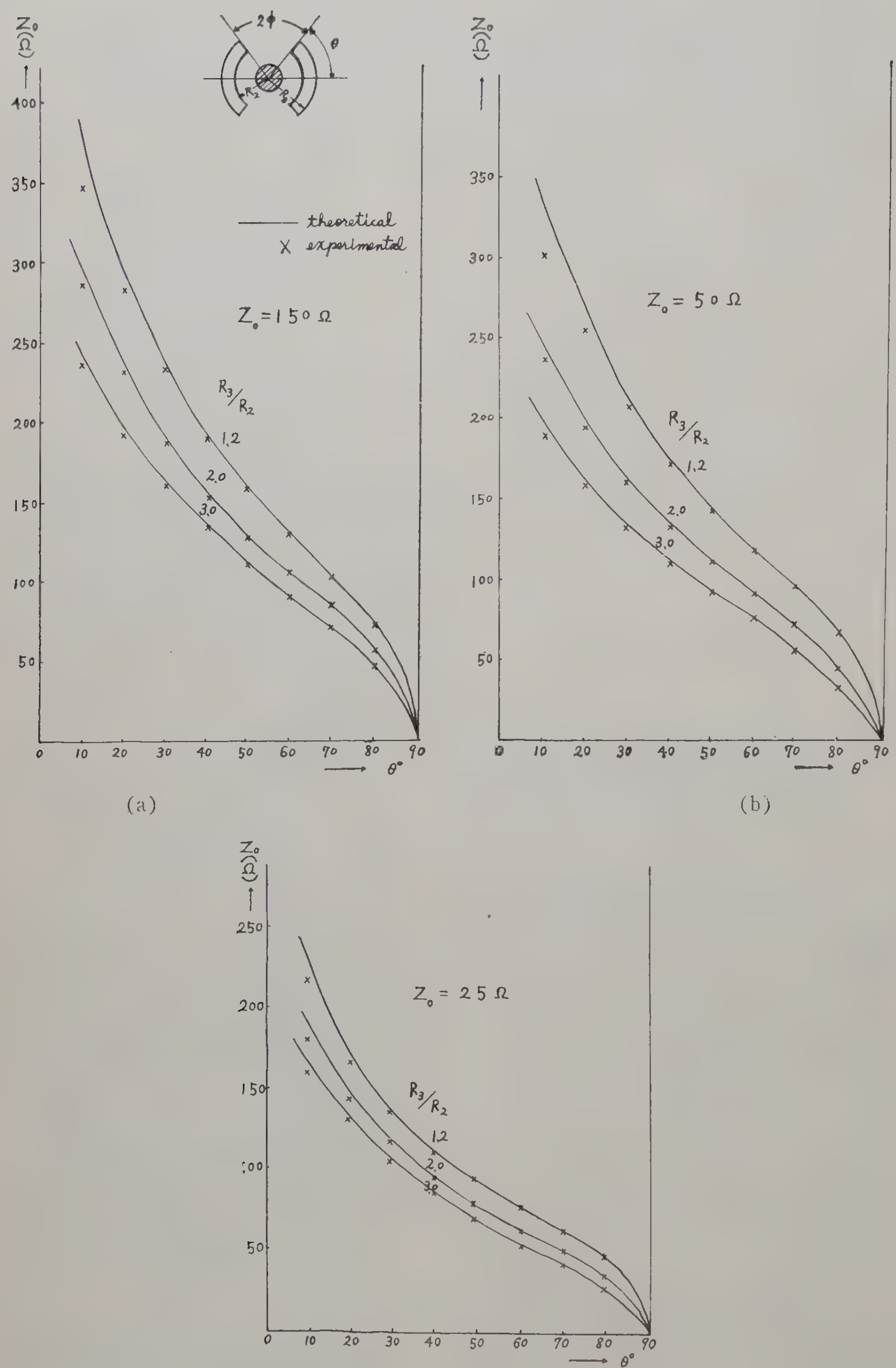

Fig. 4—Characteristic impedance of Split coaxial line; (a) case of 150 ohms for the no slit, (b) case of 50 ohms for the no slit, and (c) case of 25 ohms for the no slit.

6) The variable range of the split width.
   A) $2\phi = 10° \sim 40°$.
   B) the whole range.
7) The split coaxial with the thickness of the wall in consideration.
   A) This is proven[4] in reference to the split cylinder with the thickness of the wall.
   B) Our treatise[3] which conducted almost the same problem in contrast with Bochenek[4] was already published.
8) Experiments.
   A) None.
   B) The results of the experiment of the water tank conform fully with the theory as shown in Fig. 4.

Hiroshi Kogō
Chiba Univ.
531 Iwase
Matsudo, Chiba, Jap.

[4] K. Bochenek, "Impedecja falowa linii wyslepujecej wjednym Z rodzajów symetryzatora," *Arch. Electrotech*, vol. 4, pp. 135–148; April, 1956.

A Method for Enhancing the Performance of Nonreciprocal Microwave Devices*

The performances of nonreciprocal microwave devices are as temperature dependent as the ferrimagnetic materials used to produce them. Hence, the operating characteristics vary markedly with incident power level and ambient temperature. In order to compensate for these temperature changes, special cooling techniques are frequently utilized. Since those are often inconvenient, devices are more usually designed to operate at a much broader frequency range than the specifications demand resulting in deterioration of performance in the specified band. In some cases, ferrites may be especially prepared to have a nearly constant saturation magnetization for a range of temperature, as illustrated in Fig. 1. Whereas both of these ferrites have the same saturation magnetization at room temperature, changing the temperature to 100°C causes a 25 per cent change in the $4\pi M_s$ of the commercially available ferrite, but only a 7 per cent variation in the especially designed one. Tailoring ferrites to the application is much too difficult to represent a solution to the problem.

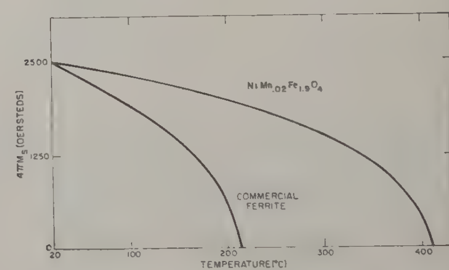

Fig. 1—Saturation magnetization curves for a simple, commercially available ferrite and for an especially designed ferrite having the same $4\pi M_s$ at room temperature.

A simpler solution may be to design devices for operation at the highest ambient temperature to be encountered, or the highest temperature developed because of high input power, and control the temperature of the ferrite to this level. Fig. 2 illustrates one method among many for accomplishing this. Alternatively, some design geometries would lend themselves to an adoption of the well-known technique used in ferromagnetic resonance research: The sample is heated directly through a metal post on which it is mounted in the resonant cavity. A very simple temperature control circuit is required, only regulating to ±10°C or more, since the saturation magnetization does not change very rapidly with temperature even in simple ferrites (Fig. 1). Operation of a nonreciprocal device at a constant elevated temperature results in optimum performance at all power levels and ambient

* Received by the PGMTT, March 18, 1959. This work was done while the author was at the Microwave Physics Lab., Sylvania Elec. Products, Inc., Mountain View, Calif.

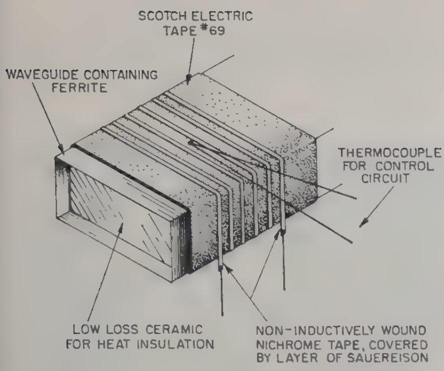

Fig. 2—Schematic diagram illustrating a method for maintaining an elevated constant operating temperature for a nonreciprocal device.

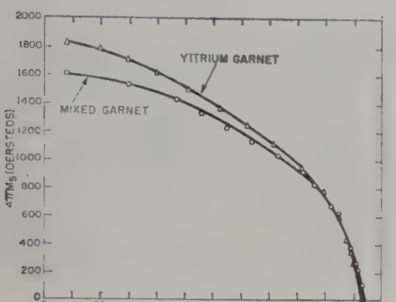

Fig. 3—Saturation magnetization as a function of temperature of yttrium iron garnet and a mixed garnet, $2.5\ Y_2O_3 \cdot 0.5\ Gd_2O_3 \cdot 5\ Fe_2O_3$.

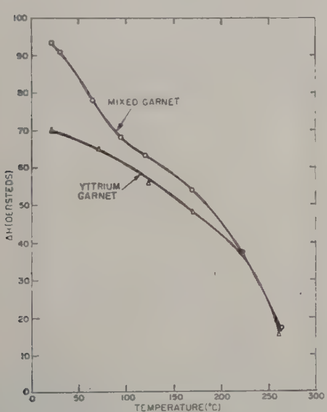

Fig. 4—Ferromagnetic resonance line width of yttrium iron garnet and the 2.5 Y to 0.5 Gd mixed garnet as a function of temperature.

temperatures over the required frequency band.

The design of very low microwave frequency nonreciprocal devices is also significantly enhanced by this method. Essential for the design of such devices are ferromagnetic materials with both narrow resonance line width and small saturation magnetization. Narrow line width materials are required for avoiding the overlap between the inevitable low magnetic field losses, which are reciprocal, and the desired nonreciprocal resonance losses. A small saturation magnetization is highly desirable to ensure stability of operation through definite saturation of the material at the small applied fields required for operating devices at low frequencies ($\omega = \gamma H$). To date, the materials most nearly fulfilling these requirements are mixed garnets in which the *c* sites are shared by yttrium and gadolinium ions.[1] However, as Figs. 3 and 4 show, the desired reduction in saturation magnetization is accompanied by an increase in the line width. Hence, mixed garnets represent, at best, only a compromise solution.

As seen in Figs. 3 and 4, *both* the line widths and saturation magnetizations of rare earth garnets decrease with increasing temperature. By maintaining ordinary yttrium ion garnet at 150°C, a $4\pi M_s$ of 1300 oersteds and a ΔH of 50 oersteds may be easily obtained. Thus, by this relatively simple means, an improvement over the previously best material for nonreciprocal low microwave frequency applications of almost 20 per cent in saturation magnetization and 50 per cent in line width is achieved.

BETSY ANCKER-JOHNSON
RCA Labs.
Princeton, N. J.

[1] B. Ancker-Johnson and J. J. Rowley, "Mixed garnets for nonreciprocal devices at low microwave frequencies," PROC. IRE, vol. 46, pp. 1421–1422; July, 1958. See also M. H. Sirvetz and J. E. Zneimer, "Microwave properties of polycrystalline rate earth garnets," *J. Appl. Phys.*, vol. 29, pp. 431–433; March, 1958.

Characteristics of Argon Noise Source Tubes at S-Band*

During the design of equipment for applications in radio astronomy, various tests were performed on argon plasma noise source discharge tubes, with emphasis on the Bendix 6358/TD-12 which is Model A148 of Johnson and DeRemer.[1] In view of the wide use of these tubes as secondary standards of microwave noise power, a brief summary of the results obtained will be given. A description of the test equipment and experimental procedures used would be repetitive of much that has been reported by Sees[2] and Hughes,[3] but is available from the writer if desired.

An absolute calibration at 2885 mc was made on the TD-12, matched to its standard waveguide mount, and operating at the recommended discharge current of 250 ma. The value obtained for the effective noise temperature, T_D, was 10,700°K, with a probable error of 150°K. (T_D is defined by taking the available noise power equal to $kT_D df$, where k is Boltzmann's constant and DF is the frequency bandwidth.) In estimating the probable error, allowance was made for the fact that individual tubes are not precisely the same in noise emission. Relative measurements were made on a sample of twenty tubes consisting of twelve A148 (Bendix TD-12), and eight A147 (Bendix TD-10 and Philco L1306A) mounted and matched in *S*-band waveguide; the difference between any two was in most cases about 50° or less, with an extreme of 80° between the highest and lowest.

Hughes'[3] value of T_D for the British CV1881,[4] which is somewhat similar to the A147, was 11,140±130°K (frequency 2860 mc, discharge current 180 ma, 90° E-plane mount). Our tests on the CV1881 yielded a result of 10,900±160°K (frequency 2885 mc, discharge current 180 ma, 20° and 30° E-plane mounts).

Less accurate calibrations on the TD-12 were also taken at a few different frequencies between 2750 and 2910 mc. The results, although not very informative, were at least consistent with the theory that any variation of emission with frequency is small.[5]

The consistency of output of a single tube operating over a period of time is very good. Relative accuracies of one part in two or three thousand were obtained with the TD-12 (frequency 2885 mc) over selected two-hour periods; and one part in one thousand over fifteen-hour periods. For these particular tests, the discharge current was set at 300 ma. Although the emission is slightly higher and less critical to small changes in discharge current at the usual setting of 250 ma,. the audio frequency oscillations characteristic of these tubes[1] were more intense and irregular, with correspondingly poorer results as to consistency of output reading over a period of time. Whether the fault should be ascribed to the tube or the particular measuring equipment used, it is probably preferable to operate at 300 ma discharge current when extreme accuracy is desired. The A147 tubes gave satisfactory results at their recommended discharge current of 250 ma.

Whether this degree of consistency of output can be maintained over much longer periods of time has not been established. Several tubes were retested after intermittent operation, continuous operation, repeated on-off cycling, or shelf-life of several months; some of these appeared to have changed in emission by as much as 50°, but these changes were not clearly related to the history of the tube. On this basis, the relative accuracy to be expected from the operation of a single tube, either continuously or intermittently, over periods of months, may not be better than one part in two hundred.

W. J. MEDD
Radio and Elec. Engrg. Div.
Nat. Res. Council
Ottawa 2, Can.

* Received by the PGMTT, April 10, 1959.

[1] H. Johnson and K. R. DeRemer, "Gaseous discharge super-high frequency noise source," PROC. IRE, vol. 39, pp. 908–914; August, 1951.

[2] J. E. Sees, "Fundamentals in Noise Source Calibrations at Microwave Frequencies," Naval Res. Lab. Rep. No. 5051; January, 1958.

[3] V. A. Hughes, "Absolute calibration of a standard temperature noise source for use with S-band radiometers," *Proc. IEE*, pt. B, vol. 103, pp. 669–672; September, 1956.

[4] N. Houlding and L. C. Miller, "Discharge tube noise sources," Radar Res. Est., Great Malvern, Worcs., Eng., T.R.E. Memo. No. 593; October, 1953.

[5] P. Parzen and L. Goldstein, "Current fluctuations in D.C. gas discharge plasma," *Phys. Rev.*, vol. 79, p. 190; July, 1950.

PGMTT News

Among those attending the PGMTT Administrative Committee luncheon meeting, held on March 23 at the Essex House, New York, N. Y., were (clockwise): R. F. Schwartz, A. G. Clavier, H. F. Engelmann, Harvey Lance, Gus Shapiro, T. S. Saad, *Chairman*, A. A. Oliver, *Vice-Chairman*, H. Magnuski, George Sinclair, Saul Rosenthal, W. W. Mumford, Donald D. King, A. C. Beck, and S. B. Cohn.

Contributors

Robert E. Beam (S'37–A'41–SM'44–F'56), for a photograph and biography, please see page 335 of the July, 1958 issue of these TRANSACTIONS.

❖

Robert W. Beatty (S'43–A'45–M'50–SM'53), for a photograph and biography please see p. 457 of the October, 1958 issue of these TRANSACTIONS.

❖

Morris E. Brodwin (A'49–M'55), for a photograph and biography, please see page 242 of the April, 1958 issue of these TRANSACTIONS.

John Brown (SM'57) was born on July 17, 1923, in Auchterdewan, Scotland. He received the M.A. degree in mathematics and natural philosophy from the University of Edinburgh, Scotland, in 1944, and the Ph.D. degree from the University of London, Eng., in 1954.

From 1944 to 1951 he was on the staff of the Radar Research and Development Establishment, Malvern, and was mainly concerned with theoretical studies of microwave tubes. In 1951, he became a lecturer in electrical engineering at the Imperial College of Science and Technology and in 1955 moved to University College, London, where he is now reader in electrical engineering.

Dr. Brown is an Associate Member of the IEE, London, and at present serves on the Electronics and Communications Section Committee.

Glenn F. Engen was born in Battle Creek, Mich., on April 26, 1925. He received the B.A. degree in physics and mathematics from Emmanuel Missionary College, Berrien Springs, Mich., in June, 1947. He has done graduate work at the Universities of Michigan, Maryland, and Colorado. After employment with the U. S. Naval Ordnance Laboratory and the Johns Hopkins University Applied Physics Laboratory, he joined the National Bureau of Standards in 1954. His present work is in the field of microwave power measurement techniques and standards.

GLENN F. ENGEN

Mr. Engen is a member of Commission I of the International Scientific Radio Union, and of the Boulder Branch of RESA.

❖

Georges Goudet (SM'50) was born in 1912, in Dijon, France. He received several scholarships at the Ecole Normale Supérieure. In 1936, he became an Agrégé (fellow) of physical science at the university. After serving as an artillery officer during the war, he completed his work for the Ph.D. degree in physics in 1942.

G. Goudet

During 1943 and 1944, he worked on microwave tubes at Laboratoire Central de Télécommunications. He then became the head of the ultra-high-frequency laboratory of the French Posts, Telegraphs and Telephones Administration. In 1951, he joined the staff of Nancy University as a professor and director of the special school of electricity and mechanics. He has served as a consultant to Laboratoire Central de Télécommunications and in 1955 became the director of that laboratory. He is the author of numerous publications and of several books.

Dr. Goudet is a member of the Société Française de Physique, the Société des Radioélectriciens, and the Société Française des Electriciens.

❖

Jôji Hamasaki was born on October 25, 1931, in Kure City, Japan. He received the B.S. degree in 1953, the M.A. degree in 1955, and the Ph.D. degree in 1958, in electrical engineering, from the University of Tokyo.

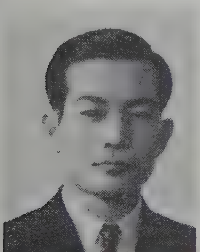

J. Hamasaki

He was engaged in research of microwave filters and power meters, and became an assistant professor of the University of Tokyo in 1958.

He is a member of the IEE of Japan and the Institute of Electrical Communication Engineers of Japan.

❖

Toshio Hosono was born on March 31, 1922, in Tokyo, Japan. He received the B.S. degree in electrical engineering in 1943 from Nihon University and the Doctor of Engineering degree in 1958 from the University of Tokyo. He joined the University of Tokyo, working on electromagnetic theory as a research fellow from 1944 to 1946 and a research assistant from 1946 to 1952. He has been an assistant professor in electrical engineering at Nihon University since 1953. He is secretary of the committee for electromagnetic fields arranged by Institute of Electrical Engineers in Japan and one of the standing committee for microwave transmission arranged by the Institute of Electrical Communication Engineers of Japan.

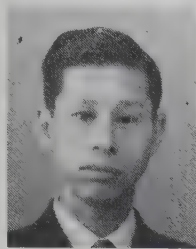

T. Hosono

❖

R. C. Johnson (M'56) was born in Eveleth, Minn., on May 9, 1930. He received the B.S. and M.S. degrees in physics in 1953 and 1958, respectively, from the Georgia Institute of Technology, Atlanta.

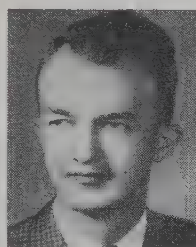

R. C. Johnson

In 1953 he entered the U.S. Navy where he attended the Naval Electronic Material School and served as Electronics Officer aboard the U.S.S. *Moale* (DD693). Since 1956 he has been employed at the Engineering Experiment Station of the Georgia Institute of Technology, working on meteor-scatter propagation, microwave components, and microwave antennas.

Mr. Johnson is a member of Tau Beta Pi and Sigma Pi Sigma.

❖

Shishu Kohno was born on March 20, 1912, in Tokyo, Japan. He received the B.S. and Ph.D. degrees in engineering from the University of Tokyo in 1936 and 1954, respectively.

S. Kohno

In 1936 he joined the Furukawa Electric Company, Ltd. and was assigned to its Yokohama Works. In 1946 he became chief of the 3rd Unit, engineering section, then assistant chief of the Communication Cable Section of the Engineering Division in 1949. In 1953 he was made chief of the Communication Cable Section, and then chief of the Research Section for the Transmission Line in 1955. In 1956 he became chief of the Research Division.

He is one of a standing committee of microwave transmission arranged by the Institute of Electrical Communication Engineers of Japan.

Kaneyuki Kurokawa was born on August 14, 1928, in Tokyo, Japan. He received the B.S. degree in electrical engineering in 1951 and the Ph.D. degree in 1958 from the University of Tokyo.

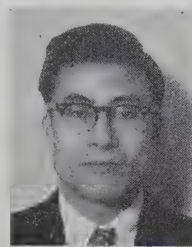

K. Kurokawa

Since 1951, he has been engaged in research on microwave measurements, microwave theory, and mm-wave transmission lines. From 1955 to 1958, he also served as a chief engineer of the Radar group for the sounding rocket research conducted by the Institute of Industrial Science, University of Tokyo. At present, he is an assistant professor of the University of Tokyo.

Dr. Kurokawa is a member of the IEE of Japan and the Institute of Electrical Communication Engineers of Japan.

❖

Tsuneo Nakahara was born on August 29, 1930 in Naruto, Japan. He graduated in 1953 from the electrical engineering department of the University of Tokyo.

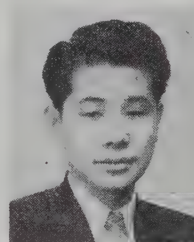

T. Nakahara

In 1953, he joined the microwave laboratory of Sumitomo Electrical Industries, Ltd., engaging in the research on microwave transmission lines and broadcast antennas.

Mr. Nakahara is a member of the Institute of Electrical Communication Engineers of Japan, and the IEE of Japan.

❖

J. Q. Owen (M'55) was born in Glasgow, Scotland, on May 30, 1923. He served with the Royal Electrical and Mechanical Engineers from 1942–1947, working on radio and communication equipment. In 1951 he received the B.S. degree in electrical engineering from Glasgow University, Scotland.

J. Q. Owen

Until 1955 he was engaged in research and development of microwave components and systems in the Microwave Division of EMI Electronics Limited, Feltham, England. From 1955–1957 he was employed by Westinghouse Electric Corp., Baltimore, Md. on the development of microwave antennas and components. He is at present engaged in research and the development of ferrite components with the Special Microwave Device Group of Raytheon Manufacturing Company, Waltham, Mass.

Mr. Owen is an associate member of the IEE.

J. K. Pulfer was born in Gordon, Manitoba, Canada, on May 4, 1932. He attended the University of Manitoba, Fort Gary, Manitoba, Canada, where he received the B.S. degree in electrical engineering in 1953.


J. K. PULFER

He worked as a summer student in the Radio and Electrical Engineering Division of the National Research Council of Canada during 1952 and 1953. After a year of post graduate work at the University of Manitoba he returned to NRC in 1954 where he has been engaged in work in defense problems.

❖

Hans Severin (SM'56) was born in Grafenwöhr, Germany, on May 6, 1920. He received the doctor rer. nat. degree from the University of Goettingen in 1943. Until 1957 he was a research physicist at the III. Physical Institute of the University at Goettingen and became a Privatdozent for physics in 1954. During two sabbatical years he was associated with the Research Laboratories of Swiss PTT Administration at Bern, Switzerland, in 1951–1952 and with RCA Laboratories at Princeton, N. J., in 1955–1956.


H. SEVERIN

He has been engaged in physics of microwaves and their applications, especially in propagation problems. He has given papers on diffraction of electromagnetic waves in international conventions at Milan in 1952, at Montreal in 1953, and at Ann Arbor in 1955. He is now Assistant Director of Philips Laboratories at Hamburg and is teaching physics at the University of Hamburg.

Dr. Severin is a member of the German Physical Society and the German Association of Electrical Engineers.

❖

Isao Someya (M'57) was born in Okayama, Japan, on March 23, 1915. He received the Ph.D. degree in electrical engineering from Tokyo University of Tokyo, Japan, in 1952.


I. SOMEYA

During 1938–1941 he was employed by the Electro Technical Laboratory, working on research of television transmission on the coaxial cable. In 1942 he was engaged in the development of radar. Since 1945, he has been with the Electrical Communication Laboratory of the Nippon Telegraph and Telephone Public Corporation, working in the field of development of VHF and microwave relay systems.

Dr. Someya is a member of the Institute of Electrical Communication Engineers of Japan.

❖

L. Solymar, for a photograph and biography, please see pp. 459–460 of the October, 1958 issue of these TRANSACTIONS.

❖

Ronald F. Soohoo was born in Canton, China, on September 1, 1928. He received the B.S. degree from the Massachusetts Institute of Technology, Cambridge, Mass., in 1948; the M.S. degree in 1952 and the Ph.D. degree in 1957, both from Stanford University, Stanford, Calif. His studies were in electrical engineering and physics.

From 1948 to 1951, he was engaged in the design and analysis of power systems while an assistant engineer for the Pacific Gas and Electric Company. He then became a research assistant at the Microwave Laboratory, W. W. Hansen Laboratories of Physics at Stanford, where he was involved with microwave tube research from 1951 to 1953. He was an electronics research assistant at the Stanford Electronics Laboratories in 1954 and 1956. From 1954 to 1955, he was a research engineer with the Cascade Research Corporation, Los Gatos, Calif., engaging in the design of ferrite devices.


R. F. SOOHOO

Since 1957, he has been Director of Research Analysis at the Cascade Research Corporation. His present duties include research in microwave ferrites, microwave tubes, and solid state physics.

❖

Masao Sugi (A'56) was born on January 19, 1918 in Kashiwazaki, Japan. He graduated in 1940 from the electrical engineering department of Tokyo Imperial University.


M. SUGI

In 1940, he joined the electrical laboratory of Sumitomo Electrical Industries, Ltd., engaging in the research on communication cables and high-frequency transmission lines. He is at present the chief of the weak current research section of the research division of the company.

Mr. Sugi is a member of the Institute of Electrical Communication Engineers of Japan, and the IEE of Japan.

❖

Leo Young (M'54–SM'57), for a photograph and biography, please see page 186 of the January, 1959 issue of these TRANSACTIONS.

for every microwave engineer...

THE NEW 1960 D-B CATALOG -320 PAGES OF HELPFUL DATA

This latest D-B catalog—a hard-cover book—gives you complete information on making microwave measurements. You get comprehensive theory, plus practical help on applications. You'll find actual drawings of test setups, and instructions on test procedures, using units in the D-B line of precision test equipment—largest line available today.

Expanded handbook section gives the latest tabulations on available microwave tubes and their characteristics . . . on conversion factors, and other daily-used design data. There are dimension drawings of all commonly-used AN flanges. There's all the information you need for assembling D-B Building-Block components.

New 140 KMC instrument section gives listings on a complete line of Ultramicrowave® equipment—units which can greatly enlarge your scope of microwave activity. There's also a special section on "New Horizons in Microwave Applications."

Write for a copy of the 1960 D-B catalog on your company letterhead. Ask for Catalog No. C4.

DE MORNAY BONARDI ®

DE MORNAY-BONARDI

780 SOUTH ARROYO PARKWAY • PASADENA, CALIF.

INSTITUTIONAL LISTINGS

The IRE Professional Group on Microwave Theory and Techniques is grateful for the assistance given by the firms listed below, and invites application for Institutional Listing from other firms interested in the Microwave field.

The charge for an Institutional Listing is $50.00 per issue or $140.00 for four consecutive issues. Applications for Institutional Listings and checks (made out to the Institute of Radio Engineers) should be sent to Tore N. Anderson, PGMTT Advertising Editor, 1539 Deer Path, Mountainside, N.J.

NOTICE TO ADVERTISERS

Effective immediately the IRE TRANSACTIONS ON MICROWAVE THEORY AND TECHNIQUES will accept display advertising. For full details contact Tore N. Anderson, Advertising Editor, PGMTT TRANSACTIONS, 1539 Deer Path, Mountainside, N. J.

NEW
—different

Neither . . .

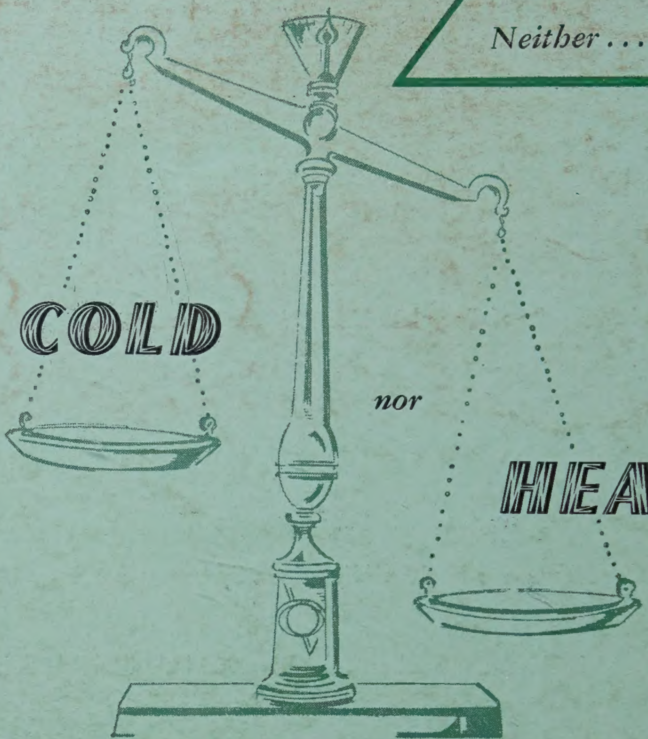

COLD

nor

HEAT

*nor microwatt range stays these instruments from drift-free measurements of RF power.**

MODEL B831A

Price $335.00
F.O.B. Woodside, N. Y.

* *With a bow to Herodotus, the 5th century B.C. Greek historian who wrote the much-quoted words appearing on the facade of the New York Post Office and paraphrased here.*

TEMPERATURE COMPENSATED POWER METER

- Temperature compensation gives greater stability and more accurate measurements.
- Readings are virtually drift-free, even in the 10 μW range.
- Accuracy: maximum positive accumulative error ± 5%. Standard deviation, or RMS probable error, ± 1.7%.
- Six direct reading ranges – 10 μW to 3 MW, full scale.
- Ranges can be switched without rebalancing.
- DC calibration at all levels.
- Self-balancing at 200 ohms.
- An *FXR SERIES 218 TEMPERATURE COMPENSATED THERMISTOR HEAD* is a required accessory. These broadband coaxial and waveguide components are available throughout the frequency range from 0.01 to 40 KMC/SEC.

FXR, Inc.

Design • Development • Manufacture •

FXR

26-12 Borough Place
Woodside 77, N. Y.

PRECISION MICROWAVE EQUIPMENT • HIGH-POWER MODULATORS • RADAR COMPONENTS • ELECTRONIC TEST EQUIPMENT